Carbon Capture by CaO in Molten Halide Salts

Karbonfangst med CaO i saltsmelter

Philosophiae Doctor (PhD) Thesis

Viktorija Tomkute

Department of Mathematical Sciences and Technology
Norwegian University of Life Sciences

Ås 2014

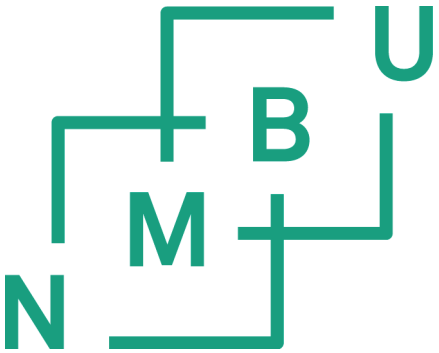

Thesis number 2014: 4
ISBN 978-82-575-1185-2
ISSN 1503-1667

The research underlying this thesis has been funded by the Research Council of Norway through the CLIMIT Research Programme (Grant No. 199900/S60, Carbon Capture in Molten Salts).

Main supervisor:

Dr. Espen Olsen
Department of Mathematical Sciences and Technology (IMT)
Norwegian University of Life Sciences (UMB)
Ås
Norway

Co-supervisor:

Asbjørn Solheim
SINTEF Materials and Chemistry
Trondheim
Norway

SUMMARY

The primary aim of commercial applications of the CO_2 capture process is to achieve efficient sorption of CO_2. Reaction of CaO with CO_2 at high temperatures is one of the promising options to reduce CO_2 concentrations from hot flue gas generated by power stations or other industrial processes. However, the main disadvantages of CaO-based materials are related to textural degradation of the sorbent during cyclic CO_2 capture, and such degradation is due to sorbent sintering, attrition, and reaction with impurities in the flue gas. Currently, there are no cost-efficient process modifications or synthesis techniques that can delay or prevent losses of the losses of calcium oxide-based sorbents in long-term and repeated CO_2 uptake cycles. Therefore, to make this technology economically attractive, future research should be focused on developing new or modified synthesis methods to improve long-term chemical and mechanical stability of CaO-based materials, or on designing a novel CO_2 removal technique that uses calcium looping.

The present research addressed a novel CO_2 capture technology using CaO dissolved or partly dissolved in molten halide salts. The use of molten salts as solvents or dispersion liquid may improve the reactivity of CO_2 with CaO by inducing more rapid gas–liquid interactions in the molten salt. Also, transport of the liquid–slurry material from the CO_2 capture unit to the CO_2 regeneration unit may not require the complex technology that is needed with solid CaO-based sorbents. Accordingly, the main goal of the current studies was to examine and verify CO_2 capture by commercially available CaO in molten metal halide salts.

The phase transitions of the NaF-CaF_2, NaF-CaF_2-CaO, NaF-CaF_2-$CaCO_3$, NaF-CaF_2-$NaCO_3$ and NaF-CaF_2-Na_2CO_3-$CaCO_3$ systems were studied primarily to examine the reactions of CaO, $CaCO_3$, and Na_2CO_3 in the eutectic mixture of NaF and CaF_2. In this work, the partial phase diagrams were obtained using thermal analysis, thermodynamic calculations (FactSage), and X-ray diffraction (XRD) of quenched samples. The experimentally derived phase relation of the NaF-CaF_2 system showed that the eutectic composition is appropriate for solid CaO reaction with CO_2. The phase diagram of the ternary CaO-NaF/CaF_2 system indicated very low CaO solubility. The data from evaluation of the $CaCO_3$-NaF/CaF_2 system suggested that the products of the reaction between $CaCO_3$ and NaF are Na_2CO_3 and CaF_2. In addition, the phase diagram of the Na_2CO_3-$CaCO_3$-NaF-CaF_2 system that was mapped using FactSage revealed formation of the intermediate compound $Na_2Ca(CO_3)_2$ (nyerereite).

Four different alkali and alkaline earth metal halide salts ($CaCl_2$, CaF_2/NaF, CaF_2/LiF, and CaF_2/$CaCl_2$) were employed as solvents for CaO dissolution or dispersion to improve sorbent activities in the CO_2 capture process. For CaF_2/NaF, CaF_2/LiF, and CaF_2/$CaCl_2$, the halide salts systems were used at a fixed composition to the eutectic mixtures. The characteristics of CO_2 uptake by CaO in the metal halide salts were optimized by evaluating the effects of the CaO mass proportion in the melt, the temperatures of the system during the carbonation/decarbonation reactions, the CO_2 content in simulated flue gas, the flue gas flow rate, and the sample weight. These tests and assessment of cyclic CO_2 capture were performed using a one-chamber reactor, Fourier transform infrared (FTIR) gas apparatus, and gravimetric and XRD analysis. The results indicate that the highest carrying capacity values

in the range 0.722–0.743 g CO_2/g CaO were achieved with the CaO-CaF_2/NaF system, because, instead of $CaCO_3$, thermodynamically stable Na_2CO_3 was formed through an ion exchange reaction. Similar high carbonation conversion values and formation of alkali metal carbonate were observed for the CaO/CaF_2/LiF system. Systematic evaluation of temperature of the carbonation reaction showed that reactivity of the sorbent with CO_2 in the CaO-CaF_2/NaF melt was highest at 826–834 ºC. Also, the carrying capacity of the sorbent was slightly affected by the concentration of CaO in the melt, but was not influenced by the CO_2 concentration. However, complete decomposition of the carbonates formed in the melt was not observed at temperatures in the range 994–1170 ºC under pure N_2 flow.

Materials for industrial applications need to be highly selective for CO_2, have a high carrying capacity, and offer good cyclic and economically acceptable regeneration performance. Therefore, in the present experiments, $CaCl_2$ and $CaCl_2$/CaF_2 (ratio set according to the eutectic composition) were utilized as the solvents for the dissolution and dispersion of CaO and $CaCO_3$ in the CaO/$CaCO_3$ carbonation/decarbonation process. Both metal halide systems showed that an increase in CaO content from 5 to 15 wt% in the molten salt enhanced the carrying capacity of the sorbent, and that a level greater than 15 wt% caused a decrease in the conversion due to sedimentation and agglomeration of the sorbent. In the CO_2 sorption tests, the CaO/CaF_2/$CaCl_2$ system resulted in more efficient CO_2 uptake behaviour compared to the CaO/$CaCl_2$ system, probably due to the lower liquidus temperature of the CaO/CaF_2/$CaCl_2$ composition, which allows performance of CaO carbonation at a lower temperature (695–705 ºC) than is possible with the CaO/$CaCl_2$ system (768–810 ºC). Desorption of CO_2 was independent of the control of carbonation and proceeded rapidly and completely at 904–950 ºC under pure N_2. Also, full decomposition of the formed carbonates was demonstrated under both a CO_2/N_2 mixture and pure CO_2. The most stable process of CO_2 absorption and desorption was reached using 15 wt% CaO in molten CaF_2/$CaCl_2$ (11.7/73.3 wt%). Most importantly, the cyclic CO_2 capture behaviour resulted in constant carrying capacity values of ~ 0.504 and ~ 0.667 g CO_2/g CaO for the CaO/$CaCl_2$ (5.32/94.68 wt%) and CaO/CaF_2/$CaCl_2$ (15/11.7/73.3 wt%) systems, respectively, over 10 CO_2 uptake cycles. Obviously, CaO dissolution/dispersion in the CaF_2/$CaCl_2$ system represents a feasible option to enhance the activity of CaO in long-term repeated CO_2 capture cycles. Notably, technical design and the selection of appropriate molten salt composition for dissolution or partial dissolution of the active sorbent are essential aspects in development of technologically and economically efficient CO_2 capture processes.

SAMMENDRAG

Hovedmålet ved kommersiell bruk av CO_2-fangstprosesser er å oppnå en effektiv sorpsjon av CO_2. Reaksjon mellom CaO og CO_2 ved høye temperaturer ("kalsiumlooping") er en av de mest lovende mulighetene til å redusere CO_2-konsentrasjonen i varme avgasser fra gasskraftverk eller andre industrielle prosesser. Hovedulempene med CaO-baserte materialer er at sorbentens overflatestruktur brytes ned under syklisk CO_2-fangst; denne nedbrytningen skjer ved at sorbenten sintrer, slites og reagerer med forurensninger i avgassen. For øyeblikket finnes det ingen kostnadseffektive prosessmodifikasjoner eller synteseteknikker som kan forsinke nedbrytningen for å unngå tap av CaO-baserte sorbenter i langvarige, repeterende sykluser med absorpsjon og desorpsjon av CO_2. For å gjøre denne teknologien attraktiv økonomisk, bør videre forskning fokusere på å utvikle en ny eller modifisert syntesemetode for å forbedre den langsiktige kjemiske og mekaniske stabiliteten til CaO-baserte materialer, eller på å utvikle en ny CO_2-fangstteknikk basert på kalsiumlooping.

Forskningen som er utført i forbindelse med denne avhandlingen er rettet mot en ny CO_2-fangstteknologi basert på kalsiumlooping, hvor CaO er oppløst (eller delvis oppløst) i en halogenid-saltsmelte. Bruken av en saltsmelte som løsemiddel eller dispersjonsvæske kan forbedre reaktiviteten mellom CO_2 og CaO, siden det vil være flere hurtige gass/væske-interaksjoner i saltsmelten. Transporten av væske-slurry fra CO_2-fangstenheten til CO_2-regenereringsenheten krever dessuten ikke like avansert teknologi som transport av faste CaO-baserte sorbenter, siden slurryen kan pumpes. Hovedhensikten med disse studiene var å undersøke og verifisere ideen om CO_2-fangst ved hjelp av kommersielt tilgjengelig CaO i metall-halogenid-saltsmelter.

Faseforholdene i systemene NaF-CaF_2, NaF-CaF_2-CaO, NaF-CaF_2-$CaCO_3$, NaF-CaF_2-$NaCO_3$ og NaF-CaF_2-Na_2CO_3-$CaCO_3$-systemene ble i hovedsak studert for å undersøke reaksjonene til CaO, $CaCO_3$ og Na_2CO_3 i en eutektiske blanding av NaF og CaF_2. I dette arbeidet ble fasediagramdata funnet ved termisk analyse, termodynamiske beregninger (FactSage) og røntgendiffraksjon (XRD) av bråkjølte prøver. De eksperimentelt utledede faselikevektene for systemet NaF-CaF_2 viste at fast CaO kan reagere med CO_2 ved de eutektiske sammensetgningen. Fasediagrammet til det ternære systemet CaO-NaF-CaF_2 viste at løseligheten av CaO er svært lav. Dataene for systemet $CaCO_3$-NaF/CaF_2 indikerer at $CaCO_3$ og NaF er Na_2CO_3 og CaF_2. Kartlegging av dette fasediagrammet med FactSage viste dessuten at det dannes $Na_2Ca(CO_3)_2$ (nyerereitt).

Fire forskjellige alkali- og jordalkalimetall-halogenidsaltsmelter ($CaCl_2$, CaF_2/NaF, CaF_2/LiF, og CaF_2/$CaCl_2$) ble brukt som løsemiddel for å oppløse eller dispergere CaO, med sikte på å finne den mest effektive prosessen for CO_2-fangst. For de binære blandingene ble det brukt eutektiske blandinger. Reaksjonen mellom CO_2 og CaO ble optimalisert ved å evaluere effekten av (1) vektprosent CaO i smelten, (2) systemets temperaturer ved karbonatiserings og dekarbonatiserings-reaksjonene, (3) CO_2-andelen i den simulerte syntesegassen, (4) avgassens strømningshastighet og (5) prøvens vekt. Disse testene og vurderingene av syklisk CO_2-fangst ble utført med en ettkammers reaktor, et FTIR massespektrometer til gassanalyser, samt røntgendiffraksjons-analyser (XRD) og gravimetri. Resultatene indikerer at de høyeste

verdiene for CO_2-bæreevnen er omkring 0.722–0.743 g CO_2/g CaO i systemet CaO-CaF_2/NaF. Dette skyldes at det termodynamisk stabile Na_2CO_3 ble dannet istedenfor $CaCO_3$, ved en ionebyttereaksjon. Tilsvarende høye konverteringsverdier for karbonatisering og dannelse av alkalimetallkarbonat ble observert for systemet CaO-CaF_2/LiF. Systematisk evaluering av temperaturen ved karbonatiseringsreaksjonen i dette systemet viste at sorbentens reaktivitet med CO_2 smelten var høyest ved 826–834 ºC. I tillegg ble sorbentens bæreevne delvis påvirket av CaO-konsentrasjonen i smelten, men ikke av CO_2-konsentrasjonen. Fullstendig dekomponering av karbonatene som ble dannet i smelten under ren nitrogen ble derimot ikke observert ved temperaturer i intervallet 994–1170 ºC.

Substansene som inngår i en industriell saltsmelte må være svært selektive for CO_2, ha en høy CO_2-bæreevne og god syklisk regenereringsytelse, samt være økonomisk fordelaktige. I de gjennomførte forsøkene ble derfor $CaCl_2$ og eutektisk $CaCl_2$/CaF_2 utnyttet som løsemiddel for oppløsning og dispergering av CaO og $CaCO_3$. I begge metallhalogenid-systemene viste det seg at en økning i CaO-andelen i saltsmelten fra 5 til 15 vekt% forbedret bæreevnen til sorbenten. Dersom CaO-innholdet overskred 15 vekt% ble konverteringen redusert, sannsynligvis på grunn av sedimentasjon og agglomerering av sorbenten. I CO_2-sorpsjonstestene ga systemet CaO-CaF_2/$CaCl_2$ mer effektivt CO_2-opptak enn systemet CaO-$CaCl_2$-systemet; sannsynligvis på grunn av den lavere liquidustemperaturen i det sistnevnte systemet, noe som tillater CaO-karbonatisering ved lavere temperatur (695–705 ºC). I systemet CaO-$CaCl_2$ ble karbonatisering utført ved 768–810 ºC.

Desorpsjon av CO_2 var uavhengig av karbonatiseringen, og forløp hurtig og fullstendig ved 904–950 ºC ved bobling med ren N_2. Fullstendig dekomponering av de dannete karbonatene ble demonstrert både under en CO_2/N_2-blanding, og under ren CO_2. Den mest stabile prosessen med CO_2-absorpsjon og desorpsjon ble oppnådd med 15 vekt% CaO i saltsmelten CaF_2/$CaCl_2$ (11.7/73.3 wt%). Ved forsøk med syklisk CO_2-absorpsjon og desorpsjon ble det oppnådd konstante bæreevner gjennom 10 sykluser, på henholdsvis 0.504 g CO_2/g CaO og 0.667 g CO_2/g CaO for CaO/$CaCl_2$-(5.32/94.68 wt%) og CaO/CaF_2/$CaCl_2$ (15/11.7/73.3 wt%). Oppløsning og dispersjon av CaO is systemet CaF_2/$CaCl_2$ er en åpenbar mulighet til å forbedre aktiviteten til CaO i langvarige, repeterende CO_2-fangstsykluser. Teknisk design og valg av en hensiktsmessig saltsmeltesammensetning for oppløsning eller delvis oppløsning av den aktive sorbenten er essensielle aspekter i utviklingen av teknologisk og økonomisk effektive CO_2-fangstprosesser.

ACKNOWLEDGMENTS

The journey leading to this thesis has been a great part of my academic experience. While reaching my goal, I have met wonderful people who have helped, supported, encouraged, and guided me throughout my research.

First of all, I gratefully acknowledge my advisor, Dr. Espen Olsen, for his professional guidance, patience, and support in academic endeavours. Above all, and most needed, he gave me the opportunity to determine carbon capture in the molten salt process. His advice in academic life and motivation helped me to manage the research leading to this thesis. I am very thankful that I was allowed to work so independently on developing a novel technological process, including freedom to make my own decisions.

In addition, I am especially grateful to Asbjørn Solheim for his valuable advice in research discussions, supervision of the phase diagram analyses, and crucial contributions to this thesis. I am indebted to him for support in the part of the research performed at the Materials and Chemistry Laboratory (SINTEF) in Trondheim. I also thank Dr. Bjarte Øye for help with the simulation of phase diagrams (FactSage).

I thank the Research Council of Norway through the CLIMIT Research Programme for funding. My gratitude also goes to Arne Svendsen and Tom Ringstad for technical support in developing the experimental setup and the data collection system. Furthermore, I am grateful to other members of the IMT Energy laboratory team for all contributions to this research, and for the generous support and advice provided by the administrative staff at IMT: Marianne Skjervold, Anita H. Habbestad, Tone Rasmussen, Mona V. Kristiansen, and Ingunn Burud.

It is also a pleasure to thank all the present and former members of the Sol–Gel chemistry group at Vilnius University for giving me the opportunity to obtain extensive knowledge about academic and social life. I appreciate all of you, particularly Professors Aivaras Kareiva and Aldona Beganskiene, and Dr. Simas Sakirzanovas for performing the XRD spectral analyses in this work.

I am sincerely grateful to Arne for his understanding, tolerance, and patience, and most importantly for encouraging me to believe in my abilities. You gave me many special moments during the final years of my PhD studies. I also want to thank all my friends, especially Audra, for support and understanding, and just for being with me through both the best and the most difficult moments of my life.

Finally, and most importantly, I want to thank my dear family. I am so grateful to my father Mecislovas and my mother Jadvyga for their faith in me and for allowing me to be as ambitious as I wanted. To my sister Erika and my brother Arvydas, I appreciate your inspiration, motivation, enthusiasm, and moral and emotional support, which I needed over this period.

CONTENTS

LIST OF PAPERS

Paper I

Viktorija Tomkute, Asbjørn Solheim, Simas Sakirzanovas, Bjarte Øye and Espen Olsen. Phase equilibria evaluation for CO_2 Capture: CaO-CaF_2-NaF, $CaCO_3$-NaF-CaF_2, and Na_2CO_3-CaF_2-NaF. Submitted to *Journal of Chemical & Engineering Data*.

Paper II

Viktorija Tomkute, Asbjørn Solheim, Simas Sakirzanovas and Espen Olsen. A Novel CO_2 Separation Process Using CaO in Molten CaF_2/NaF. Submitted to *Environmental Science & Technology*.

Paper III

Viktorija Tomkute, Asbjørn Solheim and Espen Olsen. Investigation of high-temperature CO_2 capture by CaO in $CaCl_2$ molten salt. *Energy & Fuels* 27 (2013) 5373–5379.

Paper IV

Viktorija Tomkute, Asbjørn Solheim and Espen Olsen. A New Optimized Process for CO_2 Capture by CaO in a CaF_2/$CaCl_2$ System. (Manuscript).

Paper V

Espen Olsen and **Viktorija Tomkute**. Carbon Capture in Molten Salts. *Energy Science & Engineering* 1 (2013) 144–150.

ABBREVIATIONS

A-B/C	A compound in B/C at a fixed eutectic composition ratio
BET	specific surface area (Brunauer-Emmett-Teller method)
CAP	chilled ammonia process
CCS	carbon capture and storage
CLC	chemical looping combustion
CFBR	circulating fluidized bed reactor
EOR	enhanced oil recovery
FBR	fluidized bed reactor
FSP	flame spray pyrolysis
FTIR	Fourier transform infrared spectroscopy
IGCC	integrated gasification combined cycle
IL	ionic liquid
IPCC	Intergovernmental Panel on Climate Change
MCFC	molten carbonate fuel cell
MEA	monoethanolamine
MFM	mass flow meter
MOF	metal-organic framework system
NG	natural gas
NGCC	natural gas combined cycle
OECD	organization for Economic Cooperation and Development
PC	pulverized coal
PCC	precipitated calcium carbonate
SCPC	supercritical pulverized coal
SI	supporting information
TA	thermal analysis
TGA	thermogravimetric analysis

USCPC	ultra-supercritical pulverized coal
XRD	X-ray diffraction
ZIF	zeolitic imidazole framework system

1.0 INTRODUCTION

The increasing global energy demand may be related to the growing number of all types of technological processes and the significant rise in the world's population. Escalating consumption of electricity leads to more extensive emission of pollutants, such as CO_2, CH_4, NO_x, SO_x, HCl, HF, and particulate matter, and this has severe consequences for biodiversity and the environment.[1-5] Climate models used in assessments performed by the Intergovernmental Panel on Climate Change (IPCC) have concluded that the emissions of greenhouse gasses will increase the average global temperature by 1.1 to 6.4 ºC by the end of the 21st century.[6] An increase of more than 2 ºC will lead to serious environmental and social consequences of global warming, and thus the IPCC has asserted that global greenhouse gas (GHG) emissions must be decreased by 50 % to 80 % by 2050.[6,7] A major cause of global warming is related to the rapid rise in anthropogenic carbon dioxide emissions from energy production and other industrial processes (e.g., production of chemicals, ethanol, fertilizers, hydrogen, cement, iron, and steel).[4,8] Therefore, it is essential that electricity and other products be generated with pollution-free methods, high round-trip efficiency, and flexible power and energy, all of which have a pronounced impact on the sustainable development of world economics and ecology.

There are many strategies aimed at significantly reducing CO_2 emissions from the global energy sector, and the following are most important[7]:

1. Energy conservation and efficiency.
2. Implementation of carbon capture and storage (CCS) in the industrial processes.
3. Use of renewable energy.

CO_2 emissions related to wasteful energy use can be minimized by increasing energy efficiency and conservation, which can be achieved by using new advanced power technology designs aimed at promoting development of sustainable global economics and ecology. If a country's economic situation is not sufficiently well structured to prioritize the implementation of more expensive modern technologies, the emissions of CO_2 will not be reduced. As mentioned above, generating energy in a renewable manner can markedly diminish emissions of greenhouse gases and other pollutants. Systems for such production are based on natural energy sources like hydropower, ocean (wave) energy, wind energy, direct solar energy, bioenergy, and geothermal energy, which are used separately or in integrated operations. However, the main issues in realization of large-scale renewable power plants are related to cost efficiency, which is associated with advances in technology, environmental/economic factors, and land use conflicts.[9] At present, electricity produced by renewable power plants is more expensive than that generated at fossil fuel or nuclear energy plants.[3] Also, it is impossible to quickly and easily reduce large CO_2 emissions simply by increasing energy efficiency and conserving or replacing fossil fuels with alternative energy sources that entail very low or no emission of pollutants. The global energy sector today depends on electricity generated chiefly (81%) from carbon-based resources such as coal, oil, and natural gas, which accounts for approximately two-thirds of all CO_2 emissions.[7]

Accordingly, implementation of large-scale CCS technology in production of power, cement, and hydrogen might make a noticeable contribution to reaching ambitious climate protection goals.[3,10,11]

CCS technology relies on separation of CO_2 from the waste gas generated by stationary emission sources, and subsequent concentration into a stream of pure CO_2 for transport to a storage site. The capture stage is much more complex than the transport and storage stages, and it also represents the major part of the total CCS process, with costs values in the range of 24–52 EUR/ton CO_2 captured.[12] Hence it is essential to improve the cost structure and efficiency of CO_2 capture.

Currently, there is no single option that can resolve the challenges that confront CO_2 capture systems, and thus it may be necessary to integrate many different technologies. The selection of materials for CO_2 separation depends on the particular technology (e.g., the stage at which CO_2 removal should occur). In this context, flue gas composition (e.g., CO_2 partial pressure and the effects of impurities on the activity of the sorbent) and the need for long-term stability can to a greater or lesser extent constitute a problem when selecting the sorbent material for CO_2 separation in power production or other industrial processes.[13] Nevertheless, the material to be used as the sorbent should have the following main characteristics: high CO_2 selectivity, a substantial carrying capacity, adequate sorption and desorption kinetics, pronounced chemical and mechanical stability throughout the cyclic operation, a low environmental impact, and low cost for purchase and operation.

There is growing interest in use of solid sorbents in CO_2 capture technology, because compounds have a high capacity for binding CO_2, and they can be carbonated in a wide temperature range from ambient[14] to 1000 ºC.[15] For example, high-temperature (> 400 ºC) CO_2 sorbents such as alkali ceramics and those based on CaO undergo textural degradation during performance of carbonation/decarbonation.[1] Some zeolites, zeolitic imidazole frameworks (ZIF), and metal–organic frameworks (MOFs) function well at low temperatures (< 200 ºC) and show high stability and capacity for CO_2 capture, but the cost of those sorbents is usually too high to permit use in large amounts.[16] Another option to create low-temperature CO_2 sorbents is to use carbon-based materials, which are cheap, abundant, and thermally and chemically stable, and can be improved by grafting functional amine groups to the carbon atoms. However, it is well known that amine-based sorbents have the major disadvantages of being expensive, corrosive in nature, and subject to oxidative/thermal degradation, and they also react with the other impurities present in the flue gas (e.g., NO_x, SO_x, HCl, HF, and particulate matter).[17] Therefore, ionic liquids (ILs) have been proposed as a “next generation” solvent technology for CO_2 capture. ILs are salt materials that are in liquid phase below 100 ºC, have low vapour pressure, and can react with CO_2 at high temperatures with a rather low energy regeneration penalty.[18] In addition, it may be possible to use ILs in multi-pollutant removal processes, such as integration of SO_2 co-capture with CO_2 capture.[19] Preparation and purification of ILs are complex and expensive operations, which means that application of these liquids in large-scale CO_2 absorption processes would be costly.[3] Therefore, future research should focus on improving the stability and use of both solid and liquid sorbent materials, and developing new materials for this purpose. Furthermore, for commercial applications, the CO_2 capture technologies must be carefully developed and established to

achieve integration in realistic processes, for example, including pilot-scale testing of modified solid sorbents, alternative chemical solvents, membranes, and other well-tested materials. A significant number of pilot-scale CO_2 capture systems are already under construction or in operation, but, before direct integration with power plants or industrial processes can be possible, it will also be necessary to make considerable improvements in the use of amine-based solvents, CaO-based sorbents, and membrane or chemical looping systems.

2.0 MOTIVATION AND OBJECTIVES

The present research activities were focused on evaluating the new and untested methodology entailing physico-chemical absorption/desorption of CO_2 by CaO dissolved or partly dissolved in molten halide salt systems. Sorbents based on calcium oxide have now been accepted as the most economically and environmentally attractive high-temperature solid sorbents for CO_2 capture. The reason for this is that these materials are inexpensive and readily available in nature (in the form of limestone and dolomite minerals), they have a high CO_2 carrying capacity and low toxicity. Moreover, they can be integrated in the cement industry, because they are associated with low specific energy consumption and do not require the complex process of flue gas treatment.[20] However, many investigations have demonstrated that the CO_2 capture capacity of limestone and dolomite decreases with an increasing number of carbonation/decarbonation cycles.[5] Various methods to delay or prevent attrition and sintering of the CaO-based sorbents have led to some improvements, such as increased thermal and mechanical stability of synthesized modified materials, but no economically attractive modification techniques have yet been successful in completely eliminating the problems associated with long-term decay related to carbonation conversion.[2,21]

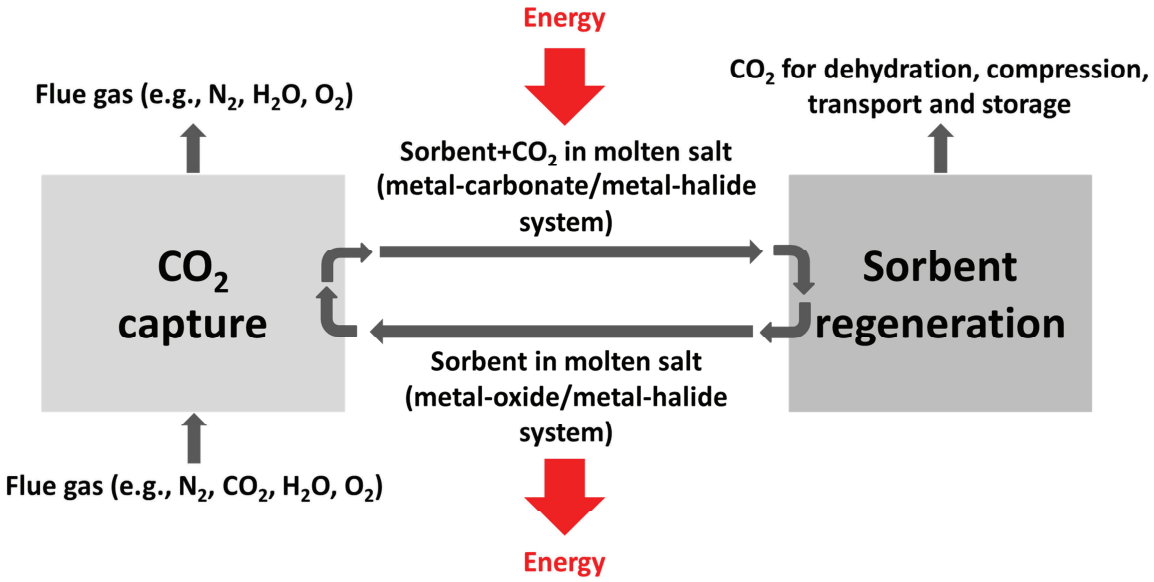

Figure 2.1. Schematic diagram of CO_2 capture by metal oxides in molten salts.

Molten halide salts may function as solvents or as a matrix for dispersion of solid sorbent particles due to some of their unique properties, including the following[22,23]: high electrical conductivity, decomposition potentials, and resistance to radiation; low vapour pressure; a manageable melting point and good heat transfer characteristics. The dissolution and/or dispersion of CaO in the molten salt matrix may increase the reactivity of the sorbent with CO_2 by causing more rapid gas–liquid interactions in the molten salt. Figure 2.1 presents a general schematic diagram of CO_2 capture by metal oxides in molten metal halide systems

based on solvent/sorbent capture technology. In this case, metal oxides are dissolved or partly dissolved in molten salt in a CO_2 capture unit, where the carbonation of the sorbent may take place. Consequently, the formed carbonates may be transported to a regenerator unit for desorption of the absorbed CO_2 and regeneration of the sorbent to enable continuous performance of the capture process. In this type of system, facilitating transport of the liquid–slurry from the carbonation unit to the sites of decarbonation and gas–liquid reactions might reduce the final cost of total CO_2 capture technology by CaO-based sorbents. Therefore, the main objective of the present research was to improve reactivity of CaO with CO_2 at high temperatures by dissolution or dispersion of the sorbent in molten halide salts, such as $CaCl_2$, CaF_2/NaF, CaF_2/LiF, and CaF_2/$CaCl_2$ systems. Parametric and cyclic studies were conducted to develop and verify the most efficient conditions for absorption/desorption of CO_2 by CaO in various metal halides when using a thermal swing method. The purpose of this work was to carry out carbonation/decarbonation tests using a fully automated one-chamber atmospheric pressure reactor, a Fourier transform infrared (FT-IR) gas detector, and gravimetric and X-ray diffraction (XRD) measurements. Another aim was to investigate the partial phase diagrams for the NaF-CaF_2, NaF-CaF_2-CaO, NaF-CaF_2-$CaCO_3$, NaF-CaF_2-$NaCO_3$, and NaF-CaF_2-Na_2CO_3-$CaCO_3$ systems by thermal analysis (TA), thermodynamic calculations (FactSage), and XRD assessment of quenched samples to ascertain how the phase transitions in molten halide salts affect CO_2 uptake characteristics and thereby enable development of a novel CO_2 capture technology.

The specific goals of the present research were as follows:

- To evaluate the phase transitions of CaO, $CaCO_3$, and Na_2CO_3 in the eutectic composition of NaF/CaF_2 (**Paper I**).
- To design and verify an experimental set up for studying the CO_2 capture mechanism of CaO dissolved/dispersed in molten salts at a fixed eutectic composition ratio (**Papers II–V**).
- To apply CaF_2/NaF (41.85/48.15 wt%) and $CaCl_2$ and CaF_2/$CaCl_2$ (13.8/86.2 wt%) melts as solvents for dissolution or partial dissolution of CaO in the carbonation and decarbonation reactions of the system (**Papers II–V**).
- To determine the optimal temperature for the carbonation/decarbonation of CaO/$CaCO_3$/Na_2CO_3 dissolved or partly dissolved in the melt (**Papers II–IV**).
- To elucidate the impact of the mass proportion of CaO in the melt on CO_2 uptake behaviour (**Papers II–IV**).
- To study the effect of the concentration of CO_2 in N_2 and the flow rate of simulated flue gas on the carrying capacity of the sorbent (**Papers II–IV**).
- To perform XRD analyses on quenched samples (**Papers I, II and V**).
- To investigate the influence of the weight of samples on the reactivity of CaO and CO_2 (**Paper III**).

- To demonstrate the possibility of regenerating CaO from the $CaCO_3$ formed in $CaCl_2$ under a stream of pure CO_2 (**Paper III**).

- To compare CO_2 capture capacities achieved in experiments using specific $CaO/CaF_2/NaF$ (10/41.8/48.2 wt%), $CaO/CaF_2/LiF$ (10/38/52 wt%), and $CaO/CaCl_2$ (5.3/94.7 wt%) systems **(Paper V)**.

- To demonstrate the characteristics of cyclic CO_2 sorption, which was considered to be one of the most important objectives of the research (**Papers III and IV**).

3.0 LITERATURE OVERVIEW

3.1 CCS technology

The integration of CCS technology in heavily CO_2-emitting industrial processes such as production of power (using fossil fuels or biomass), steel, cement, and hydrogen can contribute substantially to reducing anthropogenic release of CO_2. The concept of this technology is that CO_2 produced from carbon-based materials (e.g., coal, oil, natural gas, and biomass) used in power and industrial processes is first captured from gas point sources and then compressed to a dense supercritical fluid that is transported to facilities offering viable storage solutions (Figure 3.1). At present, pipelines represent the most economically attractive and reliable option for transport of dense CO_2[12], and this strategy is already a reality and has been used primarily in enhanced oil recovery (EOR) reservoirs. Notwithstanding, CO_2 transport by tanker is an effective method when the gas has to be shipped over large distances or to overseas locations. The dominant CO_2 storage options are injection in deep saline aquifers, deposition in depleted oil/gas reservoirs, and re-use in hydrocarbon production via an EOR process.[7] Transport and storage of CO_2 are relatively straightforward, and the fundamental challenges in this context are connected with characteristics of the storage location, safety distances for CO_2 pipelines, risk assessments, and public involvement/communication.[4] It is well known that the CO_2 capture stage represents the major portion of the total cost of CCS, and hence it is considered essential to improve the techno-economic structure and efficiency of CO_2 capture by employing pollution-free technological operation.[12]

3.2 Power and industrial plants with CO_2 capture

The CO_2 capture approaches applicable in power generation stations are based on three different technological processes: post-combustion (low pressure, predominantly CO_2/N_2 separation), pre-combustion (high pressure, chiefly CO_2/H_2 separation), and oxyfuel combustion (high pressure, mainly O_2/N_2 separation). Figure 3.2 outlines the technical concepts for processing of CO_2 in carbon-based power plants and industrial processes. In each CO_2 capture strategy, the selection of fuel or raw material and process scheme affects the total cost of the technology.[5,24] Table 3.1 outlines CO_2 concentration and pressure in relation to the CO_2 capture strategy and fuel type applied.[24] In pre-combustion, the release of CO_2 is significantly lower with natural gas as fuel (CO_2 concentrations in the range 15–25 mole %) than with coal synthesis gases (after water gas shift, CO_2 30–45 mole %). However, post-combustion of natural gas/flue gas typically yields 3–4 mole % CO_2, and the partial pressure of CO_2 is close to 0.1 atm, whereas the pressure of pre-combustion synthesis gases varies between 25 and 70 bar. The oxy-combustion route reuses CO_2 and H_2O to control combustor temperature; the composition of CO_2 and H_2O depends on fuel type and can contain from 75 up to 90 mole % of CO_2 after water removal, and the pressure is close to 1 atm. All of these processes release other pollutants (e.g., NO_x, NH_3, SO_x, H_2S, HCl, HF, and particulate matter), the concentrations of which depend on the type of fuel/material used in the process.

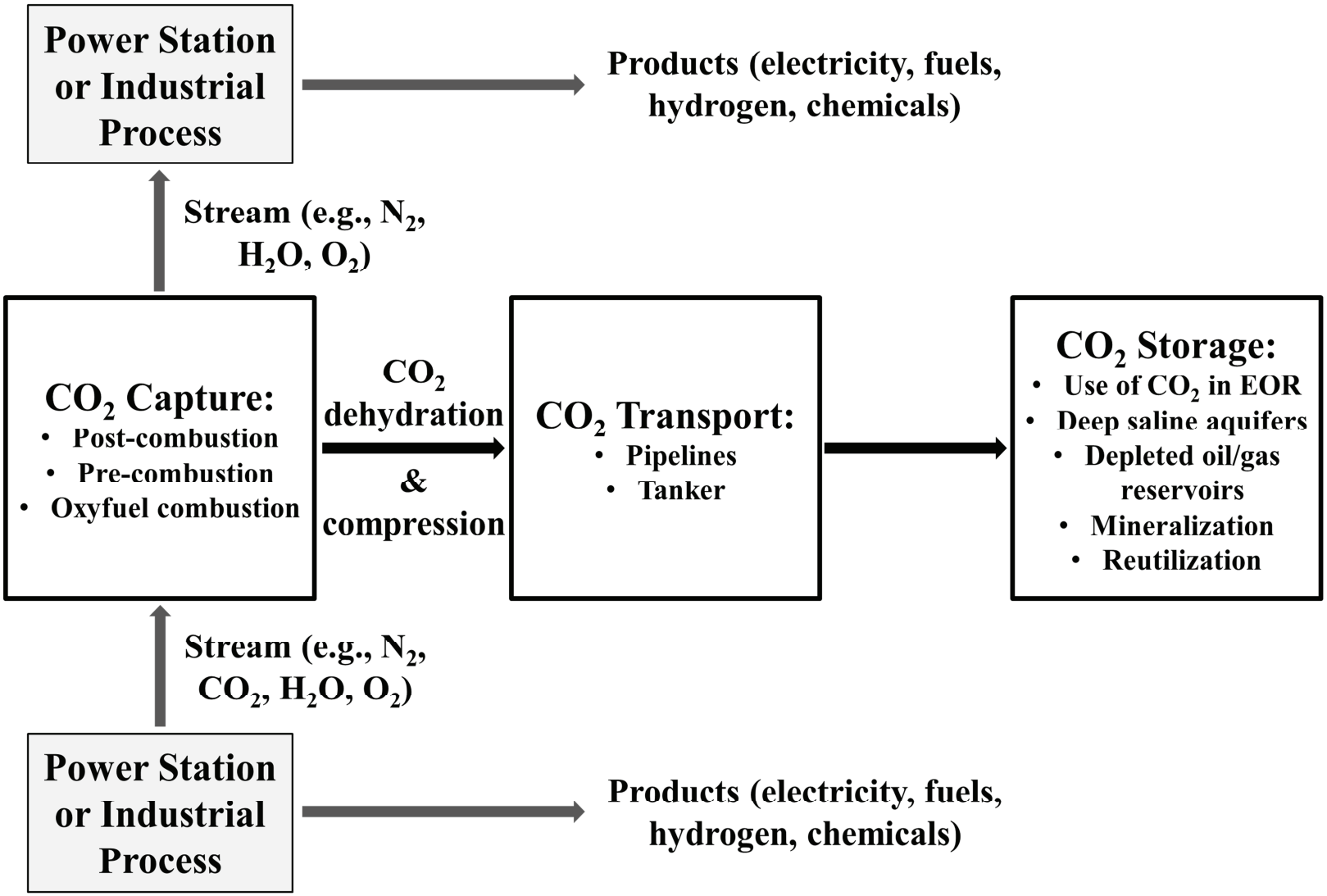

Figure 3.1. General diagram of different technical options in CO_2 capture, transport, and storage. EOR = enhanced oil recovery.

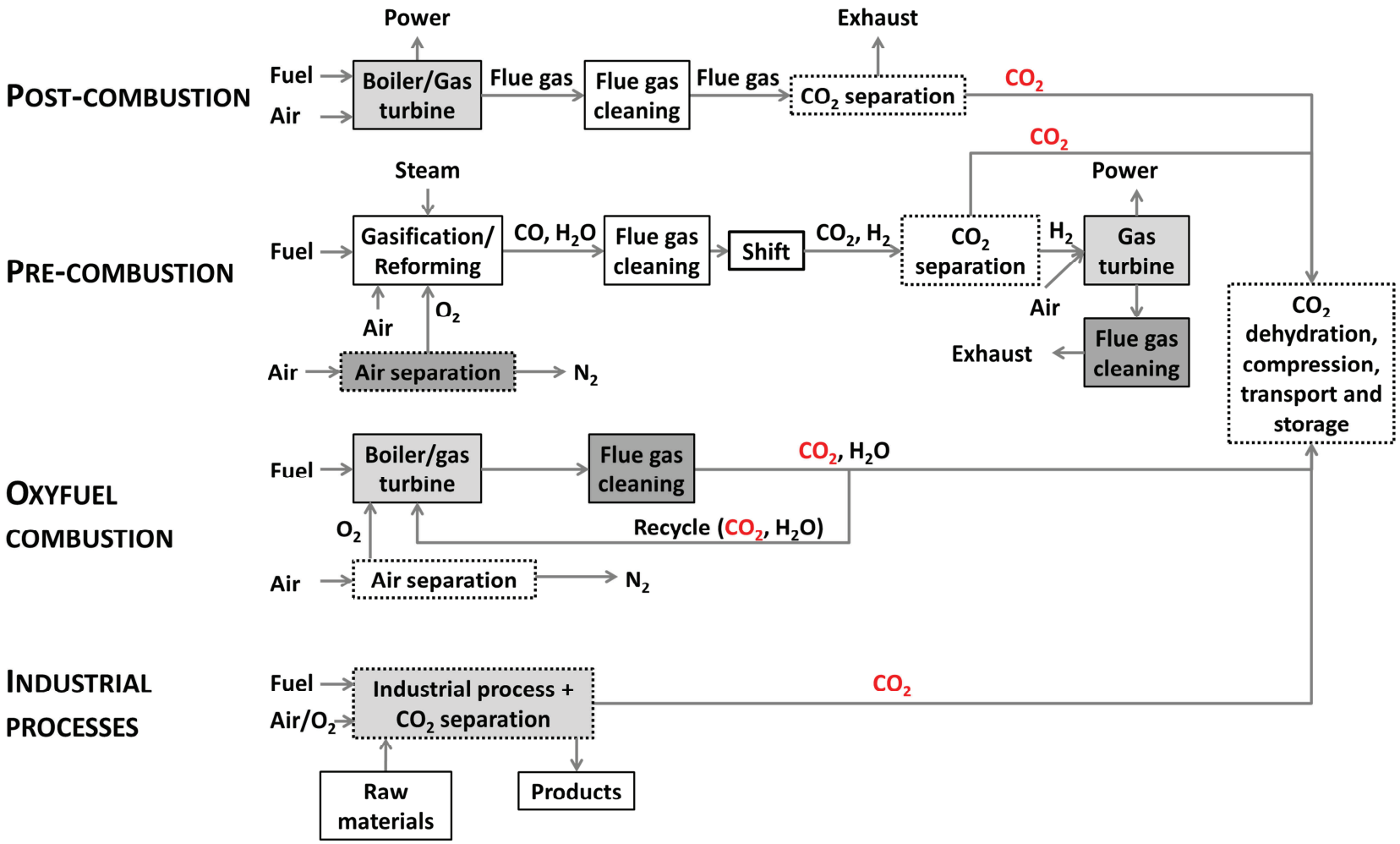

Figure 3.2. Overview of capture of CO_2 at power generation stations and in industrial processes. Light grey boxes indicate generation of power or other industrial products; boxes with dotted borders signify processes with a major impact on generation efficiency[8]; dark grey boxes denote optional technological processes.

For example, flue gas from combustion of pulverized coal can contain 10–55 mole % of SO_2 and 10–20 mole % of NO_x gas.[8] Therefore, when selecting CO_2 capture technology, in some cases it is important to include other techniques for removal of flue gas impurities.

Table 3.1. Typical or estimated CO_2 content in flue gas and CO_2 partial pressure for pre-combustion, post-combustion, and oxyfuel combustion.[8,24-26]

Capture technology	CO_2, mole %			CO_2 partial pressure, bar	Capture efficiency, %		
	IGCC	NG	PC		IGCC	NG	PC
Pre-combustion	30–45	15–20	–	25–70	85–90	85~100	–
Post-combustion	–	3–4*	12-15	~ 1	–	85–90*	85–90
Oxyfuel combustion	2–19^	60–85	60–90	~ 1	50–100^	50–100	90~100

Abbreviations: IGCC, integrated gasification combined cycle; NG, natural gas; PC, pulverized coal; NGCC*, natural gas combined cycle; GC^, gas cycles.

3.3 CO_2 separation and capture methods

The diverse strategies for CO_2 capture in power production plants and other industries are based on the major CO_2 gas separation methods: absorption[3,27-29], adsorption[1-3,10,30,31], cryogenic distillation, gas separation with membranes[1,30,32,33] and microbial/algal systems (Figure 3.3)[25,34-36]. When choosing a CO_2 capture strategy to be applied in generation of power or other industrial processes which is optimal with regard to energy and economic costs, it is important to specify the purity of the final product and the parameters of the stream/raw material treatment (e.g., temperature, pressure, concentration, the level of impurities). For example, CO_2 capture systems that are already available additionally contains gas cleaning technique that removes impurities from flue gas originating from natural gas or coal used in the production of ammonia, hydrogen, and other chemicals.[35] The separated CO_2 gas is usually vented to the atmosphere or used in the manufacture of other products.[12,25]

To be suitable for commercial use, CO_2-reducing technologies must be carefully developed and well tested. There are numerous methods that can be applied to CCS activities for post-combustion capture of CO_2 (Figure 3.3). However, as of yet, few of those techniques have been considered appropriate for use in large-scale processes such as those involving amine-based solvents, physical solvents, calcium looping technology, or cryogenic oxygen separation for oxyfuel combustion.[34-37]

3.4.1 Process using amine-based solvents

For more than 80 years, amine solutions have been used to capture CO_2 from concentrated CO_2 streams, and they are now regarded as one of the most suitable technologies for

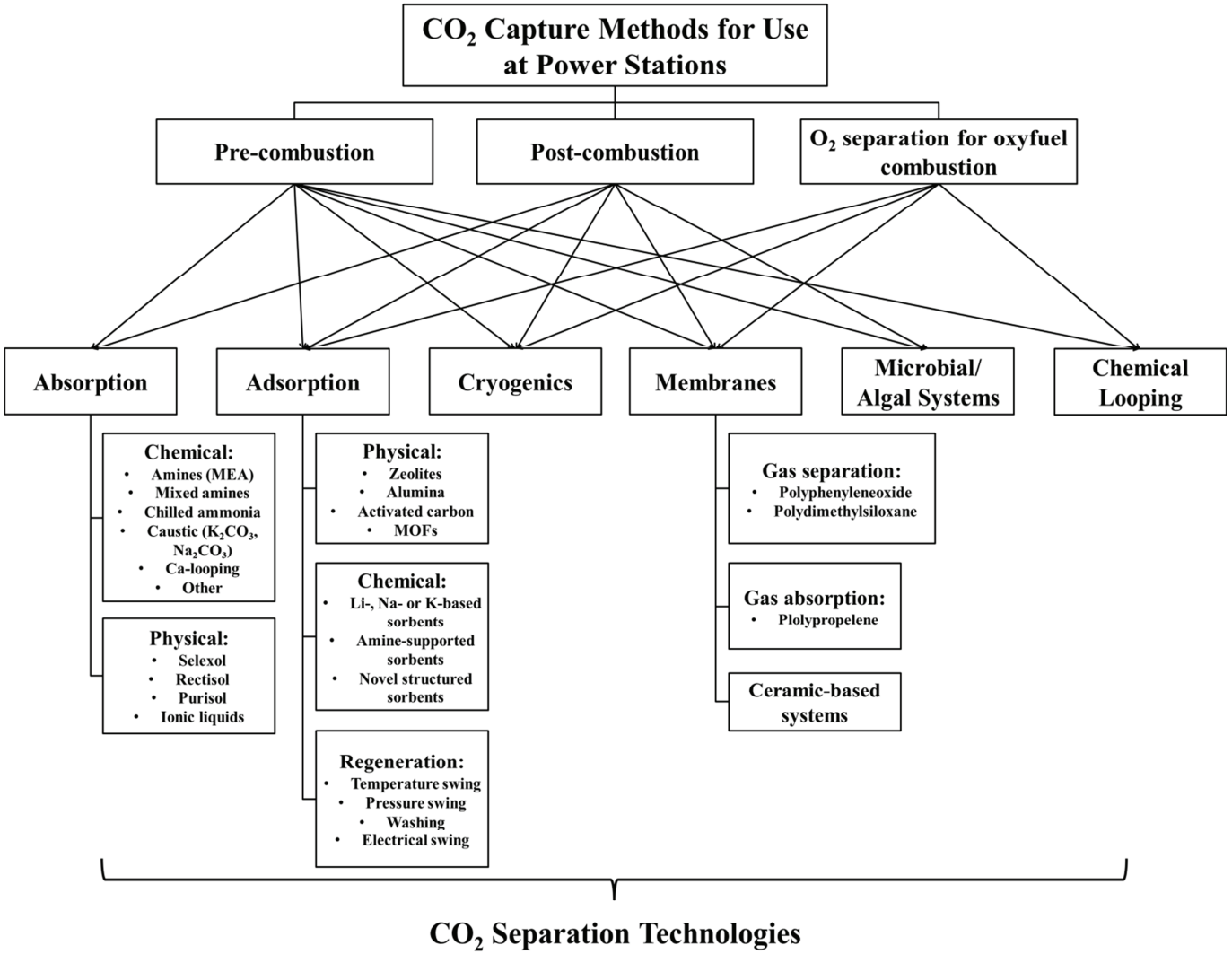

Figure 3.3. Technical gas separation options for CO_2 capture processes.[25,38]

commercial applications.[3,35] The screened absorbents that are frequently used in post-combustion CO_2 capture are 25–40 wt% aqueous solutions containing monoethanolamine (MEA) and diethanolamine (DEA), which react with CO_2 at 20–50 ºC to form carbamates and bicarbonates.[27-29] Stripping of CO_2 can be accomplished by thermal desorption of CO_2 at 100–110 ºC, and this can constitute approximately 70% of the total operational costs of a full-scale CO_2 capture plant.[35] Lee et al.[39] have demonstrated that solutions of primary amines exhibited the most efficient CO_2 removal at a load of 2 tons of CO_2 per day in a pilot plant. However, CO_2 uptake technology based on amine solutions is connected with many challenges related to the following aspects: cost, corrosiveness, oxidative/thermal degradation of the amines, and the reaction of amines with other pollutants in the flue gases, such as typical acid gases (NO_x, SO_x, HCl, and HF) and particulate matter.[17]

3.4.2 Process using chilled ammonia

A CO_2 absorption technology based on a chilled ammonia process (CAP) shows good promise in lowering the energy requirements in the CO_2 removal stage (carbonation temperature 0–20 ºC).[12,40] Products of the reaction of CO_2 with ammonia include ammonium carbonate and bicarbonate precipitates, which decompose at 100–200 ºC.[40] Estimations indicate that CAP should cost 60% less than the MEA process, but the flue gas from the former requires numerous pretreatments, such as oxidation of SO_2 to SO_3, and NO to NO_2. Also, the cleaning of exhaust gas from the emission of ammonia must be considered.[28,35]

3.4.3 Process using cryogenic separation

Although the oxyfuel combustion process is not a CO_2 capture technology, it is used for gas separation. This process requires denitrification of the atmosphere in the system to enable combustion of the fuel under pure O_2, which yields an exhaust gas consisting only of concentrated CO_2 and water vapour (can be used in boilers and gas turbines and applied extensively in the power industry).[25,41,42] Therefore, an oxy-combustor must be supplied with substantial quantities of pure O_2, which can be generated by a large-scale air separator, such as cryogenic air separation units or membranes. Equipment of that type that is currently available for air denitrification is not economically efficient in the oxyfuel combustion process.[42,43] Consequently, further development of this technology should focus on improvement and investigation of oxygen separation methods. Also, recycling of the flue gases for combustor temperature control makes oxyfuel combustion more cost effective.[34] Other challenges that are related to this combustion technology are fouling, corrosion, slagging, changes in the chemical composition of the fly ash, and leakages.[25]

3.4.4 Process using potassium- and sodium-based sorbents

An alternative method of CO_2 removal involves use of inorganic sorbents, such as hydroxides of the alkali and alkaline earth metals. A column system packed with this type of sorbent solution has been used in industries as a wet scrubbing technique to remove acidic gases from the product stream[44,45], and this method can be applied to both pre- and post-combustion CO_2 capture.[5] A number of research projects have demonstrated the solubility of CO_2 in aqueous

alkaline absorbent solutions with low CO_2 desorption requirements and slow reaction rates. Currently, interest is being focused primarily on sodium hydroxide solution, which has a high pH value that gives good selectivity for CO_2 at room temperature.[45-47] The reaction of CO_2 with NaOH leads to formation of dissolved Na_2CO_3, as shown in Equation 1.[47]

$$2NaOH(aq) + CO_2(g) \leftrightarrow Na_2CO_3(aq) + H_2O(l), \Delta H^0 = -109.4 \frac{kJ}{mol} \quad (1)$$

The production of Na_2CO_3 during the absorption process is simple, slow, and economically attractive, whereas the regeneration process is not cost effective because it requires water evaporation and thermal/pressure swing decomposition of Na_2CO_3.[11,44]. This decomposition can be achieved by performing conventional "causticization" or "caustic recovery" that to remove carbonate ions from the solution by using $Ca(OH)_2$ to precipitate $CaCO_3$ (Eq. 2).[48] Thereafter, $CaCO_3$ can be converted back to solid CaO and a pure stream of < 90 vol% CO_2 (Eq. 3) by thermal/pressure swing desorption, and finally CaO can be hydrated to form $Ca(OH)_2$ (Eq. 4).[3]

$$Na_2CO_3(aq) + Ca(OH)_2(s) \leftrightarrow 2NaOH(aq) + CaCO_3(s),\ \Delta H^0 = -5.3 \frac{kJ}{mol} \quad (2)$$

$$CaO(s) + CO_2(g) \leftrightarrow CaCO_3(s),\ \Delta H^0 = +179.2 \frac{kJ}{mol} \quad (3)$$

$$CaO(s) + H_2O(l) \leftrightarrow Ca(OH)_2(s),\ \Delta H^0 = -64.5 \frac{kJ}{mol} \quad (4)$$

Another method of Na_2CO_3 recovery is to use non-conventional causticization technology that is based on addition of a metal oxide (Me_xO_y) or salt in Na_2CO_3 solution.[48,49] A study assessing this technique suggested that initially $Na_2Me_xO_{y+1}$ and CO_2 gas is formed during the reaction between Na_2CO_3 and metal oxide (Me_xO_y), after which NaOH can be generated by dissolving $Na_2Me_xO_{y+1}$ in water.[3]

Dry inorganic chemical adsorbents such as K_2CO_3 and Na_2CO_3 have been tested in CO_2 removal processes, because they are inexpensive and have low energy requirements and a good CO_2 sorption capacity.[14,50-53] This technology itself is not corrosive and does not result in emissions of secondary pollutants.[54] CO_2 uptake characteristics have been investigated in the presence of water at 60 ºC, using K_2CO_3 as active material and activated carbon (AC), Al_2O_3, and MgO as support materials.[14,53-56] The results showed that K_2CO_3 promoted sorption of CO_2 on the AC and TiO_2, which led to formation of $KHCO_3$ that subsequently decomposed back to K_2CO_3 and CO_2, and this process was fast and complete at 150 ºC.[53] However, other researchers [14] have observed that a composite of 30 wt% K_2CO_3 in MgO produced by wet chemistry exhibited the most efficient carrying capacity of 0.197 g CO_2/g K_2CO_3/MgO, and that study also showed that, during the reaction with CO_2, K_2CO_3/Al_2O_3 and K_2CO_3/MgO produced various carbonates, such as $KAl(CO_3)_2(OH)_2$, $K_2Mg(CO_3)_2$ and $K_2Mg(CO_3)_2 \bullet 4(H_2O)$. These complex carbonates affect the efficiency of regeneration, and thus they are not fully decomposed back to the K_2CO_3 phase.[53] Two recent investigations also evaluated CO_2 uptake by Na_2CO_3-based sorbents on MgO[57] and Al_2O_3[58] supports. In one of

those studies[57], sorption tests using Na_2CO_3–MgO showed that a double salt ($Na_2Mg(CO_3)_2$) was generated during the carbonation step, and that the CO_2 capture capacity decreased to 15 % of the initial capacity after only eight carbonation/decarbonation cycles. In the other study[58], performance of 150 CO_2 sorption cycles 35wt% Na_2CO_3 in γ-Al_2O_3 resulted in a residual carrying capacity of about 0.14 g CO_2/g Na_2CO_3. The carrying capacities of these composites are relatively low for commercial applications, hence it is important to establish novel adsorbents that have good selectivity for CO_2 and a high capture capacity, and can also achieve fast, easy, and repeatable operation.

3.4.5 Calcium looping technology

Alkaline earth metal oxides are used as CO_2 sorbents due to their high CO_2 capture capacity: theoretically, 1 mole of metal oxide should react chemically with 1 mole of CO_2 to form a metal carbonate. Furthermore, materials based on calcium oxide have been accepted as the most attractive CO_2 capture agents for industrial application, because, of all the naturally occurring alkaline earth metal oxides, CaO is the most abundant (limestone and dolomite minerals), and it has low toxicity and a high CO_2 carrying capacity.[21,59,60] The process generally known as carbonate or calcium looping is based on the gas–solid exothermic reaction between CaO and CO_2 that yields calcium carbonate ($CaCO_3$), which can be decomposed (endothermically) by the thermal or the pressure swing method (Eq. 3).

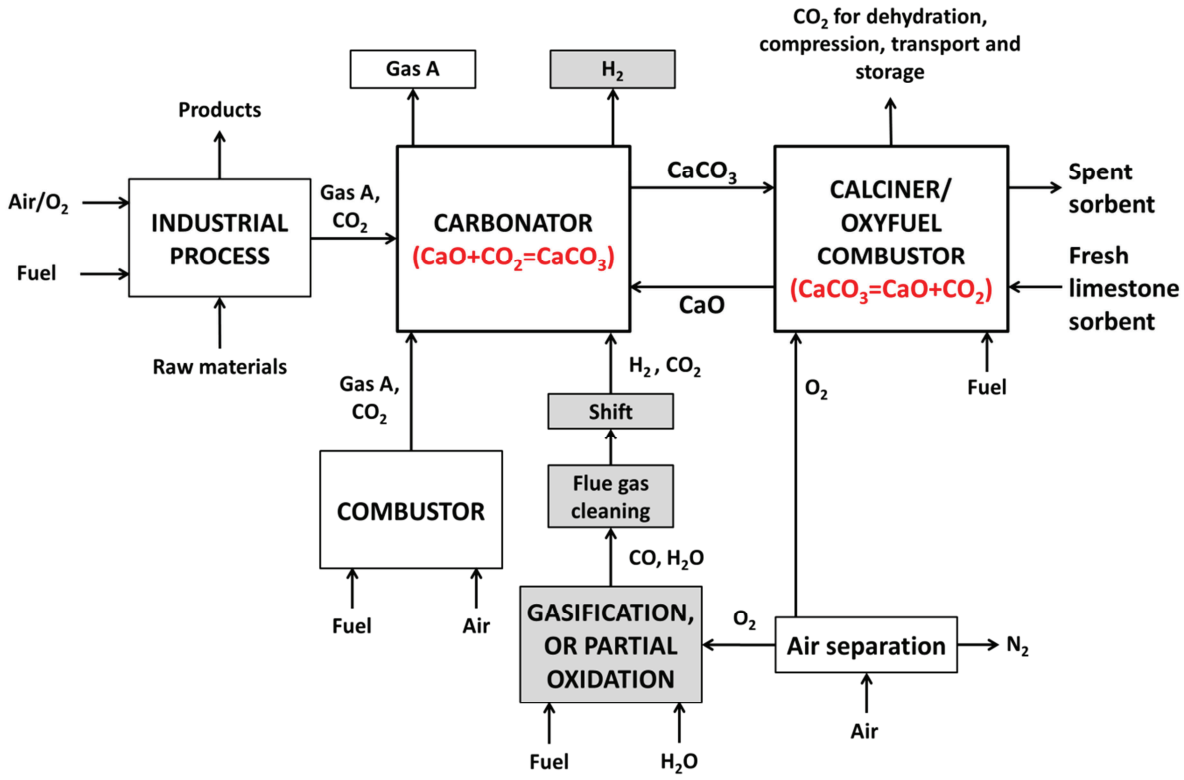

Figure 3.4. Schematic diagram of calcium looping technology integrated with chemical looping combustion (CLC) as an application for removal of CO_2 from post-combustion, pre-combustion (grey boxes), and industrial processes. Such CO_2 capture is done using two interconnected units: a carbonator and a calciner.

The general setup of calcium looping technology consists of two reactors (a carbonator and a calciner)[61] that are interconnected to enable continuous CO_2 capture. Figure 3.4 illustrates a flow diagram of a simplified system comprising $CaO/CaCO_3$ integrated with chemical looping combustion (CLC) that can be used to recover CO_2 from post-combustion, pre-combustion, and industrial processes.[20] All applications using the calcium looping cycle operate on similar principles. The reaction of a CaO-based sorbent with CO_2 occurs in the carbonator unit at > 850 ºC (~1 atm). It has been demonstrated that carbonation of CaO is a two-phase reaction: initially, CaO undergoes rapid chemical reaction with CO_2, and then a slower step occurs that is induced by CO_2 diffusion through the layer of $CaCO_3$ that is formed around unreacted CaO particles.[20,61-63] The transition from the fast to the slow reaction step is attributed to the accumulation of a layer of $CaCO_3$ on the unreacted sorbent particles, which decreases the access of CO_2 molecules to the active CaO.[64] $CaCO_3$ formed after the carbonation reaction is transferred to a second unit (a calciner) in which there is rapid regeneration of CaO and desorption of CO_2 at < 850 ºC (~1 atm). Thereafter, a stream of pure CO_2 is transported for dehydration and compression, and then transported to the storage site. The carbonation/calcination cycle of the $CaO/CaCO_3$ system is repeated a certain number of times and can be operated under a range of conditions (e.g., with temperature or pressure of the system favourable for thermodynamic equilibrium, or using CO_2 partial pressure swing or hydration).

Recent research has demonstrated that the $CaO/CaCO_3$ looping process can satisfactorily reduce CO_2 emission reductions from fossil-fuel-fired power plants and cement manufacturing.[10,25] Figure 3.4 illustrates various applications of the calcium looping cycle with operational concepts comparable to those outlined above. It should be mentioned that the heat required for the calcination unit shown in the figure is provided by oxyfuel combustion, for example, using coal under extremely pure O_2.[20] The calcium looping cycle technology is now one of the emerging options for post-combustion CO_2 removal (i.e., separation of CO_2 from flue gases produced by burning fossil fuels in air).[65] This method was created by Shimizu et al.[61], and the general concept involves a modified version of the calcium looping process for pre-combustion CO_2 capture[66], which includes production of H_2 and CO_2 by the water gas shift reaction (Eq. 5) after gasification of the fuel.[10]

$$CO(g) + H_2O(g) \leftrightarrow CO_2(g) + H_2(g),\ \Delta H^0 = -41\,\frac{kJ}{mol} \qquad (5)$$

3.4.5.1 Temperature and pressure evaluation for CO_2 capture using CaO-based sorbents

Numerous articles in the literature have described the properties and operation of $CaO/CaCO_3$ looping. As mentioned above, the carbonation reaction of CaO is exothermic, and decomposition of the $CaCO_3$ formed is endothermic. The dependence of equilibrium CO_2 partial pressure ($p_{eq.(3)}$) on temperature in Equation 3 has been investigated by use of thermodynamic coefficients.[20,21] In the cited studies, the value of $p_{eq.(3)}$ approached to overcome the CO_2 pressure in air (~0.35 x 10^{-3} bar) at ~550 ºC but, compared to flue gas from fuel combustion (which can have a pressure of ~0.2 bar), was similar to the $p_{eq.(3)}$ at

~800 ºC.[20,21,63,67] The rapid regeneration of CO_2 and CaO must be carried out in a high level of CO_2 at a pressure higher than the atmospheric pressure, which occurs at ~890 ºC. This demonstrates that CO_2 capture technology based on the $CaO/CaCO_3$ looping process is easy to accomplish by either thermal or pressure swing sorption, although the former is more attractive from an economic perspective.[68-70] Accordingly, efficient CaO carbonation can be carried out in the temperature range 650–800 ºC and with $CaCO_3$ calcination at > 900 ºC, using the thermal swing method.[68]

In experiments involving carbonation of limestone performed using thermogravimetric analysis (TGA) at carbonation temperatures in the range 650–850 ºC, the highest conversion of limestone (~77 %) in the initial cycle was observed at 650 ºC and decreased with an increasing number of CO_2 uptake cycles (conversion 28.4 % after 30 cycles).[71] However, analysis of the cyclability of CO_2 capture by limestone indicated a similar carbonation conversion value of ~44 % after 10 cycles at 650 and 700 ºC.[71] Blamey et al.[72] used a fluidized bed reactor (FBR) to determine the effect of calcination temperature on cyclic removal of CO_2 by use of a solid CaO-based sorbent. The carbonation of limestone was performed at 700 ºC, and subsequent calcination was done at 840–1000 ºC under 15 vol% CO_2 in N_2. The results showed that CaO activity decreased with increasing CO_2 desorption temperature. It was suggested that the reduction in the activity of CaO-based material is affected by sintering and attrition of the sorbent at high system temperatures.[2]

Butler et al.[68] evaluated the impact of carbonation pressure (6–21 bar) on CaO-based sorbent conversion at 1000 ºC under pure CO_2 flow. In that study, stripping of CO_2 and regeneration of sorbent were done at 1000 ºC under atmospheric pressure, and the most efficient long-term (250 cycle) limestone conversion (~27.7 %) was achieved with a pressure swing of 1 to 11 bar. It has also been demonstrated that the pressure-cycling method achieves higher long-term calcium-based sorbent activity when performed using CO_2 than with temperature swing or CO_2 partial pressure swing operation under comparable conditions.[68]

3.4.5.2 Sorbent performance along CO_2 capture cycles

A great number of investigations of long-term cyclic carbonation/decarbonation runs using various CaO-based minerals have demonstrated that the degradation of the sorbents is rapid during CO_2 capture cycles.[21,68,73,74] The loss of sorbent reactivity over long-term CO_2 capture was attributed to loss of the active surface area and porosity of the sorbent caused by sintering, attrition, and reaction with impurities in the flue gas (e.g., sulphur-containing species, HCl, and particulate matter).[21,59,60]

Grasa et al.[74] have proposed a model of the decay of CaO-based sorbents during conversion of carbonates achieved by increasing the number of cycles (Eq. 6). In this model, X_N is the maximum carbonation conversion in cycle N (> 20), X_R is the residual carbonation conversion after numerous CO_2 capture cycles, and k is the deactivation constant:

$$X_N = \frac{1}{\frac{1}{1+X_R}+kN} + X_R \qquad (6)$$

This model is semi-empirical, and applying it to limestone or dolomite with different origins and characteristic properties (e.g., structure, particle size, porosity, and surface area) can provide inaccurate results regarding CO_2 uptake behaviour.[10,75] Also, the use of calcium looping in a full-scale power station unavoidably entails reactions of calcium compounds with sulphur-containing components, ash, and other flue gas components, which may strongly alter the residual carbonation conversion. Therefore, application of the $CaO/CaCO_3$ looping process requires tremendous quantities of fresh limestone or dolomite to retain an acceptable CO_2 capture capacity.[76] However, the total cost of the calcium looping technology can be acceptable due to the low price of CaO-based minerals, not requirements to use complex flue gas-cleaning technologies, and the possibility of using the CaO materials as feedstock for generating cement.[67]

3.4.5.3 Modification of CaO-based sorbents

A number of pilot-scale calcium looping systems are now in operation or under construction, and a large number of scientific articles have been published that describe investigation of the properties and performance of CaO-based sorbents. However, an evaluation of the decay of carbonation/decarbonation conversion of natural limestone showed that, after around 20 CO_2 absorption/desorption cycles, the conversion stabilized at around 25% of the initial carbonation efficiency of ~70%.[77] Therefore, it is essential to make improvements in the macro- and microstructural properties of the sorbent, such as the surface area, the volume and structure of pores, and orientation of the calcium oxide crystals.[74,78] The main modification strategies for enhancing the activity of CaO-based sorbents in long-term calcium looping performance include the following: (a) spent sorbent reactivation by hydration[72,79,80]; (b) synthesis of CaO-based sorbents from various precursors[81,82]; (c) doping with trace amounts of foreign ions and precipitation[83]; (d) CaO-based sorbents on inert porous supports[84-86]; (e) thermal pretreatment[87] of spent sorbents; and (f) pelletization[88,89]. Ideally, these modified sorbents should possess high mechanical strength, while the active surface area is preserved during repeated cycling of CO_2 capture.

Introduction of an intermediate hydration step in between the CO_2 capture cycling of CaO-based sorbent has been shown to enhance the carrying capacity of the sorbent.[72,80] Hydration of the CaO with water vapour leads to the formation of $Ca(OH)_2$ that has an increased active surface area due to surface cracking (which allows water vapour to penetrate to the core of CaO particles).[21] In experiments evaluating the effects of CaO hydration with water vapour in a FBR under atmospheric pressure and temperature after 10 CO_2 capture cycles, it was found that such treatment led to recovery of the carrying capacity of the sorbent from ~18 % to ~30 %.[90] This enhanced conversion was observed only in the first step in carbonation of the sorbent, after the hydration stage, and the subsequent carbonation conversion value of ~18 % was achieved after 10 additional CO_2 uptake cycles. Also, sorbent hydration with steam at 200 ºC resulted in ~22 % conversion after 10 repeated CO_2 capture cycles[90,91]. Donat et al.[60] demonstrated that application of high-temperature steam (1–20 % H_2O in N_2, 800 ºC) in both the carbonation and decarbonation stages had a slightly greater effect on limestone conversion (~25 %). In another study[92], it was shown that hydration of CaO-based minerals is an

effective method for enhancing CO_2 capture activity, although this technique raised the particle attrition rates in a FBR.

Table 3.2. Carrying capacity and morphological properties of various sorbents (data collected before carbonation/decarbonation cycles unless otherwise indicated).

Material	Synthesis method	$T_{carb.}$, °C	$T_{decarb.}$, °C	Weight of the sample, mg	No. of cycles	Surface area, m^2/g	Pore volume, cm^3/g	Carrying capacity, %
Limestone (Havelock)[70]	–	650	900	5	30	–	–	18
Limestone (Tamuin)[75]	–	650	850	5.65	40	–	0.05	20
$CaCO_3$[93]	–	650	700	5–20	3	–	–	50
$CaCO_3$ ($Ca(OH)_2$)[93]	Precipitation	650	700	5–20	2	20.93	0.05	70
$CaCO_3$ ($Ca(CH_3COO)_2$)[94]	Precipitation	700	–	4–8	1	20	0.22	80
$CaCO_3$ $Ca(C_2H_5COO)_2$)[94]	Precipitation	700	–	4–8	1	15	0.18	77
$CaCO_3$ $Ca(CH_3COO)_2 \bullet H_2O$)[95]	Precipitation	600	750	–	27	20.2	0.23	62
$CaCO_3$ ($Ca(OH)_2$)[70]	Precipitation	650	900	5	30	–	–	20
$CaO/Ca_{12}Al_{14}O_{33}$ (85/15)[70]	Precipitation	650	900	5	30	8.44**	–	22
Zr/Ca (3:10)[96]	Flame spray pyrolysis	700	750	4	100	71	0.24	50
Al/Ca (3:10)[97]	Flame spray pyrolysis	700	750	–	100	63	0.18	67
CG-MG (25/75)[59]	Spray drying	650	900		44	–	–	59
$CaO/Ca_9Al_6O_{18}$ (20/80)[98]	Sol-gel/support	650	800	10	35	19.7	0.04	75
CaO ($Ca(NO_3)_2$)[99]	Sol-gel	650	800	10	20	6.8*	–	65

*After 5 cycles.

**After 10 cycles.

Abbreviations: CG, calcium D-gluconate; MG, magnesium D-gluconate hydrate; $T_{carb.}$, carbonation temperature; $T_{decarb.}$, decarbonation temperature.

The morphology and structure of the Ca-based sorbents has a marked impact on CO_2 uptake behaviour. Accordingly, various synthesis techniques have been used to produce modified calcium-based sorbents with high selectivity for CO_2, and examples of these approaches include the following: precipitation[70,100,101], flame spray pyrolysis[96,97], spray drying technique[59], thermal treatment[82], addition of inert support materials[102], and the sol-gel

method[98,99]. Data concerning the morphological and structural characteristics and the carrying capacity of CaO-based sorbents prepared using different techniques or precursors vary to some extent between studies in the literature, even when similar methods and conditions were used. The selected results are summarized in Table 3.2. It should be noted that the carrying capacity of evaluated sorbents differs strongly depending on the experimental setup employed[75], for example, regarding the amount of sample used, the size of the particles, and the sample preparation technique and treatment conditions, which may alter the reactivity of CO_2 with the sorbent.[103]

Much work has been focused on precipitation methods with the aim of synthesizing sorbents with a large active surface and substantial pore volume that can provide efficient CO_2 capture. Lu et al.[94,95] demonstrated that using a precipitation strategy to achieve synthetic generation of CaO from calcium propionate and calcium acetate monohydrate resulted in the greatest surface area, although the sorbent comprising $Ca(CH_3COO)_2 \cdot H_2O$[95] exhibited a better pore volume. It was observed ~62 % conversion after 27 carbonation/calcination cycles with Ca-based sorbent produced from calcium acetate monohydrate.[95] Moreover, other researchers[70] found that the calcium carbonate precipitated by bubbling CO_2 through $Ca(OH)_2$ slurry generated a sorbent with slightly higher CO_2 activity than seen in natural limestone. This enhancement of the carbonation conversion of the sorbent was attributed to the morphology of the CaO produced, which included pore size distribution in the mesoporous range (5–20 nm) and was achieved by using an anionic dispersing agent during the synthesis operation.[93]

An alternative method to delay or prevent sintering of calcium-based sorbents is to use dopants or supports instead of changing the precursor in the synthesis of CaO. For example, flame spray pyrolysis (FSP; converts the precursor into solid nanoparticles in flames) can be used to produce well-dispersed doped CaO nanoparticles with a large surface area and high thermal stability. Koirala et al.[97] and Lu et al.[96] showed that the surface area of all sorbents prepared by FSP was at least twice that of sorbents generated by other techniques. It was also observed that FSP-produced calcium-based sorbents had a significantly improved long-term carrying capacity after 100 CO_2 capture cycles. Furthermore, other researchers[97] found ~51% better CO_2 sorption behaviour after 100 cycles when using Al-doped CaO sorbent, with Al and Ca at a molar ratio of 3:10; this sorbent exhibited very good long-term conversion stability, which the authors suggested was affected by increased formation of inert $Ca_{12}Al_{14}O_{33}$ (mayenite). There are also other promising methods for preparing modified or unmodified CaO that has high selectivity for CO_2 and offers stable carbonation conversions during CO_2 capture cycles, and these strategies include spray drying, the sol-gel technique, and use of inert support materials, as well as combinations of these techniques.[59,98,99,104]

Notably, doping CaO with inorganic salts has provided various results with regard to carbonation conversion of the sorbent. Havelock limestone doped with NaCl and Na_2CO_3 was experimentally investigated using a TGA apparatus.[105,106]. The results showed that limestone impregnated with aqueous solutions of NaCl (0.002–0.5 M) slightly increased the carbonation conversion from 30% to 40% over 15 CO_2 capture cycles, whereas Na_2CO_3 (0.002–0.5 M) had no effect. However, the reactivity of the sorbent with CO_2 was greatly improved by use of pretreated CaO doped with dry 1 wt% Li_2CO_3, but was decreased by CaO doped with 1 wt% K_2CO_3.[81] More recent research on application of inorganic salts such as $MgCl_2$, $CaCl_2$, and

$Mg(NO_3)_2$ as dopants has also demonstrated increment of carbonation conversion of calcium-based sorbents when using characteristic concentrations of the dopant.[83,107] It has been suggested that, in some cases, if the concentrations of dopants are too low, these additives may have no impact on the carrying capacity of the sorbent; conversely, if the concentrations are too high, it may lead to more rapid sintering or attrition of calcium-based sorbents due to pore-blocking effect.[10] Thus the efficiency of doping depends largely on the amount of dopant used in the modification process.

3.4.5.4 Effects of SO_2 and HCl on efficiency of CO_2 capture

Clean conversion of energy to electricity or other products is essential for reducing anthropogenic CO_2 emissions. When applying the calcium looping process for capture of CO_2 from power plants and other industries, a fundamental issue to consider is related to the occurrence of competing reactions between CaO and flue gas components. Reaction of CaO with compounds/substances such as sulphur-containing species, halides, ash, and particulate matter can affect sintering and attrition of the sorbent.[108,109] For example, CaO has high affinity for SO_2 and form thermodynamically stable $CaSO_4$ via direct (Eq. 7) or indirect (Eq. 8) sulphation under the oxidizing conditions that exist in the carbonator and the regenerator (post-combustion and oxyfuel combustion).[110] Also, chemical reaction between CaO and H_2S can occur to form CaS by direct (Eq. 9) or indirect (Eq. 10) sulphidation under reducing conditions (pre-combustion flue gas).[10] Therefore, CaO-based materials have been used as effective and inexpensive alternatives for removal of sulphur-containing species from molten metal processing or other industrial operations.[111,112] However, decomposition of sulphated sorbent back to CaO must be performed under harsh conditions (high temperature or reducing parameters), whereas regeneration of sulphided sorbent requires less energy.[10,113]

$$CaO(s) + SO_2(g) + \frac{1}{2}O_2(\mathrm{g}) \leftrightarrow CaSO_4(s),\ \Delta H^0 = -502\frac{kJ}{mol} \quad (7)$$

$$CaCO_3(s) + SO_2(g) + \frac{1}{2}O_2(\mathrm{g}) \leftrightarrow CaSO_4(s) + CO_2(g),\ \Delta H^0 = -502\frac{kJ}{mol} \quad (8)$$

$$CaO(s) + H_2S(g) \leftrightarrow CaS(s) + H_2O(g),\ \Delta H^0 = -61.3\frac{kJ}{mol} \quad (9)$$

$$CaCO_3(s) + H_2S(g) \leftrightarrow CaS(s) + CO_2(g) + H_2O(g),\ \Delta H^0 = +117\frac{kJ}{mol} \quad (10)$$

The reaction efficiency of sulphation and sulphidation can depend on many factors, primarily the following: system design, operational parameters, fuel type, and O_2/CO_2 ratio.[114] Liu et al.[110] investigated the behaviour of CaO and $CaCO_3$ sulphation by performing FBR at 610–850 ºC under $O_2/CO_2/SO_2$ conditions, and their results demonstrated that the degree of the sulphation reaction was affected by the temperature of the system and the type of sorbent used. It was found that raising the temperature of the system from 610 to 850 ºC under 80 vol% CO_2, 10 vol% O_2, and 1920 ppm SO_2 in Ar increased the direct sulphation of CaO from ~10 to 45 %.[110] Research has also shown that the direct sulphation is affected by chemical- and diffusion-controlled reactions (e.g., the reaction of CO_2 with solid calcium-

based sorbents), and the diffusion-controlled reaction of SO_2 particles with limestone generates porous products that may lead to efficient CO_2/SO_2 capture technology.[110,115] Nevertheless, the regeneration of the sulphated sorbents back to CaO-based materials occurs at very high temperatures, which increases the cost of the total process, and more extensive attrition of the particles has also been observed throughout cyclic CO_2 capture.[110,116]

CaO-based sorbents are also capable of removing halides from flue gas, and thus carbonation conversion of the sorbent can be effected by the concentration of halides in the system.[66] Dry removal of HCl by CaO (Eq. 11) and $CaCO_3$ (Eq. 12) is influenced by the reaction conditions and the morphology and structure of the sorbent. Partanen et al.[117] found that the activity of limestone and dolomite was increased when the gas mixture had a higher content of moisture, and they also observed the most efficient sorption of HCl when using dolomite, which contains the highest level of MgO compared to other natural composites. Sun et al.[118] tested HCl removal by use of $CaCO_3$, CaO, and hydrated CaO (all three synthesized by PCC), and limestone; the results indicated that the most extensive conversion of sorbent to $CaCl_2$ was achieved by chloridation at 550 ºC using CaO synthesized by PCC technology. It was found that smaller particles had a greater potential to absorb hydrochloric acid.[117,118] Morphological and structural evaluation of the sorbents confirmed that the precipitation synthesis method is effective in generating sorbents with well-defined mesoporous structure for removal of CO_2, HCl, and SO_2.

$$CaO(s) + 2HCl(g) \leftrightarrow CaCl_2(s,l) + H_2O(g),\ \Delta H^0 = -217.8\frac{kJ}{mol} \quad (11)$$

$$CaCO_3(s) + 2HCl(g) \leftrightarrow CaCl_2(s,l) + CO_2(g) + H_2O(g),\ \Delta H^0 = -39.5\frac{kJ}{mol} \quad (12)$$

3.4.5.5 Pilot-scale dual fluidized beds

Several pilot-scale dual fluidized bed combustion systems have been constructed to demonstrate the feasibility of using CO_2 capture by calcium looping technology in continuous operation.[119,120] Lu et al.[116] tested the effect of numerous operating conditions (e.g., flue gas volume, CaO/CO_2 ratio, and sorbent looping rate) on the performance of limestone (Havelock) in cyclic CO_2 capture using CANMET 75 kW_{th} in pilot-scale dual fluidized bed reactors (FBRs). The results showed a high carbonation conversion efficiency of ~72 % after more than 25 cycles of CO_2 absorption/desorption (simulated flue gas composition: 15 % CO_2 in air), but it was also found that the attrition of the CaO-based sorbent was enhanced with an increasing number of cycles. Therefore, ~60 % of fine particles occurred in agglomerated form after 25 cycles, which significantly reduced the CO_2 capture rate in subsequent cycles. Similar cyclic carrying capacity efficiencies > 70 % have been found in other evaluations using 30 kW_{th} in circulating fluidized bed reactors (CFBRs).[121] Researchers have noted that decay of the activity of CaO-based sorbents over repeated CO_2 capture cycles was successfully counteracted by using large amounts of fresh sorbent in the carbonators.[116,119-121] Furthermore, the estimation of sulphation of limestone in 30 kW_{th} CFB facility has shown the feasibility of using the calcium looping process for co-capture of CO_2 and SO_2, an approach that can be used to avoid desulphurization of the flue gas.[122] Although these pilot-scale

investigations of calcium looping technologies for CO_2 capture have demonstrated high removal efficiencies under various operating conditions, there is still a need to evaluate the issues of sorbent loss via sintering and attrition, sulphation, sulphidation, and hydration, and the effects of other flue gas components, as well as optimization of the process.

To summarize, a great number of scientific studies concerning modification of the properties of calcium-based sorbents have been to some extent successful in achieving enhanced carbonation conversion leading to increased mechanical and thermal stability, although none of the strategies used have completely prevented sintering or attrition of the sorbents. Interaction of CaO with CO_2 during cyclic carbonation is effected by several variables, such as treatment of the sorbent, and the structure and morphology of that material (e.g., particle size, impurities, surface area, volume and structure of the pores, and orientation of calcium oxide crystals); temperature and time of the carbonation and decarbonation stages; CO_2 partial pressure and gas composition (e.g., levels of N_2, H_2O, He, Ar, SO_x, and HCl) during carbonation and decarbonation. These aspects make it difficult to compare the results of different investigations. However, when selecting a CO_2 capture method for commercial application, it is fundamental to specify the purity of the final product and the strategy selected for operation of the flue gas and raw material in order to ensure that operation will be optimal with respect to energy use and cost. Considering the increased interest in employing modified and/or synthesized CaO-based materials as CO_2 sorption agents, it is necessary to make improvements throughout the removal process or to create new methodology that can achieve technically and economically efficient CO_2 capture using the calcium looping method.

3.4 Comparison of CO_2 capture cost and energy penalty

As noted above, energy generation techniques that offer pollution-free performance, high efficiency and operational reliability, and low capital costs are economically attractive technologies for industrial applications.[123,124] Economic data on CO_2 capture processes have been approximated in numerous studies focused on this technology, but those calculations have underestimated realistic commercial costs.[25] Variation in the approximate price of the captured CO_2 may be explained by differences in the following: national and regional policies and regulatory structure, emission and power markets, risks assessments, technical and financial factors, quality of available fuels, and public interest.[125] Rubin et al.[14] summarized the available literature on this subject and reported approximate energy penalties of CO_2 capture efficiency for different power plants with or without a fixed energy input (Table 3.3). These estimated techno-economic data for power generation stations were based on CO_2 capture achieved by use of physical solvents in different approaches: pre-combustion removal of CO_2 from flue gas from combined-cycle integrated coal gasification; application of cryogenic air separation units for oxyfuel combustion capture of CO_2 from burning of pulverized coal (PC); amine solvents for post-combustion CO_2 capture from coal-fired and natural gas plants.[6] The results show that the energy input requirements of post-combustion capture at a supercritical (low net efficiency) PC (SPCPC) plant are twice as high as at a new facility using integrated gasification combined cycle (IGCC) technology. It is plausible that the lower efficiency at the former is related to the need to use more fuel to generate energy

and thereby enable CO_2 capture. For example, coal combustion plants will produce more processed fuel solid waste, ammonia, and limestone waste from cleaning flue gas (SO_2, NO_x). In addition, increased need for cooling of the system units significantly raises the total plant cost.[7] In general, plant efficiency is reduced by the energy requirements for operation of fans, pumps, and CO_2 compressors, as well as thermal energy losses due to solvent regeneration (PC plants) and the water–gas shift reaction (IGCC plants). However, innovations in technological processes are improving the efficiency of power plants, and thus the energy penalty for CO_2 capture at these facilities is lower.[25] Accordingly, there is a need to evaluate the general efficiency of CO_2 capture in terms of energy penalty for individual power plants.[6]

Table 3.3. Average cost efficiency of power plant and CCS energy penalty (OECD only).[6,25]

Power plant, fuel type and CO_2 capture system	New plant efficiency without CCS, %	New plant efficiency with CCS, %	CCS energy penalty		Relative overnight cost increase, %	Cost of CO_2 avoided, US$/$t_{CO2}$
			Additional energy input per net kWh output, %	Reduction in net kWh output for a fixed energy input, %		
Coal/Post-combustion (SPCPC)	33	23	43	30	75	58
Coal/Post-combustion (USPCPC)	40	31	29	23	75	58
Coal/Oxyfuel combustion (USPCPC)	40	32	25	20	74	52
Coal/Pre-combustion (IGCC)	40	33	21	18	44	43
NG/Post-combustion (NGCC)	50	45	16	14	82	80

Abbreviations: SPCPC, supercritical pulverized coal; USCPC, ultra-supercritical pulverized coal; IGCC, integrated gasification combined cycle; NG, natural gas; NGCC, natural gas combined cycle.

3.5 Application of molten salts in CO_2 capture

High-temperature CO_2 adsorbents such as lithium zirconate (Li_2ZrO_3)[126,127] and lithium silicate (Li_4SiO_4)[128,129] that are activated with alkali metal salts are known as alkali ceramics, and the adsorbent capacity of these materials is due to mobility of the lithium in ceramic beds.[5] Adsorption of CO_2 on lithium atoms is rapid and involves diffusion from the core of the ceramic material particles to the surface of the ceramic bed that to form Li_2CO_3; in comparison, diffusion of CO_2 molecules in the solid Li_2CO_3 is slow (Eqs. 13 and 14).

$$Li_2ZrO_3(s) + CO_2(g) \leftrightarrow Li_2CO_3(s) + ZrO_2(s) \quad (13)$$

$$Li_4SiO_4(s) + CO_2(g) \leftrightarrow Li_2CO_3(s) + Li_2SiO_3(s) \quad (14)$$

The main obstacles to commercial application of Li_2ZrO_3 and Li_4SiO_4 are the kinetic limitations of these compounds and the cost of lithium-based materials. The chemical and mechanical stability of lithium ceramics depends on the change in texture caused by lithium sublimation.[5] Therefore, the CO_2 sorption capacity of Li_2ZrO_3[127,130,131] and Li_4SiO_4[129,132] can be improved by using alkali carbonates as an active molten carbonate layer on the outer surface of the lithium zirconate or silicate particles. Various eutectic compositions of alkali carbonates and their mixtures with alkali metal halides, such as $KCl/NaCl/Na_2CO_3$, K_2CO_3/Li_2CO_3, $K_2CO_3/Li_2CO_3/Na_2CO_3$, $NaCl/Na_2CO_3/NaF$, and $K_2CO_3/Na_2CO_3/NaF$, have been used to enhance Li_2ZrO_3 reactivity with CO_2.[127] It was observed that the CO_2 sorption capacity of Li_2ZrO_3 activated with ternary eutectic $K_2CO_3/Na_2CO_3/NaF$ increased from 13 wt% to 75 wt% at 700 ºC under 100 % CO_2 atmosphere.[127] In other studies, modification of Li_4SiO_4 by K_2CO_3 resulted in increased and stable carrying capacity of 0.101 g CO_2/g sorbent, and an increased concentration of K_2CO_3 was found to improve CO_2 sorption behaviour by leading to higher diffusion rates of lithium and CO_2 in the molten salt layer.[129] However, these processes still require extensive development, which can be achieved by investigating novel materials, evaluating long-term cyclability, and determining how fuel-bound impurities affect the sorption capacity of the sorbent.

Interest in electrochemical conversion and utilization of CO_2 in ionic liquids (ILs) has grown considerably over the past few years.[133,134] ILs have unique properties such as low vapour pressure, high thermal stability, and strong solubility capacity, but they are also very expensive, which has a pronounced impact on the total cost of the process.[18,135] Therefore, high-temperature molten salts have been selected as an alternative to avoid some of the challenges related to ILs.[136] Molten salts have some distinct advantages in electrochemical reactions, including substantial electrical conductivity, a high degree of ionization, good thermal energy transfer, and considerable thermal stability and inertia.[22,23]

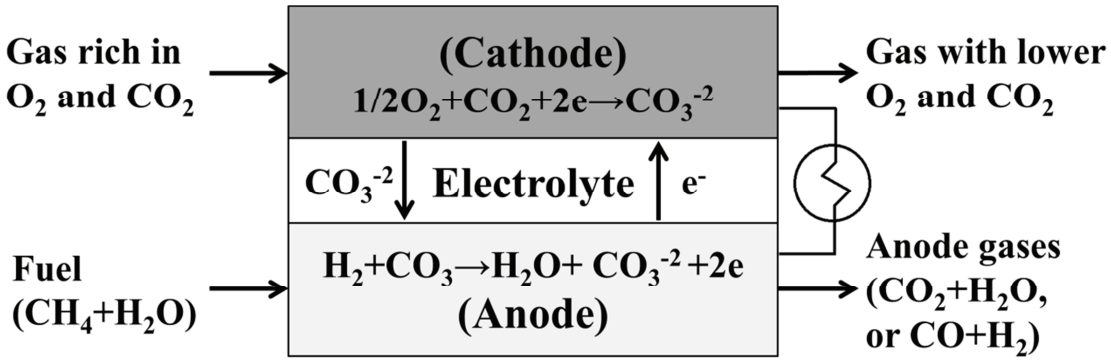

Figure 3.5. Operating principle of MCFCs used for CCS.

Molten salts are used as electrolytic media in energy conversion and storage devices (e.g., batteries, fuel cells, and solar/thermal energy collection, storage and transfer) and thus represent important applications in pollution-free generation of electric power.[137] Molten

carbonate fuel cells (MCFCs) represent one category of the hydrogen fuel cells that are classified according to the type of electrolyte used.[138] MCFCs are accepted as *in situ* CO_2 capture technology, and studies have also examined the possibility of integrating MCFCs in CO_2 separation from waste gas produced by fossil-fired power plants.[137,139] MCFC operation (illustrated in Figure 5) requires a constant supply of fuel and oxygen (fuel is fed to the anode, oxygen near the cathode) and can proceed without interruption if this criterion is met. MCFCs are high-temperature (650 ºC) systems in which a molten carbonate (e.g., Li_2CO_3, Na_2CO_3, or K_2CO_3) serves as the reaction medium, hydrogen is typically the fuel, and oxygen is the oxidant.[137] Water and carbon dioxide or carbon monoxide and hydrogen are the by-products of the MCFC reaction.[140] The cell, which can have a high current density, is completely pollution free.[141,142] Discepoli et al.[137] observed that MCFCs can remove 70 % of CO_2 from the flue gas produced by the power plant in Norcia, Italy. The advantage of this type of fuel cell is that it can also use CO, CO_2, and certain hydrocarbons (e.g., methanol and gasoline) directly in the production of carbon materials and electricity.[23,143]

As noted above, an alternative to exploiting the unique properties of molten salts is to perform electro-reduction of CO_2 to carbon-based materials rather than to CO.[144] Yin et al.[49] found that carbon-based materials that were electrochemically deposited at the cathode (500 ºC) in a $Li_2CO_3/Na_2CO_3/K_2CO_3$ mixture had a high specific surface area (BET > 400 m^2/g), and hence might be useful in other industrial processes and decrease the cost of the technology. The electrochemical transformation of CO_2 in molten $LiCl/Li_2O$ (650 ºC) or $CaCl_2/CaO$ (900 ºC) has also been investigated regarding potential use in production of carbon-based materials and utilization of CO_2.[136] In the cited study, the higher system temperature used for $CaCl_2/CaO$ molten salt resulted in lower CO_2 separation compared to that achieved in the $LiCl/Li_2O$ system. Also, the current required for reduction of CO_2 to CO and aggregation of graphite crystals did not depend on the amount of CO_2 in the simulated gas mixture or the flow rate of the gas, but it was affected by the electrical properties of ZrO_2 solid electrolyte, which was used to remove oxygen in melts.[136] The main disadvantages of molten carbonate fuel cells are that they must be operated at a high temperature, the corrosive electrolyte promotes device breakdown, and the electrodes are very expensive. Therefore, MCFCs represent a good alternative to reduce CO_2 emissions from small fossil fuel power stations.[138] Investigations are needed to evaluate different oxygen ionic transfer media and new molten salt materials and operational designs for use in large-scale fossil fuel power plants or other industrial operations.[138]

4.0 MATERIALS AND METHODS

4.1 Materials

In most of the present experiments, the initial material used for CO_2 removal and phase transitions was a powder composed of the following (purity within parentheses): CaO (96–100 %), NaF (98.5–100 %), LiF (99 %), $CaCl_2$ (≥ 97.0 %), CaF_2 (97–100 %), $CaCO_3$ (99.95 %), and Na_2CO_3 (99.5 %). Commercially available CaO was utilized as the sorbent in the CO_2 capture study. Powdered $CaCl_2$ and the mixtures CaF_2/NaF (41.85 wt% CaF_2 in NaF), CaF_2/LiF (42.2 wt% CaF_2 in LiF), and CaF_2/$CaCl_2$ (13.8 wt% CaF_2 in $CaCl_2$) were used as the molten salts, because their melting points are suitable for reaction of solid CaO with CO_2. All fluorides and oxides of the alkali and alkaline earth metals were dried at 200 °C for at least 24 h. The compositions of the salt mixtures used in the present investigations (to obtain phase diagrams and study CO_2 capture) are given in the respective papers. AGA (Oslo, Norway) provided the gases used in all experiments, namely, carbon dioxide (purity 99.99 %), nitrogen (purity 99.999 %, $H_2O \leq 3$ ppm, $O_2 \leq 3$ ppm, $C_nH_m \leq 1$ ppm), and argon (purity 95 %).

4.2 Methods

4.4.1 Phase diagram analysis

In the study reported in **Paper I**, thermal analysis (TA) was used to evaluate the phase transitions in the NaF-CaF_2, NaF-CaF_2-CaO, NaF-CaF_2-$CaCO_3$, NaF-CaF_2-$NaCO_3$ and NaF-CaF_2-Na_2CO_3-$CaCO_3$ systems. The design of the experimental setup is presented in Figure 1 in **Paper I**. The crucible, stirrer, and radiation shields were made of nickel. The sample (150 g) was put in the crucible (inner diameter 6.2 cm, height 6.0 cm) and heated to 870–1150 ºC in a sealed furnace under N_2 flow. Pure CO_2 gas flow was used in the NaF/CaF_2-$CaCO_3$ and NaF/CaF_2-Na_2CO_3 systems investigations. The sample was kept at a stabilized temperature (870–1150 ºC, depending on the melt composition) for approximately 3 h, after which the temperature was decreased to investigate the freezing points of the melts (see Table 2 in **Paper I**). The heating and cooling rates in the furnace (5 and 0.6–0.7 ^{o}C/min, respectively) were regulated by a computer program (LabView) interfaced with the furnace controller. A calibrated type S thermocouple (Pt-Pt10Rh, ±1.1 ºC) was used to record temperature changes in the melts during heating and cooling.

4.4.2 Operation of CO_2 capture

Sample preparation for the CO_2 capture process

A series of mixtures comprising CaO in $CaCl_2$ (**Paper III**), CaF_2/NaF (41.85 wt% CaF_2 in NaF; **Papers II and V**), CaF_2/LiF (42.2 wt% CaF_2 in LiF; **Paper V**), and CaF_2/$CaCl_2$ (13.8 wt% CaF_2 in $CaCl_2$; **Paper IV**) with various loads of CaO (5–20 wt%) were prepared, each as a liquid column (height 10 cm) in a nickel crucible (inner diameter 5.2 cm, height

35.0 cm). The weights of the mixtures varied from 470 to 650 g. The samples were fused under argon and kept at 850–970 °C (heating rate: 200 °C/h) for 10 h. Thereafter, the system was set at the carbonation temperature, which was maintained for 2 h while bubbling pure N_2 through the melt.

Experimental setup for CO_2 capture studies

The general experimental setup used to study CO_2 capture is illustrated in **Papers III** and **IV** (Figure 1 in both). A one-chamber atmospheric pressure reactor consisting of an inner nickel crucible and an outer stainless steel compartment was placed in a ceramic tube furnace (< 1250 ºC). A FTIR gas analytical cell (Nicolet 6700 FTIR spectrometer, Thermo Scientific) and a weighing scale (MS8001S, Mettler Toledo; accuracy 0.1 g) were used in all the CO_2 capture experiments, unless otherwise indicated. The Nicolet 6700 FTIR apparatus has a 2-m gas cell (volume 200 ml) with KBr windows, the temperature of which was monitored by a Digi-Sense controller (Eutech Instruments Pte Ltd). The gas cell temperature was kept at 120 ºC for 24 h before the start of an experiment and was purged with N_2 (0.7 l/min) for at least 30 min to record background N_2. All CO_2 quantification was performed using OMNIC Series software (Thermo Scientific). PTFE (Teflon) tubes previously purged with N_2 were used for gas injection to the reactor and transport from the reactor to the FTIR apparatus. A nickel tube (inner diameter 1.0 cm [**Papers II–IV**] or 0.4 cm [**Paper V**]) was used to transport the CO_2/N_2 gas mixtures into the liquid–slurry through the top of the sealed reactor. The gas feed tube was immersed to a depth of 1 cm from the bottom of the crucible. The composition and flow rates of the simulated flue gas were regulated using mass flow controllers (MASS-STREAM, M+W Instruments GmbH), unless otherwise indicated. The temperature of the system was monitored with a type S thermocouple (Pt–Pt10Rh, ±1.1 ºC) immersed in the melt (to 5 cm from the bottom of the nickel crucible). The reaction gases at the outlet of the reactor were passed through an integrated electrostatic filter. A mass flow meter (MFM; Sierra Instruments, Inc.) was used at the outlet of the FTIR detector to monitor the tightness of the assembly. Argon gas was fed continuously (0.20 l/min) through the bottom of the furnace to avoid corrosion of the reactor. All experimental data presented in this thesis were collected using settings operated by LabView computer software (temperature, composition and flow rate of CO_2/N_2, and weight changes in the molten salt systems), data visualization, and processing and analytical tools (integrated OMNIC Series [Thermo Scientific] and NI cRIO-907x integrated systems)

CO_2 capture parameters

As mentioned above, various CaO-$CaCl_2$ (**Paper III**), CaO-CaF_2/NaF (**Papers II and V**), CaO-CaF_2/LiF (**Paper V**), and CaO-CaF_2/$CaCl_2$ (**Paper IV**) systems, gas compositions (CO_2/N_2), and operational conditions were used to evaluate the efficiency of carbonation and decarbonation reactions. More detailed information on experimental parameters such as material/gas composition, gas flow rate, temperature of the systems, temperature increase/decrease, and times used for CO_2 absorption and desorption are given in the papers included in this thesis. In general, the carbonation reaction was considered to be complete when the composition of CO_2/N_2 at the inlet corresponded to that at the outlet. Decomposition

of the formed carbonates was terminated when the FTIR detector indicated that the CO_2 content in the outlet gas was close to 0 ppm. The weight of the reactor and the outlet gas composition were measured continuously.

4.4.3 Characterization

Powder X-ray diffraction (XRD) data were collected from $5^\circ \leq 2\theta \leq 110^\circ$ (scan rate 0.01 degree per second) using Ni-filtered Cu K_α on a Bruker D8 Advance diffractometer working in Bragg-Brentano ($\theta/2\theta$) geometry (**Papers I and II**) or using Cu-Kα (1.5418 Å) radiation on a Philips PW1730/10 diffractometer with a Philips PW1711/10 proportional detector (**Paper V**). All samples used for structure analysis were collected by quenching the melts on a stainless steel plate at room temperature and ambient air pressure. All measurements were performed at room temperature and ambient air pressure.

4.4.4 Thermodynamic modelling

The thermodynamic phase diagrams (for NaF-CaO-CaF_2 and NaF-CaF_2-$CaCO_3$-Na_2CO_3) were mapped using FactSage thermochemical software and databases (version 6.3).[145] This method for calculating physicochemical data is based on the Gibbs free energy minimum principle. The computation was carried out using the OptiSage module (as general module), which accesses and manipulates information from the thermodynamic databases in FactSage. Decomposition of $CaCO_3$ to CaO and CO_2 was inhibited in the calculation of phase equilibria of the NaF-CaF_2-$CaCO_3$-Na_2CO_3 system. Thermodynamic data (ΔH *and* ΔG) were also calculated using HSC Chemistry software (version 6.1).

5.0 GENERAL RESULTS AND DISCUSSION

The fundamental objective of the present research was to develop a high-temperature CO_2 capture process using CaO in molten alkali and alkaline earth metal halides. To our knowledge, no previous studies had used molten salts as a dissolution/dispersion medium for metal oxides as a means of improving the reactivity of the active substance for absorption of CO_2. Therefore, to address this issue, we performed experiments using CaO-$CaCl_2$, CaO-CaF_2/NaF, CaO-CaF_2/LiF and CaO-CaF_2/$CaCl_2$ systems under various conditions. In short, the intention was to improve carbonation and decarbonation of CaO by dissolution/dispersion of the sorbent in a molten salt matrix. The alkali and alkaline earth metal halides were selected due to their high thermal stability, low vapour pressure, and acceptable liquidus temperature for carbonation/decarbonation reactions.[146-149] As described in a previous section (3.4.5), reversible carbonation of CaO can be achieved by applying a temperature or pressure in the system that ensures thermodynamic equilibrium (Eq. 3). Considering cost, the thermal swing method is more attractive than the pressure swing technique, because the latter requires a reactor construction that is more expensive to run at elevated pressure.[34] Therefore, we investigated CO_2 desorption at the increased temperature required to achieve thermodynamic equilibrium.

Hydrolysis of the metal halides produces metal oxides that may have an impact on the liquidus temperatures and on the CO_2 capture capacity. In addition, the formation of trace amounts of complex intermediates can occur in the melt systems. Accordingly, the phase diagram data presented below were based on the precursor concentrations that were initially used in the experiments. In all cases, the carrying capacity of the sorbent (g CO_2/g CaO) or CaO/$CaCO_3$ conversion was calculated with reference to the initial amounts of CaO in the molten salts. Unless otherwise indicated, the carbonation and decarbonation conversions were computed using data from the FTIR gas analysis and weight change measurements. Corrosion of the stainless steel chamber had a small effect on the recorded reactor weight change, and this was taken into account when calculating the total carbonation/decarbonation conversions of the sorbent.

5.1 Phase diagram analysis

Thermodynamic data on molten salts are essential in the development of many industrial operations, including extractive metallurgy and electrochemical processes.[146-148,150,151] However, it is difficult to obtain experimental physicochemical data on the metal halides, because these compounds function at high temperatures or are hygroscopic or corrosive in nature. Thermodynamic modelling is more attractive for studying the phase activities in the melts. The phase transitions of CaO, $CaCO_3$, and Na_2CO_3 in CaF_2/NaF have not been investigated or simulated experimentally in earlier studies, and thus the work done in this part of the thesis aimed to develop the partial phase diagrams of NaF-CaF_2, NaF-CaF_2-CaO, NaF-CaF_2-$CaCO_3$, NaF-CaF_2-$NaCO_3$ and NaF-CaF_2-Na_2CO_3-$CaCO_3$ systems by TA, thermodynamic calculations (FactSage) and XRD.

$NaF\text{-}CaF_2$

Initially, phase diagram of the $NaF\text{-}CaF_2$ system was experimentally investigated to find the most suitable melting temperature for CaO carbonation. This system was experimentally investigated and the results show the eutectic composition at 68.1 mole% NaF, and the eutectic temperature at 814.8 ºC (Figure 2 in **Paper I**). It was also noted that $NaF\text{-}CaF_2$ is a simple eutectic system. Comparing these findings with data reported by Fedotieff et al.[152] and by Beilmann et al.[147] it was demonstrated that the composition of the binary eutectic between NaF and CaF_2 determined in our study corresponds well with values found in the accessible literature. The solidus line presented at 1151 ºC describes the transition of alpha-CaF_2 solid solution to beta-CaF_2 that was obtained by Beilmann et al.[147] and Kim et al.[153]. Furthermore, the XRD pattern peaks of the quenched molten samples may be assigned to the characteristic peaks of CaF_2 and NaF.

$CaO\text{-}CaF_2\text{-}NaF$

A good description of CaO solubility in the $NaF\text{-}CaF_2$ melt might facilitate selection of the most suitable chemical composition for the CO_2 capture process. Therefore, the liquidus and solidus lines of the CaO in the $NaF\text{-}CaF_2$ melt were experimentally investigated by TA method and calculated using FactSage software (Figure 4 in **Paper I**). CaO solubility was found to be very low at a fixed NaF/CaF_2 ratio in the eutectic composition. The partial phase diagram of the $CaO\text{-}CaF_2/NaF$ system resulted in a eutectic temperature of 814.7 ºC, which agrees with the eutectic point of CaF_2/NaF. In addition, the simulated phase equilibria resulted in a eutectic point of 813 ºC, which is similar to that determined by TA, and the eutectic coordinates were determined to be 0.202 mole% CaO and 31.55 mole% CaF_2 close to the NaF corner. Enhancement of CaO solubility was observed at increased CaF_2 concentrations. The compositions with higher CaO concentrations in the CaF_2 corner had high liquidus temperatures, and thus they might lead to substantial difficulties when experimentally operating at those temperatures. Consequently, it was selected to study CaO conversion to carbonates and regeneration in the NaF/CaF_2 melt at a fixed eutectic composition.

$CaCO_3\text{-}CaF_2\text{-}NaF$

When using a fixed eutectic ratio of NaF/CaF_2 to optimize the absorption/desorption of CO_2 by CaO, one of the most important goals was to achieve thermal stability of the formed carbonates. To accomplish that objective, we used a TA technique to investigate the liquid phase of the $CaCO_3\text{-}CaF_2/NaF$ system under a pure CO_2 atmosphere. During the measurements of the $CaCO_3\text{-}CaF_2/NaF$ melt with increased $CaCO_3$ mass proportion in the fluoride melt, the liquidus temperature increased significantly and the eutectic point was not detected in the temperature range 750–900 ºC (Figure 5 in **Paper I**). This may be explained by the additional formation of CaF_2 in the reaction between $CaCO_3$ and NaF, as described in Equation 15. The calculations of Gibbs free energy for this equation demonstrated that the reaction can occur at any temperature. It was also plausible that sodium–calcium carbonates could have been formed rather than sodium bicarbonates such as $Na_2Ca_2(CO_3)_3$ (shortite) and $Na_2Ca(CO_3)_2$ (nyerereite). However, structural analysis of the sample consisting of 10 wt%

$CaCO_3$ in the CaF_2/NaF mixture suggested that the pattern of XRD peaks may be attributed to the crystal structures of Na_2CO_3, NaF, and CaF_2.

$$CaCO_3 + 2NaF \leftrightarrow Na_2CO_3 + CaF_2 \quad (15)$$

Na_2CO_3-CaF_2-NaF

An experimental analysis of Na_2CO_3 phase transitions in the eutectic composition of the CaF_2/NaF melt is illustrated in Figure 8 in **Paper I**. This partial phase diagram demonstrates solidus lines, liquidus lines, and estimated solvus lines that may be attributed to CaF_2, CaF_2/NaF. The solvus line projected at 720 ºC (indicated by the dashed red line in the Figure 8 in **Paper I**) near the CaF_2/NaF corner may be explained by formation of a homogeneous solid solution of CaF_2/NaF. As mentioned above, sodium or calcium carbonates in the NaF-CaF_2 system can cause formation of sodium–calcium carbonates through the substitution of a calcium or a sodium cation in Na_2CO_3 or Ca_2CO_3, respectively. Cooper et al.[154] have demonstrated a phase diagram of the Na_2CO_3/Ca_2CO_3 system that shows shortite formation at temperatures below 335 ºC and nyerereite a temperature lower than 817 ºC. In our study, the impact of the concentration of Na_2CO_3 in the CaF_2/NaF system on the liquidus temperature was evaluated at 600–870 ºC, and thus the phase transition from nyerereite to shortite was not observed. Also, TA data suggested that formation of nyerereite could be assigned to the solidus lines in the NaF/CaF_2 corner at 721 ºC and in the Na_2CO_3 corner at 665 ºC. Furthermore, the intensities of the diffraction peaks of Na_2CO_3 and $Na_2Ca(CO_3)_2$ were enhanced at reduced concentrations of NaF/CaF_2 in the Na_2CO_3-CaF_2/NaF system (Figure 6 in **Paper I**).

Na_2CO_3-$CaCO_3$-CaF_2-NaF

The phase equilibrium diagram of the Na-Ca//F-CO_3 system was calculated using FactSage to comprehensively demonstrate the activity of the carbonates in the NaF-CaF_2 melt (Figure 7 in **Paper I**). The results showed that this system has three phase boundary points at 541, 553, and 567 ºC. A ternary eutectic was observed at 541 ºC, the temperature at which decomposition of nyerereite to Na_2CO_3 and CaF_2 was found to occur. The data also indicated that a solid solution of $CaCO_3$ is formed from the decomposition of $Na_2Ca(CO_3)_2$ at 553 ºC in fractions of 74 mole% carbonates in fluorides and 56 mole% of calcium ions. Other solid solution transitions were also demonstrated, such as of alpha-CaF_2, beta-CaF_2, NaF, Na_2CO_3, and $CaCO_3$. The solidification temperature of the intermediate compound $Na_2Ca_2(CO_3)_3$ (shortite) was not determined in the FactSage simulation.

5.2 CO_2 capture by CaO in CaF_2/MF (M=Li or Na)

Use of the CaO-CaF_2/NaF and CaO-CaF_2/LiF systems in the CO_2 capture processes was evaluated in two studies (**Papers II and V**). The eutectic compositions of 41.85 wt% CaF_2 in NaF (**Paper I**) and 42.2 wt% CaF_2 in LiF[147,155] were selected as dissolution/dispersion liquids for CaO to investigate the sorption characteristics of CO_2. First, the Gibbs free energy values

for possible reactions, as described by Equations 3, 16, and 17 (M = Li or Na), were simulated using HSC Chemistry software (version 6.1), and the results are depicted in Figure 5.1.

$$CaCO_3 + 2MF \leftrightarrow M_2CO_3 + CaF_2 \quad (16)$$

$$CaO(s) + CO_2(g) + 2MF \leftrightarrow M_2CO_3 + CaF_2 \quad (17)$$

As mentioned above, formation of alkali and alkaline earth metal carbonates might also be expected (Eqs. 18 and 19). However, the results demonstrated that such complexes are thermodynamically stable at lower temperatures than the melting points of the chemical components.

$$3CaCO_3 + 2MF \leftrightarrow M_2Ca_2(CO_3)_3 + CaF_2 \quad (18)$$

$$M_2Ca_2(CO_3)_3 \leftrightarrow M_2Ca(CO_3)_2 + CaCO_3 \quad (19)$$

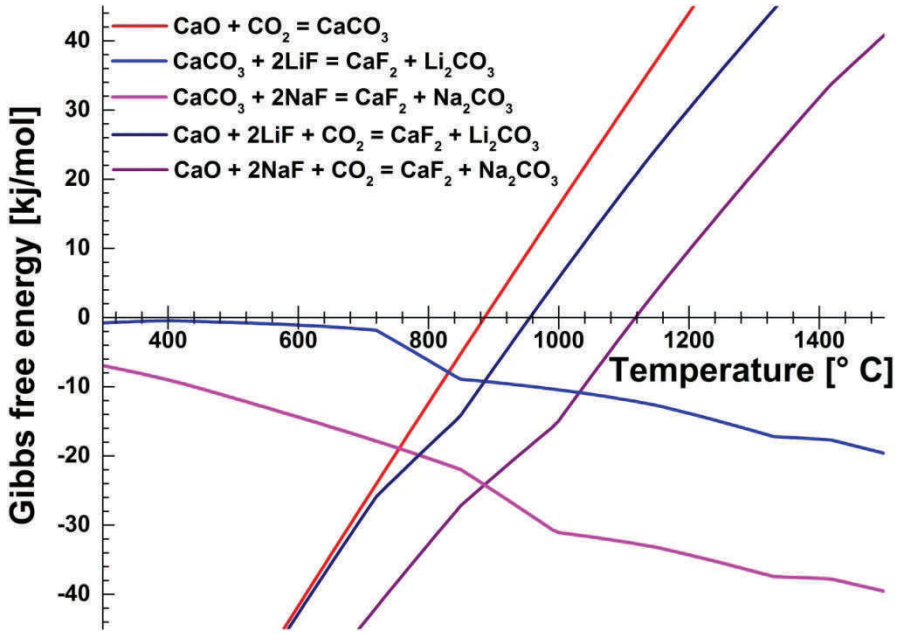

Figure 5.1 Gibbs free energy versus temperature for possible carbonation/decarbonation reactions in the CaO-CaF_2/MF system (M = Li or Na).

The Gibbs free energy for Equation 3 becomes negative at around 900 ºC, which agrees well with the results of other thermodynamic simulations and experiments.[20,21,63,67] In Figure 5.1, it can be seen that the alkali metal carbonates are thermodynamically more stable than calcium carbonate at all temperatures in the range 200–1500 ºC. For Equation 17, Gibbs free energy is close to zero at 1120 ºC for sodium carbonate and at 960 ºC for lithium carbonate formation. Therefore, decomposition should be performed at > 1120 ºC for the Na_2CO_3 formed and at > 960 ºC for the Li_2CO_3. The formation of Na_2CO_3 was confirmed by XRD analysis of the quenched samples collected during performance of the carbonation and decarbonation steps (Figures 2 and 3 in **Paper II**). In addition, a baseline study of CO_2 absorption/desorption by

the CaF_2/NaF melt without CaO was conducted to confirm that CaO is an active material (SI Figure S2 for **Paper II**). It was observed that all the CO_2 applied was emitted from the reactor, and thus there was no sorption of CO_2. Therefore, we suggest that the total reaction occurring in the CaO-CaF_2/MF system (M = Li or Na) can be described by Equation 17, where CaO initially reacts with CO_2 to form $CaCO_3$, which is simultaneously converted to the more stable alkali metal bicarbonate (M_2CO_3).

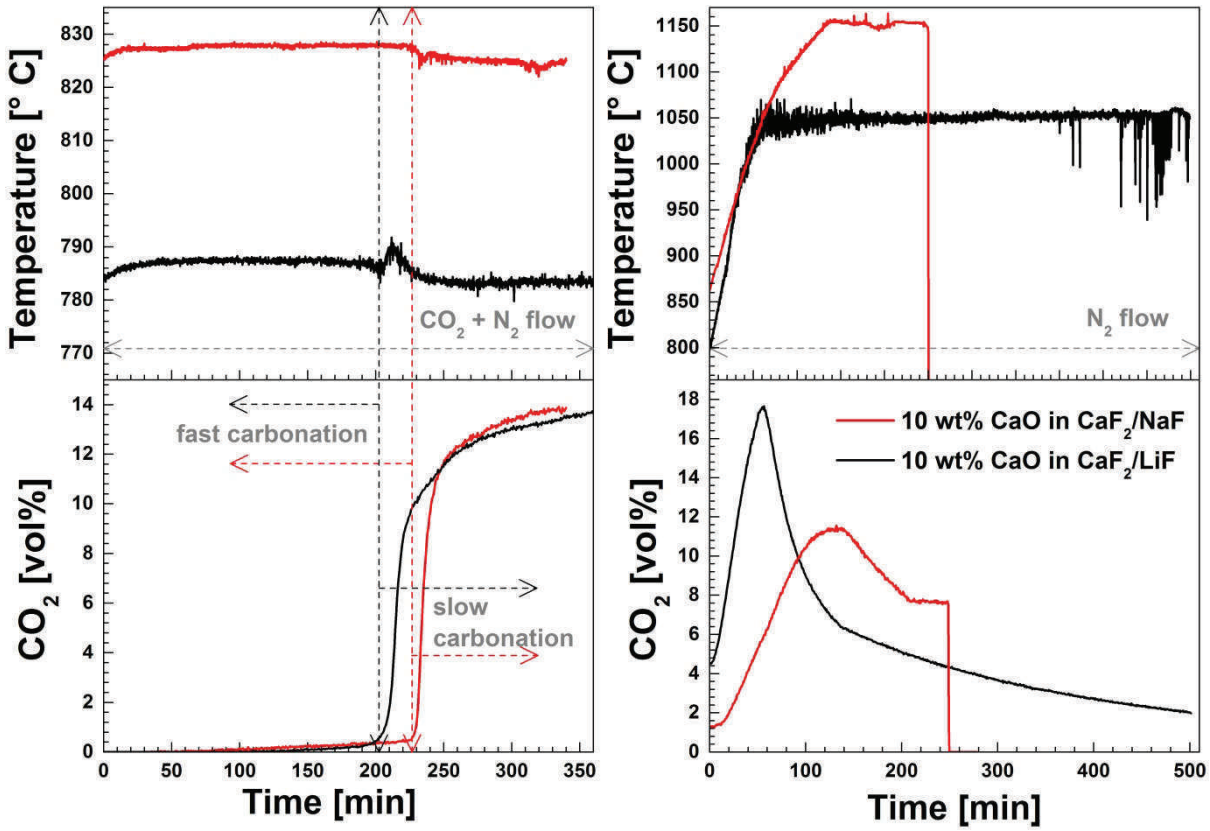

Figure 5.2. The influence of the composition of the molten halide salts on 10 wt% CaO carbonation (left side) and decarbonation of the formed carbonates (right side). CO_2 absorption/desorption was carried out using CaO/CaF_2/NaF (10/41.8/48.2 wt%) and CaO/CaF_2/LiF (10/38/52 wt%) (**Paper V**). The carbonation step was conducted by bubbling 14 vol% CO_2 in N_2 through the melt, and this was done at 826 and 787 ºC for CaO/CaF_2/NaF and CaO/CaF_2/LiF, respectively. Decarbonation was performed under flow of pure N_2 at 1153 ºC for CaO/CaF_2/NaF and at 1050 ºC for CaO/CaF_2/LiF.

The composition of the outlet gas during carbonation and decarbonation of the CaO/CaF_2/NaF (10/41.8/48.2 wt%) and CaO/CaF_2/LiF (10/38/52 wt%) samples was evaluated (**Paper V**), and the results are presented in Figure 5.2. The liquidus temperature of the eutectic composition of CaF_2/LiF (765 ºC)[147] is lower than that of CaF_2/NaF (814.8 ºC), thus we investigated CO_2 absorption by the CaF_2/LiF system at 787 ºC, which was 40 ºC lower than the temperature used for carbonation of CaO/CaF_2/NaF. The temperatures recorded using a Type S thermocouple indicated that the melt temperature increased by 4–6 ºC compared to the set point, possibly due to the exothermic reaction of CaO with CO_2 (Eq. 3). The CO_2 concentration curves clearly exhibit two stages: fast and slow carbonation reactions. The

initial carbonation reaction stage might be attributed to fast CaO carbonation, which is highly selective for CO_2 (99.9 % of the CO_2 applied is removed). The fast carbonation stage is due to the reaction of CO_2 with solid CaO dispersed in the CaF_2/MF melt. When the melt temperature returns to the set point, and there is a significant increase in the concentration of CO_2, the slow carbonation stage begins, which is known to be completed when the level of CO_2 in the outlet gas is equal to that in the inlet gas. This second carbonation stage might be the result of carbonation of the dissolved and agglomerated CaO that is covered by a layer of carbonate. The total carrying capacity of both CaO-CaF_2/MF melt systems was around 0.73 g CO_2/g CaO. However, decomposition of the formed carbonates was not complete. Greater efficiency of CO_2 and CaO regeneration was achieved using the CaO-CaF_2/LiF system than with the CaO-CaF_2/NaF system (83.8 % and 47.5 %, respectively).

CaO-CaF_2/NaF and CaO-CaF_2/LiF had similar carbonation characteristics, thus we suggest that the same reaction occurs in both systems and involves formation of alkali metal carbonates due to the thermodynamically favourable reaction (Eq. 17). The economically efficient sorbents are preferred for industrial applications, and hence the carbonation/decarbonation process was further investigated using the CaO-CaF_2/NaF system (**Paper II**). Effects of the following operating conditions were evaluated: temperature for the carbonation/decarbonation reactions, CaO concentration in the melt, and CO_2 content in the inlet gas.

The impact of CO_2 absorption temperature was investigated by bubbling 14 vol% CO_2 in N_2 through a melt consisting of 5 wt% CaO and 44.2 wt% CaF_2 in NaF for 300 min at temperatures in the range 821–950 ºC. The most efficient CO_2 capture capacity was observed at 826–834 ºC (SI Figure S3 for **Paper II**). The carbonation conversion efficiency was slightly reduced from 95 to 91 wt% by increasing CO_2 absorption temperature from 834 to 950 ºC (Figure 4 in **Paper II**), possibly due to thermodynamically stable formation of alkali metal carbonates (Eq. 17). Therefore, the optimum carbonation temperature for CaO-CaF_2/NaF system was assumed to be in the range 820–840 ºC.

As outlined above, it is necessary to determine the mechanism of the decarbonation reaction. Accordingly, the impact of the temperature of the system on CO_2 desorption by raising the temperature to values in the range 994–1163 ºC was investigated (SI Figure S4 for **Paper II**). For this purpose, a sample of 5 wt% CaO and 44.2 wt% CaF_2 in NaF was prepared and carbonated at 830 ºC under 14 vol% CO_2 in N_2 flow for 300 minutes. The calculated CaO regeneration efficiency for 170 minutes of desorption indicated enhanced CO_2 regeneration at increased temperatures (Figure 5 in **Paper II**). FTIR gas analysis did not detect complete regeneration of the formed carbonates back to CaO and CO_2, because the nickel tube was blocked by CaO precipitation.

The carbonation temperature parameters elucidated at this stage in our study had shown promising carrying capacities of the sorbents. It is also of interest to know how the content of CaO in CaF_2/NaF (46.5/53.5 wt%) affects the CO_2 sorption behaviour (Figure 6 in **Paper II**). To address this issue, carbonation of the samples with various amounts of CaO (5–20 wt%) in CaF_2/NaF was carried out at 825–835 ºC under 14 vol% CO_2 in N_2, and the decarbonation step was performed at 1160–1170 ºC in an atmosphere of pure N_2. In these experiments,

increasing the CaO concentration from 10 to 20 wt% reduced the carrying capacity of the sorbent from 0.74 to 0.59 g CO_2/g CaO (Figure 7 in **Paper II**), possibly due to deposition and agglomeration of CaO present at > 10 wt% in the melt. The regeneration efficiency of CaO calculated for the total amount carbonated sorbent showed increased desorption of CO_2 at higher metal oxide concentrations (Figure 7 in **Paper II**). This improvement in regeneration efficiency when using higher CaO concentrations in the melt might be explained by slower CaO solidification and agglomeration on carbonated particles, and in the nickel tube caused by a reduction in the melting point of the total chemical composition, which is significantly affected by the formed carbonates.

The influence of composition of the inlet gas on carbonation/decarbonation of CaO in the CaO/CaF_2/NaF (5/44.2/50.8 wt%) system was also investigated. In this case, the concentration of CO_2 in N_2 was varied between 1.3 and 14 vol% at 825–835 ºC during carbonation, and decarbonation was carried out at 1160–1170 ºC under pure N_2 (Figure 8 in **Paper II**). It was observed that the carrying capacity of the sorbent was not affected by the CO_2 concentration and was in the range 0.72–0.74 g CO_2/g CaO. Nevertheless, evaluation of the fast and slow carbonation reactions demonstrated that the conversion of CaO in the former decreased from 89.5 % to 70.1 % when the concentration of CO_2 in N_2 was decreased from 14 to 1.3 vol%. Thus the reactivity of the sorbent with CO_2 was prolonged during the slow carbonation stage. In this case, the fast and slow carbonation reaction rates might be explained by the liquidus temperature of the CaO-NaF/CaF_2 system. As mentioned above, the fast carbonation reaction might be affected by the reaction of dispersed CaO with CO_2. It is possible that slow formation of the carbonates occurring in the melt when a smaller amount of CO_2 is applied can influence the solubility, dispersion, and deposition of unreacted CaO, as well as the liquidus temperature of the melt. Therefore, further studies are needed to elucidate the additional dissolution/dispersion of solid CaO caused by reducing/increasing reaction rates.

5.3 CO_2 capture by CaO in $CaCl_2$

Substantial amounts of energy were required to regenerate the carbonates that were formed during capture of CO_2 by CaO that was dissolved or partly dissolved in CaF_2/MF (M = Li or Na) melts. Therefore, a study in which it was assumed that the ion exchange reaction could not take place in the melts was conducted (**Paper III**). $CaCl_2$ was selected as the molten liquid for the dissolution or partial dissolution of CaO. Initially, parametric evaluations of CO_2 capture by CaO in $CaCl_2$ were performed. The efficiency of the carbonation and decarbonation reactions was assessed at 768–830 ºC by bubbling simulated flue gas (14 vol% CO_2 in N_2) through the melt (5 wt% CaO in $CaCl_2$). Thereafter, desorption of CO_2 was performed at temperatures in the range 910–950 ºC under pure N_2, which showed that the optimum carbonation temperature for this system was 768–800 ºC (Figure 2 in **Paper III**). Regeneration of the carbonated sample (initially consisting of 5 wt% CaO in $CaCl_2$) performed at 900–948 ºC resulted in complete desorption of CO_2.

Large-scale CO_2 capture units can consist of the reactors, the height of which should be chosen in relation to the capture characteristics of the sorbent in molten salt and the operating

conditions. The impact of the weight of the sample (5.32 wt% CaO in $CaCl_2$) on the conversion of CaO to $CaCO_3$ was evaluated by increasing the height of the melt column from 10 cm to 20 cm (Figure 3 in **Paper III**). A slightly improved sorbent initial carbonation conversion efficiency of 57.5 wt% was achieved when using a sample column with a height of 20 cm, as compared to 56.0 wt% conversion in the 10 cm column. This might be attributed to prolonged contact time between the gas and liquid as a result of the increased reactive surface area of the sorbent.

Increasing the CaO content in $CaCl_2$ from 5.32 to 15 wt% significantly enhanced the total carbonation conversion at 790–800 ºC from 56 to 69 wt% (Figure 4 in **Paper III**). The CO_2 absorption efficiency was slightly decreased at > 15 wt% CaO. It is plausible that the reduction in the carrying capacity of the sorbent in the melts saturated with CaO was due to the decrease in the available CaO surface area caused by agglomeration and sedimentation of the CaO particles. Decomposition of the carbonates that were formed was complete at 930–940 ºC under N_2, when the samples contained less than 10 wt% sorbent. Assessments of CO_2 desorption of the carbonated samples prepared with 15–20 wt% CaO in the melt under ~14 vol% of CO_2 in N_2 (Figure 4 in **Paper III**) and pure CO_2 (Figure 7 in **Paper V**) indicated nearly 100 % efficient decomposition of the carbonates. This observation suggested that agglomeration and sedimentation of CaO in the nickel tube (which was used to transport the simulated flue gases through the melt) occurred when the melt was saturated with CaO, and therefore use of either the CO_2/N_2 gas mixture or pure CO_2 reduced the sedimentation of CaO in the tube due to fast reaction of this compound with CO_2 and rapid decomposition during decarbonation.

5.4 CO_2 capture by CaO in $CaCl_2/CaF_2$

The study reported in **Paper IV** examined the CO_2 uptake behaviour of CaO in a $CaF_2/CaCl_2$ melt. Absorption of CO_2 by CaO (5–20 wt%) dissolved or partly dissolved in $CaF_2/CaCl_2$ (13.8 wt% CaF_2 in $CaCl_2$) was conducted at various carbonation temperatures (658–759 ºC, depending on the chemical composition) under ~14 vol% CO_2 in N_2. The results show that the efficiency of conversion to carbonates was enhanced at low temperatures and at increased CaO content (Figure 2 in **Paper IV**). The most stable carrying capacities were achieved using 15 and 20 wt% CaO in the molten salt with the carbonation reaction at 675–715 ºC (Figure 3 in **Paper IV**). Also, the CO_2 concentration curves exhibited two reaction stages (slow and fast) for 15 and 20 wt% CaO in the $CaF_2/CaCl_2$ melt, which might be attributed to the phase relationships in the CaO-$CaF_2/CaCl_2$ melt at various temperatures and compositions. By comparison Wenz et al.[146] obtained a phase diagram of the CaO/$CaF_2/CaCl_2$ system showing a eutectic mixture of 2.5 wt% CaO, 12.9 wt% CaF_2 in $CaCl_2$, and melts at 625 ºC. Thus the fast and efficient carbonation stage may be related to reaction of dispersed CaO with CO_2 and the lower CO_2 uptake efficiency of the carbonation of dissolved/agglomerated CaO.

CO_2 desorption temperature is another operating parameter of the CO_2 capture process that was evaluated. Our initial work showed that CO_2 absorption by 15 wt% CaO in $CaF_2/CaCl_2$ (11.7/73.3 wt%) exhibited good carbonation conversion, thus this composition was selected for further analysis. Carbonation of the sample was initially conducted at 695–705 ºC under

14 vol% CO_2 in N_2 for 550 minutes. The conversion of CaO to $CaCO_3$ over the initial CO_2 absorption cycle was observed to be ~76.5 %. When the carbonation stage was complete, the supply of CO_2 gas was discontinued, and desorption of CO_2 was performed by raising the temperature of the system to the specific desorption temperature (899–947 ºC) under pure N_2 for 550 minutes. CaO regeneration was calculated on the basis of the total amount of CaO reacted during the carbonation process. As shown in Figure 4 in **Paper IV**, the efficiency of CO_2 and CaO regeneration in the molten $CaF_2/CaCl_2$ system decreased at temperatures lower than 927 ºC, and the decomposition process was rapid and complete at higher temperatures.

The desorption characteristics of various concentrations of CaO in $CaF_2/CaCl_2$ at 935–945 ºC under pure N_2 are illustrated in Figure 5 in **Paper IV**. The effect of CaO concentration on CO_2 and CaO regeneration was negligible in the melts comprising less than 15 wt% CaO, and this may have been related to the data showing that solubility in the $CaF_2/CaCl_2$ melt was lower for CaO than for $CaCO_3$.[146] In this case, formation of the $CaF_2/CaCl_2$ melt saturated with CaO from the decomposition of $CaCO_3$ influenced the performance of the CO_2 desorption process. It was observed that the gas transport was blocked by precipitation of the regenerated CaO in the nickel tube used to handle the flow of N_2. Therefore, the carbonates initially formed in the experiment using 20 wt% CaO in the $CaF_2/CaCl_2$ system were almost completely decomposed under ~14 vol% CO_2 in N_2.

When evaluating CO_2 sorbents, it is essential to assess the impact of the CO_2 concentration in the inlet gas on the characteristics of CO_2 absorption. Figure 6 in **Paper IV** shows the effect of the content of CO_2 in N_2 on the carrying capacity of 15 wt% CaO in $CaF_2/CaCl_2$ (11.7/73.3 wt%). The carbonation of the sample was conducted by varying the amount of CO_2 from 0.8 to 14 vol% (total gas flow rate 0.6 l/min) at 700–710 ºC, which showed that conversion of CaO to $CaCO_3$ was not affected by CO_2 concentrations higher than 5.6 vol% in the inlet gas. A rapid decrease in CaO activity from 0.601 to 0.427 g CO_2/g CaO occurred when the CO_2 content in N_2 was reduced from 9.7 to 0.8 vol%. Under pure N_2 at 935–945 ºC, desorption of CO_2 was rapid, complete, and independent of the CO_2 concentration.

5.5 Cyclic CO_2 capture by CaO in calcium halides

Studies are needed to elucidate the cyclic carbonation behaviour of CaO in metal halides salts. Figure 5.3 shows the cyclic carbonation conversions of 5.32 wt% CaO in $CaCl_2$ and 15 wt% $CaF_2/CaCl_2$ (11.7/73.3 wt%) melts at different carbonation and decarbonation temperatures (**Papers III and IV**). The lower eutectic temperature of the $CaF_2/CaCl_2$ melt (645 ºC) made it possible to perform the carbonation of CaO at a lower temperature in this system than in the $CaCl_2$ system (melting temperature 750 ºC).[146,156] Hence, CaO exhibited higher conversion efficiency when dissolved/dispersed in the $CaF_2/CaCl_2$ melt than in the $CaCl_2$ (**Papers III and IV**). The stabilized carrying capacities of CaO in the CO_2 cyclability tests were achieved after the initial 4–6 cycles. Furthermore, average carrying capacities of 0.498 g CO_2/g CaO at 799 ºC and 0.504 g CO_2/g CaO at 787 ºC for the $CaO/CaCl_2$ (5.32/94.68 wt%) system, and 0.667 g CO_2/g CaO at 705 ºC for the $CaO/CaF_2/CaCl_2$ (15/11.7/73.3 wt%) system were observed after 10–12 CO_2 capture cycles.

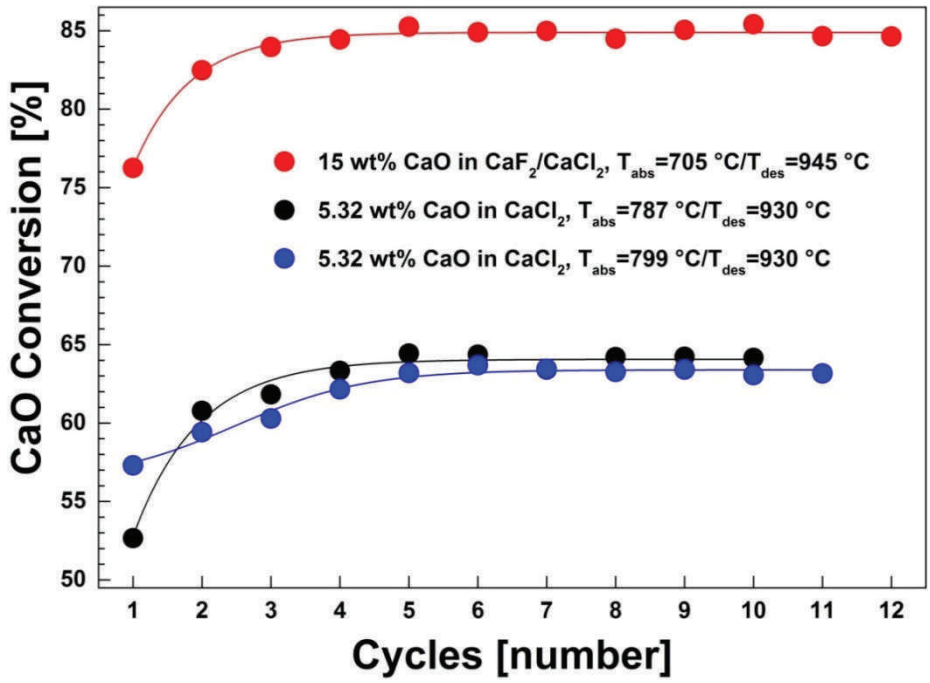

Figure 5.3. CaO conversion during the cyclic carbonation/decarbonation of the $CaO/CaCl_2$ (5.32/94.68 wt%) and $CaO/CaF_2/CaCl_2$ (15/11.7/73.3 wt%) samples. Carbonation of the samples was conducted at 705 (●), 787 (●) and 799 (●) ºC while bubbling 14 vol% CO_2 in N_2 through the melt. Decomposition of the formed carbonates was performed by raising the temperature of the system to 930 (● and ●) and 945 (●) ºC under pure N_2.

5.6 Effect of the formation of CO, HF, and HCl

It has been demonstrated that calcium looping technology can be used in multi-pollutant removal processes in which sulphur-containing species, halides, ash, and particulate matter are co-captured with CO_2 from flue gases.[117,119] However, these pollutants have an important impact on reversible absorption of CO_2 by CaO-based sorbents that leads to a decrease in long-term CO_2 removal capacity.[8,108,119] As noted above, the hydration of metal halides can result in formation of metal oxides and hydroxides, and complexes of those compounds, as well as halide species (HX or X_2, where X represents a halide ion).[157,158] Also, the CO_2 reduction process can generate CO or ash, which can affect the efficiency of carbonation conversion of CaO. Thus, the influence of these impurities on industrial performance and environment should be taken into consideration. Accordingly, the concentrations of HF, HCl, and CO in the outlet gas were also examined in all of the present CO_2 capture tests using CaO dissolved/dispersed in molten salts.

CaO-CaF_2/NaF

Investigation of the formation of HF and CO during CO_2 capture using 5 and 20 wt% CaO in CaF_2/NaF (41.85/48.15 wt%) showed that the release of HF did not depend on the concentration of CaO in the molten salt (Figure 9 in **Paper II**). The trace amounts of HF (10–50 ppm) that were detected might be explained by hydrolysis of the metal fluorides, which is

affected by the moisture in the inlet gas. The concentration of CO in the outlet gas was also determined by FTIR gas analysis (Figure 9 in **Paper II**) and, in contrast to the level of HF, was found to depend on the amount of CaO in the molten salt. The formation of CO was close to 0 ppm during the initial rapid carbonation step at 821–826 ºC for both the CaO concentrations in the melt. However, the slow carbonation step using 5 wt% CaO in CaF_2/NaF exhibited a CO peak of 470 ppm, which was more than twice as high as that seen for the sample containing 20 wt% CaO. Decomposition of the formed carbonates was conducted at elevated temperatures (1125 and 1158 ºC), which significantly affected the release of CO, with a peak of 9000 ppm detected in both the CaO-CaF_2/NaF systems. Such formation of CO is induced by reduction of CO_2 by iron at high temperatures, or by the Boudouard reaction.

CaO-$CaCl_2$ and CaO-CaF_2/$CaCl_2$

In analyses of the emissions of CO, HCl (Figure 8 in **Paper III** and Figure 10 in **Paper IV**), and HF (Figure 10 in **Paper IV**) during the cyclic CO_2 capture, trace amounts of CO were detected when using 5.32 wt% CaO in $CaCl_2$ and 15 wt% CaO in CaF_2/$CaCl_2$ (11.7/73.3 wt%). A closer evaluation of these results showed that the concentration of CO detected in each carbonation stage performed was only 0–180 ppm in the CaO-CaF_2/$CaCl_2$ system at ~705 ºC compared to 0–470 ppm in the CaO-$CaCl_2$ system at 787 ºC. Also, a CO peak of around 2900–3000 ppm was observed in all decarbonation steps. The concentration of the CO emitted in the outlet gas depends on the amount of CO_2 released from the reactor, and higher levels of CO may be explained by increased production from the reduction of CO_2 or from the reaction of carbon with CO_2 at high temperatures.

The HCl concentration curves demonstrate that the volume of HCl was affected by the temperature of the system (Figure 8 in **Paper III** and Figure 10 in **Paper IV**). Higher levels of HCl were detected during the initial carbonation step in the CaO-$CaCl_2$ system than in the CaO-CaF_2/$CaCl_2$ system. In the CaO-$CaCl_2$ system a peak of 1500 ppm HCl was observed during the initial decarbonation step at 930 ºC, which decreased to 350 ppm in the last CO_2 capture cycle. By comparison, less HCl (1160 ppm) was formed in the CaO-CaF_2/$CaCl_2$ system during the initial decarbonation at 945 ºC, which significantly reduced to stable peak of ~100 ppm after 6 CO_2 capture cycles. This disparity might be related to the use of a lower amount of $CaCl_2$ in the CaO-CaF_2/$CaCl_2$ than in the CaO-$CaCl_2$ system, which was registered because $CaCl_2$ is more hygroscopic than CaF_2.[159] The HCl concentration during the carbonation stage was close to 10–40 ppm after 10 carbonation/decarbonation cycles.

The concentration of hydrofluoric acid showed a higher peak of 90 ppm in the initial CO_2 capture cycle, which was similar to the concentration curve for HCl (Figure 10 in **Paper IV**), but the level decreased to 14–10 ppm over the rest of the carbonation/decarbonation cycles. The release of HCl and HF in the initial CO_2 capture cycle indicates that there was incomplete drying of the chemical powders used and that trace amounts of moisture affected the hydration of calcium halides. The stable emissions of HF and HCl may have been related to the hydrolysis of calcium halides induced by the moisture in the inlet gas. This finding

indicated that the formation of HF and HCl is affected primarily by the preparation of the sample, the carbonation/decarbonation temperature, and the composition of the system.

It should also be mentioned that hydration of metal halides produces metal oxides that can potentially enhance the CO_2 capture capacity. However, only trace amounts of these species were detected by FTIR gas analysis, and thus the weight change caused by the hydration of the molten salts was considered negligible. In addition, the HCl and HF released may have been co-captured by CaO.[117]

6.0 CONCLUSIONS

This main objective of the present research was to develop a novel CO_2 capture technique using CaO dissolved or partly dissolved in molten halide salts, mainly to investigate the impact of dissolution/dispersion of CaO in the melts on the carbonation/decarbonation reactions. Initially, thermodynamic data on the NaF-CaF_2, NaF-CaF_2-CaO, NaF-CaF_2-$CaCO_3$, NaF-CaF_2-$NaCO_3$, and NaF-CaF_2-Na_2CO_3-$CaCO_3$ systems were examined for investigation of the CO_2 capture technology. The phase diagram of the NaF-CaF_2 system demonstrated a eutectic composition at 814.8 ºC and 31.9 mol% CaF_2, which is appropriate for reaction of CaO with CO_2. The phase relation of the CaO-CaF_2/NaF system indicated low CaO solubility. Increasing the concentration of $CaCO_3$ in CaF_2/NaF (41.85/48.15 wt%) resulted in the raised liquidus temperature of the system, possibly due to the formation of CaF_2 and Na_2CO_3 in the reaction between $CaCO_3$ and NaF. This reaction could have occurred because more stable Na_2CO_3 than $CaCO_3$ is formed at any temperature. In addition, formation of the sodium–calcium carbonate complex ($Na_2Ca(CO_3)_2$, nyerereite) was indicated in the phase diagram of the NaF-CaF_2-Na_2CO_3-$CaCO_3$ system obtained using FactSage. These observations suggest that using the CaO-CaF_2/NaF system for CO_2 capture can result in formation of several carbonates during the carbonation reaction, for example, $CaCO_3$, $Na_2Ca(CO_3)_2$, and Na_2CO_3.

The characteristics of carbonation/decarbonation were investigated experimentally using a one-chamber reactor, FTIR gas apparatus, and gravimetric analysis. The physical basis for CO_2 capture by CaO in a molten eutectic mixture of 41.85 wt% CaF_2 in NaF was also evaluated. Calculations of Gibbs free energy, assessment of carbonation and decarbonation temperatures, and XRD analyses of quenched samples taken during CO_2 absorption and desorption were performed to identify the phases present in the melt. Efficient absorption of CO_2 from a simulated flue gas and desorption of pure CO_2 were observed. The CO_2 was present mainly as Na_2CO_3 formed by an ion exchange reaction (Eq. 17), and the sorbent activity was highest in the temperature range 826–834 ºC. The increase in CaO concentration from 5 to 20 wt% in the molten salt led to reduced efficiency of CO_2 absorption due to precipitation and agglomeration of the sorbent. The total carbonation conversion was independent of the CO_2 concentration in the inlet gas, and the sorbent carrying capacity was in the range 0.722–0.743 g CO_2/g CaO. Decarbonation was conducted by raising the temperature above 1048 ºC. The CO_2 concentration curves revealed a rapid absorption step followed by a slow step, and structure analysis of the reaction products indicated that full decomposition of the formed carbonates could be achieved.

Similar CO_2 uptake characteristics were observed when using the CaO/CaF_2/LiF (10/38/52 wt%) system. A eutectic composition of 42.2 wt% CaF_2 in LiF melted at 765 ºC[147,155], which was lower than the corresponding temperature for 41.85 wt% CaF_2 in NaF (814.8 ºC), thus the carbonation of the CaO/CaF_2/LiF (10/38/52 wt%) system was conducted at 787 ºC. The total carbonation conversion of 10 wt% CaO in the CaF_2/MF (M = Li or Na) melts was around 93 wt%. Nevertheless, regeneration of CaO and CO_2 from the formed carbonates was found to be more efficient in the CaO-CaF_2/LiF system (desorption temperature: 1050 ºC) than in the CaO-CaF_2/NaF system (desorption temperature: 1153 ºC), as demonstrated by values of 83.8 % and 47.5 %, respectively, for the total amount

of reacted CO_2. CO_2 desorption was incomplete in both cases due to the sedimentation and deposition of CaO. Therefore, further research using different reactor designs is needed.

The last part of the research investigated a novel CO_2 capture process using CaO-$CaCl_2$ and CaO-CaF_2/$CaCl_2$ systems. The composition of the calcium halides mixture was chosen at a fixed ratio to the eutectic composition (CaF_2/$CaCl_2$ = 11.7/73.3 wt%), with a liquidus temperature at 645 ºC[147]. The absorption and desorption of CO_2 were examined at various carbonation/decarbonation temperatures, which indicated efficient CaO conversion to carbonates at 768–810 and 658–710 ºC for the CaO-$CaCl_2$ and CaO-CaF_2/$CaCl_2$ systems, respectively. The content of CaO in calcium halides was found to enhance the carbonation conversion when the sorbent concentration was increased from 5 to 15 wt% in the molten salts. Furthermore, CaO concentrations higher than 15 wt% decreased the CO_2 capture capacity of the sorbent, because the active surface area of the CaO was reduced due to sedimentation and agglomeration. For the chemical compositions containing less than 15 wt% CaO, decarbonation of the formed carbonates was complete and rapid at temperatures in the range 904–950 ºC under pure N_2. The actual process of desorption of CO_2 was not dependent on the carbonation conditions used. It was also found that complete regeneration of CaO and CO_2 could be achieved under flow of pure CO_2 or a N_2/CO_2 gas mixture, and that increasing the height of the melt column increased the carbonation rates. Evaluation of the influence of the concentration of CO_2 in N_2 showed that carbonation conversion was significantly diminished at a CO_2 content lower than 5.6 vol%, possibly due to formation of a carbonate layer on unreacted calcium oxide particles. Higher rates of the sorbent conversion to $CaCO_3$ were obtained using CaO/CaF_2/$CaCl_2$ than CaO-$CaCl_2$ system. For example, the maximum carbonation conversion with 15 wt% CaO in $CaCl_2$ was 68.9 wt% at 804 ºC, and the sample consisting of 15 wt% CaO in molten CaF_2/$CaCl_2$ (11.7/73.3 wt%) resulted in sorbent conversion efficiency of 76.7 wt% at 677 ºC. This might have occurred because, at lower carbonation temperatures, the solid CaO reacted more readily with CO_2 to form $CaCO_3$.[20,21]

One of the most promising results for large-scale process integration was observed during the operation of cyclic CO_2 capture. CaO exhibited a more efficient cyclic carrying capacity when using molten CaF_2/$CaCl_2$ as a liquid for CaO dissolution/dispersion than when using molten $CaCl_2$. After the initial 4–6 carbonation/decarbonation cycles, a sustained CO_2 capture capacity was observed in all multiple tests. After 10 CO_2 absorption/desorption cycles, the efficiency of CaO in carbonation conversion had increased from 52.8 to 64.2 wt% at 787 ºC in the CaO/$CaCl_2$ (5.32/94.68 wt%) system, and from 76.4 to 85.5 wt% in the CaO/CaF_2/$CaCl_2$ (15/11.7/73.3 wt%) system. This shows that the dissolution/dispersion of CaO in molten CaF_2/$CaCl_2$ is a promising pathway for improving the reactivity of CaO in long-term cyclic CO_2 capture operation. Further research should consider the possible occurrence of secondary reactions, use of other molten salt compositions, and technical design applications.

7.0 FUTURE PERSPECTIVES

The scope of this thesis focused on development of a novel CO_2 capture process using CaO in molten halide salts. Dissolution and dispersion of CaO in molten alkali and alkaline earth metal halide salts ($CaCl_2$, CaF_2/NaF, CaF_2/LiF, and CaF_2/$CaCl_2$) was performed to enhance the reactivity of CaO with CO_2. It was demonstrated that the CO_2 capture behaviour of CaO in a molten salt is strongly affected by the molten salt itself. Also, the temperature of the system has an important effect on the cyclic CO_2 capture capacity of the sorbent. It appears that the optimum carbonation/decarbonation temperature can be selected based on the salt composition, and therefore research concerning the solubility and activity coefficients of various metal oxides and carbonates in such melts is fundamental for development of the CO_2 capture process. In particular, the mechanisms of the carbonation and decarbonation reactions, which may occur in the molten phase due to the secondary reactions, should be investigated by experimental evaluations of CO_2 capture. Thus different compositions of molten salts and metal oxides/carbonates should be tested in the future.

Industrial processes require the use of CO_2 sorbent material that has a sustained long-term carrying capacity in the presence of other impurities in the flue gas, such as CO, NO_x, SO_x, HCl, HF, and particulate matter, which can have a significant impact on CO_2 capture by CaO in molten salts. Thus it is also essential to assess the effects of other pollutants on the efficiency of cyclic CaO conversion to carbonates.

Most importantly, technical and economic data that realistically simulate the conditions prevailing in post-combustion, pre-combustion, and industrial processes should be investigated. In this context, the selection of a suitable molten salt composition and the structure of the reactor are central to achieving a process that is economically and technically attractive for commercial applications.

REFERENCES

(1) Choi, S.; Drese, J. H.; Jones, C. W.: Adsorbent materials for carbon dioxide capture from large anthropogenic point sources. *Chemsuschem* **2009**, *2*, 796-854.

(2) MacDowell, N.; Florin, N.; Buchard, A.; Hallett, J.; Galindo, A.; Jackson, G.; Adjiman, C. S.; Williams, C. K.; Shah, N.; Fennell, P.: An overview of CO_2 capture technologies. *Energy & Environmental Science* **2010**, *3*, 1645-1669.

(3) Goeppert, A.; Czaun, M.; Prakash, G. K. S.; Olah, G. A.: Air as the renewable carbon source of the future: an overview of CO_2 capture from the atmosphere. *Energy & Environmental Science* **2012**, *5*, 7833-7853.

(4) Jacobson, M. Z.: Review of solutions to global warming, air pollution, and energy security. *Energy & Environmental Science* **2009**, *2*, 148-173.

(5) Zaman, M.; Lee, J. H.: Carbon capture from stationary power generation sources: a review of the current status of the technologies. *Korean Journal of Chemical Engineering* **2013**, *30*, 1497-1526.

(6) Finkenrath, M.: Carbon dioxide capture from power generation - status of cost and performance. *Chemical Engineering & Technology* **2012**, *35*, 482-488.

(7) "The global status of CCS: 2013," Global CCS Institute, 2013.

(8) Koornneef, J.; Ramirez, A.; Turkenburg, W.; Faaij, A.: The environmental impact and risk assessment of CO_2 capture, transport and storage - an evaluation of the knowledge base. *Prog Energ Combust* **2012**, *38*, 62-86.

(9) Edenhofer, O.; Pichs-Madruga, R.; Sokona, Y.; Seyboth, K.; Matschoss, P.; Kadner, S.; Zwickel, T.; Eickemeier, P.; Hansen, G.; Schloemer, S.; Von Stechow, C. "Renewable energy sources and climate change mitigation," Cambridge University Press, 2011.

(10) Dean, C. C.; Blamey, J.; Florin, N. H.; Al-Jeboori, M. J.; Fennell, P. S.: The calcium looping cycle for CO_2 capture from power generation, cement manufacture and hydrogen production. *Chem. Eng. Res. Des.* **2011**, *89*, 836-855.

(11) Zeman, F.: Energy and material balance of CO_2 capture from ambient air. *Environ. Sci. Technol.* **2007**, *41*, 7558-7563.

(12) Pires, J. C. M.; Martins, F. G.; Alvim-Ferraz, M. C. M.; Simoes, M.: Recent developments on carbon capture and storage: an overview. *Chem. Eng. Res. Des.* **2011**, *89*, 1446-1460.

(13) D'Alessandro, D. M.; Smit, B.; Long, J. R.: Carbon dioxide capture: prospects for new materials. *Angewandte Chemie-International Edition* **2010**, *49*, 6058-6082.

(14) Lee, S. C.; Chae, H. J.; Lee, S. J.; Choi, B. Y.; Yi, C. K.; Lee, J. B.; Ryu, C. K.; Kim, J. C.: Development of regenerable MgO-based sorbent promoted with K_2CO_3 for CO_2 capture at low temperatures. *Environ. Sci. Technol.* **2008**, *42*, 2736-2741.

(15) Stendardo, S.; Andersen, L. K.; Herce, C.: Self-activation and effect of regeneration conditions in CO_2-carbonate looping with CaO-$Ca_{12}Al_{14}O_{33}$ sorbent. *Chem. Eng. J.* **2013**, *220*, 383-394.

(16) Sumida, K.; Rogow, D. L.; Mason, J. A.; McDonald, T. M.; Bloch, E. D.; Herm, Z. R.; Bae, T. H.; Long, J. R.: Carbon dioxide capture in metal-organic frameworks. *Chemical Reviews* **2012**, *112*, 724-781.

(17) Zhao, M.; Minett, A. I.; Harris, A. T.: A review of techno-economic models for the retrofitting of conventional pulverised-coal power plants for post-combustion capture (PCC) of CO_2. *Energy & Environmental Science* **2013**, *6*, 25-40.

(18) Li, H.; Bhadury, P. S.; Song, B. A.; Yang, S.: Immobilized functional ionic liquids: efficient, green, and reusable catalysts. *Rsc Advances* **2012**, *2*, 12525-12551.

(19) Figueroa, J. D.; Fout, T.; Plasynski, S.; McIlvried, H.; Srivastava, R. D.: Advances in CO_2 capture technology - The U.S. Department of Energy's Carbon Sequestration Program. *Int. J. Greenh. Gas Control* **2008**, *2*, 9-20.

(20) Blamey, J.; Anthony, E. J.; Wang, J.; Fennell, P. S.: The calcium looping cycle for large-scale CO_2 capture. *Prog Energ Combust* **2010**, *36*, 260-279.

(21) Valverde, J. M.: Ca-based synthetic materials with enhanced CO_2 capture efficiency. *J. Mater. Chem. A* **2013**, *1*, 447-468.

(22) Siefert, N.; Shekhawat, D.; Litster, S.; Berry, D.: Molten catalytic coal gasification with *in situ* carbon and sulphur capture. *Energy & Environmental Science* **2012**, *5*, 8660-8672.

(23) Ray, H. S.: *Introduction to melts. Molten salts, slags and glasses*; Allied Publishers Pvt, Ltd., 2006.

(24) Berstad, D.; Anantharaman, R.; Neksa, P.: Low-temperature CO_2 capture technologies - applications and potential. *International Journal of Refrigeration-Revue Internationale Du Froid* **2013**, *36*, 1403-1416.

(25) Rubin, E. S.; Mantripragada, H.; Marks, A.; Versteeg, P.; Kitchin, J.: The outlook for improved carbon capture technology. *Prog Energ Combust* **2012**, *38*, 630-671.

(26) Di Lorenzo, G.; Barbera, P.; Ruggieri, G.; Witton, J.; Pilidis, P.; Probert, D.: Pre-combustion carbon-capture technologies for power generation: an engineering-economic assessment. *International Journal of Energy Research* **2013**, *37*, 389-402.

(27) Scheffknecht, G.; Al-Makhadmeh, L.; Schnell, U.; Maier, J.: Oxy-fuel coal combustion - a review of the current state-of-the-art. *Int. J. Greenh. Gas Control* **2011**, *5*, S16-S35.

(28) Zhang, M. K.; Guo, Y. C.: Process simulations of large-scale CO_2 capture in coal-fired power plants using aqueous ammonia solution. *Int. J. Greenh. Gas Control* **2013**, *16*, 61-71.

(29) Han, K.; Ahn, C. K.; Lee, M. S.; Rhee, C. H.; Kim, J. Y.; Chun, H. D.: Current status and challenges of the ammonia-based CO_2 capture technologies toward commercialization. *Int. J. Greenh. Gas Control* **2013**, *14*, 270-281.

(30) Hedin, N.; Andersson, L.; Bergstrom, L.; Yan, J. Y.: Adsorbents for the post-combustion capture of CO_2 using rapid temperature swing or vacuum swing adsorption. *Applied Energy* **2013**, *104*, 418-433.

(31) Huang, Q. L.; Eic, M.: Commercial adsorbents as benchmark materials for separation of carbon dioxide and nitrogen by vacuum swing adsorption process. *Separation and Purification Technology* **2013**, *103*, 203-215.

(32) Liu, Y. Y.; Wang, Z. Y. U.; Zhou, H. C.: Recent advances in carbon dioxide capture with metal-organic frameworks. *Greenhouse Gases-Science and Technology* **2012**, *2*, 239-259.

(33) Adewole, J. K.; Ahmad, A. L.; Ismail, S.; Leo, C. P.: Current challenges in membrane separation of CO_2 from natural gas: a review. *Int. J. Greenh. Gas Control* **2013**, *17*, 46-65.

(34) Mondal, M. K.; Balsora, H. K.; Varshney, P.: Progress and trends in CO_2 capture/separation technologies: a review. *Energy* **2012**, *46*, 431-441.

(35) Yang, H. Q.; Xu, Z. H.; Fan, M. H.; Gupta, R.; Slimane, R. B.; Bland, A. E.; Wright, I.: Progress in carbon dioxide separation and capture: a review. *Journal of Environmental Sciences-China* **2008**, *20*, 14-27.

(36) Koros, W. J.; Mahajan, R.: Pushing the limits on possibilities for large scale gas separation: which strategies? *Journal of Membrane Science* **2000**, *175*, 181-196.

(37) Vatopoulos, K.; Tzimas, E.: Assessment of CO_2 capture technologies in cement manufacturing process. *J. Clean Prod.* **2012**, *32*, 251-261.

(38) Rao, A. B.; Rubin, E. S.: A technical, economic, and environmental assessment of amine-based CO_2 capture technology for power plant greenhouse gas control. *Environ. Sci. Technol.* **2002**, *36*, 4467-4475.

(39) Lee, S.; Maken, S.; Park, J. W.; Song, H. J.; Park, J. J.; Shim, J. G.; Kim, J. H.; Eum, H. M.: A study on the carbon dioxide recovery from 2 ton-CO_2/day pilot plant at LNG based power plant. *Fuel* **2008**, *87*, 1734-1739.

(40) Yang, Z. Z.; He, L. N.; Gao, J.; Liu, A. H.; Yu, B.: Carbon dioxide utilization with C-N bond formation: carbon dioxide capture and subsequent conversion. *Energy & Environmental Science* **2012**, *5*, 6602-6639.

(41) Stadler, H.; Beggel, F.; Habermehl, M.; Persigehl, B.; Kneer, R.; Modigell, M.; Jeschke, P.: Oxyfuel coal combustion by efficient integration of oxygen transport membranes. *Int. J. Greenh. Gas Control* **2011**, *5*, 7-15.

(42) Wall, T.; Liu, Y. H.; Spero, C.; Elliott, L.; Khare, S.; Rathnam, R.; Zeenathal, F.; Moghtaderi, B.; Buhre, B.; Sheng, C. D.; Gupta, R.; Yamada, T.; Makino, K.; Yu, J. L.: An overview on oxyfuel coal combustion - state of the art research and technology development. *Chem. Eng. Res. Des.* **2009**, *87*, 1003-1016.

(43) Pfaff, I.; Kather, A.: Comparative thermodynamic analysis and integration issues of CCS Steam power plants based on oxy-combustion with cryogenic or membrane based air separation. In *Greenhouse Gas Control Technologies 9*; Gale, J., Herzog, H., Braitsch, J., Eds.; Elsevier Science Bv: Amsterdam, 2009; Vol. 1; pp 495-502.

(44) Baciocchi, R.; Storti, G.; Mazzotti, M.: Process design and energy requirements for the capture of carbon dioxide from air. *Chemical Engineering and Processing* **2006**, *45*, 1047-1058.

(45) Chen, W. H.; Tsai, M. H.; Hung, C. I.: Numerical prediction of CO_2 capture process by a single droplet in alkaline spray. *Applied Energy* **2013**, *109*, 125-134.

(46) Stolaroff, J. K.; Keith, D. W.; Lowry, G. V.: Carbon dioxide capture from atmospheric air using sodium hydroxide spray. *Environ. Sci. Technol.* **2008**, *42*, 2728-2735.

(47) Nikulshina, V.; Ayesa, N.; Galvez, M. E.; Steinfeld, A.: Feasibility of Na-based thermochemical cycles for the capture of CO_2 from air - thermodynamic and thermogravimetric analyses. *Chem. Eng. J.* **2008**, *140*, 62-70.

(48) Mahmoudkhani, M.; Keith, D. W.: Low-energy sodium hydroxide recovery for CO_2 capture from atmospheric air - thermodynamic analysis. *Int. J. Greenh. Gas Control* **2009**, *3*, 376-384.

(49) Yin, H. Y.; Mao, X. H.; Tang, D. Y.; Xiao, W.; Xing, L. R.; Zhu, H.; Wang, D. H.; Sadoway, D. R.: Capture and electrochemical conversion of CO_2 to value-added carbon and oxygen by molten salt electrolysis. *Energy & Environmental Science* **2013**, *6*, 1538-1545.

(50) Duan, Y. H.; Sorescu, D. C.: CO_2 capture properties of alkaline earth metal oxides and hydroxides: a combined density functional theory and lattice phonon dynamics study. *Journal of Chemical Physics* **2010**, *133*.

(51) Xiao, G. K.; Singh, R.; Chaffee, A.; Webley, P.: Advanced adsorbents based on MgO and K_2CO_3 for capture of CO_2 at elevated temperatures. *Int. J. Greenh. Gas Control* **2011**, *5*, 634-639.

(52) Li, L.; Li, Y.; Wen, X.; Wang, F.; Zhao, N.; Xiao, F. K.; Wei, W.; Sun, Y. H.: CO_2 capture over $K_2CO_3/MgO/Al_2O_3$ dry sorbent in a fluidized bed. *Energ Fuel* **2011**, *25*, 3835-3842.

(53) Lee, S. C.; Choi, B. Y.; Lee, T. J.; Ryu, C. K.; Soo, Y. S.; Kim, J. C.: CO_2 absorption and regeneration of alkali metal-based solid sorbents. *Catalysis Today* **2006**, *111*, 385-390.

(54) Wu, Y.; Chen, X. P.; Zhao, C. W.: Study on the failure mechanism of potassium-based sorbent for CO_2 capture and the improving measure. *Int. J. Greenh. Gas Control* **2011**, *5*, 1184-1189.

(55) Zhao, C. W.; Chen, X. P.; Zhao, C. S.: CO_2 absorption using dry potassium-based sorbents with different supports. *Energ Fuel* **2009**, *23*, 4683-4687.

(56) Zhao, C. W.; Chen, X. P.; Zhao, C. S.: Multiple-cycles behavior of K_2CO_3/Al_2O_3 for CO_2 capture in a fluidized-bed reactor. *Energ Fuel* **2010**, *24*, 1009-1012.

(57) Zhang, K. L.; Li, X. H. S.; Duan, Y. H.; King, D. L.; Singh, P.; Li, L. Y.: Roles of double salt formation and $NaNO_3$ in Na_2CO_3-promoted MgO absorbent for intermediate temperature CO_2 removal. *Int. J. Greenh. Gas Control* **2013**, *12*, 351-358.

(58) Kondakindi, R. R.; McCumber, G.; Aleksic, S.; Whittenberger, W.; Abraham, M. A.: Na_2CO_3-based sorbents coated on metal foil: CO_2 capture performance. *Int. J. Greenh. Gas Control* **2013**, *15*, 65-69.

(59) Liu, W. Q.; Yin, J. J.; Qin, C. L.; Feng, B.; Xu, M. H.: Synthesis of CaO-based sorbents for CO_2 capture by a spray-drying technique. *Environ. Sci. Technol.* **2012**, *46*, 11267-11272.

(60) Donat, F.; Florin, N. H.; Anthony, E. J.; Fennell, P. S.: Influence of high-temperature steam on the reactivity of CaO sorbent for CO_2 capture. *Environ. Sci. Technol.* **2012**, *46*, 1262-1269.

(61) Shimizu, T. H., T.; Hosoda, H.; Kitano, K.; Inagaki, M.; Tejima, K.: A twin fluid-bed reactor for removal of CO_2 from combustion processes. *Chem. Eng. Res. Des.* **1999**, *77*, 62-68.

(62) Valverde, J. M.; Perejon, A.; Perez-Maqueda, L. A.: Enhancement of fast CO_2 capture by a nano-SiO_2/CaO composite at Ca-looping conditions. *Environ. Sci. Technol.* **2012**, *46*, 6401-6408.

(63) Li, Z. S.; Fang, F.; Tang, X. Y.; Cai, N. S.: Effect of temperature on the carbonation reaction of CaO with CO_2. *Energ Fuel* **2012**, *26*, 2473-2482.

(64) Stamnore, B. R.; Gilot, P.: Review-calcination and carbonation of limestone during thermal cycling for CO_2 sequestration. *Fuel Processing Technology* **2005**, *86*, 1707-1743.

(65) Huang, C. M.; Hsu, H. W.; Liu, W. H.; Cheng, J. Y.; Chen, W. C.; Wen, T. W.; Chen, W.: Development of post-combustion CO_2 capture with CaO/$CaCO_3$ looping in a bench scale plant. In *10th International Conference on Greenhouse Gas Control Technologies*; Gale, J., Hendriks, C., Turkenberg, W., Eds.; Elsevier Science Bv: Amsterdam, 2011; Vol. 4; pp 1268-1275.

(66) Li, F. X.; Fan, L. S.: Clean coal conversion processes - progress and challenges. *Energy & Environmental Science* **2008**, *1*, 248-267.

(67) Anthony, E. J.: Ca looping technology: current status, developments and future directions. *Greenhouse Gases-Science and Technology* **2011**, *1*, 36-47.

(68) Butler, J. W.; Lim, C. J.; Grace, J. R.: CO_2 capture capacity of CaO in long series of pressure swing sorption cycles. *Chemical Engineering Research and Design* **2011**, *89*, 1794-1804.

(69) Wang, W. R., S.; Fan, L. S.: Energy penalty of CO_2 capture for the carbonation-calcination reaction (CCR) process: parametric effects and comparisons with alternative processes. *Fuel* **2013**, *104*, 561-574.

(70) Florin, N. H.; Blamey, J.; Fennell, P. S.: Synthetic CaO-based sorbent for CO_2 capture from large-point sources. *Energ Fuel* **2010**, *24*, 4598-4604.

(71) Manovic, V.; Anthony, E. J.: Parametric study on the CO_2 capture capacity of CaO-based sorbents in looping cycles. *Energ Fuel* **2008**, *22*, 1851-1857.

(72) Blamey, J.; Paterson, N. P. M.; Dugwell, D. R.; Stevenson, P.; Fennell, P. S.: Reactivation of a CaO-based sorbent for CO_2 capture from stationary sources. In *P Combust Inst*, 2011; Vol. 33; pp 2673-2681.

(73) Gonzalez, B.; Grasa, G. S.; Alonso, M.; Abanades, J. C.: Modeling of the deactivation of CaO in a carbonate loop at high temperatures of calcination. *Ind Eng Chem Res* **2008**, *47*, 9256-9262.

(74) Grasa, G. S.; Abanades, J. C.: CO_2 capture capacity of CaO in long series of carbonation/calcination cycles. *Ind Eng Chem Res* **2006**, *45*, 8846-8851.

(75) Bouquet, E.; Leyssens, G.; Schonnenbeck, C.; Gilot, P.: The decrease of carbonation efficiency of CaO along calcination-carbonation cycles: experiments and modelling. *Chemical Engineering Science* **2009**, *64*, 2136-2146.

(76) Martinez, A.; Lara, Y.; Lisbona, P.; Romeo, L. M.: Energy penalty reduction in the calcium looping cycle. *Int. J. Greenh. Gas Control* **2012**, *7*, 74-81.

(77) Abanades, J. C.; Alvarez, D.: Conversion limits in the reaction of CO_2 with lime. *Energ Fuel* **2003**, *17*, 308-315.

(78) Fennell, P. S.; Pacciani, R.; Dennis, J. S.; Davidson, J. F.; Hayhurst, A. N.: The effects of repeated cycles of calcination and carbonation on a variety of different limestones, as measured in a hot fluidized bed of sand. *Energ Fuel* **2007**, *21*, 2072-2081.

(79) Martinez, I.; Grasa, G.; Murillo, R.; Arias, B.; Abanades, J. C.: Evaluation of CO_2 carrying capacity of reactivated CaO by hydration. *Energ Fuel* **2011**, *25*, 1294-1301.

(80) Materic, V.; Sheppard, C.; Smedley, S. I.: Effect of repeated steam hydration reactivation on CaO-based sorbents for CO_2 capture. *Environ. Sci. Technol.* **2010**, *44*, 9496-9501.

(81) Florin, N. H.; Harris, A. T.: Screening CaO-based sorbents for CO_2 capture in biomass gasifiers. *Energ Fuel* **2008**, *22*, 2734-2742.

(82) Yu, F. C.; Phalak, N.; Sun, Z. C.; Fan, L. S.: Activation strategies for calcium-based sorbents for CO_2 capture: a perspective. *Ind Eng Chem Res* **2012**, *51*, 2133-2142.

(83) Al-Jeboori, M. J.; Fennell, P. S.; Nguyen, M.; Peng, K.: Effects of different dopants and doping procedures on the reactivity of CaO-based sorbents for CO_2 capture. *Energ Fuel* **2012**, *26*, 6584-6594.

(84) Wu, G. W.; Zhang, C. X.; Li, S. R.; Huang, Z. Q.; Yan, S. L.; Wang, S. P.; Ma, X. B.; Gong, J. L.: Sorption enhanced steam reforming of ethanol on Ni-CaO-Al_2O_3 multifunctional catalysts derived from hydrotalcite-like compounds. *Energy & Environmental Science* **2012**, *5*, 8942-8949.

(85) Guo, M.; Zhang, L.; Yang, Z. Q.; Tang, Q.: Removal of CO_2 by CaO/MgO and CaO/$Ca_9Al_6O_{18}$ in the presence of SO_2. *Energ Fuel* **2011**, *25*, 5514-5520.

(86) Manovic, V.; Anthony, E. J.: Integration of calcium and chemical looping combustion using composite CaO/CuO-based materials. *Environ. Sci. Technol.* **2011**, *45*, 10750-10756.

(87) Manovic, V.; Anthony, E. J.: Thermal activation of CaO-based sorbent and self-reactivation during CO_2 capture looping cycles. *Environ. Sci. Technol.* **2008**, *42*, 4170-4174.

(88) Manovic, V.; Anthony, E. J.: Long-term behavior of CaO-based pellets supported by calcium aluminate cements in a long series of CO_2 capture cycles. *Ind Eng Chem Res* **2009**, *48*, 8906-8912.

(89) Manovic, V.; Wu, Y. H.; He, I.; Anthony, E. J.: Spray water reactivation/pelletization of spent CaO-based sorbent from calcium looping cycles. *Environ. Sci. Technol.* **2012**, *46*, 12720-12725.

(90) Blamey, J.; Paterson, N. P. M.; Dugwell, D. R.; Fennell, P. S.: Mechanism of particle breakage during reactivation of CaO-based sorbents for CO_2 capture. *Energ Fuel* **2010**, *24*, 4605-4616.

(91) Manovic, V. A., E. J.: Steam Reactivation of Spent CaO-based Sorbent for Multiple CO_2 Capture Cycles. *Environ. Sci. Technol.* **2007**, *41*, 1420-1425.

(92) Materić, V.; Edwards, S.; Smedley, S. I.; Holt, R.: Ca(OH)2 Superheating as a Low-Attrition Steam Reactivation Method for CaO in Calcium Looping Applications. *Ind Eng Chem Res* **2010**, *49*, 12429-12434.

(93) Gupta, H.; Fan, L. S.: Carbonation-calcination cycle using high reactivity calcium oxide for carbon dioxide separation from flue gas. *Ind Eng Chem Res* **2002**, *41*, 4035-4042.

(94) Lu, H.; Khan, A.; Smirniotis, P. G.: Relationship between structural properties and CO_2 capture performance of CaO–based sorbents obtained from different organometallic precursors. *Ind Eng Chem Res* **2008**, *47*, 6216-6220.

(95) Lu, H.; Reddy, E. P.; Smirniotis, P. G.: Calcium oxide based sorbents for capture of carbon dioxide at high temperatures. *Ind Eng Chem Res* **2006**, *45*, 3944-3949.

(96) Lu, H.; Khan, A.; Pratsinis, S. E.; Smirniotis, P. G.: Flame-made durable doped-CaO nanosorbents for CO_2 capture. *Energ Fuel* **2009**, *23*, 1093-1100.

(97) Koirala, R.; Reddy, G. K.; Smirniotis, P. G.: Single nozzle flame-made highly durable metal doped Ca-based sorbents for CO_2 capture at high temperature. *Energ Fuel* **2012**, *26*, 3103-3109.

(98) Xu, P.; Xie, M. M.; Cheng, Z. M.; Zhou, Z. M.: CO_2 capture performance of CaO-based sorbents prepared by a sol-gel method. *Ind Eng Chem Res* **2013**, *52*, 12161-12169.

(99) Luo, C.; Zheng, Y.; Zheng, C. G.; Yin, J. J.; Qin, C. L.; Feng, B.: Manufacture of calcium-based sorbents for high temperature cyclic CO_2 capture via a sol-gel process. *Int. J. Greenh. Gas Control* **2013**, *12*, 193-199.

(100) Karami, D.; Mahinpey, N.: Highly active CaO-based sorbents for CO_2 capture using the precipitation method: preparation and characterization of the sorbent powder. *Ind Eng Chem Res* **2012**, *51*, 4567-4572.

(101) Kierzkowska, A. M.; Poulikakos, L. V.; Broda, M.; Muller, C. R.: Synthesis of calcium-based, Al_2O_3-stabilized sorbents for CO_2 capture using a co-precipitation technique. *Int. J. Greenh. Gas Control* **2013**, *15*, 48-54.

(102) Kim, J. N.; Ko, C. H.; Yi, K. B.: Sorption enhanced hydrogen production using one-body CaO-$Ca_{12}Al_{14}O_{33}$-Ni composite as catalytic absorbent. *International Journal of Hydrogen Energy* **2013**, *38*, 6072-6078.

(103) Karami, D. M., N.: Highly Active CaO-Based Sorbents for CO_2 Capture Using the Precipitation Method: Preparation and Characterization of the Sorbent Powder. *Ind Eng Chem Res* **2012**, *51*, 4567-4572.

(104) Santos, E. T.; Alfonsin, C.; Chambel, A. J. S.; Fernandes, A.; Dias, A. P. S.; Pinheiro, C. I. C.; Ribeiro, M. F.: Investigation of a stable synthetic sol-gel CaO sorbent for CO_2 capture. *Fuel* **2012**, *94*, 624-628.

(105) Salvador, C.; Lu, D.; Anthony, E. J.; Abanades, J. C.: Enhancement of CaO for CO_2 capture in an FBC environment. *Chem. Eng. J.* **2003**, *96*, 187-195.

(106) Manovic, V.; Anthony, E. J.; Grasa, G.; Abanades, J. C.: CO_2 looping cycle performance of a high-purity limestone after thermal activation/doping. *Energ Fuel* **2008**, *22*, 3258-3264.

(107) Sun, P.; Grace, J. R.; Lim, C. J.; Anthony, E. J.: Investigation of attempts to improve cyclic CO_2 capture by sorbent hydration and modification. *Ind Eng Chem Res* **2008**, *47*, 2024-2032.

(108) Partanen, J.; Backman, P.; Backman, R.; Hupa, M.: Absorption of HCl by limestone in hot flue gases. Part II: importance of calcium hydroxychloride. *Fuel* **2005**, *84*, 1674-1684.

(109) Fang, F.; Li, Z. S.; Cai, N. S.: CO_2 capture from flue gases using a fluidized bed reactor with limestone. *Korean Journal of Chemical Engineering* **2009**, *26*, 1414-1421.

(110) Liu, H.; Katagiri, S.; Kaneko, U.; Okazaki, K.: Sulfation behavior of limestone under high CO_2 concentration in O_2/CO_2 coal combustion. *Fuel* **2000**, *79*, 945-953.

(111) Cho, M. K.; Cheng, J.; Park, J. H.; Min, D. J.: Hot metal desulfurization by $CaO-SiO_2-CaF_2-Na_2O$ slag saturated with MgO. *Isij International* **2010**, *50*, 215-221.

(112) Susaki, K.; Maeda, M.; Sano, N.: Sulfide capicity of $CaO-CaF_2-SiO_2$ slags. *Metallurgical Transactions B-Process Metallurgy* **1990**, *21*, 121-129.

(113) Luo, C.; Zheng, Y.; Yin, J. J.; Qin, C. L.; Ding, N.; Zheng, C. G.; Feng, B.: Effect of support material on carbonation and sulfation of synthetic CaO-based sorbents in calcium looping cycle. *Energ Fuel* **2013**, *27*, 4824-4831.

(114) Manovic, V.; Anthony, E. J.; Loncarevic, D.: Sulphation of CaO-based sorbent modified in CO_2 looping cycles. In *Proceedings of the 20th International Conference on Fluidized Bed Combustion*; Yue, G., Zhang, H., Zhao, C., Luo, Z., Eds.; Springer Berlin Heidelberg, 2010; pp 987-992.

(115) Manovic, V.; Anthony, E. J.; Lu, D. Y.: Sulphation and carbonation properties of hydrated sorbents from a fluidized bed CO_2 looping cycle reactor. *Fuel* **2008**, *87*, 2923-2931.

(116) Lu, D. Y.; Hughes, R. W.; Anthony, E. J.: Ca-based sorbent looping combustion for CO_2 capture in pilot-scale dual fluidized beds. *Fuel Processing Technology* **2008**, *89*, 1386-1395.

(117) Partanen, J.; Backman, P.; Backman, R.; Hupa, M.: Absorption of HCl by limestone in hot flue gases. Part I: the effects of temperature, gas atmosphere and absorbent quality. *Fuel* **2005**, *84*, 1664-1673.

(118) Sun, Z. C.; Yu, F. C.; Li, F. X.; Li, S. G.; Fan, L. S.: Experimental study of HCl capture using CaO sorbents: activation, deactivation, reactivation, and ionic transfer mechanism. *Ind Eng Chem Res* **2011**, *50*, 6034-6043.

(119) Fang, F.; Li, Z. S.; Cai, N. S.: Continuous CO_2 capture from flue gases using a dual fluidized bed reactor with calcium-based sorbent. *Ind Eng Chem Res* **2009**, *48*, 11140-11147.

(120) Abanades, J. C.; Anthony, E. J.; Lu, D. Y.; Salvador, C.; Alvarez, D.: Capture of CO_2 from combustion gases in a fluidized bed of CaO. *Aiche Journal* **2004**, *50*, 1614-1622.

(121) Rodriguez, N.; Alonso, M.; Abanades, J. C.: Experimental investigation of a circulating fluidized-bed reactor to capture CO_2 with CaO. *Aiche Journal* **2011**, *57*, 1356-1366.

(122) Arias, B.; Cordero, J. M.; Alonso, M.; Diego, M. E.; Abanades, J. C.: Investigation of SO_2 capture in a circulating fluidized bed carbonator of a Ca looping cycle. *Ind Eng Chem Res* **2013**, *52*, 2700-2706.

(123) Bowen, F.: Carbon capture and storage as a corporate technology strategy challenge. *Energy Policy* **2011**, *39*, 2256-2264.

(124) Von Stechow, C.; Watson, J.; Praetorius, B.: Policy incentives for carbon capture and storage technologies in Europe: a qualitative multi-criteria analysis. *Glob. Environ. Change-Human Policy Dimens.* **2011**, *21*, 346-357.

(125) Davison, J.; Thambimuthu, K.: An overview of technologies and costs of carbon dioxide capture in power generation. *Proceedings of the Institution of Mechanical Engineers Part a-Journal of Power and Energy* **2009**, *223*, 201-212.

(126) Nakagawa, K.; Ohashi, T.: A novel method of CO_2 capture from high temperature gases. *Journal of the Electrochemical Society* **1998**, *145*, 1344-1346.

(127) Fauth, D. J.; Frommell, E. A.; Hoffman, J. S.; Reasbeck, R. P.; Pennline, H. W.: Eutectic salt promoted lithium zirconate: novel high temperature sorbent for CO_2 capture. *Fuel Processing Technology* **2005**, *86*, 1503-1521.

(128) Ozaki, Y.; Kanai, Y.; Terasaka, K.; Kobayashi, D.: Hot CO_2 recovery using lithium silicate suspended in molten salt. *Journal of Chemical Engineering of Japan* **2010**, *43*, 546-552.

(129) Olivares-Marin, M.; Drage, T. C.; Maroto-Valer, M. M.: Novel lithium-based sorbents from fly ashes for CO_2 capture at high temperatures. *Int. J. Greenh. Gas Control* **2010**, *4*, 623-629.

(130) Nair, B. N.; Yamaguchi, T.; Kawamura, H.; Nakao, S. I.; Nakagawa, K.: Processing of lithium zirconate for applications in carbon dioxide separation: structure and properties of the powders. *Journal of the American Ceramic Society* **2004**, *87*, 68-74.

(131) Olivares-Marin, M.; Castro-Diaz, M.; Drage, T. C.; Maroto-Valer, M. M.: Use of small-amplitude oscillatory shear rheometry to study the flow properties of pure and potassium-doped Li_2ZrO_3 sorbents during the sorption of CO_2 at high temperatures. *Separation and Purification Technology* **2010**, *73*, 415-420.

(132) Terasaka, K.; Suyama, Y.; Nakagawa, K.; Kato, M.; Essaki, K.: Absorption and stripping of CO_2 with a molten salt slurry in a bubble column at high temperature. *Chemical Engineering & Technology* **2006**, *29*, 1118-1121.

(133) Zhang, X. P.; Zhang, X. C.; Dong, H. F.; Zhao, Z. J.; Zhang, S. J.; Huang, Y.: Carbon capture with ionic liquids: overview and progress. *Energy & Environmental Science* **2012**, *5*, 6668-6681.

(134) Spinner, N. S.; Vega, J. A.; Mustain, W. E.: Recent progress in the electrochemical conversion and utilization of CO_2. *Catalysis Science & Technology* **2012**, *2*, 19-28.

(135) Mignard, D. S., M.; Duthie, J. M.; Whittington, H. W.: Methanol synthesis from flue-gas CO_2 and renewable electricity: a feasibility study. *International Journal of Hydrogen Energy* **2003**, *28*, 455-464.

(136) Otake, K.; Kinoshita, H.; Kikuchi, T.; Suzuki, R. O.: CO_2 gas decomposition to carbon by electro-reduction in molten salts. *Electrochim. Acta* **2013**, *100*, 293-299.

(137) Discepoli, G.; Cinti, G.; Desideri, U.; Penchini, D.; Proietti, S.: Carbon capture with molten carbonate fuel cells: Experimental tests and fuel cell performance assessment. *Int. J. Greenh. Gas Control* **2012**, *9*, 372-384.

(138) Cassir, M.; McPhail, S. J.; Moreno, A.: Strategies and new developments in the field of molten carbonates and high-temperature fuel cells in the carbon cycle. *International Journal of Hydrogen Energy* **2012**, *37*, 19345-19350.

(139) Campanari, S.; Chiesa, P.; Manzolini, G.: CO_2 capture from combined cycles integrated with molten carbonate fuel cells. *Int. J. Greenh. Gas Control* **2010**, *4*, 441-451.

(140) Abanades, A.; Rubbia, C.; Salmieri, D.: Thermal cracking of methane into Hydrogen for a CO_2-free utilization of natural gas. *International Journal of Hydrogen Energy* **2013**, *38*, 8491-8496.

(141) Sanchez, D.; Monje, B.; Chacartegui, R.; Campanari, S.: Potential of molten carbonate fuel cells to enhance the performance of CHP plants in sewage treatment facilities. *International Journal of Hydrogen Energy* **2013**, *38*, 394-405.

(142) Spallina, V.; Romano, M. C.; Campanari, S.; Lozza, G.: Application of MCFC in coal gasification plants for high efficiency CO_2 capture. *J. Eng. Gas. Turbines Power-Trans. ASME* **2012**, *134*.

(143) Wang, X.; Hu, C. G.; Xiong, Y. F.; Liu, H.; Du, G. J.; He, X. S.: Carbon-nanosphere-supported Pt nanoparticles for methanol and ethanol electro-oxidation in alkaline media. *Journal of Power Sources* **2011**, *196*, 1904-1908.

(144) Zhao, G. Y. J., T.; Han, B. X.; Li, Z. H.; Zhang, J. M.; Liu, Z. M.; He, J.; Wu, W. Z.: Electrochemical reduction of supercritical carbon dioxide in ionic liquid 1-n-butyl-3-methylimidazolium hexafluorophosphate. *Journal of Supercritical Fluids* **2004**, *32*, 287-291.

(145) Bale, C. W.; Belisle, E.; Chartrand, P.; Decterov, S. A.; Eriksson, G.; Hack, K.; Jung, I. H.; Kang, Y. B.; Melancon, J.; Pelton, A. D.; Robelin, C.; Petersen, S.: FactSage thermochemical software and databases - recent developments. *Calphad-Computer Coupling of Phase Diagrams and Thermochemistry* **2009**, *33*, 295-311.

(146) Wenz, D. A.; Johnson, I.; Wolson, R. D.: $CaCl_2$-rich region of $CaCl_2$-CaF_2-CaO system. *J. Chem. Eng. Data* **1969**, *14*, 250-&.

(147) Beilmann, M.; Benes, O.; Konings, R. J. M.; Fanghanel, T.: Thermodynamic investigation of the (LiF + NaF + CaF_2 + LaF_3) system. *J. Chem. Thermodyn.* **2011**, *43*, 1515-1524.

(148) Wang, S. L. Z., F. S.; Liu, X.; Zhang, L. J.: CaO solubility and activity coefficient in molten salts $CaCl_2$-x (x=0, NaCl, KCl, $SrCl_2$, $BaCl_2$ and LiCl). *Thermochim. Acta* **2008**, *470*, 105-107.

(149) Forsberg, C. W.; Peterson, P. F.; Zhao, H. H.: High-temperature liquid-fluoride-salt closed-Brayton-cycle solar power towers. *Journal of Solar Energy Engineering-Transactions of the Asme* **2007**, *129*, 141-146.

(150) Freidina, E. B.; Fray, D. J.: Study of the ternary system $CaCl_2$-NaCl-CaO by DSC. *Thermochim. Acta* **2000**, *356*, 97-100.

(151) Freidina, E. B.; Fray, D. J.: Phase diagram of the system $CaCl_2$-$CaCO_3$. *Thermochim. Acta* **2000**, *351*, 107-108.

(152) Fedotieff, P. P.; Iljinsky, W. P.: Uber die schmelzbarkeit des ternaren systems: natriurnfluorid, calciumfluorid, aluminiumfluorid. *Zeitschrift für anorganische und allgemeine Chemie* **1923**, *1*, 93-107.

(153) Kim, D. G.; Van Ende, M. A.; Van Hoek, C.; Liebske, C.; Van der Laan, S.; Jung, I. H.: A critical evaluation and thermodynamic optimization of the CaO-CaF_2 system. *Metall. Mater. Trans. B-Proc. Metall. Mater. Proc. Sci.* **2012**, *43*, 1315-1325.

(154) Cooper, A. F.; Gittins, J.; Tuttle, O. F.: System Na_2CO_3-K_2CO_3-$CaCO_3$ at 1 kilobar and its significance in carbonatite petrogenesis. *American Journal of Science* **1975**, *275*, 534-560.

(155) Kostensk, I.; Vrbenska, J.; Malinovs, M.: Equilibrium solidus-liquidus in system lithium fluoride-calcium fluoride. *Chemicke Zvesti* **1974**, *28*, 531-538.

(156) Poletaev, I. F.; Lyudomirskaya, A. P.; Ismailov, A. I.; Tsiklina, N. D.: $CaCl_2$-$CaCO_3$-CaO system. *Zhurnal Neorg. Khimii* **1976**, *21*, 2281-2284.

(157) Kondo, H.; Asaki, Z.; Kondo, Y.: Hydrolysis of fused calcium-chloride at high-temperature. *Metallurgical Transactions B-Process Metallurgy* **1978**, *9*, 477-483.

(158) Molenda, M.; Stengler, J.; Linder, M.; Worner, A.: Reversible hydration behavior of $CaCl_2$ at high H_2O partial pressures for thermochemical energy storage. *Thermochim. Acta* **2013**, *560*, 76-81.

(159) Sudha, V.; Harinipriya, S.; Sangaranarayanan, M. V.: Dehydration energies of alkaline earth metal halides - a novel simulation methodology. *Chemical Physics* **2005**, *310*, 59-66.

PAPERS

Paper I

Viktorija Tomkute, Asbjørn Solheim, Simas Sakirzanovas, Bjarte Øye and Espen Olsen. Phase equilibria evaluation for CO_2 Capture: CaO-CaF_2-NaF, $CaCO_3$-NaF-CaF_2, and Na_2CO_3-CaF_2-NaF. Submitted to *Journal of Chemical & Engineering Data*.

Phase equilibria evaluation for CO_2 Capture: CaO-CaF_2-NaF, $CaCO_3$-NaF-CaF_2, and Na_2CO_3-CaF_2-NaF

Viktorija Tomkute[1], Asbjørn Solheim[2], Simas Sakirzanovas[3], Bjarte Øye[2], Espen Olsen[1]*

[1] Department of Mathematical Sciences and Technology, Norwegian University of Life Sciences (UMB), Post Office Box 5003, Drøbakveien 31, NO-1432 Ås, Norway

[2] SINTEF Materials and Chemistry, Post Office Box 4760, Sluppen, NO-7465 Trondheim, Norway

[3] Department of Applied Chemistry, Vilnius University (VU), Naugarduko 24, LT-03225, Vilnius, Lithuania

Abstract

This paper presents partial phase relations for the systems NaF-CaF_2, NaF-CaF_2-CaO, NaF-CaF_2-$CaCO_3$, NaF-CaF_2-$NaCO_3$ and NaF-CaF_2-Na_2CO_3-$CaCO_3$. The data were obtained by thermal analysis (TA), thermodynamic calculations (FactSage), and X-ray diffraction (XRD) of quenched samples. There was particular emphasis on revealing the phase formations of CaO, $CaCO_3$, and Na_2CO_3 in the eutectic composition of NaF-CaF_2 for development of a novel carbon capture technology. Therefore, a thermal analysis of the binary CaF_2-NaF system was performed first. A eutectic point was found at 31.9 mole % CaF_2 and 814.8 ºC. The liquidus isotherms and phase regions of the Na-Ca//F-O and Na-Ca//F-CO_3 systems were mapped using FactSage. In addition, some compositions in the NaF-CaF_2-CaO and NaF-CaF_2-Na_2CO_3-$CaCO_3$ systems were studied by TA. XRD analysis of the quenched samples was applied for phase identification. Based on the FactSage simulation and the experimental data, the solubility of CaO increases with increasing CaF_2 concentration in NaF melt. It was derived that carbonates (Na_2CO_3 and $CaCO_3$) in NaF-CaF_2 are present as intermediate compounds. The reactions of NaF and $CaCO_3$ and the formation of complex carbonates are discussed. In general, there is good agreement between experimental data and simulations.

Keywords: NaF-CaF_2; NaF-CaF_2-CaO; NaF-CaF_2-Na_2CO_3-$CaCO_3$; Phase diagrams; Molten Salts; FactSage

Introduction

Electrochemical decomposition of CO_2 has been investigated in various electrolytes, including aqueous solutions, room temperature ionic liquids (RTILs) and low cost carbonate and chloride molten salt mixtures.[1-4] The CO_2 solubility is higher in RTILs and molten salts

than in aqueous solutions.[1,4] In addition, it is possible to generate valuable carbon materials and oxygen by molten salt CO_2 capture and electrochemical transformation (MSCC-ET), which reduces the total cost of the process.[1] However, the current MSCC-ET technology is not suitable for use in large-scale fossil fuel power plants, cement manufacturing, or other industrial operations. Therefore, a low toxicity and inexpensive $CaCl_2$ melt was applied as the solvent for the dissolution/dispersion of CaO and $CaCO_3$ in a carbon capture process.[5] This concept is based on a solvents/sorbents capture technology, where oxides are dissolved and dispersed in molten salt in a CO_2 capture chamber, and consequently, the formed carbonates are dissolved and dispersed in molten salt in the CO_2 regenerator chamber. The chambers are interconnected to create a continuous capture process. So far, no calculations on the economy of this process have been published. However, the CO_2 capture efficiency of CaO decreases with increasing number of carbonation-decarbonation cycles in the solid Ca-looping technology.[6,7] This is apparently not the case when CaO is dissolved in molten salt; the conversion of CaO to carbonate increased from 55.4 up to 64.2% after 10 cycles, and the decomposition of the carbonate was complete in all cycles.[5]

Molten alkali and alkaline earth metal fluoride mixtures have been utilized in many industrial processes, including extractive metallurgy and electrochemical processes.[8] The application of fluoride-liquid-salt compositions in energy production and thermal-energy storage processes[8-10] is a rapidly growing field. Molten salts containing CaF_2 are utilized as heat transport and reaction media in high-temperature nuclear reactor fuel processing.[10-12] Molten NaF-AlF_3-CaF_2 is the base solvent for alumina in Hall-Héroult electrolysis cells for primary aluminium production.[13,14] The physical and chemical properties of the CaO-based slag systems such as CaO-CaF_2, CaO-BaO-CaF_2 and CaO-SiO_2-CaF_2 have been investigated for the purpose of obtaining a steel grade with low oxygen and high hydrogen contents.[11,12,15] For example, removal of sulphur-containing species from molten metal by CaO-based slags is a well-known, effective and inexpensive process for sulphur capture.[16,17]

The selection of fluoride salts for these processes is based on their high-temperature heat transfer, thermal stability, radiation resistance, low vapour pressure, and manageable melting point.[10] Therefore, the data from phase diagrams of the salt systems is indispensable in all the technological processes. It is known that NaF-CaF_2 forms a simple eutectic system, and some experimental and calculation cases on the eutectic data are presented in Table 1.[8,18,19] Kim et al.[15] used a modified quasi-chemical model to evaluate the solubility of CaO in CaF_2 melt. Comparison with all available literature data showed good agreement with the experimental results (Table 1).[15,20,21] In the evaluation of the $CaCO_3$-Na_2CO_3 system the compounds Na_2CO_3, $Na_2Ca(CO_3)_2$ (nyerereite), $Na_2Ca_2(CO_3)_3$ (shortite) and $CaCO_3$ (calcite) were identified in the solid phase, while the corresponding anion complexes may be present in the melt.[22] However, phase diagrams for the CaO/CaO_3-Na_2CO_3/NaF-CaF_2 systems have not been calculated or experimentally determined so far as we are aware. Therefore, in this study we focused on the evaluation of the phase diagrams for the CaO-NaF-CaF_2 system in the composition range of interest for application in CO_2 capture technology.

TABLE 1

Experimental

In the experimental thermal analysis study, CaF_2 (Merck reagent, 97-100 % purity, CAS-No: 7789-75-5), CaO (Alfa Aesar reagent, 99.95 % purity, CAS-No: 1305-78-8), $CaCO_3$ (Alfa Aesar reagent, 99.95 % purity, CAS-No: 471-34-1), NaF (Merk reagent, 99 % purity, CAS-No: 7681-49-4) and Na_2CO_3 (Alfa Aesar reagent, 99.5 % purity, CAS-No: 497-19-8) were used. All fluoride powders were dried at 200 °C for 24 h. The samples were prepared by direct mixing of the pure compounds. Each melt composition data and evaluated temperature region employed in this work are represented in Table 2.

The crucible assembly (Figure 1) was positioned in a vertical tube furnace (< 1200 ºC) supplied with a ceramic tube. Nickel radiation shield were applied above and below the crucible. The heating or cooling rate of the furnace was controlled by a computer program (LabView) connected with the furnace controller. The sample (150 g) was placed in the nickel crucible and heated to 870-1150 ºC (5 ºC/min), and kept for around 3 h, followed by controlled cooling (0.6-0.7 ^{o}C/min). The temperature was measured using calibrated Type S thermocouples (Pt-Pt10Rh, ±1.1 ºC). Vigorous stirring was applied to avoid supercooling. The systems Na-Ca-F and Na-Ca-F-O were studied under N_2 atmosphere, while CO_2 gas was used for the Na-Ca-F-CO_3 systems. The thermodynamic calculations of phase equilibria and the projection of phase diagrams were performed utilizing the FactSage thermochemical software and databases, version 6.3.[23]

Powder XRD analysis was employed for phase identification. The samples for structural analysis were prepared by quenching the molten chemical mixtures on a stainless steel plate at room temperature and ambient air pressure. XRD data were collected from 5º $\leq 2\theta \leq$110º (scan rate 0.01 degree per second) using Ni-filtered Cu K_α on Bruker D8 Advance diffractometer working in Bragg-Brentano ($\theta/2\theta$) geometry. All measurements were performed at room temperature and ambient pressure in air.

FIGURE 1

TABLE 2

Results and discussion

NaF-CaF_2 system

All compositions and measured temperatures are given in Table 2.

Figure 2 depicts the phase diagram of the simple NaF-CaF_2 binary system derived by thermal analysis. As can be observed, it is a simple eutectic system without solid solubility.[14] The liquidus and solidus lines experimentally determined by Fedotieff et al.[18] and calculated by Beilmann et al.[8] are also shown. Beilmann et al.[8] used classical polynomial as well as modified quasi-chemical models to determine the solidus and liquidus planes, which provided eutectic composition of 68.6 mole% and 67.2 mole% NaF in CaF_2, respectively. In addition, both models produced a eutectic temperature of 816 ºC, which is close to the eutectic temperature established by Fedotieff et al.[18] (Table 1). In the present work, the eutectic composition for NaF-CaF_2 is at 68.1 mole% NaF, and the eutectic temperature is 814.8 ºC. This agrees well with most of the earlier results.[14,18,19] In addition, the phase transition

projection of alpha-CaF_2 solid solution to beta-CaF_2 at 1151 ºC was included.[15] X-ray diffraction measurements of the quenched molten samples on the stainless steel plate were performed, and a representative XRD pattern of NaF-CaF_2 is plotted in Figure 3. The phases were identified as a blend of CaF_2 and NaF single cubic phases.

FIGURE 2 and 3

NaF-CaF_2-CaO system

A series of TA measurements were performed, starting at the NaF-CaF_2 eutectic point and keeping the NaF/CaF_2 ratio constant while adding CaO (compositions represented by the open circles in Figure 4). It was found that the CaO solubility was very low and the eutectic point was observed at 814.7 ºC, which is equal to the eutectic point in the binary system of NaF-CaF_2. At higher CaO concentrations only the eutectic points could be obtained experimentally. Therefore, the NaF-CaF_2-CaO phase diagram was carried out using FactSage and is shown in Figure 4. The calculations were performed based on information from the FToxid database and FToxid-SlagH database. There is good agreement between the simulation data and experiments, as demonstrated in Table 2 and Figure 4. The calculated phase diagram presents two ternary invariant points marked "1" and "2" in Figure 4. The eutectic mixture (Point 2) consists of 0.202 mole% CaO and 68.248 mole% NaF in CaF_2 and melts at 813 ºC, which is in agreement with experimental data (Table 2). The composition of the peritectic point (Point 1) is 70.9 mole% CaF_2 and 10.5 mole% CaO in NaF at 1151 ºC. This point may be attributed to the transition between alpha-CaF_2 and beta-CaF_2 (also, see Figure 2). The increase in CaO solubility by increasing the CaF_2 concentration in NaF melt may be observed also. CaF_2, CaO, and NaF represent cubic crystal systems, where CaF_2 crystallizes in space group cF12[24], and CaO and NaF crystallizes in Fm3m.[25,26] The structural analysis of a sample consisting of 9.6 mole% CaO and 28.8 mole% CaF_2 in NaF by X-ray diffraction (XRD) (Figure 3) demonstrate that diffraction pattern peaks may be attributed to the pure initial compounds without any impurities or intermediate compounds.

FIGURE 4

NaF-CaF_2-$CaCO_3$ system

Analysis of the system $CaCO_3$-Na_2CO_3 revealed that there are two intermediate compounds; $Na_2Ca(CO_3)_2$ (nyerereite) and $Na_2Ca_2(CO_3)_3$ (shortite).[22] The decomposition of synthesised $Na_2Ca_2(CO_3)_3$ to $CaCO_3$ and $Na_2Ca(CO_3)_2$ starts at around 400 ºC, and $Na_2Ca_2(CO_3)_3$ has an upper stability of 817 ºC at $CaCO_3$ concentration higher than 53 mole% and 725 ºC at the Na_2CO_3-corner.[22] Thus, it is fundamentally important to estimate the stability of carbonates in the fluoride melt. For this reason, $CaCO_3$ as well as Na_2CO_3 were added to the NaF-CaF_2 base melt with fixed NaF/CaF_2 ratio; see Table 2.

$CaCO_3$ must be expected to react with the melt to form CaF_2 and Na_2CO_3 (Eq. (1) below). This reaction proceeds at any actual temperature. In addition, sodium-calcium complex carbonates may be formed, as shown in eqs. 2-4. Formation of $Na_2Ca_2(CO_3)_3$ may be expected at temperatures lower than 400 ºC, and at higher temperature, shortite is replaced by $Na_2Ca(CO_3)_2$, which has a melting point of 817 ºC.[22]

$$CaCO_3 + 2NaF \leftrightarrow Na_2CO_3 + CaF_2 \quad (1)$$

$$3CaCO_3 + 2NaF \leftrightarrow Na_2Ca_2(CO_3)_3 + CaF_2 \quad (2)$$

$$2CaCO_3 + 2NaF \leftrightarrow Na_2Ca(CO_3)_2 + CaF_2 \quad (3)$$

$$Na_2Ca_2(CO_3)_3 \leftrightarrow Na_2Ca(CO_3)_2 + CaCO_3 \quad (4)$$

The experimentally determined liquidus and solidus temperature obtained by adding $CaCO_3$ to the fluoride based melt under CO_2 atmosphere is shown in Figure 5. The increasing liquidus temperature reflects the formation of CaF_2 according to eq. 1 (also, see Figure 2). A ternary eutectic in the system $CaCO_3$-NaF-CaF_2 could not be detected. The presence of Na_2CO_3 (space group P6(3)/m)[27] in $CaCO_3$-NaF-CaF_2 composition was confirmed by XRD analysis (Figure 6). The peaks of $CaCO_3$ (space group R3C), $Na_2Ca(CO_3)_2$ (space group Cmc21)[28] and $Na_2Ca_2(CO_3)_3$ (space group C2mm) crystal structures were not determined in the XRD pattern of the sample, which contained 8.6 mole% $CaCO_3$, 29.1 mole% CaF_2, and 62.2 mole% NaF.

FIGURE 5 and 6

NaF-CaF_2-$CaCO_3$-Na_2CO_3 system

To fully understand the stability of $CaCO_3$ in the NaF-CaF_2 melt, the quaternary phase diagram for the system NaF-CaF_2-$CaCO_3$-Na_2CO_3 was computed, using FactSage. In the calculation, $CaCO_3$ decomposition to CaO and CO_2 was suppressed. The result is shown in Figure 7. As can been seen from the figure, the phase diagram contains three invariant points at 567, 553 and 541 ºC. The point at 567 ºC is located where the fraction of carbonates in fluorides is around 64 mole% and 60 mole% of sodium ions in cationic mole fraction region. This phase boundary connects the liquidus planes of NaF, Na_2CO_3 and alpha-CaF_2 phases projected onto the basis plane. Solid solution of calcite appears at the $CaCO_3$-CaF_2 side of the phase diagram (not shown in the figure). The alpha-CaF_2 solid solution transition line to beta is observed at 1151 ºC close to the CaF_2 corner. A field of primary crystallization of the intermediate compound $Na_2Ca(CO_3)_2$ (nyerereite) can be seen in the upper part of the phase diagram. Nyerereite decomposition occurs at 541 ºC in the sodium carbonate side and at 553 ºC in the calcium carbonate corner.[22] At low temperatures, calcium may be substituted in sodium carbonate solid solution and the $Na_2Ca(CO_3)_2$ solid solution to form the more stable complex carbonate compound $Na_2Ca_2(CO_3)_3$ (shortite). However, the shortite phase was not observed in the FactSage calculation.

FIGURE 7

NaF-CaF_2-Na_2CO_3 system

Figure 8 presents experimental data on the effect of adding Na_2CO_3 to the fluoride base melt (Table 2) under CO_2 atmosphere. Solidus lines, liquidus lines, and estimated solvus lines are shown. As described above, Na_2CO_3 and Ca_2CO_3 may form the intermediate compounds

($Na_2Ca(CO_3)_2$ and $Na_2Ca_2(CO_3)_3$) in the NaF-CaF_2 melt. According to the thermodynamic calculations, shortite formation is caused by calcium cation substitution in Na_2CO_3 at temperatures below 335 ºC.[22] However, above this temperature, in the presence of Na_2CO_3, shortite may react with Na_2CO_3 to form nyerereite (eq. 5).

$$Na_2Ca_2(CO_3)_3 + Na_2CO_3 \leftrightarrow 2Na_2Ca(CO_3)_2 \quad (5)$$

Since the thermal analysis was conducted at 600-870 ºC, the phase boundary point of nyerereite to shortite was not detected. The data indicated that the compound $Na_2Ca(CO_3)_2$ could decompose at 721 ºC in the high NaF/CaF_2 content and at 665 ºC in the Na_2CO_3-corner. Formation of Na_2CO_3 solid solution may take place at around 665 ºC in the Na_2CO_3 end of the diagram. XRD phase identification of the samples prepared with Na_2CO_3 shown in Figure 6. All investigated samples represents characteristic peaks of NaF, CaF_2, Na_2CO_3 and $Na_2Ca(CO_3)_2$. It was observed that the intensity of the Na_2CO_3 and $Na_2Ca(CO_3)_2$ peaks increased with decreasing concentrations of NaF and CaF_2.

FIGURE 8

Uncertainties in the experimental data may be attributed to the hygroscopic properties of some of the compounds. Hydrolysis of metal fluorides leads to the formation of metal oxides, which affect the liquidus temperatures. The formation of small amounts of complex carbonates not detected by XRD cannot be ruled out. The experimental data are comparable with the results obtained by the FactSage simulations.

Conclusions

Parts of the NaF-CaF_2-CaO-Na_2CO_3-$CaCO_3$ systems were studied with the primary intent of examining phase transitions of CaO, $CaCO_3$ and Na_2CO_3 in the eutectic composition of NaF-CaF_2 for development of CO_2 capture technology. The experimentally obtained phase diagram of the NaF-CaF_2 system shows a eutectic point at 814.8 ºC and 31.9 mole% CaF_2, which is suitable for solid CaO reaction with CO_2. The partial phase diagram of the NaF-CaF_2-CaO system determined by thermal analysis showed very low CaO solubility; a ternary eutectic was observed at 814.7 ºC. The mapped phase relation of the ternary CaO-NaF-CaF_2 system using FactSage exhibits a eutectic composition of 68.248 mole% NaF and 31.75 CaF_2 at 813 ºC. Information on the solubility of CaO in the fluoride melts demonstrates the possibility of using a eutectic mixture of NaF-CaF_2 as the solvent for the dissolution and dispersion of CaO for a high-temperature CO_2 capture technology. Addition of $CaCO_3$ to the NaF/CaF_2 binary mixture resulted in increased liquidus temperature, which can be explained by additional CaF_2 formation due to reaction between $CaCO_3$ and NaF. This was confirmed by thermodynamic calculations using FactSage. Formation of the intermediate compound $Na_2Ca(CO_3)_2$ (nyerereite) was indicated. Thus, CaO-based sorbents in molten NaF-CaF_2 may form several kinds of carbonates during carbonation, such as $CaCO_3$, $Na_2Ca(CO_3)_2$, and Na_2CO_3. Additionally, the presence of NaF, CaF_2, CaO, Na_2CO_3 and $Na_2Ca(CO_3)_2$ was determined by XRD.

AUTHOR INFORMATION

Corresponding Author

*Email: viktorija.tomkute@gmail.com

Notes

The authors declare no competing financial interest.

ACKNOWLEDGMENTS

We thank the Research Council of Norway for financial support through the CLIMIT research Programme (199900/S60). The primary data have been deposited for open access with the Norwegian University of Life Sciences (UMB).

References

(1) Yin, H. Y.; Mao, X. H.; Tang, D. Y.; Xiao, W.; Xing, L. R.; Zhu, H.; Wang, D. H.; Sadoway, D. R.: Capture and electrochemical conversion of CO_2 to value-added carbon and oxygen by molten salt electrolysis. *Energy & Environmental Science* **2013**, *6*, 1538-1545.

(2) Zhao, G. Y. J., T.; Han, B. X.; Li, Z. H.; Zhang, J. M.; Liu, Z. M.; He, J.; Wu, W. Z.: Electrochemical reduction of supercritical carbon dioxide in ionic liquid 1-n-butyl-3-methylimidazolium hexafluorophosphate. *Journal of Supercritical Fluids* **2004**, *32*, 287-291.

(3) Otake, K.; Kinoshita, H.; Kikuchi, T.; Suzuki, R. O.: CO_2 gas decomposition to carbon by electro-reduction in molten salts. *Electrochim. Acta* **2013**, *100*, 293-299.

(4) Mignard, D. S., M.; Duthie, J. M.; Whittington, H. W.: Methanol synthesis from flue-gas CO_2 and renewable electricity: a feasibility study. *International Journal of Hydrogen Energy* **2003**, *28*, 455-464.

(5) Tomkute, V.; Solheim, A.; Olsen, E.: Investigation of high-temperature CO_2 capture by CaO in $CaCl_2$ molten salt. *Energ Fuel* **2013**, *27*, 5373-5379.

(6) Liu, W. Q.; Yin, J. J.; Qin, C. L.; Feng, B.; Xu, M. H.: Synthesis of CaO-Based Sorbents for CO2 Capture by a Spray-Drying Technique. *Environ. Sci. Technol.* **2012**, *46*, 11267-11272.

(7) Valverde, J. M.: Ca-based synthetic materials with enhanced CO_2 capture efficiency. *J. Mater. Chem. A* **2013**, *1*, 447-468.

(8) Beilmann, M.; Benes, O.; Konings, R. J. M.; Fanghanel, T.: Thermodynamic Investigation of the (LiF + NaF + CaF_2 + LaF_3) System. *J. Chem. Thermodyn.* **2011**, *43*, 1515-1524.

(9) Babaev, B. D. G., A. M.: Phase Diagram of the System LiF-NaF-CaF_2-BaF_2-$BaMoO_4$. *Inorganic Materials* **2003**, *39*, 1203-1207.

(10) Forsberg, C. W.; Peterson, P. F.; Zhao, H. H.: High-temperature liquid-fluoride-salt closed-Brayton-cycle solar power towers. *Journal of Solar Energy Engineering-Transactions of the Asme* **2007**, *129*, 141-146.

(11) Choi, C. H. J., S. K.; Kim, S. H.; Lee, K. R.; Kim, J. T.: The Effect of CaF_2 on Thermodynamics of CaO-CaF_2-SiO_2(-MgO) Slags. *Metall. Mater. Trans. B-Proc. Metall. Mater. Proc. Sci.* **2004**, *35*, 115-120.

(12) Wenz, D. A. J., I.; Wolson, R. D.: $CaCl_2$-rich region of $CaCl_2$-CaF_2-CaO system. *J. Chem. Eng. Data* **1969**, *14*, 250-&.

(13) Sterten, A. S., P. A.; Skybakmoen, E.: Influence of Electrolyte Impurities on Current Efficiency in Aluminium Electrolysis Cells. *Journal of Applied Electrochemistry* **1998**, *28*, 781-789.

(14) Zaitseva, J. N.; Yakimov, I. S.; Kirik, S. D.: Thermal transformation of quaternary compounds in NaF-CaF2-AlF_3 system. *Journal of Solid State Chemistry* **2009**, *182*, 2246-2251.

(15) Kim, D. G. V. E., M. A.; Van Hoek, C.; Liebske, C.; Van der Laan, S.; Jung, I. H.: A Critical Evaluation and Thermodynamic Optimization of the CaO-CaF_2 System. *Metall. Mater. Trans. B-Proc. Metall. Mater. Proc. Sci.* **2012**, *43*, 1315-1325.

(16) Cho, M. K. C., J.; Park, J. H.; Min, D. J.: Hot Metal Desulfurization by CaO-SiO_2-CaF_2-Na_2O Slag Saturated with MgO. *Isij International* **2010**, *50*, 215-221.

(17) Susaki, K.; Maeda, M.; Sano, N.: Sulfide Capicity of CaO-CaF_2-SiO_2 Slags. *Metallurgical Transactions B-Process Metallurgy* **1990**, *21*, 121-129.

(18) Fedotieff;, P. P.; Iljinsky, W. P.: Uber die Schmelzbarkeit des ternaren Systems: Natriurnfluorid, Calciumfluorid, Aluminiumfluorid. *Zeitschrift für anorganische und allgemeine Chemie* **1923**, *1*, 93-107.

(19) Lin, P. L.; Pelton, A. D.; Saboungi, M. L.: Computer-Analysis of Phase-Diagrams and Thermodynamic Properties of Cryolite Based Systems. 2. The AlF_3-CaF_2-LiF, AlF_3-CaF_2-NaF and CaF_2-LiF-NaF Systems. *Metallurgical Transactions B-Process Metallurgy* **1982**, *13*, 61-69.

(20) Seo, W. G.; Zhou, D. H.; Tsukihashi, F.: Calculation of thermodynamic properties and phase diagrams for the CaO-CaF_2, BaO-CaO and BaO-CaF_2 systems by molecular dynamics simulation. *Materials Transactions* **2005**, *46*, 643-650.

(21) Chatterj.Ak; Zhmoidin, G. I.: Phase equilibrium diagram of system CaO-Al_2O_3-CaF_2. *Journal of Materials Science* **1972**, *7*, 93-&.

(22) Cooper, A. F.; Gittins, J.; Tuttle, O. F.: System Na_2CO_3-K_2CO_3-$CaCO_3$ at 1 kilobar and its significance in carbonatite petrogenesis. *American Journal of Science* **1975**, *275*, 534-560.

(23) Bale, C. W.; Belisle, E.; Chartrand, P.; Decterov, S. A.; Eriksson, G.; Hack, K.; Jung, I. H.; Kang, Y. B.; Melancon, J.; Pelton, A. D.; Robelin, C.; Petersen, S.: FactSage thermochemical software and databases - recent developments. *Calphad-Computer Coupling of Phase Diagrams and Thermochemistry* **2009**, *33*, 295-311.

(24) Gerward, L.; Olsen, J. S.; Steenstrup, S.; Malinowski, M.; Asbrink, S.; Waskowska, A.: X-Ray-Difraction Investigations of CaF2 at High-Pressure. *Journal of Applied Crystallography* **1992**, *25*, 578-581.

(25) Kubo, K.: Dislocations observed in NaF crystals. 1. Rosette structure and its changes under external stress. *Journal of the Physical Society of Japan* **1970**, *28*, 177-&.

(26) Shen, C. H.; Liu, R. S.; Lin, J. G.; Huang, C. Y.: Phase stability study of $La_{1.2}Ca_{1.8}Mn_2O_7$. *Materials Research Bulletin* **2001**, *36*, 1139-1148.

(27) Swainson, I. P.; Dove, M. T.; Harris, M. J.: Neutron Powder Diffraction Study of the Ferroelastic Phase-Transition and Lattice Melting in Sodium-Carbonate, Na_2CO_3. *Journal of Physics-Condensed Matter* **1995**, *7*, 4395-4417.

(28) McKie, D.; Frankis, E. J.: Nyerereite - New Volcanic Carbonate Mineral from Oldoinyo-Lengai Tanzania. *Zeitschrift Fur Kristallographie* **1977**, *145*, 73-95.

Table 1. Summary of the experimental and computation studies on the eutectic data in the system NaF-CaF_2-CaO.

No.	Author	Method	Eutectic composition, mole%			Eutectic temperature, °C
			NaF	CaF_2	CaO	
1	Fedotieff et al.[18]	Experimental	67.5	32.5	-	813
2	Beilmann et al.[8]	Classical polynomial	68.6	31.4	-	816
3	Beilmann et al.[8]	Modified quasichemical model	67.2	32.8	-	816
4	Lin et al.[19]	Conformal ionic solution (CIS) theory	67.7	32.3	-	817
5	Kim et al.[15]	Modified quasichemical model	-	84.7	15.3	1362
6	Seo et al.[20]	Molecular dynamics model	-	80	20	1377
7	Chatterjee et al.[21]	Quenching	-	80	20	1360

Table 2. The composition of the samples and investigated temperature region used in thermal analysis. Liquidus temperatures of the analysed samples.

Sample No.	Samples mixture					Temperature evaluation range, °C	Eutectic Temperature, °C
	NaF, mole%	CaF_2, mole%	CaO, mole%	$CaCO_3$, mole%	Na_2CO_3, mole%		
1	44.35	55.65	-	-	-	800-1100	813.3
2	50.03	49.97	-	-	-	800-1100	813.8
3	55.49	44.51	-	-	-	800-1100	814.7
4	60.37	39.63	-	-	-	800-1100	814.6
5	64.11	35.89	-	-	-	800-1100	814.9
6	65.03	34.97	-	-	-	800-1100	814.8
7	65.93	34.07	-	-	-	800-1100	814.8
8	66.37	33.63	-	-	-	800-1100	814.9
9	66.85	33.15	-	-	-	800-1100	814.7
10	67.26	32.74	-	-	-	800-1100	814.8
11	67.71	32.29	-	-	-	800-1100	814.9
12	68.15	31.85	-	-	-	800-1100	814.8
13	68.58	31.42	-	-	-	800-1100	814.8
14	69.44	30.56	-	-	-	800-1100	814.8
15	73.61	26.39	-	-	-	800-1150	814.8
16	84.86	15.14	-	-	-	800-1100	813.3
17	88.15	11.85	-	-	-	800-1100	812.3
18	68.08	31.82	0.09	-	-	800-1100	814.7
19	68.01	31.80	0.19	-	-	800-1100	814.5
20	67.94	31.77	0.29	-	-	800-1100	815
21	67.89	31.73	0.38	-	-	800-1100	814.7
22	67.82	31.70	0.48	-	-	800-1100	814.2
23	67.50	31.55	0.95	-	-	800-1100	814.5
24	66.94	31.29	1.77	-	-	800-1100	814.3
25	65.54	30.64	3.82	-	-	800-1100	814.2
26	67.78	31.68	-	0.54	-	750-900	813.0
27	67.43	31.52	-	1.05	-	750-900	811.8
28	67.04	31.33	-	1.63	-	750-900	809.8
29	66.85	31.25	-	1.90	-	750-900	808.8
30	66.66	31.16	-	2.18	-	750-900	807.5
31	66.28	30.98	-	2.74	-	750-900	805.9
32	65.90	30.80	-	3.30	-	750-900	803.8
33	64.33	30.07	-	5.60	-	750-900	794.3
34	62.27	29.11	-	8.62	-	750-900	779.3
35	60.11	28.10	-	11.78	-	750-900	761.2
36	64.33	30.07	-	-	5.60	600-870	796.7
37	62.87	29.39	-	-	7.74	600-870	787.3
38	55.45	25.92	-	-	18.63	600-870	739.7
39	53.60	25.05	-	-	21.35	600-870	721.3
40	44.41	20.76	-	-	34.83	600-870	721.2
41	41.28	19.30	-	-	39.42	600-870	721.3
42	37.83	17.68	-	-	44.49	600-870	721.3
43	35.68	16.68	-	-	47.64	600-870	630.3
44	34.24	16.00	-	-	49.76	600-870	633.9
45	30.33	14.18	-	-	55.49	600-870	651.0
46	29.27	13.68	-	-	57.05	600-870	654.7
47	27.04	12.63	-	-	60.33	600-870	662.0
48	26.37	12.33	-	-	61.30	600-870	664.5
49	25.70	12.01	-	-	62.29	600-870	664.4
50	21.90	10.23	-	-	67.87	600-870	665.5
51	16.92	7.91	-	-	75.17	600-870	670.4

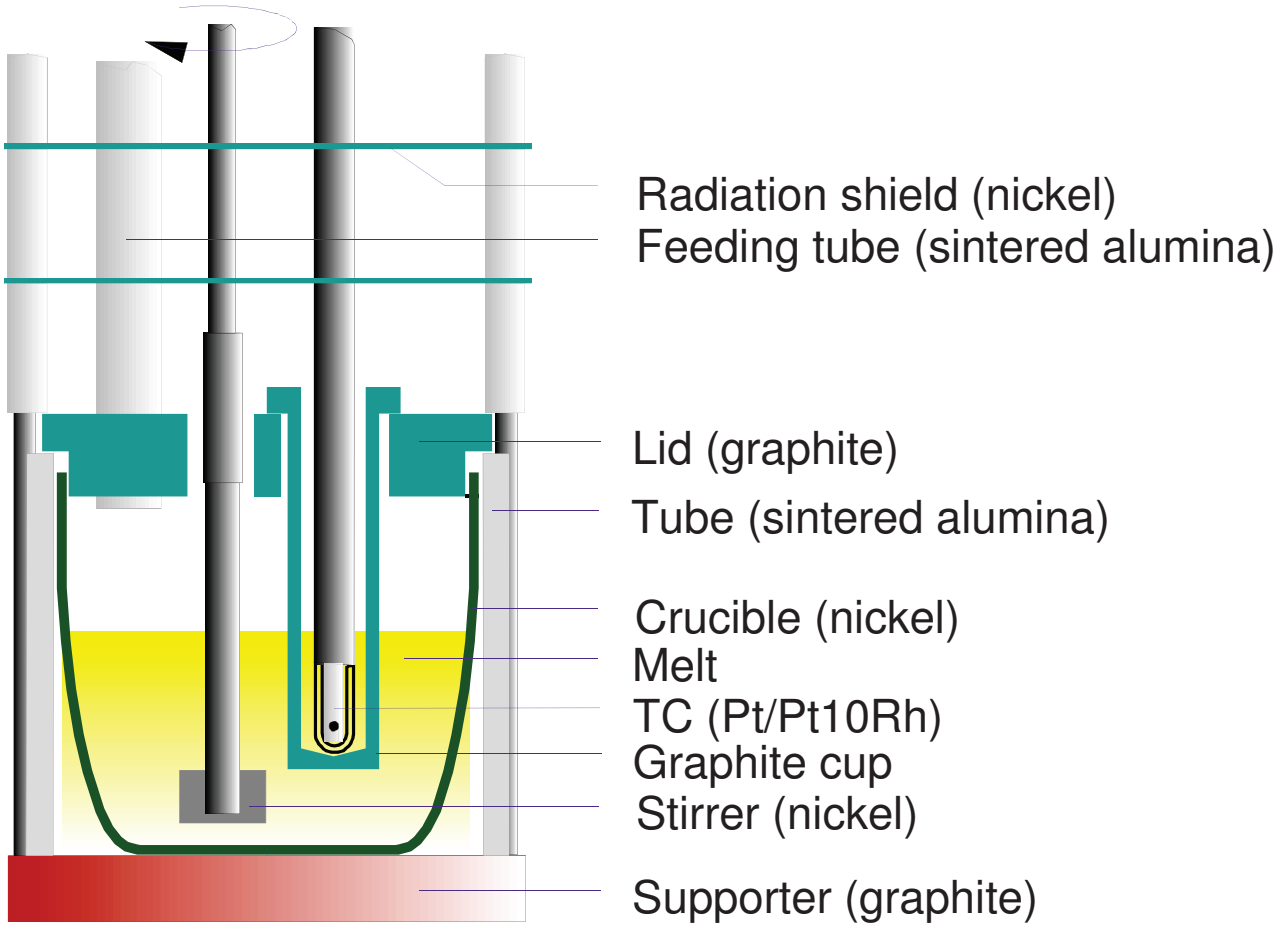

Figure 1. Design of the experimental set up for thermal analysis (TA). TC – thermocouple.

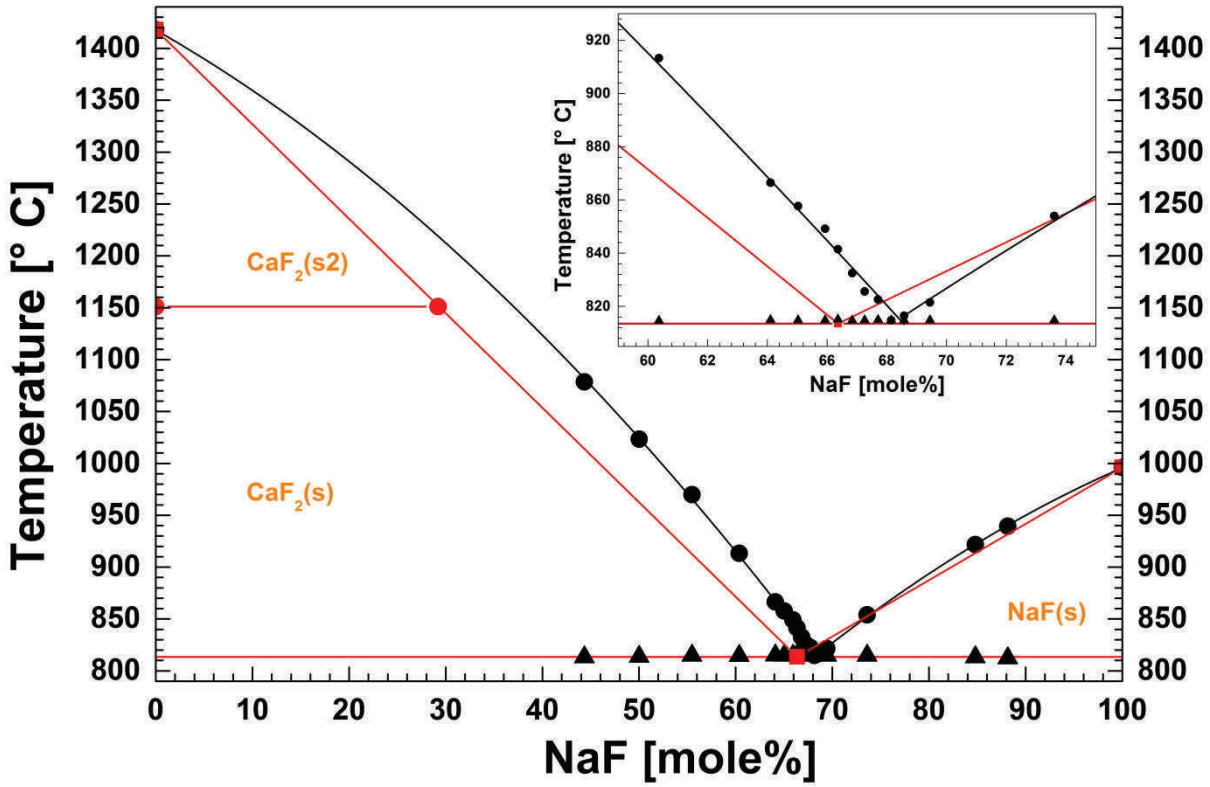

Figure 2. Binary phase diagram for the system NaF- CaF_2: experimental points by Fedotieff et al.[18] (■), simulation data by Beilmann et al.[8] (●) and experimental data of this work (● – liquidus line, ▲- eutectic line). Inset: As above, in the range 59-75 mole% NaF. Crystal structures: CaF_2 (s) – alpha state (monoclinic); CaF_2 (s2) – beta state (cubic); NaF (s) – villiaumite.

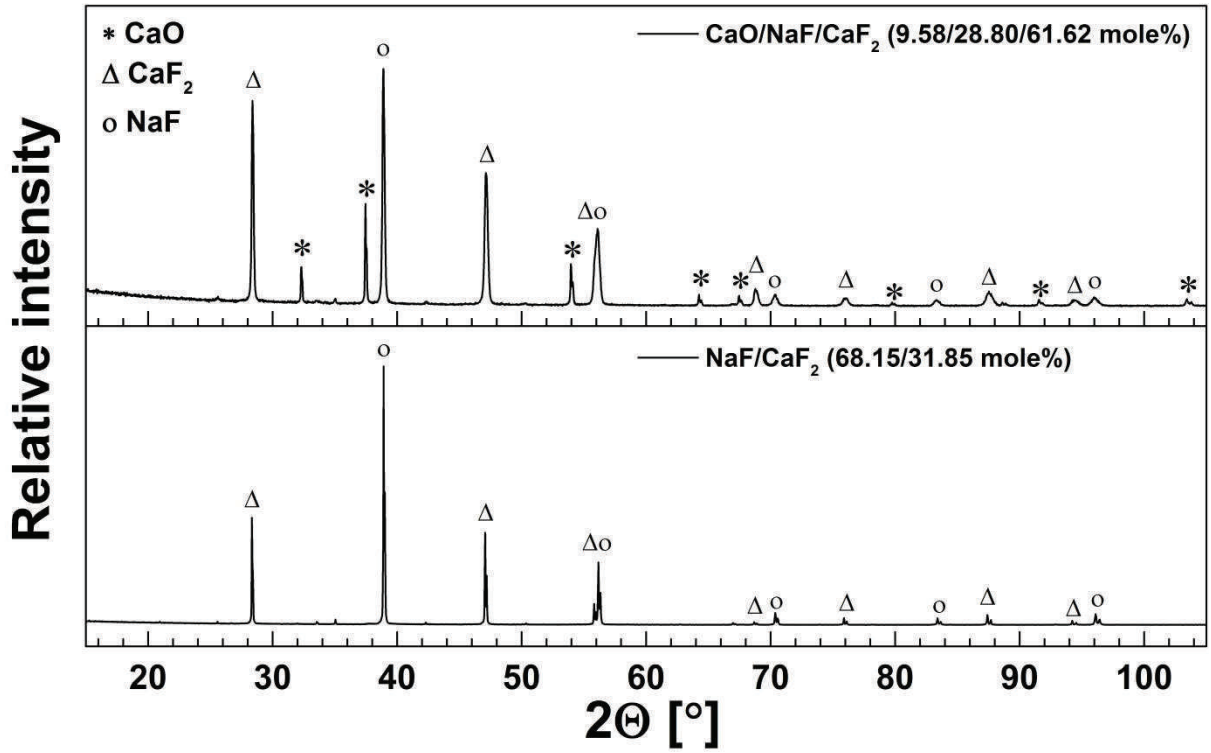

Figure 3. XRD patterns of quenched samples, NaF-CaF_2 and CaO-NaF-CaF_2.

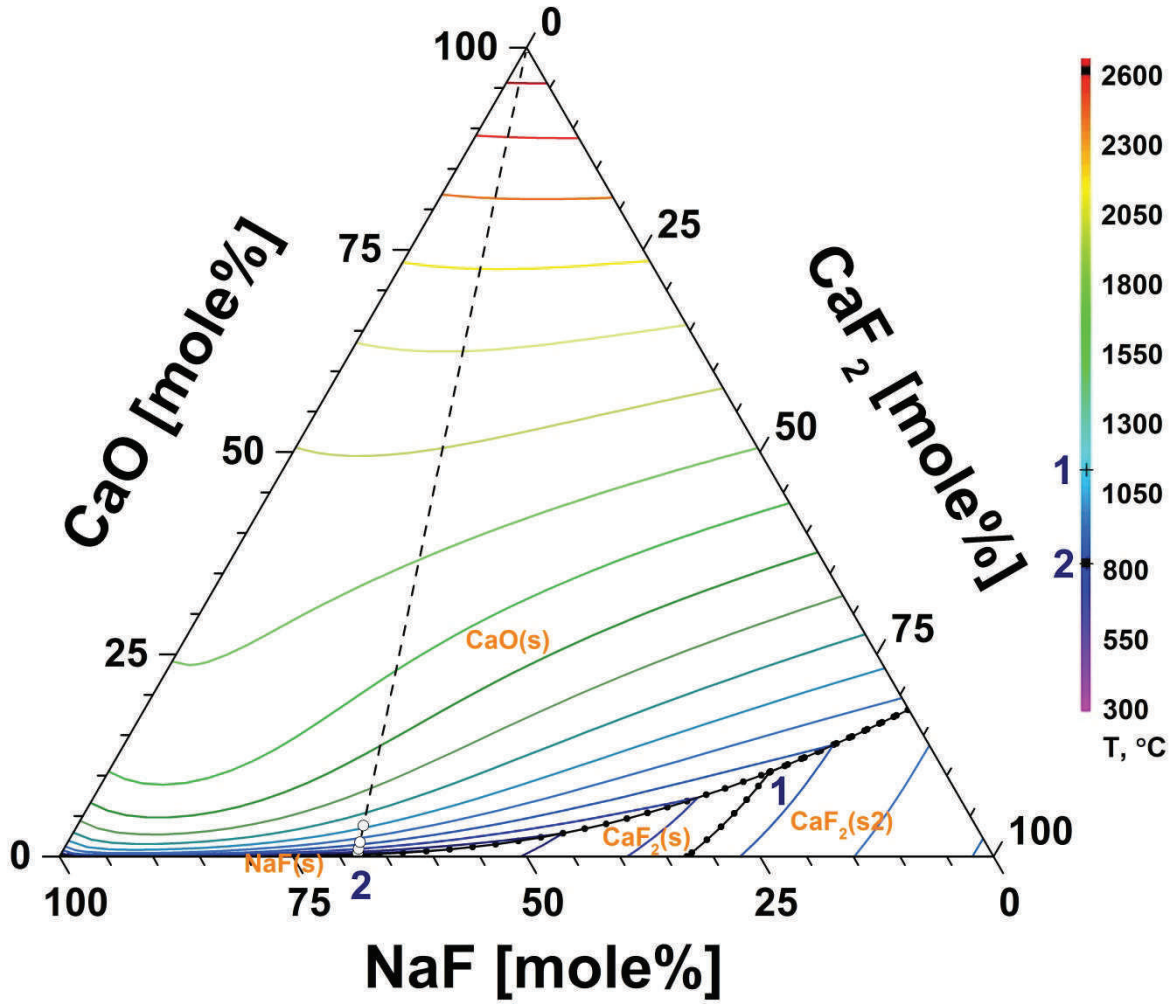

Figure 4. Projection of the liquidus planes and liquidus isotherms (the difference between the lines is 100 ºC) for the ternary CaO-NaF-CaF_2 system, as calculated by FactSage. The positions of experimentally analysed phase transitions are marked (○). Crystal structures: CaO (s) – lime (cubic); CaF_2 (s) – alpha state (monoclinic); CaF_2 (s2) – beta state (cubic) and NaF (s) – villiaumite (cubic).

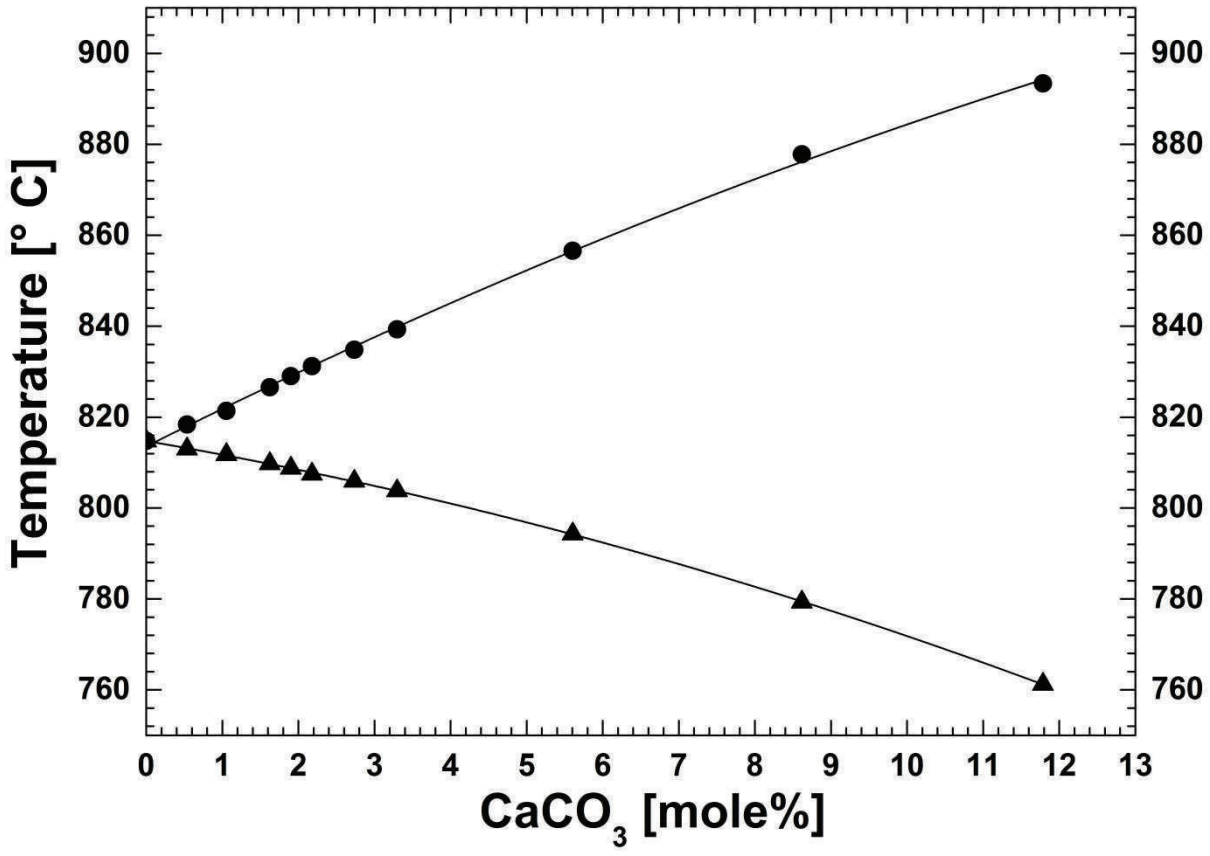

Figure 5. Experimentally derived data obtained by adding $CaCO_3$ to a melt with fixed CaF_2/NaF ratio (initially 31.9 mole% CaF_2), ● – liquidus line, ▲- solidus line.

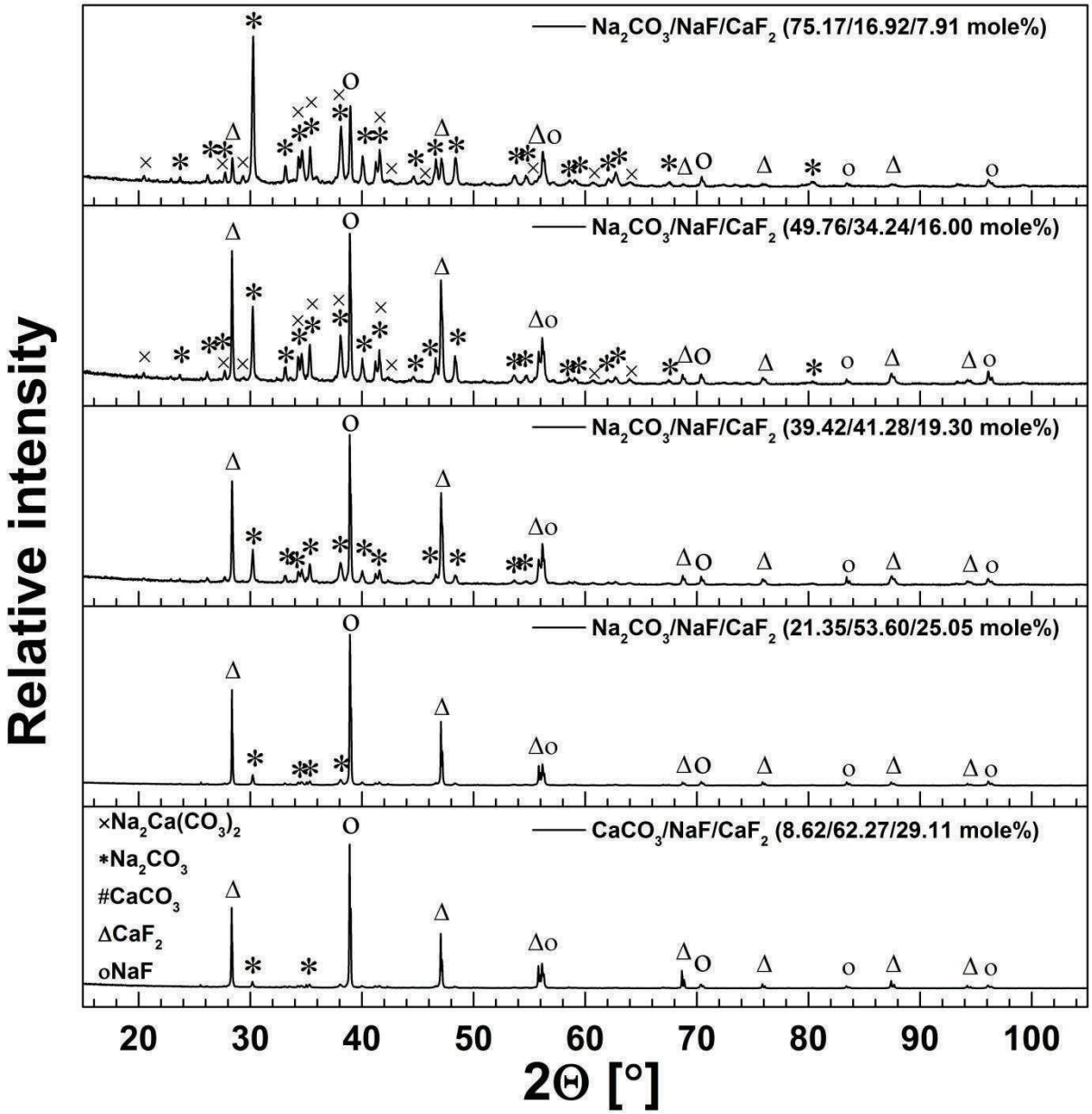

Figure 6. XRD patterns of quenched samples with different concentrations in a melt with fixed NaF/CaF_2 ratio (initially 31.9 mole% of CaF_2).

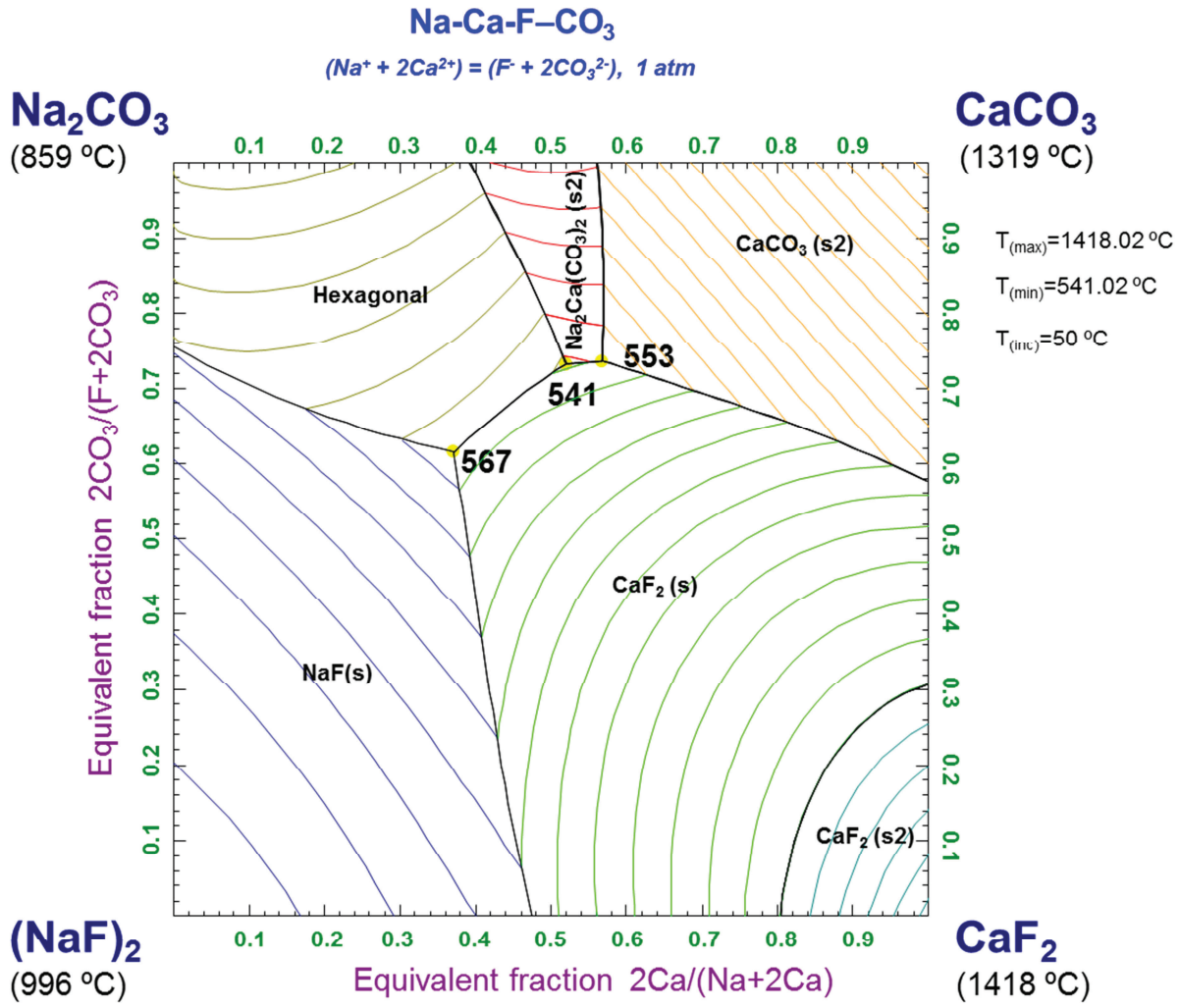

Figure 7. Phase diagram of Na-Ca-F-CO_3 calculated by FactSage. Crystal structures: CaF_2 (s) – alpha state (monoclinic); CaF_2 (s2) – beta state (cubic); NaF (s) – villiaumite (cubic); Na_2CO_3 – hexagonal and $Na_2Ca(CO_3)_2$ (s2) – orthorhombic-pyramidal. The distance between the liquidus isotherms is 50 ^oC.

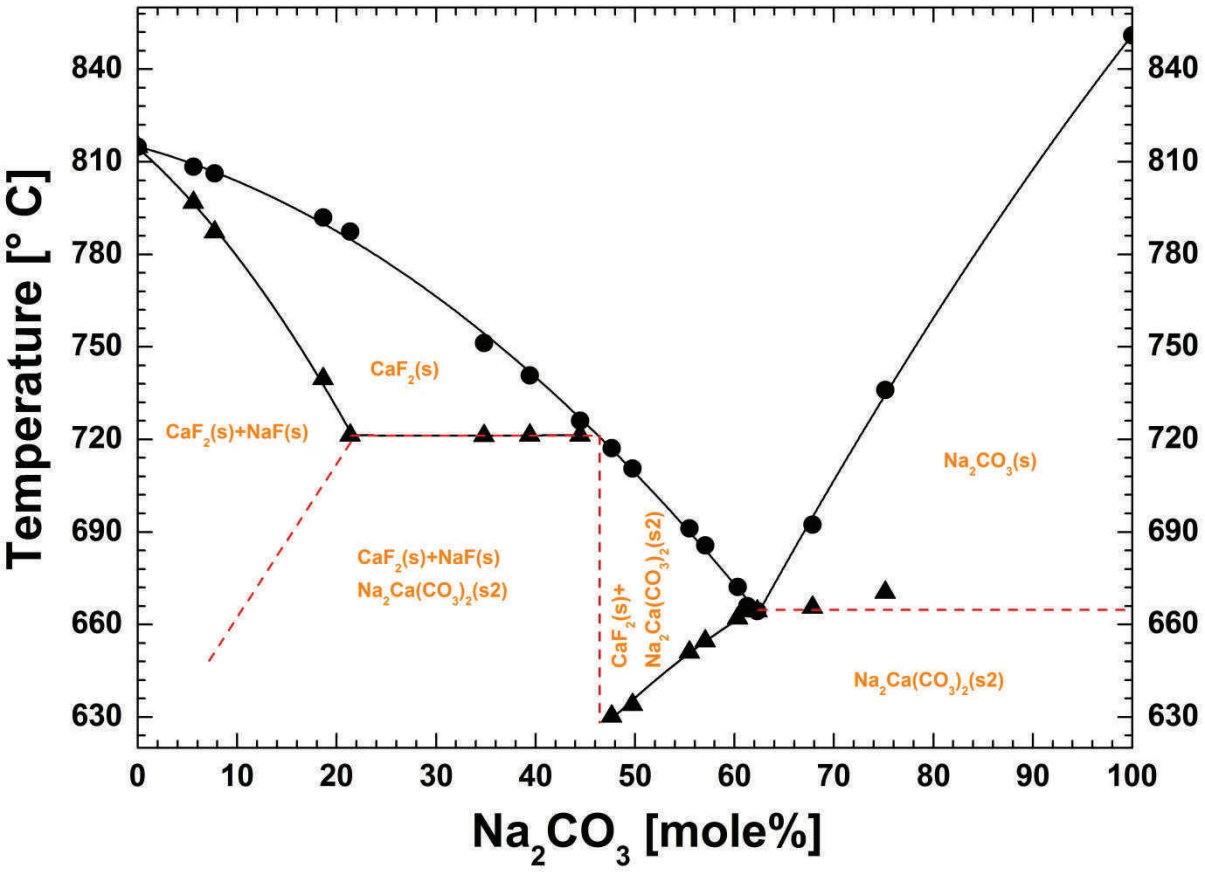

Figure 8. Experimental data on the solubility of Na_2CO_3 in a melt containing CaF_2 and NaF at a fixed ratio (initially 31.9 mole% of CaF_2). Crystal structures: CaF_2 (s) – alpha state (monoclinic); CaF_2 (s2) – beta state (cubic); NaF (s) – villiaumite (cubic); Na_2CO_3 – hexagonal and $Na_2Ca(CO_3)_2$ (s2) – orthorhombic-pyramidal (● – liquidus line, ▲- eutectic line, --- estimated liquidus and solidus lines).

Paper II

Viktorija Tomkute, Asbjørn Solheim, Simas Sakirzanovas and Espen Olsen. A Novel CO_2 Separation Process Using CaO in Molten CaF_2/NaF. Submitted to *Environmental Science & Technology*.

A Novel CO_2 Separation Process Using CaO in Molten CaF_2/NaF

Viktorija Tomkute[1], Asbjørn Solheim[2], Simas Sakirzanovas[3], Espen Olsen[1]*

[1] Department of Mathematical Sciences and Technology, Norwegian University of Life Sciences (UMB), Post Office Box 5003, Drøbakveien 31, NO-1432 Ås, Norway

[2] SINTEF Materials and Chemistry, Post Office Box 4760, Sluppen, NO-7465 Trondheim, Norway

[3] Department of Applied Chemistry, Vilnius University (VU), Naugarduko 24, LT-03225 Vilnius, Lithuania

Keywords: Post-combustion CO_2 Capture; Calcium Oxide; Molten Salt; Calcium Fluoride; Sodium Fluoride

Abstract. It has been demonstrated that the dissolution/dispersion of CaO in $CaCl_2$ melt enhances the cyclic capacity of the sorbent. We here report on the study on CO_2 removal from simulated flue gas by CaO in molten CaF_2/NaF. A salt system consisting of CaF_2-NaF at eutectic composition ratio was utilized as the solvent for the dissolution/dispersion of CaO. The impacts on the CO_2 capture efficiency by the CaO mass proportion in the molten salt, the temperatures for the carbonation/decarbonation reactions, the flue gas flow rate, and the CO_2 concentration were investigated. The experiments were performed in a one-chamber atmospheric pressure reactor, utilizing a Fourier transform infrared (FT-IR) gas detector and gravimetric analysis. CO_2 separation from N_2 was carried out at 821-948 ºC and decomposition of the formed carbonates was accomplished at 994-1170 ºC. Our studies showed high CO_2 removal efficiency where >99 % of the applied CO_2 was captured in the initial carbonation reaction stage. This may be attributed to the simultaneously occurring ion exchange reaction in CaO-CaF_2/NaF melt, where initially CO_2 reacts with CaO, and the calcium ion is subsequently substituted by sodium to give Na_2CO_3. The mechanisms concerning formation of carbonates are explained using experimentally derived as well as simulated data. The formation of Na_2CO_3 and $Na_2Ca(CO_3)_2$ was confirmed by X-ray diffraction analysis.

Introduction

Several concepts are under investigation for the capture of CO_2, such as physical and chemical absorption, adsorption, use of membranes, and removal via cryogenic separation.[1] CO_2 capture is frequently performed using amine solutions which reacts with CO_2 to form carbamates and bicarbonates.[2] It has been demonstrated that the main disadvantages of processes based on amine solutions are high cost, corrosion oxidative/thermal degradation of

the sorbent, and reactions with the other impurities existing in the synthesis gas (NO_x, SO_x, HCl, HF and particulate matter).[2,3] An alternative pathway investigated for CO_2 capture is the use of inorganic sorbents, such as the oxides or hydroxides of the alkali and alkaline earth metals which possess basic properties.[2] Calcium oxide has been accepted as the most attractive solid sorbent because of its high availability, low toxicity, and high CO_2 carrying capacity.[4-7] Analysis of the limestone carbonation conversion decay shows that after application of around 20 CO_2 absorption/desorption cycles, the performance stabilizes at only 25% of the initial carbonation efficiency.[8]

A packed tower with aqueous alkaline absorbent solution has been applied as a wet scrubbing technique for treating processing gases in industry.[9-11] One of the most studied of these solutions is NaOH with high pH for selective absorption of CO_2 from air at room temperature.[10-13] Although the collection of Na_2CO_3 for regeneration is easy and economically attractive, the process itself requires a lot of energy for water evaporation and thermal decomposition of Na_2CO_3. Therefore, a conventional "causticization" or "caustic recovery" process is usually selected for NaOH regeneration, where Na_2CO_3 reacts with $Ca(OH)_2$ resulting in the formation of NaOH and $CaCO_3$.[14] Decomposition of the formed $CaCO_3$ back to CaO and pure stream of CO_2 may be carried out at 900-950 ºC[15], CaO then needs to be hydrated with water to form $Ca(OH)_2$.[2] Also, non-conventional "causticization" technologies based on metal oxide (Me_xO_y) or salts in the Na_2CO_3 solution have been investigated for the pulp and paper industry.[14,16]

The reactivity of metal oxides promoted with alkali and alkali earth metals salts with CO_2 has been widely reported in recent years.[17-23] Sorption of CO_2 was tested by using K_2CO_3 as active material on carbon (AC) and MgO supports in the presence of water.[20] K_2CO_3 with 70 wt% MgO prepared by wet-chemistry method exhibited a highest carrying capacity of 0.197 g of CO_2/g of sorbent.[20] It has been demonstrated that MgO based sorbents induced with K_2CO_3 form several kinds of carbonates during the carbonation step, such as $K_2Mg(CO_3)_2$ and $K_2Mg(CO_3)_2 \bullet 4(H_2O)$. Also, Na_2CO_3-based sorbents with[22] and MgO[23] investigation showed the formation of a double salt ($Na_2Mg(CO_3)_2$) during the carbonation step.

Transport of liquid sorbents from the CO_2 capture chamber to the regenerator does not require complex technology as with solid sorbents. On the other hand, the carbonation reaction may be accomplished in a wider temperature range, from ambient temperature[20] to 1000 ºC with solid sorbents.[24] The dissolution/dispersion of sorbent particles in a molten salt matrix may enhance the reactivity of the sorbent with CO_2 due to more efficient gas-liquid-solid reactions than in gas-solid. Thus, CO_2 capture by CaO dissolved/dispersed in inexpensive $CaCl_2$ melt was investigated.[25] Studies of cyclic CO_2 absorption/desorption by CaO in 94.68 wt% $CaCl_2$ melt showed a stable carrying capacity of 0.504 g CO_2/g CaO. In all cases, the decomposition of the formed carbonates proceeded rapidly and completely.[25]

The aim of this work was to investigate the efficiency of a process based on CaO dissolved/dispersed in a eutectic mixture of CaF_2 and NaF. The eutectic composition of CaF_2/NaF (41.85 wt% CaF_2 in NaF, 815 ºC) was chosen due to its suitable melting point for the carbonation reaction and high boiling point, which allows low-pressure operation.[26,27] The CO_2 sorption/desorption behavior was studied using a Fourier transform infrared (FTIR) gas

detector and gravimetric analysis. Particularly, the impacts of the CaO mass proportion in the melt, the temperatures of the system for the carbonation/decarbonation reactions, the CO_2 content and the simulated flue gas flow rate were examined to determine the efficient CO_2 sorption process by the CaO-CaF_2/NaF system.

Materials and methods

Materials

CaO (Sigma-Aldrich reagent, 96-100 % purity), CaF_2 (Sigma-Aldrich reagent, 99.0 – 100.0 % purity) and NaF (Sigma-Aldrich reagent, 98.5-100.0 % purity) were used for preparing the molten salt for carbonation/decarbonation tests. The powders were dried at 200 °C for 24 h. All sorbents were prepared by direct mixing of the appropriate amounts of NaF/CaF_2 (41.85 wt% CaF_2 and 48.15 wt% NaF) and CaO (5, 10, 15, 20 wt%) to form a 10 cm high liquid column in a nickel crucible (5.2 cm dia. x 35.0 cm height). The weight varied from 630 to 650 g depending on the composition, unless otherwise mentioned. The mixtures were melted in argon atmosphere and kept at 970 °C for 10 h before carbonation, unless otherwise mentioned. Pure gases provided by AGA were used for all experiments and the mixtures of carbon dioxide (purity of 99.99 %) in nitrogen (purity of 99.999%, $H_2O \leq 3$ ppm, $O_2 \leq 3$ ppm, $C_nH_m \leq 1$ ppm) were controlled by mass flow controllers (MASS-STREAM, M+W Instruments GmbH).

Experimental set-up and methods

The absorption and desorption of CO_2 were carried out in an automated one-chamber atmospheric pressure reactor.[25] The nickel crucible mentioned above was placed inside a stainless steel outer chamber, and this assembly was fixed in a ceramic tube vertical furnace. The carbonation/decarbonation experiments were followed using a FTIR gas analyzer (Thermo Scientific, Nicolet 6700 model) and an industrial weighing scale (MS8001S, Mettler Toledo, accuracy of 0.1 g). Before each sorption measurement the melts were stirred by bubbling N_2 (0.5 l/min) through the melt at different absorption temperatures in the range 820-950 °C for 2 h before carbonation. The N_2 and CO_2-N_2 gas mixtures (total flow 0.6 l/min, 1.3-14.0 vol% CO_2) were controlled by mass flow controllers (MASS-STREAM, M+W Instruments GmbH) and bubbled into the CaO-CaF_2/NaF melt via a nickel pipe passed through the top of the sealed reactor assembly and immersed to a depth of 1 cm from the bottom of the crucible. A constant argon flow of 0.20 l/min was applied as a purge flow over the assembly in the ceramic tube furnace to avoid corrosion of the chamber. The temperature measurements were performed using a type S (Pt–Pt10Rh, ±1.1 °C) thermocouple immersed in the melt. The tightness of the system was controlled by a mass flow meter (Sierra 820 Series, Sierra Instruments, Inc.) supplied at the outlet of the FTIR gas cell. In each test, the carbonation process was determined to be complete when the inlet and outlet CO_2-N_2 stream composition was nearly matching. Decomposition of the formed carbonates back to oxide was conducted at temperatures ranging from of 994 ^oC to 1163 °C. The total weight of the assembly and the gas composition were continuously monitored. All experimental information represented in this study were collected using computer controlled change of settings (temperature, CO_2 and N_2 gases composition and weight changes), data collection,

visualization, processing and analysis tools (OMNIC Series Thermo Scientific and NI cRIO-907x integrated systems).

The weight increase is due to absorbed CO_2, and weight decrease is caused by CO_2 liberation during decarbonation of the formed carbonates. Correction for the weight change due to corrosion of the stainless steel compartment was taken into the calculations. For this purpose, a baseline study of the corrosion of the reactor was performed at different temperatures.

Characterization

Powder X-ray diffraction (XRD) analysis was carried out for phase identification in samples collected during carbonation and decarbonation reaction stages. Samples consisting of 20 wt% of CaO in NaF-CaF_2 were analysed. The samples were collected by quenching the melts on a stainless steel plate. XRD data were collected from $5^o \leq 2\theta \leq 110^o$ (scan rate 0.01 degree per second) using Ni-filtered Cu K_α on a Bruker D8 Advance diffractometer working in Bragg-Brentano ($\theta/2\theta$) geometry. All measurements were performed at room temperature and ambient pressure in air.

Results and discussion

Evaluation of the CaO-CaF_2/NaF system for the CO_2 sorption processes

Figure 1 depicts measurements of the melt temperature, CO_2 concentration in N_2 leaving the sealed reactor, and the weight changes of the reactor assembly detected during the experiments. First, the melt consisting of 5 wt% CaO, 50.8 wt% NaF and 44.2 wt% CaF_2 was kept under N_2 atmosphere at 824 ºC for 2 h before initiating the carbonation. The CO_2 flow was started at time t = 0. This caused an increase in the temperature, which can be attributed to the exothermic reaction of CaO with CO_2 (Eq. 1).

$$CaO(s) + CO_2(g) \leftrightarrow CaCO_3(s) \quad (1)$$

The weight and CO_2 concentration curves reveal a period with fast carbonation followed by slow carbonation. The initial fast carbonation reaction represents a highly efficient CO_2 removal stage where close to 99.9 % of the applied CO_2 is captured; this stage can be related to CO_2 reaction with dispersed CaO. The second carbonation stage may be assigned to the reaction of the dissolved and deposited CaO (which is covered by carbonate layer) with CO_2. This slow stage is considered to be finished when the CO_2 concentration recorded by the FTIR analyzer becomes equal to the inlet concentration. Decomposition of the formed carbonates was conducted by raising the temperature to 1156 ºC bubbling pure N_2 through the melt which also resulted in a rapid step and a slow step (Figure 1). The total conversion efficiency of CaO to carbonates at 824 ºC was around 94 wt%, but complete decomposition of the formed carbonates was not reached (65 wt% of CO_2 released). The high carbonation efficiency is enabled by the ion exchange reaction described by eq. 2.

$$CaCO_3 + 2NaF \leftrightarrow Na_2CO_3 + CaF_2 \quad (2)$$

$$CaO(s) + CO_2(g) + 2NaF \leftrightarrow Na_2CO_3 + CaF_2 \quad (3)$$

At temperatures lower than 335 ºC[28], formation of shortite may take place (Eq. 4), but above this temperature shortite decomposes to nyerereite which melts at 817 ºC (Eq. 5).

$$3CaCO_3 + 2NaF \leftrightarrow Na_2Ca_2(CO_3)_3 + CaF_2 \quad (4)$$

$$Na_2Ca_2(CO_3)_3 \leftrightarrow Na_2Ca(CO_3)_2 + CaCO_3 \quad (5)$$

FIGURE 1

The Gibbs free energy for possible carbonation/decarbonation reactions as described by Eqs. 1, 2 and 3 were calculated using the HSC Chemistry program (version 6.1), and the results are provided in Supporting Information (SI) Figure S1. In addition, the Gibbs free energy for the reaction between solid sodium oxide and CO_2 was calculated. The results indicate that Na_2CO_3 is thermodynamically more stable than $CaCO_3$, because the Gibbs free energy for Eq. 2 is negative over the temperature range 400-2300 ºC. It is shown that decomposition of $CaCO_3$ appears at around 900 ºC and the reaction between Na_2O and CO_2 occurs at temperatures lower temperature than 2200 ºC. The value of the Gibbs free energy for Eq. 3 is negative at low temperatures and becomes positive above 1120 ºC, indicating that the equilibrium is shifted towards the left as the temperature increases. This reaction was verified experimentally by conducting the baseline study of CO_2 capture using the CaF_2/NaF system without addition of CaO (SI Figure S2). In this study, 14 vol% CO_2 in N_2 was bubbled through the CaF_2/NaF melt at 820 ºC after approximately 2 minutes of pure N_2 flow. No CO_2 removal from the gas mixture was observed.

Structural analysis

XRD analysis was carried out on quenched samples collected during the performance of the carbonation step using CaO/CaF_2/NaF (20/37.2/42.8 wt%) melt and 14 vol% CO_2 in N_2 gas mixture at 830 ºC). The results are shown in Figure 2. For the sample taken before the start of CO_2 flow through the melt, the XRD pattern peaks must be assigned to the pure initially weighed in CaO, CaF_2 and NaF. The intensity of the characteristic peaks belonging to NaF and CaO decrease was observed after a prolonged period of carbonation. The X-ray diffraction pattern of the sample taken after 100 minutes of CO_2 absorption illustrates a new phase formation which can be indexed as Na_2CO_3 (space group P6(3)/m)[29]. It is suggested that the ion exchange reaction forming Na_2CO_3 takes place immediately during carbonation step (Eq. 2). After 480 minutes of CO_2 absorption most of the CaO was converted to CaF_2, and the NaF has been partly converted to Na_2CO_3. No $CaCO_3$, $Na_2Ca(CO_3)_2$ or $Na_2Ca(CO_3)_2$ characteristic peaks were found during the carbonation. The formation of $Na_2Ca_2(CO_3)_3$ and $Na_2Ca_2(CO_3)_3$ may be expected at temperatures lower than 400 ºC and 817 ºC, respectively[28]. Therefore, we suggest that complete sodium cation substitution in $CaCO_3$ occurs, and that Na_2CO_3 and CaF_2 are formed by Eq. 3. The concentration of the formed double carbonates appears to be too low for detection by XRD.

FIGURE 2

The formed carbonates were decomposed by rising the temperature to 1170 ºC under pure N_2 atmosphere. The X-ray diffraction patterns of the assembled samples are shown in Figure 3. The intensity of the Na_2CO_3 peaks decreased with increasing decarbonation time. In addition,

the presence of CaO can clearly be seen after 120 minutes of CO_2 desorption. As would be expected, the intensity of peaks characteristic for CaO increased with time, indicating that the reversible reaction occurs (Eq. 3). Finally, there were no intensive Na_2CO_3 peaks detected in the XRD pattern after 480 minutes of decarbonation, which indicates that full decomposition of the formed carbonates was accomplished.

FIGURE 3

From the analysis of the peaks it is still difficult to calculate the accurate amount of the active CaO that takes place in the carbonation/decarbonation process, because of the complexity in the undergoing reactions between $CaCO_3$ and NaF. The formation of small amounts of complex carbonates in the CaO-CaF_2/NaF system not identified in the XRD pattern may influence the results. Therefore, the conversions of the sorbent to carbonates for all tests were calculated on the basis of the initially added amounts of CaO in the CaF_2/NaF eutectic mixture.

Effect of carbonation temperature

The effect of temperature on the carbonation reaction in CaO/CaF_2/NaF (5/44.2/50.8 wt%) was investigated to determine the most efficient temperature conditions for the sorbent conversion (SI Figure S3). A rise in the melt temperature by 4-6 ºC was detected in all initial fast carbonation reaction stages. The slow carbonation reaction stage starts when the measured melt temperature is returning to the initial temperature and a rapid increase in the recorded CO_2 concentration was observed. As mentioned above; according to the thermodynamics, the reaction of CO_2 with solid-CaO dispersed in the CaF_2/NaF melt constitutes the fast reaction stage and the reaction of CO_2 with dissolved/agglomerated CaO takes place in the slow reaction stage. The results indicate that CaO conversion in the initial fast carbonation reaction is close to 90 wt% of total reacted sorbent (Figure 4). The highest carbonation efficiency was observed at 826-834 °C, where the fast reaction was completed after 117 minutes and the final CaO conversion was 94-95 wt%. At temperatures higher than 834 °C the total conversion efficiency decreased from 95 to 91 wt%. High carbonation conversion achieved in temperature range 821-950 °C indicates formation of the thermodynamically stable carbonate (Na_2CO_3, see Eq. 2)

FIGURE 4

Effect of decarbonation temperature

To investigate the decarbonation reaction mechanism, decomposition of the carbonates was carried out at temperatures ranging from 994 to 1163 ºC (SI Figure S4). The initial CO_2 carbonation was carried out at 830 ºC by bubbling 14 vol% CO_2 in N_2 through the melt consisting of dissolved/dispersed CaO in CaF_2/NaF (5/50.8/44.2 wt%) for 300 minutes. The decarbonation was performed by increasing the temperature. It was observed that the CO_2 concentration curves recorded at 1048-1163 ºC exhibit two peaks, and the curves recorded at lower temperature show one single peak (SI Figure S4). As described above, the calculation of the standard Gibbs free energy for the reaction where CaO reacts with CO_2 and NaF to form CaF_2 and Na_2CO_3 (Eq. 3) indicates that the equilibrium may be achieved at around 1120 ºC. Therefore, the faster decomposition of the formed sodium carbonate should appear

at temperatures higher than 1120 ºC (this temperature is not corrected for activities lower than unity for all substances other than CaO). We suggest that the first peak in the CO_2 concentration curve may be assigned to the decomposition of a small amount of $CaCO_3$, while the second peak is due to decomposition of Na_2CO_3. The results in Figure 5 demonstrate the effect of decarbonation temperature on CaO regeneration. The degree of conversion of the formed carbonates was calculated from the amount of CO_2 released from the reactor during 170 minutes. It can be observed that the efficiency of CO_2 regeneration increases rapidly at higher temperatures. However, complete decomposition of the formed carbonates was not observed due to the reactor design; it was observed that the nickel tube which was used to transport the gases into the melt was blocked due to sorbent precipitation on the walls.

FIGURE 5

Effect of CaO variation in the fluoride melts

The influence of CaO mass proportion in the CaF_2/NaF (46.5/53.5 wt%) eutectic mixture on the CO_2 uptake is shown in Figure 6. As noted above, we have established that the conversion of CaO in the molten fluoride based salt is highest between 826 ºC and 834 ºC. Accordingly, the experiments with variable CaO concentration were carried out within this temperature range. The gas composition in the carbonation step was 14 vol% CO_2 in N_2. Regeneration was performed at 1160 – 1170 ºC under pure N_2 atmosphere. It was found out that 99.9 % of total applied CO_2 was removed from the N_2 in the initial carbonation stage with 5 wt% CaO in CaF_2/NaF. The CO_2 adsorption efficiency decreased to 98.1 % by increasing the CaO concentration from 5 to 20 wt%. The total CaO conversion efficiency decreased rapidly from 94.6 to 75.2 wt% when increasing the CaO concentration from 10 to 20 wt% (Figure 7). The loss in CaO activity above 10 wt% may be attributed to deposition and agglomeration of CaO. Regeneration of the metal oxide was performed by raising the temperature to 1160-1170 ºC under pure N_2, resulted in incomplete CO_2 desorption (Figure 6 and 7). In this case, the regeneration efficiency of CaO was calculated for the total reacted CaO with CO_2. The highest CO_2 release from the carbonated sample (84.5 % of total captured CO_2) was achieved with 20 wt% CaO in CaF_2/NaF. The formation of carbonates in the CaO/NaF/CaF_2 system influences the liquidus temperature of the mixture, and also the solubility of CaO. The carbonates have higher solubility than CaO, so higher carbonate concentration due to increased amounts of CaO would lead to a lower melting point. Therefore, the enhancement in the regeneration efficiency with higher CaO amounts may be related to slower CaO solidification and agglomeration on carbonated particles and around the nickel tube.

FIGURE 6 and 7

Effect of CO_2 concentration in the simulated flue gas

The impact of the inlet gas composition on sorbent conversion efficiency was examined by varying the CO_2 concentration in N_2 between 1.3 and 14 vol% at 825-835 ºC. For this purpose, the melt containing of 5 wt% CaO was tested. Figure 8 shows the concentration of CO_2 versus time in the outlet gas as recorded the FTIR gas detector. It was found out that the total carbonation conversion is independent on the inlet CO_2 concentration in N_2, and it was around 93.3 wt% (0.733 g CO_2/g of CaO). However, a closer examination of these results reveals that the regions of fast and slow carbonation reaction are affected by the inlet steam

composition. The conversion of CaO in the fast carbonation stage is reduced from 89.5 to 70.1 % by increasing the CO_2 concentration from 1.3 vol% to 14 vol%. In addition, the duration of the slow carbonation reaction was prolonged when the CO_2 concentration decreased. This may be related to phase transitions in the CaO-NaF/CaF_2 system due to formation of carbonates which influence the solubility of unreacted CaO as well as the liquidus temperature of the melt. As mentioned above, the fast carbonation reaction may be attributed to reaction between CO_2 and dispersed CaO. Therefore, the additional dissolution/dispersion of solid CaO would influence the fast and slow carbonation reactions rates.

FIGURE 8

Effect of CO and HF formation

The concentrations of carbon monoxide (CO, from the reduction of CO_2) and hydrofluoric acid (HF, from the hydrolysis of fluoride salts) are shown in Figure 9. The data were recorded during carbonation experiments using 14 vol% CO_2 in N_2 and 5 or 20 wt% CaO in CaF_2/NaF. Desorption of CO_2 was conducted under pure N_2. The results indicate that the CaO concentration does has no effect on the HF formation. The HF peak at 50 ppm was detected after 100 minutes of carbonation at 821 and 826 ºC, decreasing to 10 ppm during the rest of the carbonation. The same value was found during the decarbonation process at elevated temperature (1125 and 1158 ºC). This indicates that metal fluoride hydrolysis is independent on the temperature in the range 821-1158 ºC, and it may be related to minor contents of moisture in the inlet gas. The weight change due to the hydrolysis of the fluoride salts was considered negligible.

The carbon monoxide concentration curves indicate that the CO release was affected by the CaO concentration. The CO emission from the reactor in the initial fast carbonation step is close to 0 ppm for both compositions (5 and 20 wt% of CaO in CaF_2/NaF), but during the slow carbonation step, a CO peak of 470 ppm is detected at low CaO concentration. However, during the decarbonation step CO contents up to 9000 ppm are observed, depending on the CO_2 release from the reactor. The carbon monoxide behavior may be explained by CO_2 reduction by iron at elevated temperatures, or by the Boudouard reaction.

FIGURE 9

ASSOCIATED CONTENT

Supporting Information. Figures S1, S2, S3 and S4. This material is available free of charge via the Internet at http://pubs.acs.org.

AUTHOR INFORMATION

Corresponding Author
*Email: viktorija.tomkute@gmail.com

Notes

The authors declare no competing financial interest.

Acknowledgments

We thank the Research Council of Norway for financial support through the CLIMIT research Programme (199900/S60). The primary data have been deposited for open access with the Norwegian University of Life Sciences (UMB).

References

(1) Wang, M.; Lawal, A.; Stephenson, P.; Sidders, J.; Ramshaw, C.: Post-combustion CO_2 capture with chemical absorption: A state-of-the-art review. *Chem. Eng. Res. Des.* **2011**, *89*, 1609-1624.

(2) Goeppert, A.; Czaun, M.; Prakash, G. K. S.; Olah, G. A.: Air as the renewable carbon source of the future: an overview of CO_2 capture from the atmosphere. *Energy & Environmental Science* **2012**, *5*, 7833-7853.

(3) Zhao, M.; Minett, A. I.; Harris, A. T.: A review of techno-economic models for the retrofitting of conventional pulverised-coal power plants for post-combustion capture (PCC) of CO_2. *Energy & Environmental Science* **2013**, *6*, 25-40.

(4) Martinez, A.; Lara, Y.; Lisbona, P.; Romeo, L. M.: Energy Penalty Reduction in the Calcium Looping Cycle. *Int. J. Greenh. Gas Control* **2012**, *7*, 74-81.

(5) Liu, W. Q.; Yin, J. J.; Qin, C. L.; Feng, B.; Xu, M. H.: Synthesis of CaO-Based Sorbents for CO2 Capture by a Spray-Drying Technique. *Environ. Sci. Technol.* **2012**, *46*, 11267-11272.

(6) Valverde, J. M.: Ca-based synthetic materials with enhanced CO_2 capture efficiency. *J. Mater. Chem. A* **2013**, *1*, 447-468.

(7) Donat, F.; Florin, N. H.; Anthony, E. J.; Fennell, P. S.: Influence of high-temperature steam on the reactivity of CaO sorbent for CO_2 capture. *Environ. Sci. Technol.* **2012**, *46*, 1262-1269.

(8) Abanades, J. C.; Alvarez, D.: Conversion Limits in the Reaction of CO_2 with Lime. *Energ Fuel* **2003**, *17*, 308-315.

(9) Baciocchi, R.; Storti, G.; Mazzotti, M.: Process design and energy requirements for the capture of carbon dioxide from air. *Chemical Engineering and Processing* **2006**, *45*, 1047-1058.

(10) Chen, W. H.; Tsai, M. H.; Hung, C. I.: Numerical prediction of CO_2 capture process by a single droplet in alkaline spray. *Applied Energy* **2013**, *109*, 125-134.

(11) Zeman, F.: Energy and material balance of CO_2 capture from ambient air. *Environ. Sci. Technol.* **2007**, *41*, 7558-7563.

(12) Stolaroff, J. K.; Keith, D. W.; Lowry, G. V.: Carbon dioxide capture from atmospheric air using sodium hydroxide spray. *Environ. Sci. Technol.* **2008**, *42*, 2728-2735.

(13) Nikulshina, V.; Ayesa, N.; Galvez, M. E.; Steinfeld, A.: Feasibility of Na-based thermochemical cycles for the capture of CO_2 from air - Thermodynamic and thermogravimetric analyses. *Chem. Eng. J.* **2008**, *140*, 62-70.

(14) Mahmoudkhani, M.; Keith, D. W.: Low-energy sodium hydroxide recovery for CO_2 capture from atmospheric air-Thermodynamic analysis. *Int. J. Greenh. Gas Control* **2009**, *3*, 376-384.

(15) MacDowell, N.; Florin, N.; Buchard, A.; Hallett, J.; Galindo, A.; Jackson, G.; Adjiman, C. S.; Williams, C. K.; Shah, N.; Fennell, P.: An overview of CO_2 capture technologies. *Energy & Environmental Science* **2010**, *3*, 1645-1669.

(16) Yin, H. Y.; Mao, X. H.; Tang, D. Y.; Xiao, W.; Xing, L. R.; Zhu, H.; Wang, D. H.; Sadoway, D. R.: Capture and electrochemical conversion of CO_2 to value-added carbon and oxygen by molten salt electrolysis. *Energy & Environmental Science* **2013**, *6*, 1538-1545.

(17) Duan, Y. H.; Sorescu, D. C.: CO_2 capture properties of alkaline earth metal oxides and hydroxides: A combined density functional theory and lattice phonon dynamics study. *Journal of Chemical Physics* **2010**, *133*.

(18) Xiao, G. K.; Singh, R.; Chaffee, A.; Webley, P.: Advanced adsorbents based on MgO and K_2CO_3 for capture of CO_2 at elevated temperatures. *Int. J. Greenh. Gas Control* **2011**, *5*, 634-639.

(19) Li, L.; Li, Y.; Wen, X.; Wang, F.; Zhao, N.; Xiao, F. K.; Wei, W.; Sun, Y. H.: CO2 Capture over K_2CO_3/MgO/Al_2O_3 Dry Sorbent in a Fluidized Bed. *Energ Fuel* **2011**, *25*, 3835-3842.

(20) Lee, S. C.; Chae, H. J.; Lee, S. J.; Choi, B. Y.; Yi, C. K.; Lee, J. B.; Ryu, C. K.; Kim, J. C.: Development of regenerable MgO-based sorbent promoted with K_2CO_3 for CO_2 capture at low temperatures. *Environ. Sci. Technol.* **2008**, *42*, 2736-2741.

(21) Lee, S. C.; Choi, B. Y.; Lee, T. J.; Ryu, C. K.; Soo, Y. S.; Kim, J. C.: CO_2 absorption and regeneration of alkali metal-based solid sorbents. *Catalysis Today* **2006**, *111*, 385-390.

(22) Kondakindi, R. R.; McCumber, G.; Aleksic, S.; Whittenberger, W.; Abraham, M. A.: Na_2CO_3-based sorbents coated on metal foil: CO_2 capture performance. *Int. J. Greenh. Gas Control* **2013**, *15*, 65-69.

(23) Zhang, K. L.; Li, X. H. S.; Duan, Y. H.; King, D. L.; Singh, P.; Li, L. Y.: Roles of double salt formation and $NaNO_3$ in Na_2CO_3-promoted MgO absorbent for intermediate temperature CO_2 removal. *Int. J. Greenh. Gas Control* **2013**, *12*, 351-358.

(24) Stendardo, S.; Andersen, L. K.; Herce, C.: Self-activation and effect of regeneration conditions in CO_2-carbonate looping with CaO-$Ca_{12}Al_{14}O_{33}$ sorbent. *Chem. Eng. J.* **2013**, *220*, 383-394.

(25) Tomkute, V.; Solheim, A.; Olsen, E.: Investigation of high-temperature CO_2 capture by CaO in $CaCl_2$ molten salt. *Energ Fuel* **2013**, *27*, 5373-5379.

(26) Beilmann, M.; Benes, O.; Konings, R. J. M.; Fanghanel, T.: Thermodynamic Investigation of the (LiF + NaF + CaF_2 + LaF_3) System. *J. Chem. Thermodyn.* **2011**, *43*, 1515-1524.

(27) Forsberg, C. W.; Peterson, P. F.; Zhao, H. H.: High-temperature liquid-fluoride-salt closed-Brayton-cycle solar power towers. *Journal of Solar Energy Engineering-Transactions of the Asme* **2007**, *129*, 141-146.

(28) Cooper, A. F.; Gittins, J.; Tuttle, O. F.: System Na_2CO_3-K_2CO_3-$CaCO_3$ at 1 kilobar and its significance in carbonatite petrogenesis. *American Journal of Science* **1975**, *275*, 534-560.

(29) Swainson, I. P.; Dove, M. T.; Harris, M. J.: Neutron Powder Diffraction Study of the Ferroelastic Phase-Transition and Lattice Melting in Sodium-Carbonate, Na_2CO_3. *Journal of Physics-Condensed Matter* **1995**, *7*, 4395-4417.

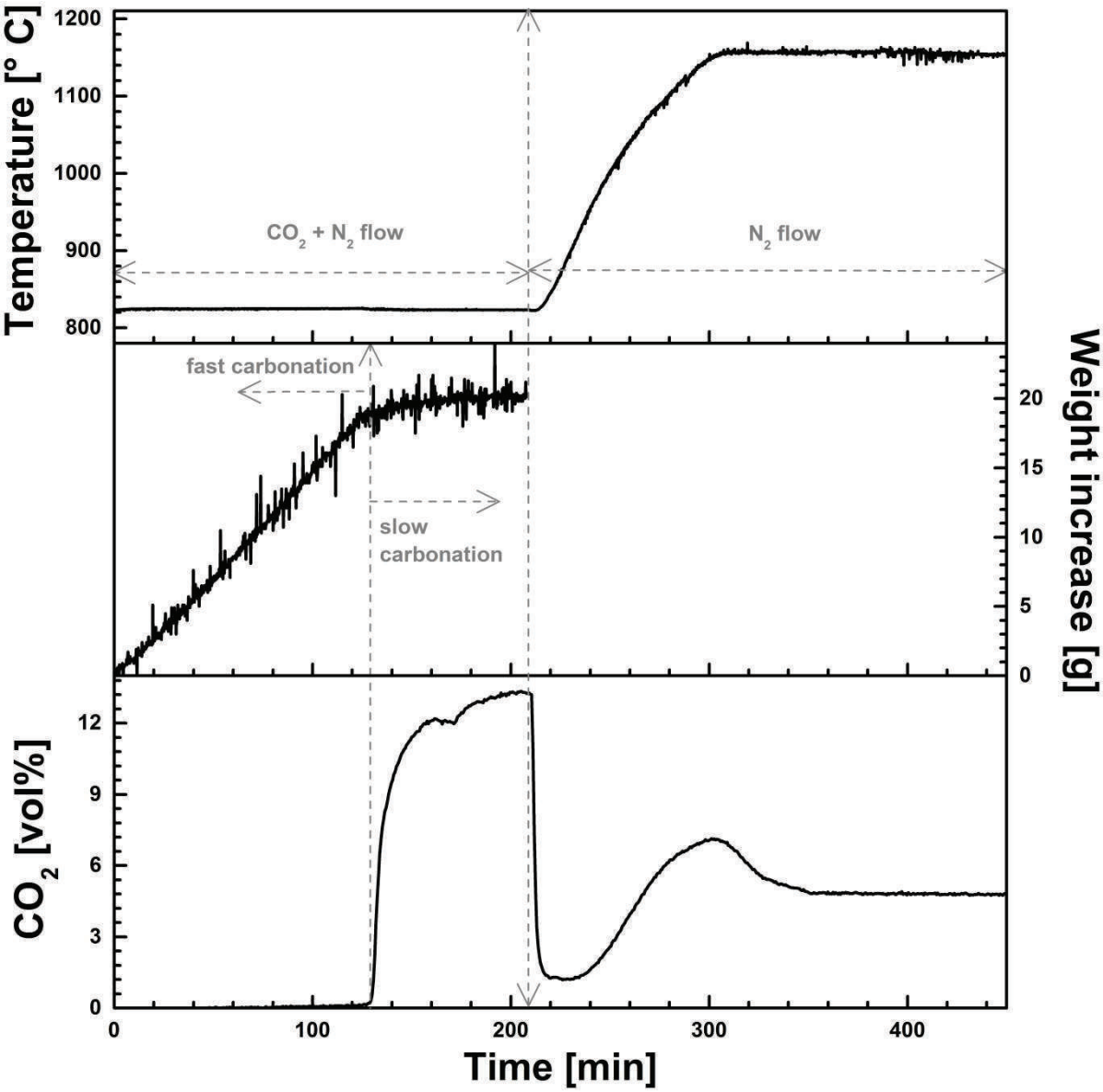

Figure 1. Separation of CO_2 from a simulated flue gas (N_2+13 vol% CO_2) by CaO/CaF_2/NaF (5/44.2/50.8 wt%) at 824 ℃. Decomposition of the formed carbonates was conducted at 1156 ℃ under N_2 atmosphere.

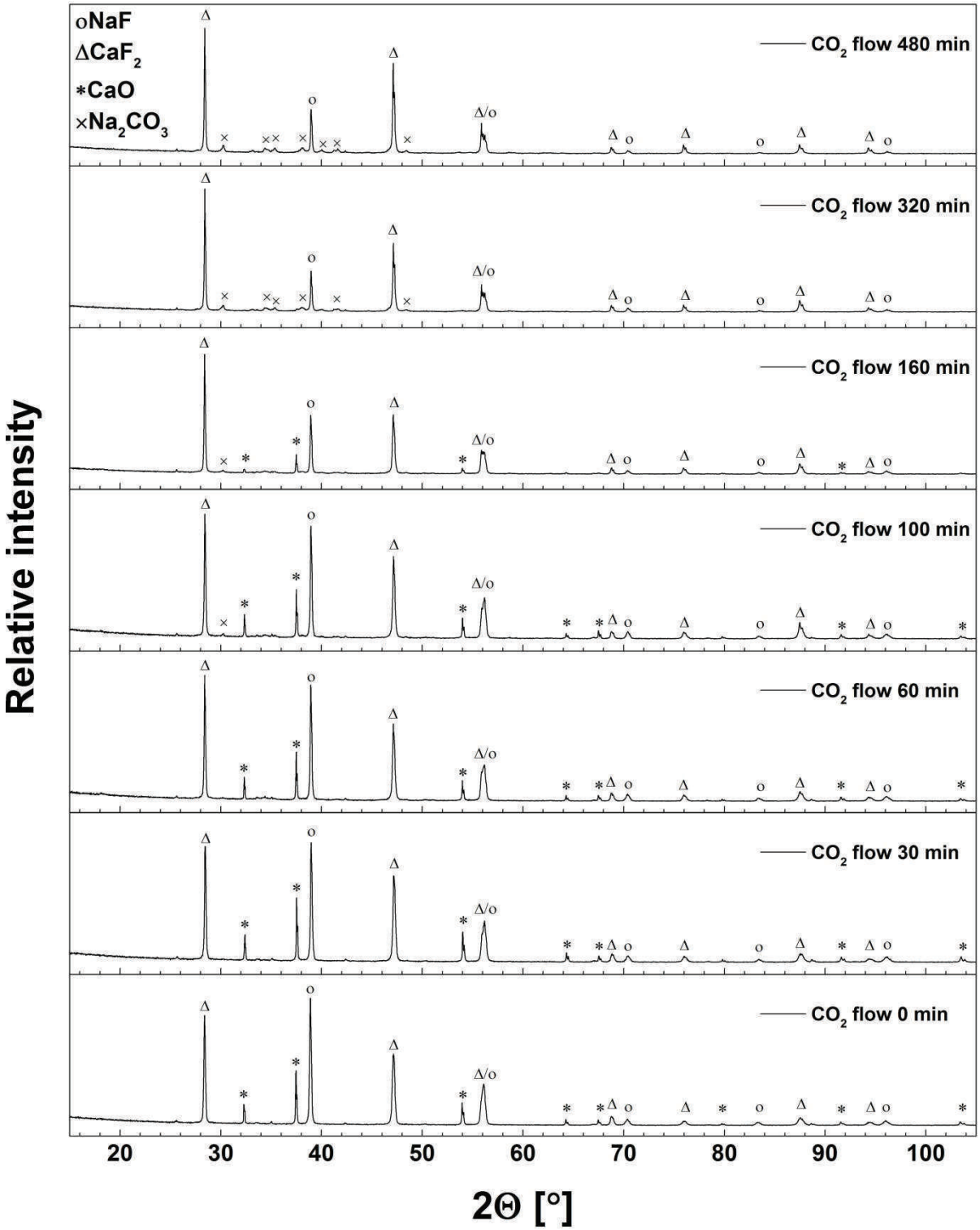

Figure 2. XRD patterns of the quenched samples collected during the carbonation step. Initial composition of the melt: 20 wt% CaO and 37.2 wt% CaF_2 in NaF. Carbonation of CaO-CaF_2/NaF was conducted by bubbling 14 vol% CO_2 in N_2 through the melt at 830 ºC.

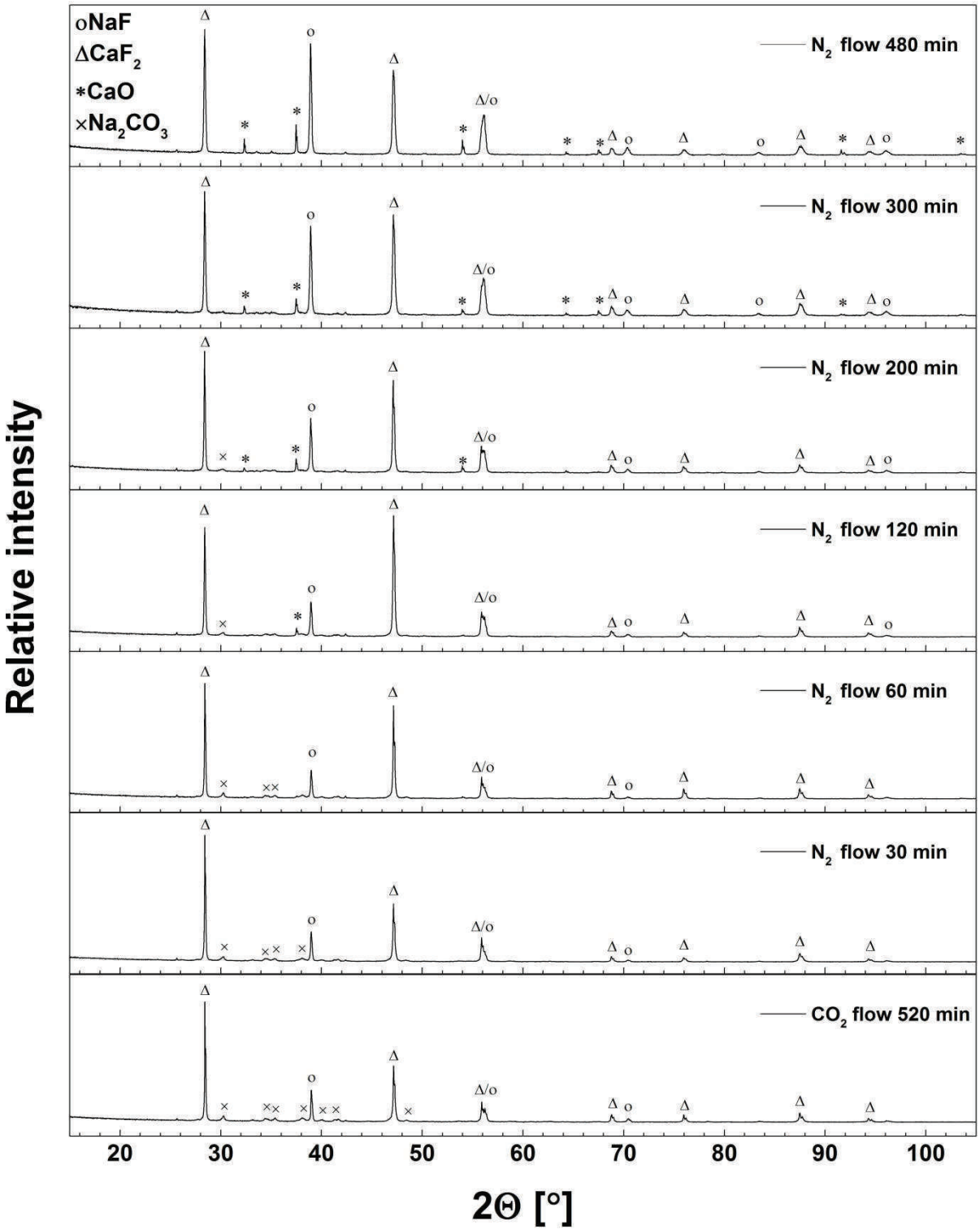

Figure 3. XRD patterns of the quenched samples collected during the decarbonation step, after carbonation of the sample ($CaO/CaF_2/NaF$=20/37.2/42.8 wt%) for 520 min under 14 vol% CO_2 in N_2. Decarbonation of the samples was carried out at 1170 ºC under pure N_2.

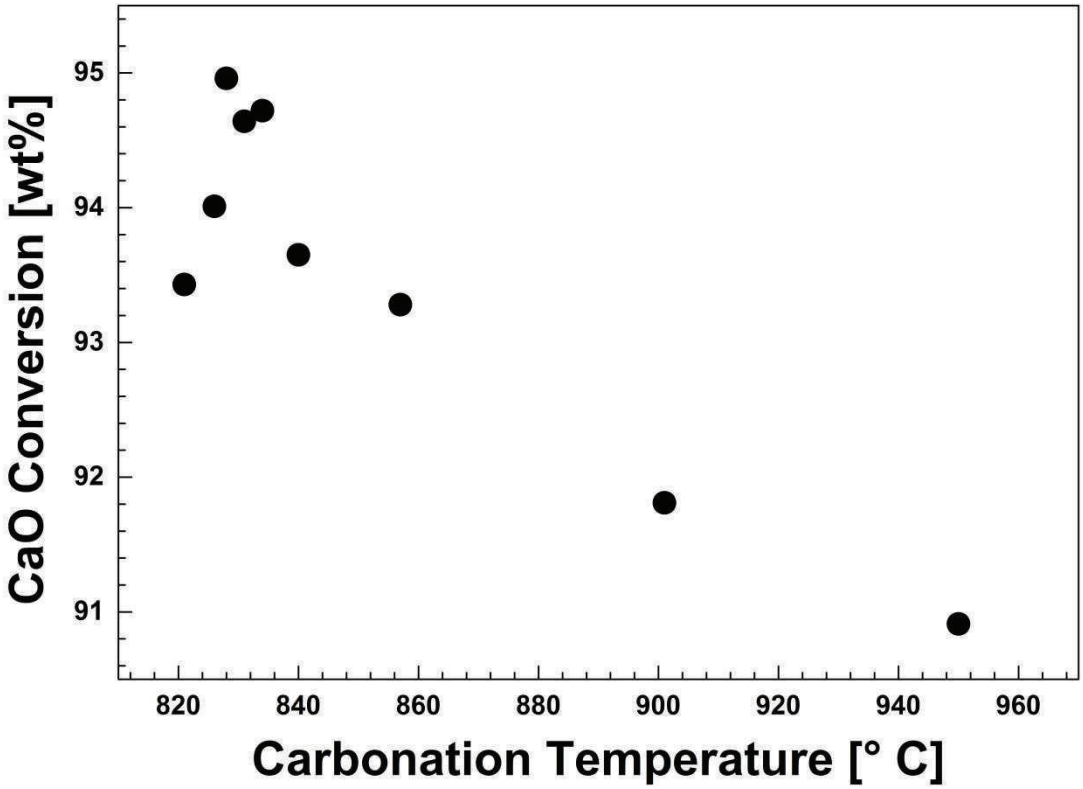

Figure 4. CaO conversion dependence on carbonation temperature. Effect of the temperature on carbonation reaction in $CaO/CaF_2/NaF$ (5/44.2/50.8 wt%) was investigated by bubbling 14 vol% CO_2 in N_2 through the melt for 300 min at temperatures in the range 821-950 ºC.

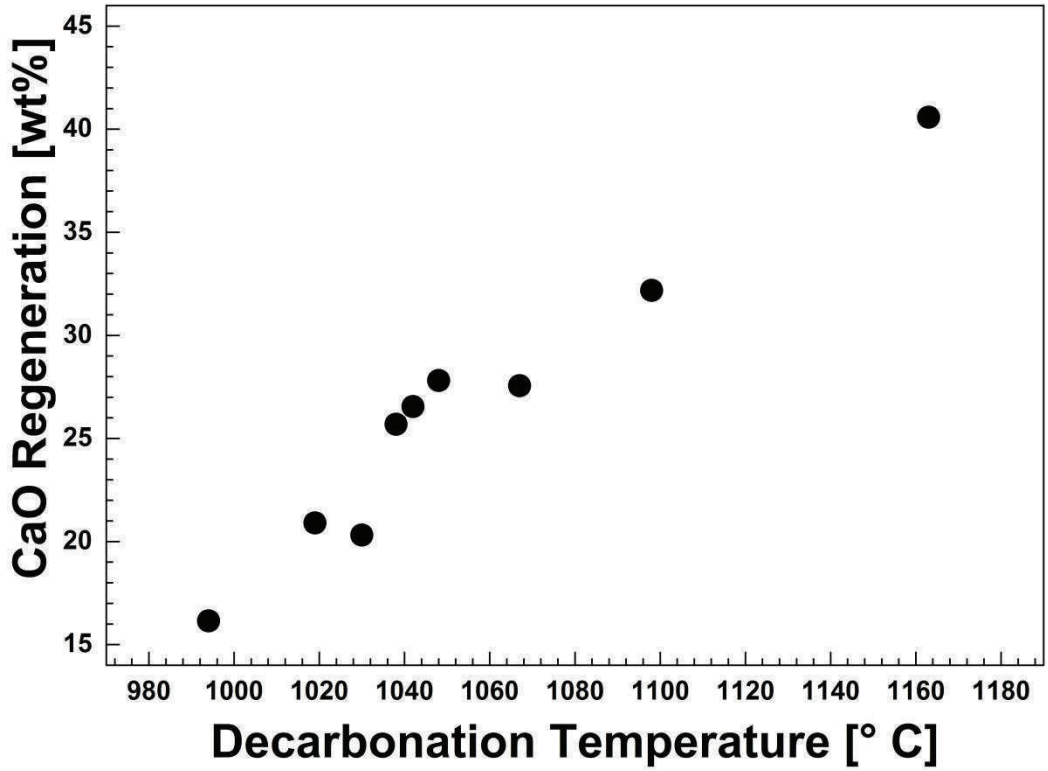

Figure 5. CaO regeneration as a function of the decarbonation temperature (the decarbonation efficiency was determined after 170 min). Firstly, the carbonation was conducted by bubbling 14 vol% CO_2 in N_2 through the melt consisting of $CaO/CaF_2/NaF$ (5/44.2/50.8 wt%) at 830 ºC for 300 min. The decarbonation step was performed under pure N_2.

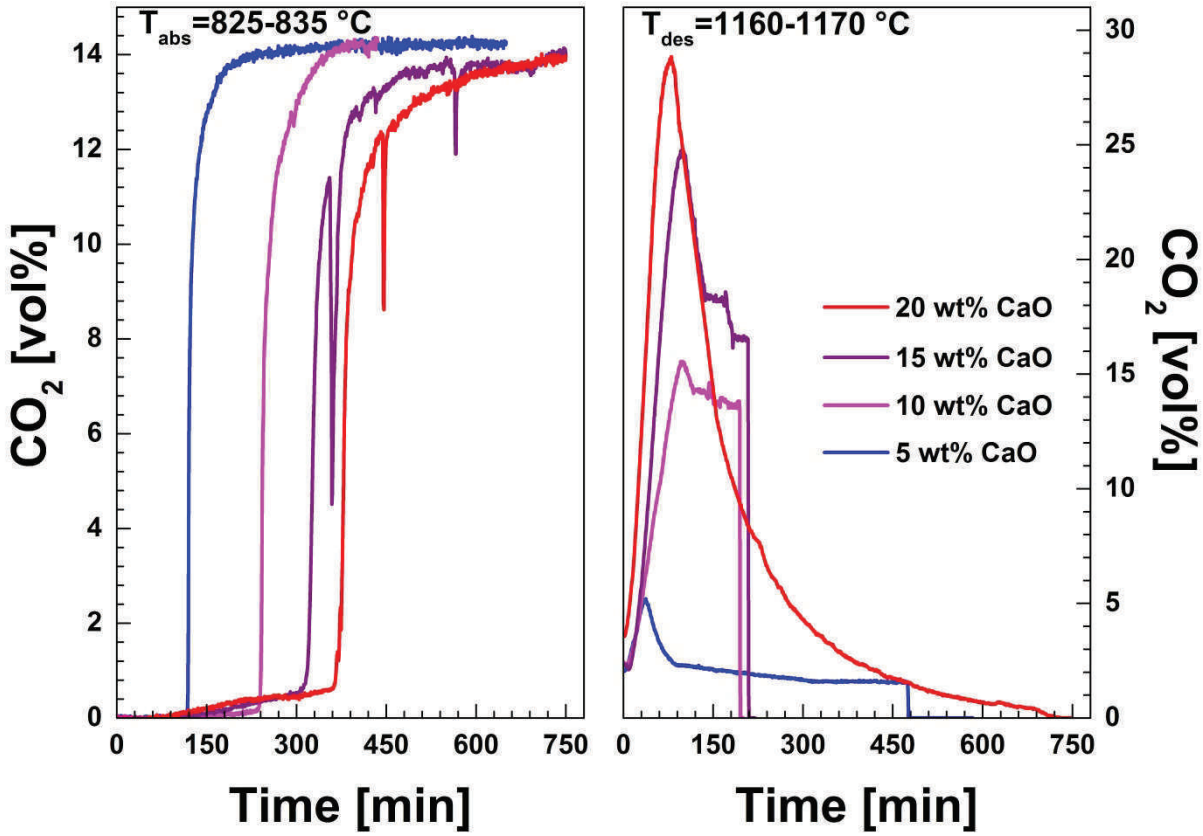

Figure 6. The influences of the CaO concentration in CaF_2/NaF eutectic mixture on CO_2 capture process. The carbonation step was conducted by transporting 14 vol% CO_2 in N_2 through the melt at 825-835 ºC. The decarbonation step was performed at 1160-1170 ºC under pure N_2.

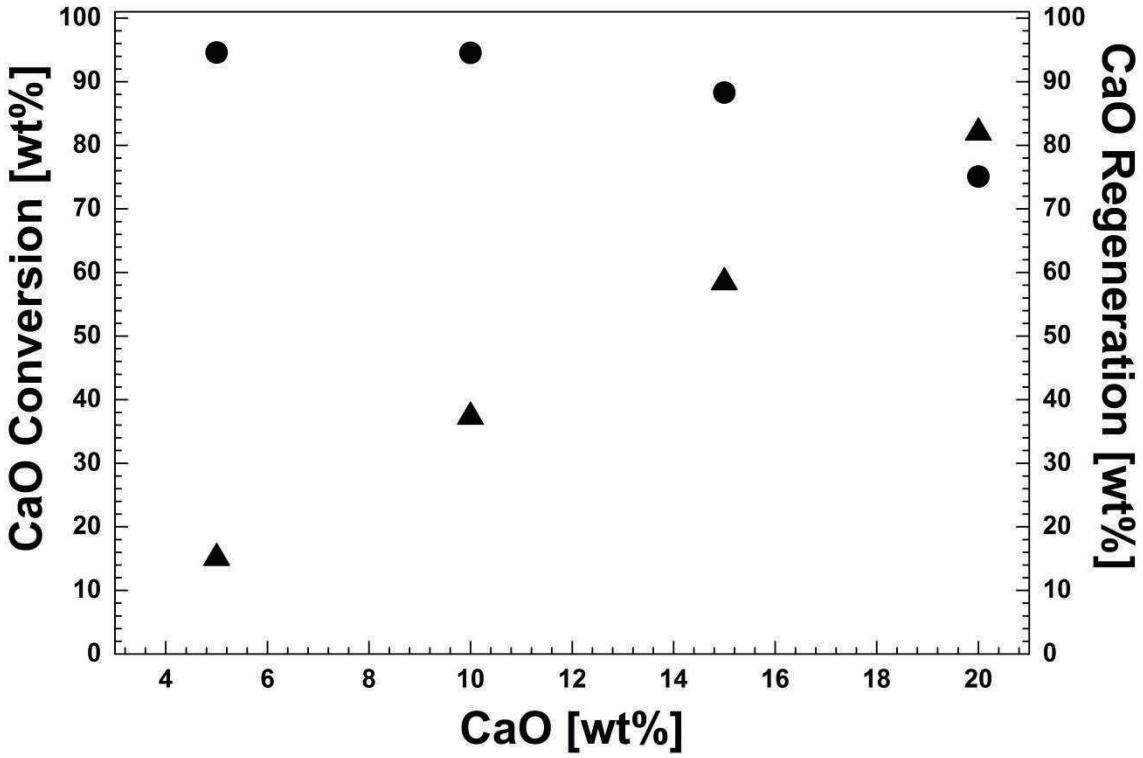

Figure 7. CaO conversion (●) and regeneration (of total reacted CaO, ▲) as a function of on the CaO concentration in the CaF_2/NaF eutectic mixture. Circles – CO_2 conversion, triangles – CO_2 regeneration.

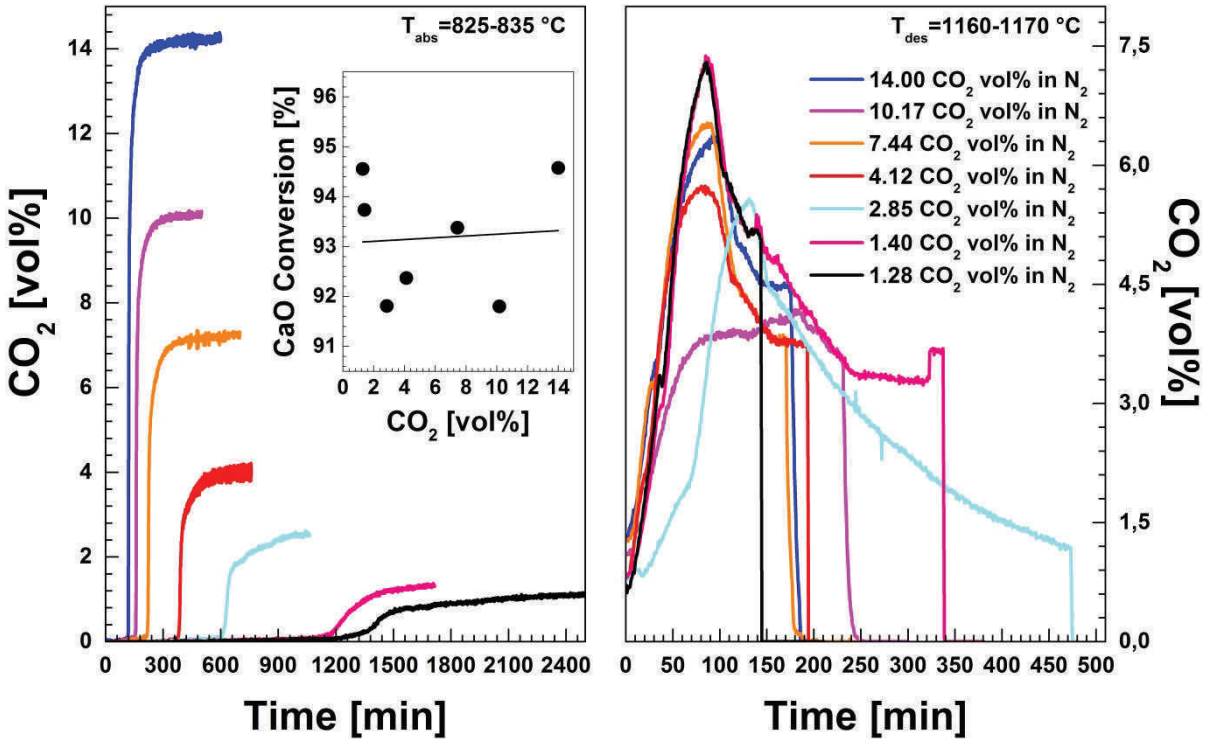

Figure 8. The influence of CO_2 concentration in N_2 on carbonation/decarbonation reactions of CaO/CaF_2/NaF (5/44.2/50.8 wt%). The carbonation step was conducted by bubbling 14 vol% CO_2 in N_2 through the melt at 825-835 ºC. The decarbonation step was performed at 1160-1170 ºC under pure N_2. Inset; CaO conversion as a function of the CO_2 concentration.

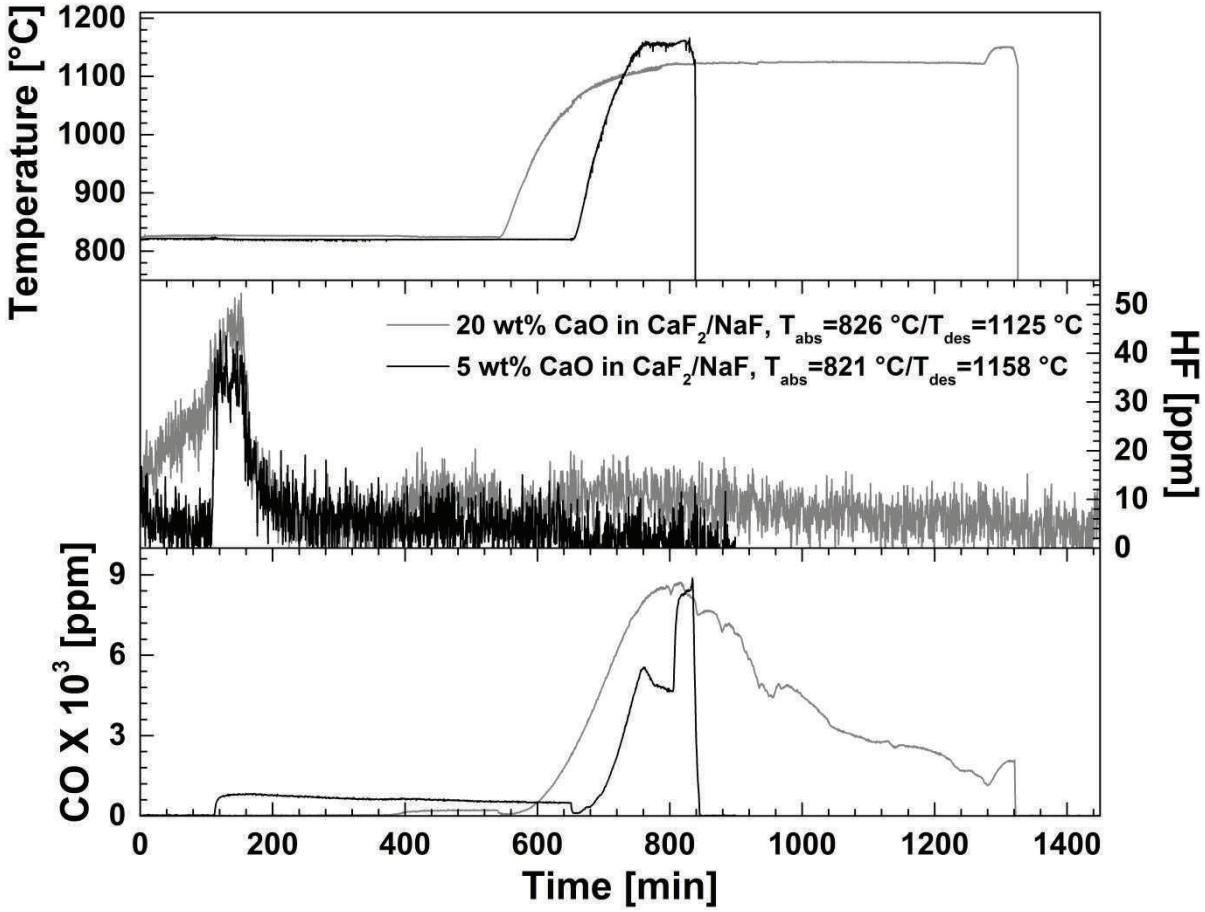

Figure 9. Hydrofluoric acid (HF) and carbon monoxide (CO) concentration during CO_2 absorption/desorption with 5 and 20 wt% of CaO in CaF_2/NaF eutectic mixture. The carbonation was carried out at 821 and 826 ºC, and the decarbonation temperatures were 1125 ºC and 1158 ºC, respectively. 14 vol% CO_2 in N_2 gas mixture was applied in carbonation step and pure N_2 in the decarbonation step.

Supporting Information

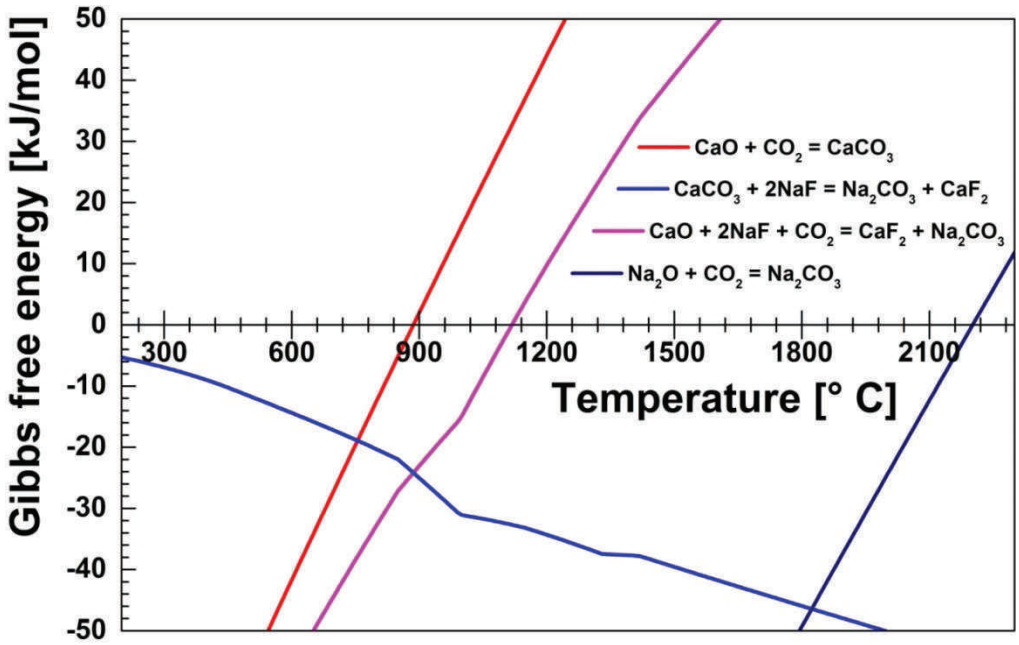

Figure S1. Gibbs free energy versus temperature for possible carbonation/decarbonation reactions in the system CaO-CaF_2-NaF and in solid Na_2O.

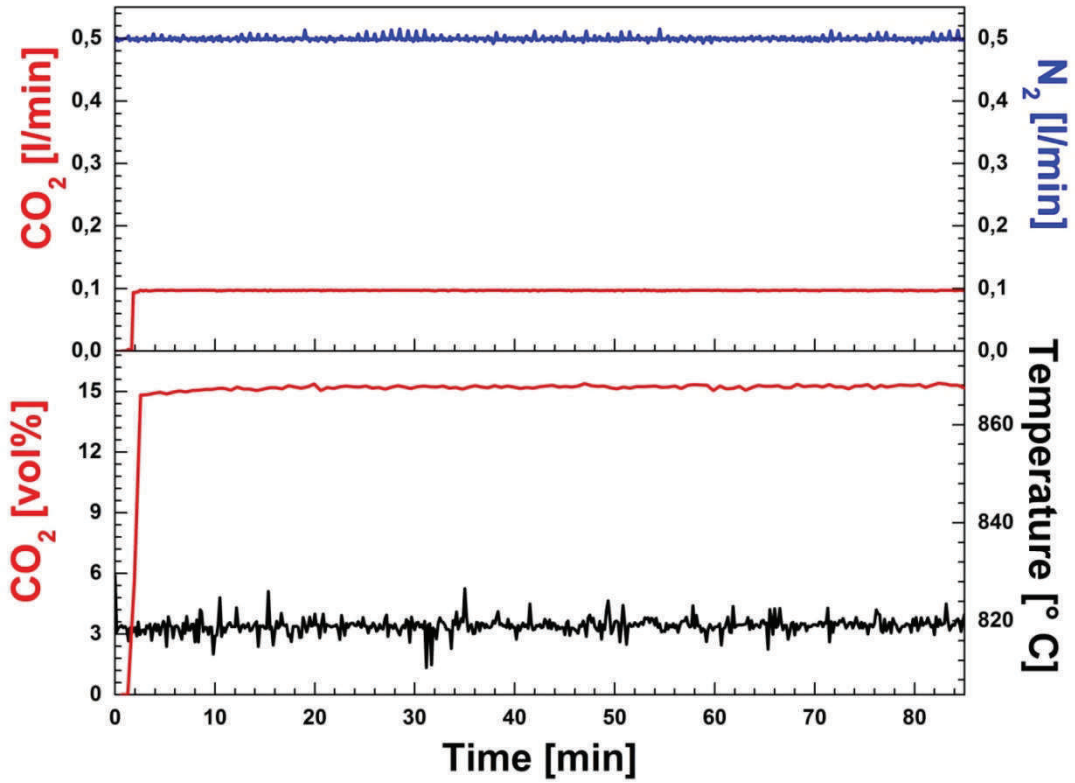

Figure S2. Baseline study of CO_2 capture at 820 ºC by bubbling 15 vol% CO_2 in N_2 through the melt consisting of 48.15 wt% NaF in CaF_2.

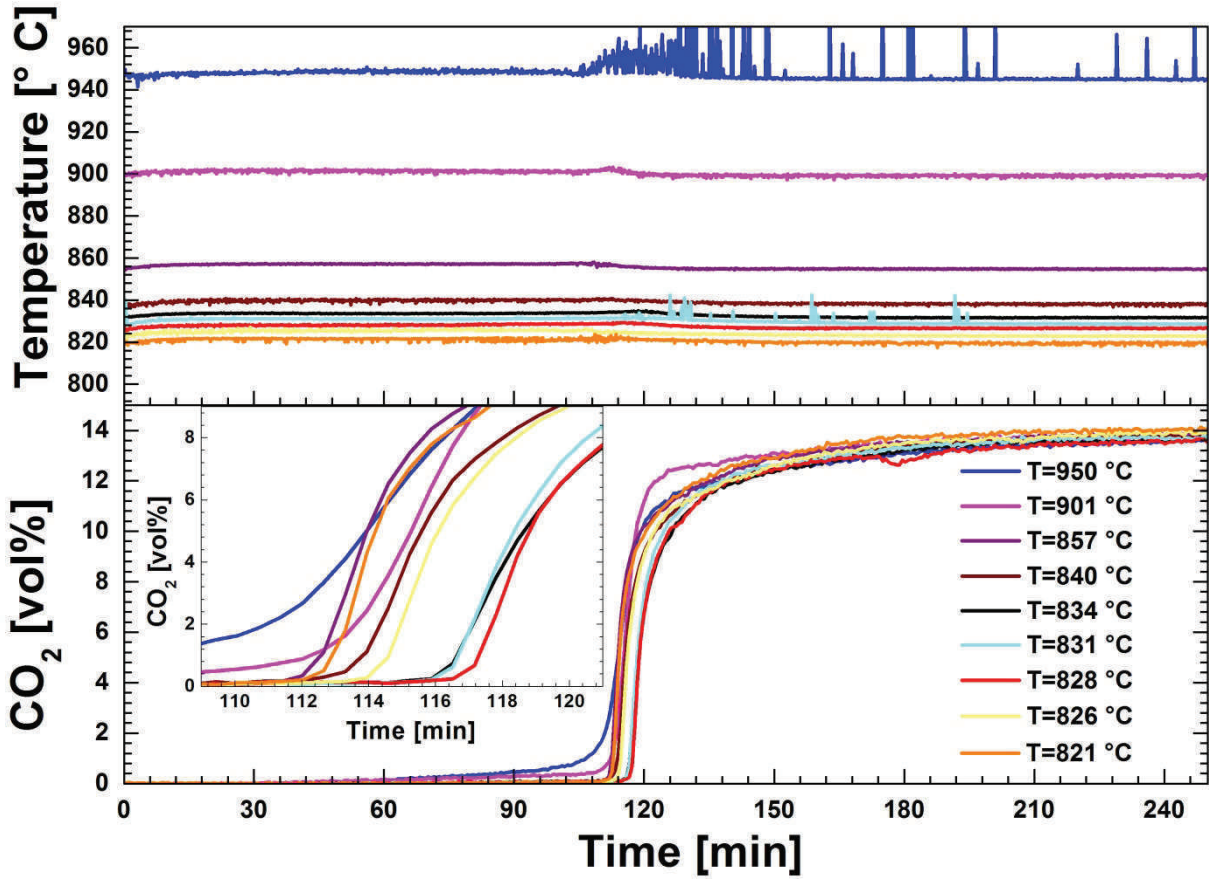

Figure S3. Effect of the temperature on carbonation reaction in $CaO/CaF_2/NaF$ (5/44.2/50.8 wt%). The carbonation step was conducted by transporting 14 vol% CO_2 in N_2 through the melt. Inset: CO_2 concentration versus time (109-121 min).

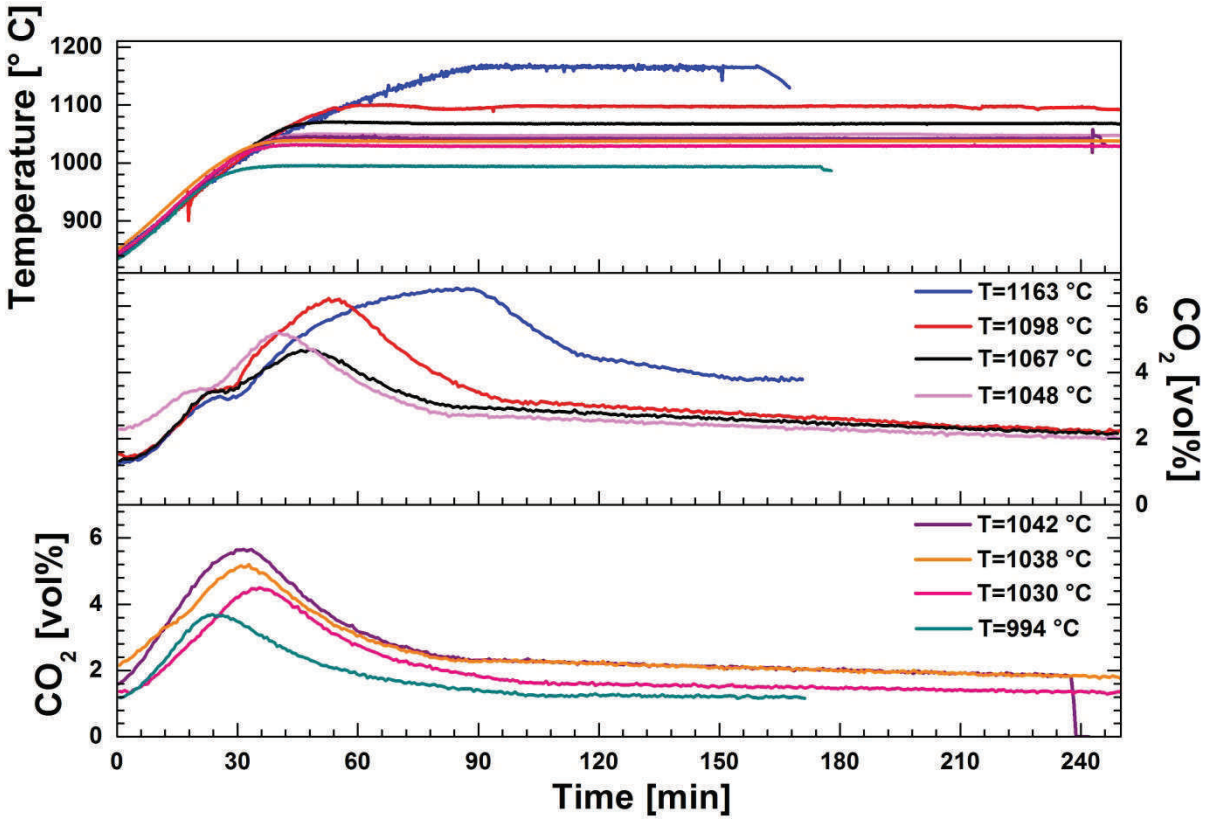

Figure S4. Effect of the temperature on decarbonation in the melt consisting of $CaO/CaF_2/NaF$ (5/44.2/50.8 wt%). Carbonation was conducted by bubbling 14 vol% CO_2 in N_2 through the melt at 830 ºC for 300 min. The decarbonation step was performed under pure N_2.

TOC:

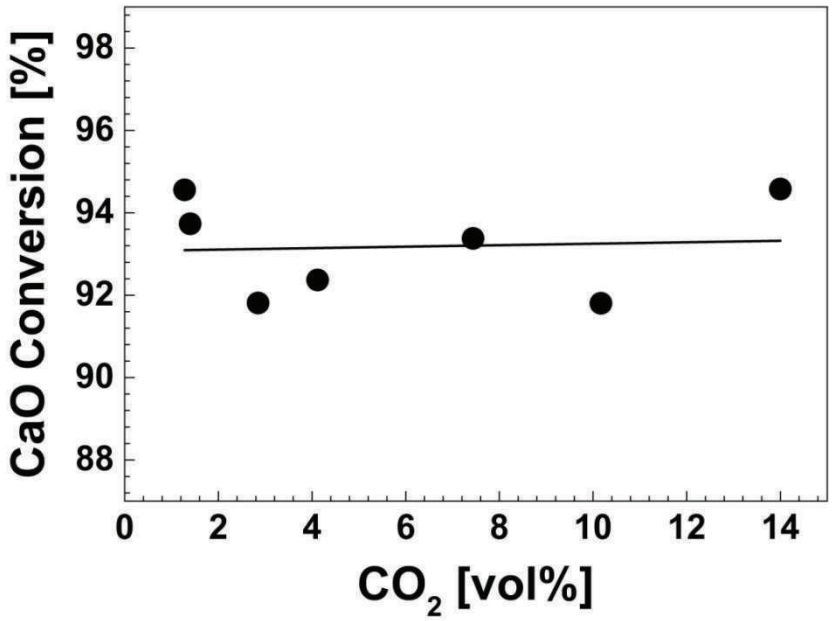

TOC 1. CaO conversion as a function of the CO_2 concentration.

Paper III

Viktorija Tomkute, Asbjørn Solheim and Espen Olsen. Investigation of high-temperature CO_2 capture by CaO in $CaCl_2$ molten salt. *Energy & Fuels* 27 (2013) 5373–5379.

energy&fuels

Article

pubs.acs.org/EF

Investigation of High-Temperature CO_2 Capture by CaO in $CaCl_2$ Molten Salt

Viktorija Tomkute,*[,†] Asbjørn Solheim,[‡] and Espen Olsen[†]

[†]Department of Mathematical Sciences and Technology, Norwegian University of Life Sciences (UMB), Post Office Box 5003, Drøbakveien 31, NO-1432 Ås, Norway

[‡]SINTEF Materials and Chemistry, Post Office Box 4760, Sluppen, NO-7465 Trondheim, Norway

ABSTRACT: Modifications of CaO-based sorbents with various inorganic salts to overcome the degradation in the reactivity between the active material and CO_2 in a carbon capture process have previously been evaluated. The present paper focuses on the performance of a novel CO_2 capture technology, where $CaCl_2$ is applied as the solvent for the dissolution/dispersion of CaO and $CaCO_3$. CO_2 capture by CaO was carried out with carbonation temperatures in the range of 770−830 °C by bubbling simulated flue gas through the melt, using a fully automated flow-through atmospheric pressure reactor. Subsequently, decomposition of the formed $CaCO_3$ to CaO and CO_2 was conducted at 910−950 °C using pure N_2. Online gas analysis was performed using a Fourier transform infrared (FTIR) gas detector and gravimetric analysis. The results indicate that the CaO carbonation efficiency decreases at temperatures higher than 800 °C. Increasing the concentration of CaO enhances the carbonation reaction. The amount of CO_2 uptake for 15 wt % CaO in calcium dichloride was 0.541 g of CO_2/g of sorbent. Moreover, investigation of CO_2 absorption/desorption by 5.32 wt % CaO in $CaCl_2$ at 787 °C showed an increase in CaO reactivity, defined as the ratio between the real and theoretical CO_2 sorption per unit of CaO, from 55.4 to 64.2% after 10 cycles. In all cases, the decarbonation process proceeded rapidly, reaching 100% efficiency.

INTRODUCTION

The fundamental obstacles in the global deployment of CO_2 capture and storage (CCS) in industrial sectors are the high operational and capital costs and also environmental issues.[1,2] There are numerous carbon capture technologies, but only post-combustion CO_2 capture using amine solvents, oxyfuel combustion, or calcium looping technologies have been considered as being appropriate for application in industrial sectors in the near future.[3] Particularly, the calcium looping technology persists as an economically and environmentally attractive high-temperature CO_2 capture process because of the low limestone cost (<$20 ton^{-1}),[4] high CO_2 carrying capacity, absence of flue gas treatment, opportunity of implementing the process in the cement industry, and low increase in specific energy consumption.[5−7] Vatopoulos et al.[8] has represented simulation data on specific energy consumption change by integrating a post-combustion CO_2 capture process at a typical cement plant, and the results demonstrate that the specific energy consumption may increase by 18% in Ca looping technology application and 45% in the case of the monoethanolamine (MEA)-based solvent process.

Recent developments show that the calcium-based looping process is an option for multiple CO_2 capture cycles in fossil-fueled power plants and cement manufacturing.[8,9] The solid looping process is based on the carbonation reaction of CaO with CO_2 and decarbonation of the formed $CaCO_3$, as shown in eq 1.

$$\mathrm{CaO(s) + CO_2(g) \leftrightarrow CaCO_3(s)}$$
$$\Delta H^0_{r,298\ K} = -178.2\ \mathrm{kJ/mol} \quad (1)$$

The conceptual design of this process comprises two interconnected reactors (absorber and regenerator) that work together to perform a continuous capture technology.[10] The carbonation of CaO is a two-stage reaction: first, a fast carbonation stage, which is controlled by chemical reaction, and second, a slower stage controlled by CO_2 diffusion through the formed $CaCO_3$ layer.[11,12] The backward reaction represents sorbent regeneration, which has been found to be fast and complete under suitable conditions.[12] Many studies have shown that CaO-based sorbents derived from limestone or dolomite are efficient just in the initial stage and the CO_2 capture capacity of the sorbent decreases with an increasing number of absorption−desorption cycles.[13] The CaO activity decay problem is influenced by sintering, attrition, and competing chemical reactions with fuel-bound impurities (sulfur-containing species, HCl, particulate matter, etc.).[4,12] Accordingly, it is indispensable to use large amounts of fresh limestone or dolomite to sustain a reasonable CO_2 capture capacity.[3,4] However, the low sorbent cost and possibility to utilize used sorbent as a feedstock for cement manufacturing may partially equilibrate the cost structure of calcium looping technology.[3,5] Still, it is essential to make improvements in CaO-based sorbent applications to enhance the reversibility for extended low-cost operation. The major strategies to limit the degradation of CaO reactivity with CO_2 for long-term calcium looping technology involve hydration of the sorbent, thermal pretreatment, implementation of nano-compounds, dispersion of CaO particles into an inert matrix, and doping with foreign ions.[3,14−22]

Strategies for the modification of the Ca-based sorbents have shown some success in preparation of materials with enhanced

Received: May 25, 2013
Revised: August 17, 2013
Published: August 19, 2013

CO_2 capture capacity, thermal stability, and mechanical strength, but still, no modification/synthesis techniques have showed complete elimination of the problems.[3,4] Therefore, there is a need for creating a new methodology for the development of inexpensive sorbent or designing a completely new process for CO_2 separation by carbonate looping technology to reduce the costs.[3]

A feasible method to reactivate CaO is using inorganic salts that enhance the long-term reactivity as dopants.[23] It has been shown that additions of $MgCl_2$, $CaCl_2$, and Grignard reagents increase the carrying capacity of limestone. The effect was explained by the change of the pore sizes in the investigated limestone to approximately the optimal diameter for repeated cycles.[24] In addition, application of different inorganic acids (HBr and HCl) during the reactivation reaction substances indicated that the cyclic reactivity of the limestone with CO_2 may be significantly improved.[25] Moreover, low-cost carbonate and chloride molten salt mixtures were examined as electrolytes for electrochemical processing of CO_2 (electrochemical deposition of C on the electrode/or reduction of CO_2 to CO).[26−28] The analysis on molten salt CO_2 capture and electrochemical transformation (MSCC-ET) showed possibility to produce carbon materials and oxygen, which may diminish the total cost of the MSCC-ET process.

Calcium chloride and mixtures of calcium chloride and alkali metal chlorides have been used in electro-deoxidation technologies of various metal oxides because of their low toxicity, low cost, and high calcium oxide solubility.[29] Furthermore, the melting points of these mixtures are not too high, and the vapor pressure is acceptable.[30−33] Therefore, CaO and $CaCO_3$ solubility and activity coefficients in molten chloride salts have been widely evaluated in research on metal electrorefining and electrowinning.[30,34−36] Many researchers have reported the liquidus line of CaO in the $CaCl_2$ binary system.[30,36] The phase diagram of the CaO−$CaCl_2$ binary system was found to have a peritectic point at approximately 835 °C and 15 wt % CaO[30] as well as a eutectic point at 750 °C and 3.4 wt % CaO.[36] In addition, Freidina et al.[35] have investigated isothermal sections of the CaO−$CaCO_3$ system by differential scanning calorimetry (DSC), and the results showed that the eutectic mixture contains 28 wt % $CaCO_3$ and melts at 635 °C.

The use of molten halide salts in a carbon capture process based on metal oxide dissolution/dispersion may enable an increase in the reactivity of the sorbent with CO_2 because of rapid gas−liquid interactions in the molten salt. Therefore, we have studied CO_2 reactivity with a commercially available CaO dissolved or partly dissolved in $CaCl_2$ melt. Optimization of CO_2 absorption/desorption by CaO in $CaCl_2$ was carried out by studying the effects of the CaO concentration in the halide salt, the temperatures for the carbonation/decarbonation reactions, and the gas flow rate. CO_2 separation from N_2 in a eutectic CaO−$CaCl_2$ melt was investigated at 768−820 °C. The thermal decomposition of the formed $CaCO_3$ has been tested at temperatures ranging from 904 to 950 °C. In addition, multiple cycles of CO_2 carbonation/decarbonation were examined using Fourier transform infrared (FTIR) gas analysis and thermogravimetric analysis.

EXPERIMENTAL SECTION

Chemicals and Gases. In this study, a powder of CaO (Sigma-Aldrich reagent, 96−100% purity) was used as the sorbent. Anhydrous calcium chloride (Sigma-Aldrich reagent, ≥97.0% purity) was selected as the solvent for CaO. All powder compounds were dried at 200 °C for 50 h. A series of CaO/$CaCl_2$ mixtures with different CaO (5, 5.32, 10, 15, and 20 wt %) concentrations was prepared. The melts were kept at 850 °C for 10 h under an argon atmosphere (heating rate of 200 °C/h) and 800 °C for 2 h under a N_2 atmosphere before the carbonation operation. A simulated flue gas consisting of pure carbon dioxide (99.99%) mixed with nitrogen (99.999%) was controlled using mass flow controllers (Sierra 820 Series, Sierra Instruments, Inc.).

Carbonation/Decarbonation. Parametric and cyclic studies of CO_2 absorption/desorption by CaO partly dissolved in $CaCl_2$ were conducted on a flow-through laboratory-scale one-chamber atmospheric pressure reactor (Figure 1). A FTIR gas analytical cell apparatus

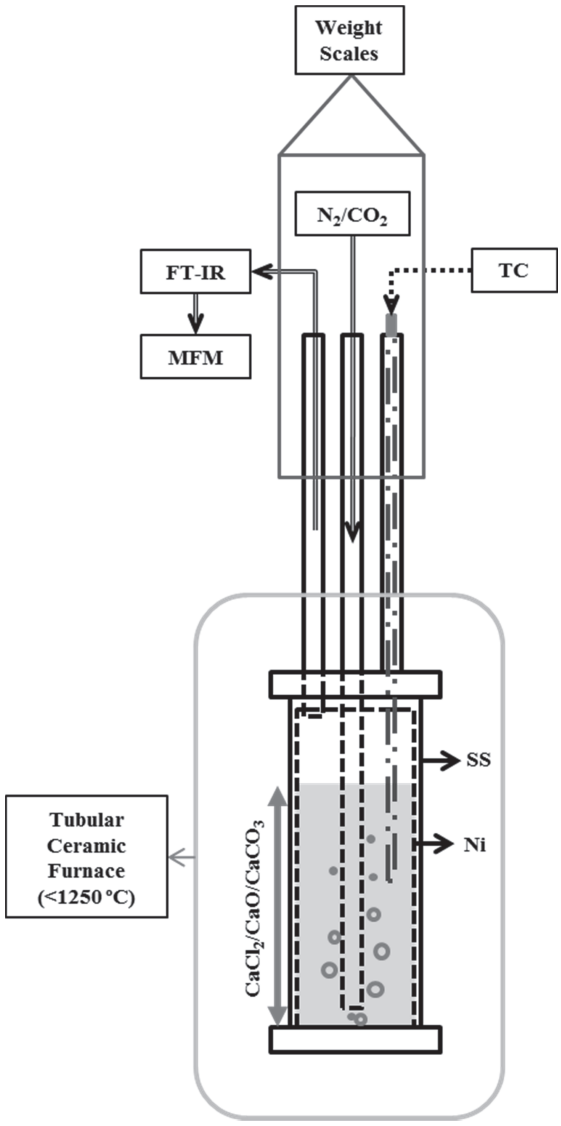

Figure 1. Design of the experimental setup: FTIR apparatus, industrial weighing balances, S-type thermocouple (TC), vertical tubular ceramic furnace, and reactor (the outer sleeve is made of stainless steel, and the inner crucible and the feed tube are made of nickel).

(Thermo Scientific, Nicolet 6700 model) and an industrial weighing scale (MS8001S, Mettler Toledo, accuracy of 0.1 g) were used for the carbonation/decarbonation reaction tests. The FTIR apparatus, which had a 2 m path length (200 mL volume) gas cell with KBr windows was kept at 120 °C for 24 h before gas analysis studies. The interferometer was purged with N_2 (0.5 L/min) for at least 30 min for N_2 background record. The CaO/$CaCl_2$ samples were placed in a nickel cell/reactor with a stainless-steel compartment (Figure 1), which was placed in a tube vertical furnace supplied with a ceramic tube. The sample

dx.doi.org/10.1021/ef4009899 | Energy Fuels 2013, 27, 5373−5379

temperature was monitored by a type S (Pt−Pt10Rh, ±1.1 °C) thermocouple in the melt. The salt melt volume in the reactor was kept constant, corresponding to a 10 cm height (470−510 g, dependent upon the CaO amount), unless otherwise mentioned. A nickel pipe was used as the inlet for N_2 and the CO_2−N_2 mixture. The gas mixture was injected through the top of the sealed reactor. In addition, before carbonation/decarbonation tests, all polytetrafluoroethylene (PTFE) (Teflon) pipes used for gas transfer were purged by N_2. The mass flow meter was applied at the outlet of the FTIR gas cell to pass a system tightness test. The CO_2 separation from N_2 was examined at 768−820 °C by bubbling simulated flue gas through the melt. The total CO_2 and N_2 flow for carbonation was about 0.6 L/min. Carbonation operation was considered to be complete when the inlet and outlet CO_2 concentrations recorded by the FTIR analyzer were nearly equal. Decarbonation of the formed $CaCO_3$ was performed at 904−962 °C (heating and cooling rates from 100 to 300 °C/h) using pure N_2, unless otherwise described. The reactor weight (Figure 1) and the gas composition were continuously recorded for evaluation of carbonation and decarbonation. All settings of the CO_2 absorption/desorption experiments, involving temperature and weight changes of the reactor and also the shifting between CO_2 and N_2 gases, were programmable and operated using NI cRIO-907x integrated systems (National Instruments).

RESULTS AND DISCUSSION

Figure 2 shows CO_2 absorption and desorption at different temperatures. The experimental data are shown as degree of

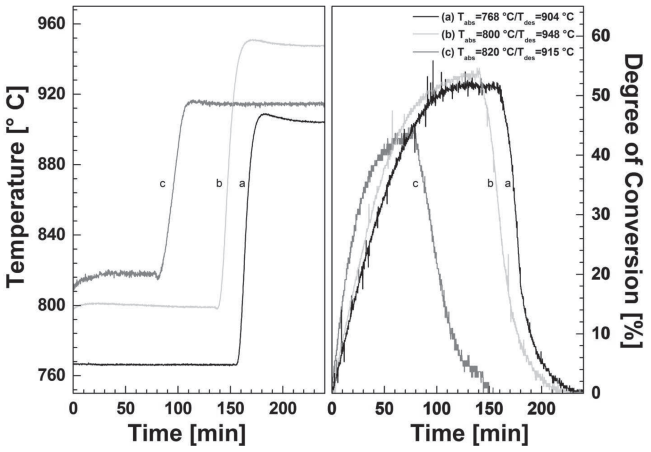

Figure 2. Effect of the temperature on carbonation and decarbonation reactions starting with 5 wt % CaO in molten $CaCl_2$. The figure show the temperature (left-hand side) and the CaO/$CaCO_3$ conversion (right-hand side) as a function of time: (a) CO_2 absorption at 768 °C and desorption at 904 °C, (b) CO_2 absorption at 800 °C and desorption at 948 °C, and (c) CO_2 absorption at 820 °C and desorption at 915 °C. All experiments were conducted with the same gas mixture (14 vol % CO_2 in N_2).

CaO/$CaCO_3$ conversion (calculated from weight change) versus time. CO_2 absorption and desorption were carried out at different temperatures by bubbling 14 vol % CO_2 in N_2 through a melt containing 5 wt % CaO in $CaCl_2$ (carbonation temperature, 768−820 °C; decarbonation temperature, 904−948 °C). CO_2 is initially absorbed rapidly up to a certain limit, followed by a slower conversion rate as the CaO concentration drops toward a low value. The results show that the highest sorbent reactivity with CO_2 was reached at 768−800 °C and CaO conversion into $CaCO_3$ differs by 2 wt % (Figure 2). In addition, the CO_2 capture capacity of CaO in molten chloride decreases above 810 °C (from 0.438 to 0.343 g of CO_2/g of CaO). This indicates that the equilibrium in eq 1 shifts toward the left as the temperature

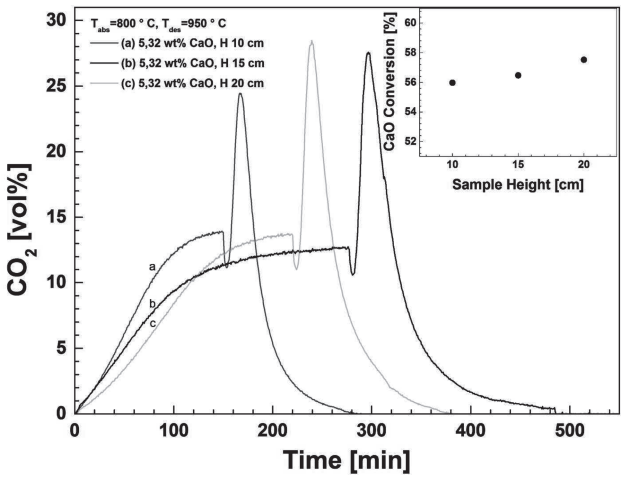

Figure 3. CO_2 absorption/desorption. Melt (5.32 wt % CaO in $CaCl_2$): (a) column height, 10 cm; mass, 639 g; (b) column height, 15 cm; mass, 705 g; and (c) column height, 20 cm; mass, 940 g. Carbonation of CaO was conducted at 800 °C by bubbling ∼14 vol % CO_2 in N_2. Decarbonation of the formed carbonate was performed at 950 °C under pure N_2. The CO_2 concentration was monitored at the gas outlet as a function of time. (Inset) CaO conversion dependence upon the carbonation sample column height.

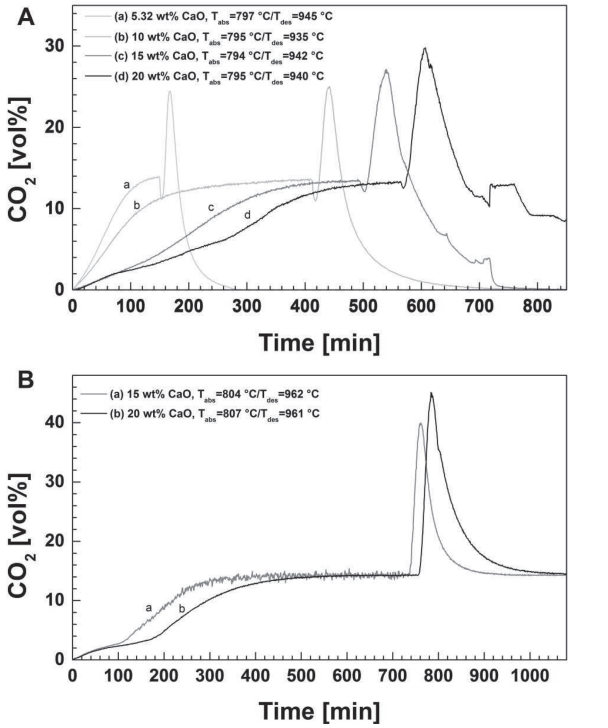

Figure 4. Effect of the CaO concentration in $CaCl_2$ melt on CO_2 absorption and desorption. The volume of the molten salts with dissolved or partly dissolved CaO was kept the same during all experiments, corresponding to a 10 cm height in the crucible: (A) carbonation, ∼14 vol % CO_2 in the N_2 gas mixture; decarbonation, pure N_2 and (B) carbonation and decarbonation, ∼14 vol % CO_2 in the N_2 gas mixture.

increases, which is in accordance with the thermodynamics (the value of the Gibbs free energy is negative at low temperatures and becomes positive above 900 °C). Regeneration of the sorbent from the formed $CaCO_3$ was conducted by raising the temperature to the range of 900−948 °C, which resulted in

dx.doi.org/10.1021/ef4009899 | Energy Fuels 2013, 27, 5373−5379

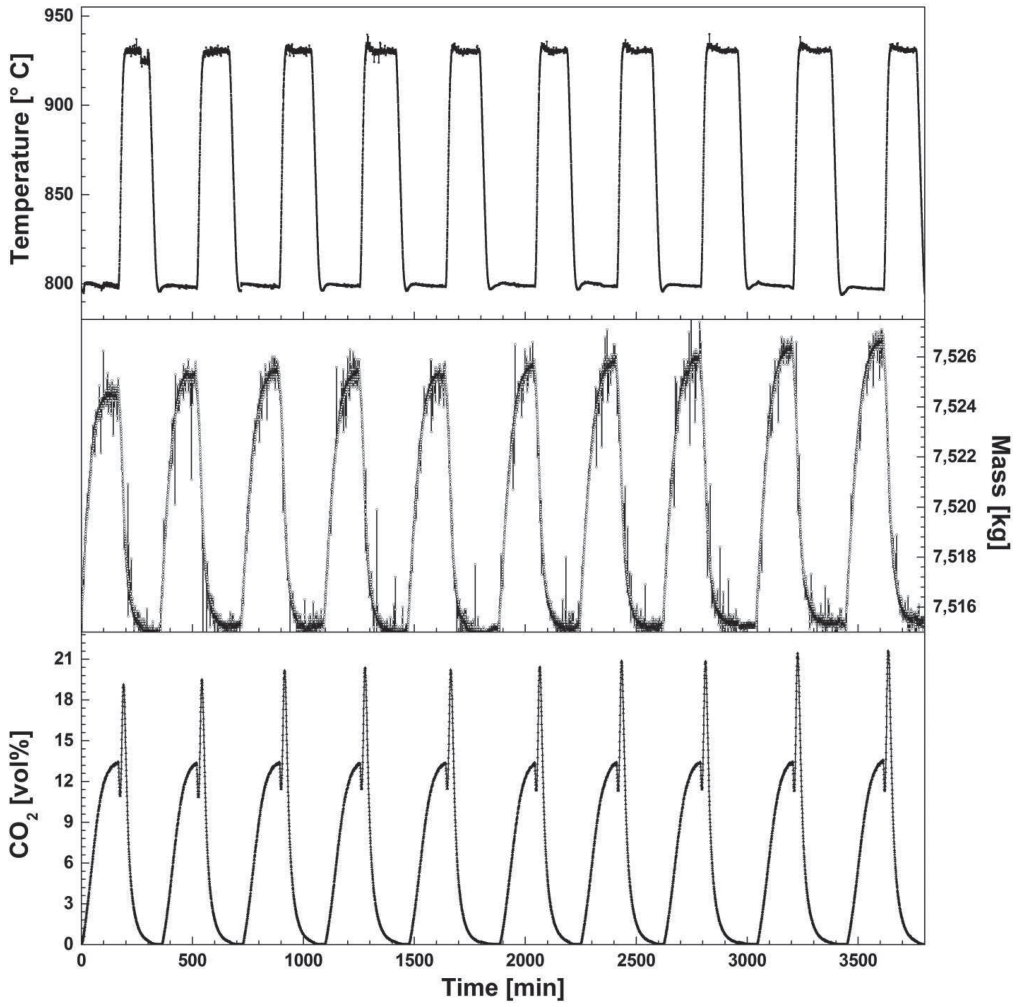

Figure 5. Cyclability analysis of CO_2 absorption/desorption by 5.32 wt % CaO in molten $CaCl_2$ (10 cycles). Carbonation was performed at 799 °C using 14 vol % CO_2 in N_2, and decarbonation was conducted under pure N_2 at 930 °C.

near 100% efficient desorption of CO_2. The decomposition rate of the formed $CaCO_3$ increases with an increasing decarbonation temperature. Therefore, for further experiments, it was chosen to use 800 °C as the absorption temperature and 940−950 °C as the desorption temperature.

Karami et al.[37] has reported that the conversion of Ca-based sorbents into carbonates decreases with increasing sample weight. In this study, the sample weight was varied by increasing the 5.32 wt % CaO in $CaCl_2$ melt column height, and the effect on the CO_2 absorption/desorption is presented in Figure 3. The experimental data show that the increase of the sample column (from 10 to 20 cm) slightly enhances the CO_2 carrying capacity of the sorbent. The first carbonation cycle in the 20 cm height melt shows higher sorbent conversion of 57.5 wt %, which can be compared to 56 wt % conversion with 10 cm sample column height. The slightly increased CO_2 capture efficiency in a taller column may be ascribed to a longer contact time between gas and liquid.

It has been reported that the mixture of 5.32 wt % (10 mol %) CaO in $CaCl_2$ melts at approximately 775 °C.[30] As mentioned above, we have demonstrated that the CO_2 capture activity of CaO in molten chloride salt is weaker at temperatures above 810 °C (Figure 2). Therefore, the focus was to investigate CaO carbonation at 790−800 °C and regeneration at 930−940 °C with the sorbent existing in a dissolved state as well as partly dissolved (CaO concentrations from 5.32 to 20 wt %). The curves of the CO_2 concentration versus time in Figure 4, recorded by the FTIR apparatus, represent the effect of the CaO concentration on the CO_2 uptake. To clarify the conversion rates of CaO into carbonate and back to oxide, the carbonation behavior was measured using both the FTIR gas analysis and reactor weight changes. The samples with different CaO concentrations (5.32−20 wt %) were prepared by keeping the same melt volume in the reactor (10 cm height); the equal carbonation/decarbonation temperature set points were monitored for all samples of the CO_2 capture process; and the same gas mixture (~14 vol % CO_2 in the N_2 gas mixture) was bubbled through the melt during all carbonation reactions (Figure 4). Nevertheless, decomposition of the formed carbonates was accomplished under pure N_2 (Figure 4A) and under ~14 vol % CO_2 in the N_2 gas mixture (Figure 4B). Looking at the shape of the CO_2 concentration versus time curves, it is evident that the efficiency of CO_2 separation from N_2 increases with an increasing CaO concentration in the melt (Figure 4). It was found that an increase in the CaO concentration from 5.32 to 15 wt % enhances the initial carbonation conversion from 56 to 69 wt % (Figure 4A). However, using more than 15 wt % sorbent, there is a slight decrease in CaO conversion efficiency. The average CO_2 sorption capacity of 15 and 20 wt % CaO was 0.541 and 0.517 g of CO_2/g of CaO, respectively (Figure 4). The decrease in CaO

dx.doi.org/10.1021/ef4009899 | *Energy Fuels* 2013, 27, 5373−5379

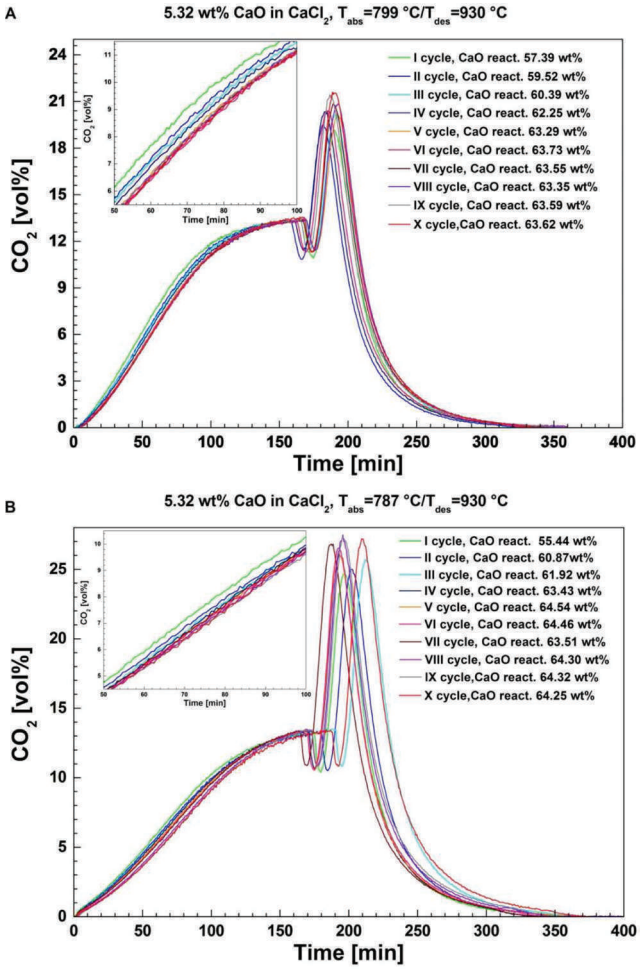

Figure 6. CO_2 separation from the gas mixture for 10 cycles with carbonation temperatures at (A) 799 °C and (B) 787 °C with 5.32 wt % CaO in $CaCl_2$ and 14 vol % CO_2 in N_2. Decarbonation was conducted at 930 °C under pure N_2. (Insets in panels A and B) CO_2 concentration versus time (50−100 min).

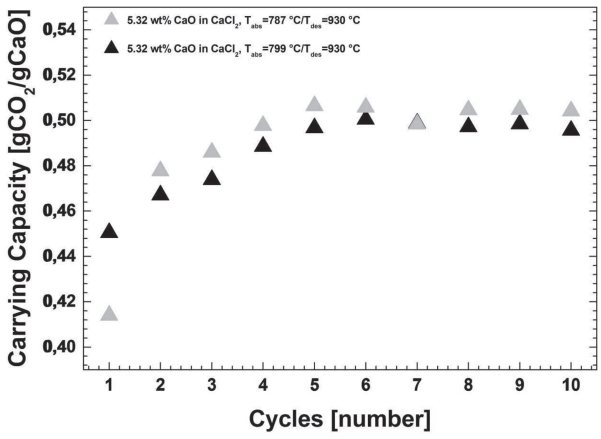

Figure 7. Carrying capacity evaluation in cyclic CO_2 absorption/desorption.

reactivity when the sorbent concentrations are above 15 wt % may be assigned to deposition and agglomeration of the sorbent. These result in a reduction in the available CaO surface area and reduced access of CO_2 molecules to the unreacted sorbent in the core. In addition, the recorded CO_2 concentration curves for the samples containing more than 10 wt % CaO reveal two carbonation reaction stages (Figure 4B). In the initial carbonation reaction, CO_2 reacts with dispersed/agglomerated CaO, while the lower rate sorption can be related to the reaction with dissolved sorbent. Complete decomposition of the formed carbonate as indicated by FTIR gas analysis and weight measurements was achieved only with the samples prepared with 5.32−10 wt % CaO under pure N_2 (Figure 4A). The tests with 15−20 wt % CaO in the melt resulted in near 100% efficient decarbonation under the CO_2−N_2 mixture (Figure 4B).

The development of the Ca-based looping technology is focused on improvement of the cyclic CO_2 capacity of the sorbent. Figure 5 shows the results for 10 repeated carbonation/decarbonation cycles with 5.32 wt % CaO in $CaCl_2$. The temperature was cycled between 799 and 930 °C. All carbonation processes were taken to be close to complete when the continuously recorded outlet CO_2 concentration was equal to the inlet value, i.e., when all available CaO had reacted to carbonate. The set point temperature was then switched to 930 °C, and the gas flow was changed to pure N_2. A small increase in the reactor weight can be attributed to corrosion of the stainless-steel compartment (Figure 5). The investigation of the results shows that the degree of carbonation increases from 57.3 to 63.7% after 6 carbonation/decarbonation cycles, which remained stable for the remaining 4 cycles. This is mostly due to the additional dissolution of CaO in the melt, which was initially in an agglomerated state or deposited on the walls of the reactor cell.

To establish the cyclic capacity of 5.32 wt % CaO in $CaCl_2$ at different CO_2 absorption temperatures, 10 carbon dioxide capture cycles were performed at 787 and 799 °C, as shown in Figures 6 and 7. The CO_2 concentrations after 10 carbonation and decarbonation cycles show a small increase during the cycle of carbonation and ∼100% desorption. The maximum carrying capacities of CaO during the CO_2 cyclability tests with carbonation at 787 and 799 °C are presented in Figure 7. The results show a slight initial increase in the capacity, followed by constant values. The enhancement of the sorbent activity is more pronounced at 787 °C than at 799 °C carbonation temperature; the carrying capacity increases from 0.396 to 0.507 g of CO_2/g of CaO during the first 6 cycles at 787 °C and from 0.451 to 0.501 g of CO_2/g of CaO at 799 °C. The cycles after the initial 6 cycles showed quite high carrying capacities, with average values of 0.504 g of CO_2/g of CaO at 787 °C and 0.498 g of CO_2/g of CaO at 799 °C carbonation temperatures. This can be related to the higher CaO solubility in the system $CaO/CaCO_3/CaCl_2$ (eutectic mixture at 615 °C and 5.5 wt % CaO[38]) than in the system $CaO/CaCl_2$ (eutectic mixture at 750 °C and 3.4 wt % CaO[36]).

Flue gases generated by burning fossil fuels contain trace amounts of sulfur-containing species, HCl, and particulate matter. This may affect the CaO conversion because of competing reactions between these compounds and the sorbent.[39] The influence of such impurities on industrial operations, biodiversity, and environment should be estimated. Therefore, the formation of CO from the CO_2 reduction and HCl from the hydrolysis of $CaCl_2$ has been studied in the cyclic CO_2 sorption operations, as shown in Figure 8. The first two cycles exhibit higher hydrochloric acid emission from the reactor, but the emission decreases in the rest of the cycles from 1500 to 350 ppm. The higher HCl concentrations appear when the temperature is increased for CO_2 desorption. Thus, HCl evolution can be attributed to the reaction between moisture

dx.doi.org/10.1021/ef4009899 | Energy Fuels 2013, 27, 5373−5379

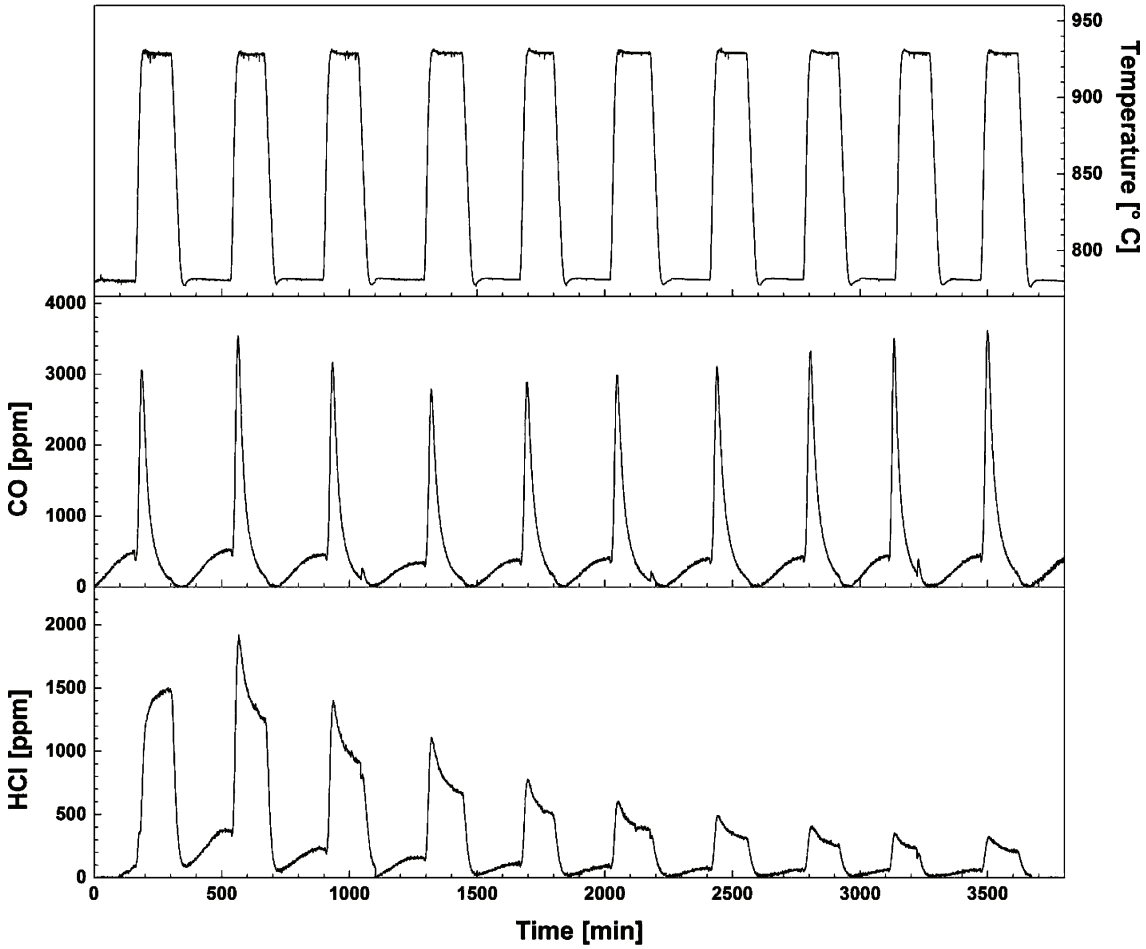

Figure 8. Hydrochloric acid (HCl) and carbon monoxide (CO) concentrations versus time in 10 CO_2 absorption/desorption cycles with 5.32 wt % CaO in $CaCl_2$. The carbonation and decarbonation temperatures are 787 and 930 °C, respectively, with 14 vol % CO_2 in N_2 during carbonation and pure N_2 during decarbonation.

and calcium chloride, leading to the formation of CaO and HCl. This additional CaO formation may be the reason for the enhancement of the sorbent reaction with CO_2. The time dependency of HCl concentration curves indicates that the concentration of released HCl depends upon CO_2 and CO emitted from the reactor during the absorption process (Figure 8). This indicates that the inlet gas contains minor amounts of moisture, which influences the hydrolysis of $CaCl_2$. However, gaseous HCl may easily be captured by CaO at ambient temperatures. Only trace amounts of CO were recorded. The carbon monoxide peak of 3000 ppm was reached at 930 °C, while the natural level in air is only 0.2 ppm. This level of the formed carbon monoxide can be related to CO formation from CO_2 reduction induced by iron at high temperatures (stainless-steel container oxidation). In addition, it can be noted that a real flue gas may contain carbon particles, and solid carbon will react with CO_2 to form CO at elevated temperatures.

■ CONCLUSION

This paper describes the experiments for optimizing the carbonation and decarbonation steps in a technique for separation of CO_2 from a flue gas stream by means of CaO dissolved in molten calcium chloride. Systematic parametric and cyclic studies of CO_2 absorption/desorption were performed, using FTIR gas analysis as well as gravimetric evaluation. It was found that, at carbonation temperatures in the range of 768−810 °C, the initial conversion of 5 wt % CaO in $CaCl_2$ to carbonate is only slightly influenced, but at higher temperatures, the conversion decreases rapidly. In the decarbonation step, the temperature was varied in the interval of 904−950 °C. Higher temperatures gave faster decomposition of the formed carbonate. The slightly higher rates of absorption were obtained by increasing the melt height from 10 to 20 cm. This may be attributed to a longer contact time between the gas and the sorbent. The increase of the CaO concentration from 5 to 15 wt % in the molten salt enhances the CO_2 removal process. The concentration of more than 15 wt % sorbent gives a decreasing CO_2 sorption capacity, probably because of sedimentation and agglomeration of the sorbent. Furthermore, several absorption/desorption cycles with 5.32 wt % CaO in $CaCl_2$ were tested at 787 and 799 °C. The results demonstrate that the sorbent activity is higher at a lower temperature and the capacity increased from 0.396 to 0.507 g of CO_2/g of CaO after application of 3 CO_2 sorption cycles. In the following carbonation/decarbonation cycles, the CaO activity was constant with a carrying capacity value of 0.504 g of CO_2/g of CaO.

■ AUTHOR INFORMATION

Corresponding Author

*E-mail: viktorija.tomkute@gmail.com.

Notes

The authors declare no competing financial interest.

■ ACKNOWLEDGMENTS

We thank the Norwegian Research Council for financial support through the CLIMIT Research Programme (199900/S60). The primary data have been deposited for open access with the Norwegian University of Life Sciences (UMB).

■ REFERENCES

(1) Bowen, F. Carbon capture and storage as a corporate technology strategy challenge. *Energy Policy* **2011**, *39*, 2256−2264.
(2) von Stechow, C.; Watson, J.; Praetorius, B. Policy incentives for carbon capture and storage technologies in Europe: A qualitative multi-criteria analysis. *Global Environ. Change* **2011**, *21*, 346−357.
(3) MacDowell, N.; Florin, N.; Buchard, A.; Hallett, J.; Galindo, A.; Jackson, G.; Adjiman, C. S.; Williams, C. K.; Shah, N.; Fennell, P. An overview of CO_2 capture technologies. *Energy Environ. Sci.* **2010**, *3*, 1645−1669.
(4) Valverde, J. M. Ca-based synthetic materials with enhanced CO_2 capture efficiency. *J. Mater. Chem. A* **2013**, *1*, 447−468.
(5) Martinez, A.; Lara, Y.; Lisbona, P.; Romeo, L. M. Energy penalty reduction in the calcium looping cycle. *Int. J. Greenhouse Gas Control* **2012**, *7*, 74−81.
(6) Florin, N. H.; Blamey, J.; Fennell, P. S. Synthetic CaO-based sorbent for CO_2 capture from large-point sources. *Energy Fuels* **2010**, *24*, 4598−4604.
(7) Wang, W.; Ramkumar, S.; Fan, L. S. Energy penalty of CO_2 capture for the carbonation−calcination reaction (CCR) process: Parametric effects and comparisons with alternative processes. *Fuel* **2013**, *104*, 561−574.
(8) Vatopoulos, K.; Tzimas, E. Assessment of CO_2 capture technologies in cement manufacturing process. *J. Clean Prod.* **2012**, *32*, 251−261.
(9) Hasanbeigi, A.; Price, L.; Lin, E. Emerging energy-efficiency and CO_2 emission-reduction technologies for cement and concrete production: A technical review. *Renewable Sustainable Energy Rev.* **2012**, *16*, 6220−6238.
(10) Shimizu, T.; Hirama, T.; Hosoda, H.; Kitano, K.; Inagaki, M.; Tejima, K. A twin fluid-bed reactor for removal of CO_2 from combustion processes. *Chem. Eng. Res. Des.* **1999**, *77*, 62−68.
(11) Valverde, J. M.; Perejon, A.; Perez-Maqueda, L. A. Enhancement of fast CO_2 capture by a nano-SiO_2/CaO composite at Ca-looping conditions. *Environ. Sci. Technol.* **2012**, *46*, 6401−6408.
(12) Liu, W. Q.; Yin, J. J.; Qin, C. L.; Feng, B.; Xu, M. H. Synthesis of CaO-based sorbents for CO_2 capture by a spray-drying technique. *Environ. Sci. Technol.* **2012**, *46*, 11267−11272.
(13) Fennell, P. S.; Pacciani, R.; Dennis, J. S.; Davidson, J. F.; Hayhurst, A. N. The effects of repeated cycles of calcination and carbonation on a variety of different limestones, as measured in a hot fluidized bed of sand. *Energy Fuels* **2007**, *21*, 2072−2081.
(14) Manovic, V.; Anthony, E. J. Steam reactivation of spent CaO-based sorbent for multiple CO_2 capture cycles. *Environ. Sci. Technol.* **2007**, *41*, 1420−1425.
(15) Manovic, V.; Anthony, E. J. Integration of calcium and chemical looping combustion using composite CaO/CuO-based materials. *Environ. Sci. Technol.* **2011**, *45*, 10750−10756.
(16) Vieille, L.; Govin, A.; Grosseau, P. Improvements of calcium oxide based sorbents for multiple CO_2 capture cycles. *Powder Technol.* **2012**, *228*, 319−323.
(17) Zhao, M.; Yang, X. S.; Church, T. L.; Harris, A. T. Novel CaO−SiO_2 sorbent and bifunctional Ni/Co−CaO/SiO_2 complex for selective H_2 synthesis from cellulose. *Environ. Sci. Technol.* **2012**, *46*, 2976−2983.
(18) Manovic, V.; Anthony, E. J.; Grasa, G.; Abanades, J. C. CO_2 looping cycle performance of a high-purity limestone after thermal activation/doping. *Energy Fuels* **2008**, *22*, 3258−3264.
(19) Li, Y. J.; Zhao, C. S.; Chen, H. C.; Liang, C.; Duan, L. B.; Zhou, W. Modified CaO-based sorbent looping cycle for CO_2 mitigation. *Fuel* **2009**, *88*, 697−704.
(20) Kim, J.; Lin, L. C.; Swisher, J. A.; Haranczyk, M.; Smit, B. Predicting large CO_2 adsorption in aluminosilicate zeolites for postcombustion carbon dioxide capture. *J. Am. Chem. Soc.* **2012**, *134*, 18940−18943.
(21) Materic, V.; Sheppard, C.; Smedley, S. I. Effect of repeated steam hydration reactivation on CaO-based sorbents for CO_2 capture. *Environ. Sci. Technol.* **2010**, *44*, 9496−9501.
(22) Guo, M.; Zhang, L.; Yang, Z. Q.; Tang, Q. Removal of CO_2 by CaO/MgO and CaO/$Ca_9Al_6O_{18}$ in the presence of SO_2. *Energy Fuels* **2011**, *25*, 5514−5520.
(23) Salvador, C.; Lu, D.; Anthony, E. J.; Abanades, J. C. Enhancement of CaO for CO_2 capture in an FBC environment. *Chem. Eng. J.* **2003**, *96*, 187−195.
(24) Al-Jeboori, M. J.; Fennell, P. S.; Nguyen, M.; Peng, K. Effects of different dopants and doping procedures on the reactivity of CaO-based sorbents for CO_2 capture. *Energy Fuels* **2012**, *26*, 6584−6594.
(25) Al-Jeboori, M. J.; Nguyen, M.; Dean, C.; Fennell, P. S. Improvement of limestone-based CO_2 sorbents for Ca looping by HBr and other mineral acids. *Ind. Eng. Chem. Res.* **2013**, *52*, 1426−1433.
(26) Yin, H. Y.; Mao, X. H.; Tang, D. Y.; Xiao, W.; Xing, L. R.; Zhu, H.; Wang, D. H.; Sadoway, D. R. Capture and electrochemical conversion of CO_2 to value-added carbon and oxygen by molten salt electrolysis. *Energy Environ. Sci.* **2013**, *6*, 1538−1545.
(27) Otake, K.; Kinoshita, H.; Kikuchi, T.; Suzuki, R. O. CO_2 gas decomposition to carbon by electro-reduction in molten salts. *Electrochim. Acta* **2013**, *100*, 293−299.
(28) Zhao, G. Y.; Jiang, T.; Han, B. X.; Li, Z. H.; Zhang, J. M.; Liu, Z. M.; He, J.; Wu, W. Z. Electrochemical reduction of supercritical carbon dioxide in ionic liquid 1-*n*-butyl-3-methylimidazolium hexafluorophosphate. *J. Supercrit. Fluids* **2004**, *32*, 287−291.
(29) Chen, G. Z.; Fray, D. J.; Farthing, T. W. Direct electrochemical reduction of titanium dioxide to titanium in molten calcium chloride. *Nature* **2000**, *407*, 361−364.
(30) Wang, S. L.; Zhang, F. S.; Liu, X.; Zhang, L. J. CaO solubility and activity coefficient in molten salts $CaCl_2$−*x* (*x* = 0, NaCl, KCl, $SrCl_2$, $BaCl_2$ and LiCl). *Thermochim. Acta* **2008**, *470*, 105−107.
(31) Panigrahi, M.; Iizuka, A.; Shibata, E.; Nakamura, T. Electrolytic reduction of mixed (Fe, Ti) oxide using molten calcium chloride electrolyte. *J. Alloys Compd.* **2013**, *550*, 545−552.
(32) Zhang, L. L.; Wang, S. B.; Jiao, S. Q.; Huang, K.; Zhu, H. M. Electrochemical synthesis of titanium oxycarbide in a $CaCl_2$ based molten salt. *Electrochim. Acta* **2012**, *75*, 357−359.
(33) Chen, Z. Y.; Liu, J. H.; Yu, Z. Y.; Chou, K. C. Electrical conductivity of $CaCl_2$−KCl−NaCl system at 1080 K. *Thermochim. Acta* **2012**, *543*, 107−112.
(34) Freidina, E. B.; Fray, D. J. Study of the ternary system $CaCl_2$−NaCl−CaO by DSC. *Thermochim. Acta* **2000**, *356*, 97−100.
(35) Freidina, E. B.; Fray, D. J. Phase diagram of the system $CaCl_2$−$CaCO_3$. *Thermochim. Acta* **2000**, *351*, 107−108.
(36) Wenz, D. A.; Johnson, I.; Wolson, R. D. $CaCl_2$-rich region of $CaCl_2$−CaF_2−CaO system. *J. Chem. Eng. Data* **1969**, *14*, 250−252.
(37) Karami, D.; Mahinpey, N. Highly active CaO-based sorbents for CO_2 capture using the precipitation method: Preparation and characterization of the sorbent powder. *Ind. Eng. Chem. Res.* **2012**, *51*, 4567−4572.
(38) Poletaev, I. F. ; Lyudomirskaya, A. P.; Ismailov, A. I.; Tsiklina, N. D. $CaCl_2$−$CaCO_3$−CaO system. *Zh. Neorg. Khim.* **1976**, *21*, 2281−2284.
(39) Sun, Z. C.; Yu, F. C.; Li, F. X.; Li, S. G.; Fan, L. S. Experimental study of HCl capture using CaO sorbents: Activation, deactivation, reactivation, and ionic transfer mechanism. *Ind. Eng. Chem. Res.* **2011**, *50*, 6034−6043.

Paper IV

Viktorija Tomkute, Asbjørn Solheim and Espen Olsen. A New Optimized Process for CO_2 Capture by CaO in a $CaF_2/CaCl_2$ System. (Manuscript)

A New Optimized Process for CO_2 Capture by CaO in a $CaF_2/CaCl_2$ System

Viktorija Tomkute[1], Asbjørn Solheim[2], Espen Olsen[1]*

1 Department of Mathematical Sciences and Technology, Norwegian University of Life Sciences (UMB), Post Office Box 5003, Drøbakveien 31, NO-1432 Ås, Norway

2 SINTEF Materials and Chemistry, Post Office Box 4760, Sluppen, NO-7465 Trondheim, Norway

Keywords: Post-combustion CO_2 Capture; Calcium Oxide; Molten Salt; Calcium Fluoride; Calcium Chloride

Abstract

CO_2 capture using the system $CaO/CaCO_3$ dissolved or partly dissolved in a molten salt can be characterized by the use of low cost CaO in the form of limestone, high CO_2 capture capacity, and the possibility of increasing the cyclic CO_2 uptake characteristics due to gas-liquid interactions in molten halide salts. Using previously obtained data on CaO reactivity with CO_2 in a $CaCl_2$ melt[1], we here describe the application of the $CaF_2/CaCl_2$ molten salt for CaO dissolution or partly dissolution in a CO_2 capture process. The effects of CaO concentration in $CaF_2/CaCl_2$ (ratio fixed to the eutectic composition), temperature, and gas composition (CO_2/N_2) on the carbonation/decarbonation reactions in a one-chamber atmospheric pressure reactor were established by means of a Fourier transform infrared (FT-IR) gas detector and gravimetric analysis. The CO_2 uptake efficiency by CaO dissolved or partly dissolved in the metal halides was found to enhance and stabilize with concentrations of CaO exceeding 10 wt% in $CaF_2/CaCl_2$ in the temperature range of 670-710 ºC. Desorption of CO_2, performed by a thermal swing technique, proceeded rapidly and completely at 927-946 ºC. The CaO activity dropped significantly when the inlet gas contained less than 5.6 vol% CO_2 in N_2. In addition, 15 wt% CaO in $CaF_2/CaCl_2$ (11.7/73.3 wt%) exhibited efficient and constant CO_2 carrying capacity of 0.667 g CO_2/g CaO after 12 carbonation/decarbonation cycles.

Introduction

The implementation of carbon capture, transport and storage (CCS) technology in power stations, cement manufacture, hydrogen production, and other heavily CO_2 emitting industrial processes could make a noticeable contribution in meeting ambitious climate protection goals.[2-4] The principle of this technology is that CO_2 is captured from point sources in the

power generation or industrial plants, compressed, and transported to the storage site. The main challenges in CCS are related to storage site characterization and public engagement/communication connected with acknowledgment of risk of leakage and induced seismicity.[5] Still, the CO_2 capture step is much more complex and expensive than other processes in the CCS technology.[6] There are various methodology options which are appropriate for CCS, but only a few are being pursued for uses in commercial deployment; among these are the use of amine-based solvents, oxyfuel combustion, and calcium looping technology.[7] At present, monoethanolamine (MEA) and diethanolamine (DEA) are usually selected as amine solvents for post-combustion CO_2 capture.[3] Nevertheless, there are a lot of disadvantages related with amine-based CO_2 removal technology, such as cost, corrosiveness, degradation of the amines, and their reaction with other constituents of the flue gases, such as typical acid gases (NO_x, SO_x, HCl and HF) and particulate matter.[8] In oxyfuel combustion carbon capture, the main challenge is that the system requires denitrification of the combustion products. Thus, combustion of fuel takes place with large quantities of pure O_2 which is produced by an expensive, large-scale air separator (cryogenic air separation unit or membranes). Also, there are more disadvantages related to the oxyfuel combustion process, such as fouling, changes in the chemical compositions of the fly ash and leakages.[6] Another technology that is attractive for commercial application is calcium looping, where CO_2 and CaO are reversibly reacted to form $CaCO_3$.[6-10] However, many investigations have shown that the degradation of CaO is rapid which may be assigned to loss of the porosity due to sintering, attrition and other competing reactions with impurities.[8,11,12]

Electrochemical reduction of CO_2 has been studied in aqueous solution and room temperature ionic liquids (RTILs).[13-15] Recent developments demonstrate that CO_2 solubility is higher in RTILs than in aqueous solution. Also, RTILs possess a wider electrochemical window which gives higher product yield. However, the fundamental barrier in the industrial application of RTILs is related to the high cost of ionic liquids.[14,16] Therefore, low cost carbonate and chloride molten salt mixtures have been studied as electrolytes for electrochemical deposition of C or reduction of CO_2 to CO.[14,15,17] Simulation data analysis on molten salt CO_2 capture and electrochemical transformation (MSCC-ET) showed possibility of producing useful carbon-based materials and oxygen which reduces the cost of the process.[14] In addition, the MSCC-ET technology is considered as a promising CO_2 capture and conversion process in renewable energy production stations and industrial operations[14], but still the total MSCC-ET process cost is too high for competing with other existing CO_2 capture technologies.

Recently, our investigation of CO_2 capture by 5.32 wt% CaO dissolved/dispersed in molten $CaCl_2$ resulted in a value of 64.3 wt% stabilized CaO conversion to carbonate. Complete decomposition of the carbonate back to CaO and CO_2 was also demonstrated.[1] Figure 1 illustrates a simplified schematic diagram of CO_2 capture by metal oxides in molten salt systems which may be operated as a large scale CO_2 capture plant. This is a two-step process where the carbonation of the metal oxides in the molten salt takes place in a CO_2 capture unit which is interconnected to a regenerator unit for metal oxide and CO_2 recovery. For this process, the selection of suitable molten salt composition and reactor design are essential in achieving the desired characteristics of the process.

FIGURE 1

Alkaline earth metal halide salts possess very high thermal stability, low viscosity, low vapour pressure, and their liquidus temperature may be easily controlled by varying chemical composition.[18] The solubility and activity coefficient of CaO in $CaCl_2$ and $CaCl_2$-CaF_2 molten salts have been widely examined for phosphate and sulfide extraction in hot metal treatment.[19-25] Tacker et al.[26] calculated $CaCl_2$-CaF_2 system liquidus curves reflecting ideal mixing between the two components, which provides a eutectic composition of 14 wt% CaF_2 in $CaCl_2$ at 645 ºC and shows good agreement with experimentally derived results reported by Wenz et al. (13.8 wt% CaF_2 in $CaCl_2$ at 645 ºC).[22] It has been demonstrated that ternary phase relations of the CaO-$CaCl_2$-CaF_2 system exhibits a eutectic point at 2.5 wt% CaO, 12.9 wt% CaF_2 in $CaCl_2$ and 625 ºC.[22] This shows that conversion of CaO to carbonates in the CaF_2-$CaCl_2$ melt enables the carbonation reaction proceeding at lower temperature than in the CaO-$CaCl_2$[1] system (eutectic temperature 750 ºC[22]).

The present study focuses on the application of the CaF_2-$CaCl_2$ molten salt as the solvent for the dissolution or partly dissolution of CaO in CO_2 capture technology. The main aims were to optimize the CO_2 absorption and desorption temperatures for the carbonation/decarbonation reactions. The effect of CaO concentration variation in the eutectic composition of the CaF_2/$CaCl_2$ system and the simulated flue gas composition (CO_2/N_2) were examined. The cyclic CO_2 capture performance was determined and compared to the previous experimentally derived data on the application of the CaO/$CaCl_2$ system in CO_2 capture[1].

Experimental

Sample preparation

Anhydrous CaO, $CaCl_2$, and CaF_2 of analytical purity (Sigma-Aldrich) were used as starting materials. All chemicals were kept in a drying cabinet at 200 ºC for 50 h before use. Various CaO-CaF_2/$CaCl_2$ mixtures were produced, keeping the same volume (10 cm height) of melt in the reactor (Figure 1). Samples were prepared with CaO contents between 5 and 20 wt% in a eutectic mixture of CaF_2/$CaCl_2$ (13.8 wt% CaF_2 in $CaCl_2$). Before the CO_2 capture experiments, the powder mixtures were placed in a nickel crucible (5.2 dia. x 35.0 cm height). To remove moisture from the compounds, the mixtures were heated slowly (heating rate 200 ºC/h) to 850 ºC under Ar and kept at that temperature for 10 h.

CO_2 capture optimization

In this study, an atmospheric pressure, one-chamber laboratory scale reactor (Figure 1) was used. The reactor comprised a nickel crucible (inner part) and a stainless-steel container (outer part), which was placed in a high temperature ceramic furnace (<1250 ºC). A nickel pipe was used to supply the CO_2/N_2 gas mixture by bubbling it into the CaO-CaF_2/$CaCl_2$ melt through the top of the sealed reactor. The flow rate and composition of the simulated flue gas (CO_2 in N_2) were adjusted by mass flow controllers (MASS-STREAM, M+W Instruments GmbH). The gases from the reactor were filtered by an electrostatic filter. The temperature of the samples was measured by a type S (Pt–Pt10Rh, ±1.1 ºC) thermocouple (TC) inserted into the melt. In addition, a mass flow meter (MFM, Sierra 820 Series, Sierra Instruments, Inc.) was integrated at the outlet of the FTIR detector to control the tightness of the assembly. Online measurements of the gas composition at the outlet of the reactor were conducted using a FTIR gas analyzer (Thermo Scientific, Nicolet 6700 model). The FTIR detector was equipped with

a 2 m path length (200 ml volume) gas cell with KBr windows, which temperature was controlled by a Digi-Sense controller (Eutech Instruments Pte Ltd). The gas cell temperature was set at 120 ºC for at least 24 h before gas analysis. The FTIR gas cell was purged with pure N_2 (0.7 l/min) for 30 minutes before N_2 background record. The detector was operated using the FTIR software package OMNIC Series (Thermo Scientific).

In all experiments, the pretreated samples (as described above) were stirred with pure N_2 (0.5 l/min) at various temperatures (658-759 ºC) for 2 h before the CO_2 absorption experiments to ensure stability of the melt temperature. CO_2 and N_2 gases of 99.99 % and 99.999 % purity, respectively, were provided by AGA. The effect of the inlet gas composition on the CaO conversion was investigated by applying different CO_2-N_2 gas mixtures (0.8-14 vol% CO_2) through the $CaO/CaF_2/CaCl_2$ (15/11.7/73.3 wt%) melt at 700-710 ºC. A controlled total inlet gas flow of 0.6 l/min was used in all experiments. The carbonation reaction commenced until the concentration of CO_2 in N_2 measured by the FTIR attained the same value as the inlet stream composition. In order to investigate the suitable temperature for CO_2 release, decomposition of the formed carbonated samples were then performed at 899-946 ºC under pure N_2 after ramping up the temperature at 300 ºC/h), unless specifically mentioned. In addition, continuous careful weighing of the reactor was performed by an industrial weighing scale (MS8001S, Mettler Toledo, accuracy 0.1 g). A baseline study of the total reactor weight change was performed at different temperatures under argon gas flow to incorporate the weight change due to stainless steel chamber corrosion in the calculations of CO_2 absorption/desorption. All experimental settings (gas composition, gas flow, temperature, and weight changes) were collected and operated by using computer integrated systems (NI cRIO-907x, National Instruments).

Cyclic CO_2 capture

To establish the cyclic carbonation/decarbonation behavior of the system, the mixture of $CaO/CaF_2/CaCl_2$ with 15/11.7/73.3 wt% was selected for the analysis. The prepared sample was fused at 850 ºC for 10 h (heating rate 200 ºC/h) in argon atmosphere. The furnace temperature was then decreased to 700 ºC and kept for 2 h while bubbling pure N_2 (0.5 l/min) through the melt. Then, the gas flow (14 vol% CO_2 in N_2, total flow 0.6 l/min) was applied for the carbonation reaction. The reactor weight change and gas analysis were conducted continuously. The CO_2 gas flow was suspended and the furnace temperature raised to 940 ºC for the decarbonation stage. Each part of the cycle lasted 600 minutes, and a total of 12 carbonation/decarbonation cycles were successively conducted.

Results and discussion

Absorption temperature evaluation

To investigate the most efficient CO_2 capture temperature, CO_2 uptake experiments on the samples containing different CaO concentrations (5-20 wt%) in $CaF_2/CaCl_2$ were performed at various carbonation temperatures. Figure 2 represents the initial CO_2 absorption cycle by CaO dissolved or partly dissolved in the molten salt. The feed stream during the carbonation stage was 14 vol% of CO_2 in N_2 and the temperature was varied from 658 to 759 ºC depending on the chemical composition. From Figure 2 it is evident that the selection of CO_2 from N_2 is enhanced at a lower carbonation temperature and at increased CaO content. The

recorded CO_2 concentration versus time curves for 15 and 20 wt% CaO indicate two distinct regions for the CO_2 uptake. This may be related to phase transitions in the $CaO/CaF_2/CaCl_2$ system at different temperatures and compositions. Thermal analysis of the $CaO\text{-}CaF_2/CaCl_2$ system demonstrated that the eutectic composition contains 2.5 wt% CaO and 12.9 wt% CaF_2 in $CaCl_2$, and melts at 625 ºC.[22] This indicates that the initial efficient carbonation reaction may be attributed to dispersed CaO reacting with CO_2, and the lower CO_2 absorption efficiency may be related to reaction with dissolved or agglomerated CaO.

FIGURE 2

The CO_2 uptake of the sorbent (g CO_2/g CaO) was calculated on the basis of the initially added amounts of CaO in $CaF_2/CaCl_2$. The dependence of carbonation temperature and CaO concentration are given in Figure 3. A significant effect of the system temperature on the sorbent sorption capacity can be observed for 10 wt% of CaO in eutectic $CaF_2/CaCl_2$ melt, as the carrying capacity drops from 0.587 g CO_2/g CaO to 0.426 g CO_2/g CaO when the CO_2 absorption was performed at 705 ºC and 755 ºC, respectively. This may be attributed to increased CaO solubility and lower concentration of solid CaO in the melt. This effect was not observed with 5 wt% CaO. The carbonation efficiency was reduced gradually from 0.456 g CO_2/g CaO to 0.393 g CO_2/g CaO by increasing the system temperature in the range 658-755 ºC. The highest initial carrying capacity of 0.616 g CO_2/g CaO was achieved at 707 ºC with the sample containing 20 wt% CaO. Also, the most effective and constant conversions of CaO to $CaCO_3$ were obtained with 15 and 20 wt% CaO at carbonation temperatures in the range 675-715 ºC. It can be noted that a uniform and stable dispersion of solid CaO in the molten salt opens the possibility for improving the CO_2 uptake characteristics.

FIGURE 3

Desorption temperature evaluation

The impact of the CO_2 desorption temperature on the carbonated $CaO/CaF_2/CaCl_2$ system was investigated during one CO_2 capture cycle as a function of the system temperature, weight changes and CO_2 concentration in the outlet stream (Figure 4). Carbonation of 15 wt% CaO partly dissolved in molten $CaF_2/CaCl_2$ (11.7/73.3 wt%) was conducted by applying gas consisting of 14 vol% CO_2 in N_2 at 695-705 ºC for 550 minutes. A carbonation conversion value of 76.5 % was detected. When carbonation had reached this value, the flow of CO_2 was stopped and regeneration of CO_2 and CaO was conducted at 899-947 ºC under pure N_2 for 550 minutes. The CO_2 concentration curves, recorded by FTIR in the stream leaving the reactor and the calculated CaO regeneration efficiency based on total reacted CO_2 describes the impact of the temperature on the CO_2 desorption, and are represented in Figure 4. The results show that decomposition of the formed carbonates in the molten $CaF_2/CaCl_2$ system is incomplete at temperatures lower than 927 ºC. Above this temperature the CO_2 desorption is rapid and approaches 100% efficiency.

FIGURE 4

Variation of CaO in the $CaF_2/CaCl_2$ system

As described above, a set of sorbents containing CaO (5, 10, 15, 20 wt%) in $CaF_2/CaCl_2$ (13.8/86.2 wt%) were examined at various carbonation temperatures for investigation of sorbent CO_2 carrying activity. Figure 5 shows the impact of the CaO concentration on the CO_2 absorption and desorption processes at selected reaction temperatures. Significantly lower carrying capacity of the sorbent was observed with the melt containing 5 wt% CaO. The sorbent carbonation conversion efficiency rapidly increased from 56.6 % to 78.5 % by increasing the CaO concentration from 5 to 20 wt% in the molten salt. The enhancement of CaO content in the melt leads to the formation of the solid-CaO solution[22], thus the efficiency of the reaction of CaO with CO_2 increases.

The effect of the CaO content in the melt on desorption of CO_2 was examined at 935-945 ºC under pure N_2 for 550 minutes (Figure 5). Complete regeneration of CO_2 and CaO was achieved in the melts containing less than 15 wt% CaO. High CaO concentrations in the molten salts increases the viscosity of the melt due to CaO saturation, and the formation of a slurry may be expected at concentrations higher than 15 wt% CaO in the $CaF_2/CaCl_2$ system. It has been demonstrated that the solubility of $CaCO_3$ in CaF_2 is higher than that of CaO. We suggest that complete decomposition of the formed carbonates in the molten halides salts with 20 wt% CaO could not be observed under pure N_2 gas flow due to CaO deposition inside the nickel tube. Thus, regeneration of 20 wt% CaO in the $CaF_2/CaCl_2$ system was conducted under 14 vol% CO_2 in N_2, which resulted in near 100 % conversion efficiency.

FIGURE 5

Concentration of CO_2 in N_2

The influence of the inlet gas composition on CaO conversion was evaluated by performing the carbonation stage under different CO_2/N_2 gas mixtures (0.8-14 vol% CO_2) at 700-710 ºC and decomposition at 935-945 ºC under pure N_2. Plots showing the recorded CO_2 concentration in the outlet stream after CO_2 absorption/desorption by 15 wt% CaO in $CaF_2/CaCl_2$ (11.7/73.3 wt%) and the calculated carrying capacity of the sorbent are presented in Figure 6. The total carrying capacity of the sorbent increased from 0.427 g CO_2/g CaO to 0.601 g CO_2/g CaO when the CO_2 content in the inlet gas increased from 0.8 vol% to 9.7 vol% (total gas flow rate 0.6 l/min). As can be observed from the registered CO_2 concentration curves, the rate of CO_2 separation from N_2 was reduced from 92.5 % to 58.1 % of the total applied CO_2 in the initial carbonation reaction step, as the CO_2 amount in the inlet gas flow decreased from 9.7 vol% to 0.8 vol%. A substantial change in the carbonation of the sorbent was observed when less than 5.60 vol% of CO_2 in N_2 was applied initially with 15 wt% CaO in $CaF_2/CaCl_2$. However, the decomposition rate of the formed carbonates in the temperature range 935-945 ºC under pure N_2 was be rapid and complete.

FIGURE 6

Cyclic CO_2 capture by CaO-$CaF_2/CaCl_2$

Sorbent systems with a high selectivity for CO_2, high carrying capacity, easy regeneration, and sustained performance upon cycling are requested for commercial applications. It has

been found that the CO_2 uptake efficiency using solid CaO based sorbents derived from limestone or dolomite rapidly decreases with increasing number of carbonation/decarbonation cycles.[6-8,10] Therefore, the cyclic CO_2 uptake by 15 wt% CaO in molten $CaF_2/CaCl_2$ (11.7/73.3 wt%) was tested for twelve complete cycles of CO_2 absorption/desorption. The system temperature, CO_2 concentration in the outlet gas and weight changes were recorded (Figure 7). The carbonation reaction was conducted at 705 ºC under feed stream consisting of 14 vol% CO_2 in N_2. Decarbonation was performed at 945 ºC under pure N_2 both reactions in each cycle were pursued for 600 minutes. The detected CO_2 concentration curves in the outlet stream are shown in Figure 8. The CO_2 separation effectiveness in the initial carbonation reaction stage (170 minutes) increased from 92.5 % to 93.6 % of total applied CO_2 after 4 CO_2 uptake cycles and remained stable over the other 8 cycles. In addition, the CO_2 regeneration behavior was rapid and accomplished at near 100 % efficiency.

FIGURE 7 and 8

The total cyclic carbonation/decarbonation conversions of CaO were calculated on the basis of the amounts of CaO used initially in the melt by FTIR gas analysis and weight change measurements. Figure 9 depicts the carrying capacity of CaO in cyclic CO_2 uptake by the system $CaO/CaF_2/CaCl_2$ (15/11.7/73.3 wt%) and the results are compared with the performance of the $CaO\text{-}CaCl_2$[1] system. Enhancement in the CO_2 uptake characteristics of the sorbent was observed after 4 cycles in the $CaO/CaF_2/CaCl_2$ system, from 0.599 g CO_2/g CaO to 0.667 g CO_2/g CaO. The following 8 cycles showed a stable carrying capacity of 0.667 g CO_2/g CaO. A similar carbonation efficiency increase and stabilization in multiple CO_2 capture cycles was detected when using 5.32 wt% CaO in $CaCl_2$[1]. The total CO_2 uptake capacity after 10 carbonation/decarbonation cycles of the systems $CaO/CaCl_2$ and $CaO/CaF_2/CaCl_2$ were 0.505 g CO_2/g CaO and 0.671 g CO_2/g CaO, respectively, while the theoretical value is 0.785 g CO_2/g CaO. This significant change in the sorbent activity may be related to the lower absorption temperature used. The lower liquidus temperature of the $CaF_2/CaCl_2$ melt (the eutectic temperature is 645 ºC) allows the carbonation to be performed at a lower temperature than in the $CaCl_2$ melt (melting temperature is 750 ºC).[22,27]

FIGURE 9

<u>CO, HCl and HF formation in Cyclic CO_2 capture by $CaO\text{-}CaF_2/CaCl_2$</u>

Carbon monoxide, hydrochloric acid (HCl) and hydrofluoric acid (HF) formation were recorded during the cyclic CO_2 capture using 15 wt% $CaO/CaF_2/CaCl_2$ (15/11.7/73.3 wt%). This is illustrated in Figure 10. The carbonation reaction was performed at 705 ºC under 14 vol% CO_2 in N_2 and decomposition of the formed carbonates was carried out at 945 ºC under pure N_2. Increasing CO release from 0 to 180 ppm was observed in each performed carbonation stage at 705 ºC. A CO peak of around 2900 ppm was recorded in all 12 decarbonation cycles, at the time when the highest CO_2 volume in the outlet gas was observed. This CO peak rapidly disappears and rises again in the next carbonation cycle. The results indicate that CO concentration in the outlet gas depends on the CO_2 content in the inlet gas and the system temperature. This demonstrates that CO formation is caused by CO_2 reduction at the temperatures used.

Hydration of calcium halides due to their hygroscopic nature leads to the formation of other substances, mainly CaO, $Ca(OH)_2$, CaClOH, HX and X_2 (X = halide ion).[28-31] Therefore, the release of HCl and HF in the outlet gas was also investigated. Figure 10 shows that the emission of HCl and HF depends on the system temperature. The HCl level of 1160 ppm was reached in the initial decarbonation reaction, but the level decreased and stabilized at 40 ppm after 5 CO_2 capture cycles. Similar behavior was observed for HF where a peak of 90 ppm was recorded in the first CO_2 uptake cycle which was reduced to 14 ppm in the next cycles. The hydration energy of CaF_2 is -24.97 eV while that of $CaCl_2$ is 22.79 eV, illustrating that $CaCl_2$ is more hygroscopic than CaF_2.[29] The higher emission of HCl and HF in the first carbonation/decarbonation cycle indicates that the initial drying of the used chemical compounds was incomplete. Stabilized formations of HCl and HF may be related to hydration of the metal halides by traces of moisture in the inlet gas. Only minor amounts of HCl and HF were recorded; thus, the change in carrying capacity of the sorbent due to the hydration of calcium halides was considered to be insignificant.

FIGURE 10

Conclusions

The present investigation demonstrates an effective CO_2 separation method with CaO dissolved or partly dissolved in the eutectic composition of the $CaF_2/CaCl_2$ molten salt. Carbonation and decarbonation in the $CaO\text{-}CaF_2/CaCl_2$ system were conducted using an atmospheric pressure reactor, a Fourier transform infrared (FT-IR) gas detector and gravimetric analysis. The efficient temperature for CO_2 gas separation from N_2 was found to be in the range 658-710 ºC and at increased CaO concentration in $CaF_2/CaCl_2$. Desorption of CO_2 in N_2 atmosphere was affected by the concentration of CaO in the melt. The optimum decomposition temperature for the formed carbonates in the metal halide salts was in the range 930-950 ºC under N_2 when the content of CaO in the melt was in the range 5-15 wt%. The most efficient performance was achieved with 15 wt% CaO. This composition exhibited a higher carrying capacity value (0.599 g CO_2/g CaO at 695-705 ºC) and complete decarbonation at 927-947 ºC. As expected, the studies of the variation of CO_2 in the inlet gas resulted in significantly reduced CaO carbonation rates when the CO_2 concentration was lower than 5.6 vol%. However, the rate of CO_2 and CaO regeneration was independent on the CO_2 content in N_2 during the carbonation reaction and proceeded rapidly and completely. In addition, it has been demonstrated that the partial dissolution of CaO in $CaF_2/CaCl_2$ enhances the cyclic CO_2 uptake behavior. After 10 carbonation/decarbonation cycles, the $CaO/CaCl_2$ (5.32/94.68 wt%)[1] and $CaO/CaF_2/CaCl_2$ (15/11.7/73.3 wt%) systems attained constant carrying capacity values of ~0.504 and ~0.667 g of CO_2/g of CaO, respectively. It is obvious that the choice of the suitable molten salt composition for dissolution or partly dissolution of the active sorbent and reactor design is essential in obtaining optimum efficiencies.

AUTHOR INFORMATION

Corresponding Author

*Email: viktorija.tomkute@gmail.com

Notes

The authors declare no competing financial interest.

ACKNOWLEDGMENTS

We thank the Research Council of Norway for financial support through the CLIMIT research Programme (199900/S60). The primary data have been deposited for open access with the Norwegian University of Life Sciences (UMB).

References

(1) Tomkute, V.; Solheim, A.; Olsen, E.: Investigation of high-temperature CO_2 capture by CaO in $CaCl_2$ molten salt. *Energ Fuel* **2013**, *27*, 5373-5379.

(2) Dean, C. C.; Blamey, J.; Florin, N. H.; Al-Jeboori, M. J.; Fennell, P. S.: The calcium looping cycle for CO_2 capture from power generation, cement manufacture and hydrogen production. *Chem. Eng. Res. Des.* **2011**, *89*, 836-855.

(3) Goeppert, A.; Czaun, M.; Prakash, G. K. S.; Olah, G. A.: Air as the renewable carbon source of the future: an overview of CO_2 capture from the atmosphere. *Energy & Environmental Science* **2012**, *5*, 7833-7853.

(4) Zeman, F.: Energy and material balance of CO_2 capture from ambient air. *Environ. Sci. Technol.* **2007**, *41*, 7558-7563.

(5) Jacobson, M. Z.: Review of solutions to global warming, air pollution, and energy security. *Energy & Environmental Science* **2009**, *2*, 148-173.

(6) Blamey, J.; Anthony, E. J.; Wang, J.; Fennell, P. S.: The calcium looping cycle for large-scale CO_2 capture. *Prog Energ Combust* **2010**, *36*, 260-279.

(7) MacDowell, N.; Florin, N.; Buchard, A.; Hallett, J.; Galindo, A.; Jackson, G.; Adjiman, C. S.; Williams, C. K.; Shah, N.; Fennell, P.: An overview of CO_2 capture technologies. *Energy & Environmental Science* **2010**, *3*, 1645-1669.

(8) Valverde, J. M.: Ca-based synthetic materials with enhanced CO_2 capture efficiency. *J. Mater. Chem. A* **2013**, *1*, 447-468.

(9) Wang, W. R., S.; Fan, L. S.: Energy penalty of CO_2 capture for the carbonation-calcination reaction (CCR) process: parametric effects and comparisons with alternative processes. *Fuel* **2013**, *104*, 561-574.

(10) Florin, N. H.; Blamey, J.; Fennell, P. S.: Synthetic CaO-based sorbent for CO_2 capture from large-point sources. *Energ Fuel* **2010**, *24*, 4598-4604.

(11) Liu, W. Q.; Yin, J. J.; Qin, C. L.; Feng, B.; Xu, M. H.: Synthesis of CaO-based sorbents for CO_2 capture by a spray-drying technique. *Environ. Sci. Technol.* **2012**, *46*, 11267-11272.

(12) Donat, F.; Florin, N. H.; Anthony, E. J.; Fennell, P. S.: Influence of high-temperature steam on the reactivity of CaO sorbent for CO_2 capture. *Environ. Sci. Technol.* **2012**, *46*, 1262-1269.

(13) Hori, Y. K., K.; Suzuki, S.: Production of CO and CH_4 in electrochemical reduction of CO_2 at metal-electrodes in aqueous hydrogencarbonate solution. *Chemistry Letters* **1985**, 1695-1698.

(14) Yin, H. Y.; Mao, X. H.; Tang, D. Y.; Xiao, W.; Xing, L. R.; Zhu, H.; Wang, D. H.; Sadoway, D. R.: Capture and electrochemical conversion of CO_2 to value-added carbon and oxygen by molten salt electrolysis. *Energy & Environmental Science* **2013**, *6*, 1538-1545.

(15) Zhao, G. Y. J., T.; Han, B. X.; Li, Z. H.; Zhang, J. M.; Liu, Z. M.; He, J.; Wu, W. Z.: Electrochemical reduction of supercritical carbon dioxide in ionic liquid 1-n-butyl-3-methylimidazolium hexafluorophosphate. *Journal of Supercritical Fluids* **2004**, *32*, 287-291.

(16) Mignard, D. S., M.; Duthie, J. M.; Whittington, H. W.: Methanol synthesis from flue-gas CO_2 and renewable electricity: a feasibility study. *International Journal of Hydrogen Energy* **2003**, *28*, 455-464.

(17) Otake, K.; Kinoshita, H.; Kikuchi, T.; Suzuki, R. O.: CO_2 gas decomposition to carbon by electro-reduction in molten salts. *Electrochim. Acta* **2013**, *100*, 293-299.

(18) Forsberg, C. W.; Peterson, P. F.; Zhao, H. H.: High-temperature liquid-fluoride-salt closed-Brayton-cycle solar power towers. *Journal of Solar Energy Engineering-Transactions of the Asme* **2007**, *129*, 141-146.

(19) Wang, S. L. Z., F. S.; Liu, X.; Zhang, L. J.: CaO solubility and activity coefficient in molten salts $CaCl_2$-x (x=0, NaCl, KCl, $SrCl_2$, $BaCl_2$ and LiCl). *Thermochim. Acta* **2008**, *470*, 105-107.

(20) Freidina, E. B.; Fray, D. J.: Study of the ternary system $CaCl_2$-NaCl-CaO by DSC. *Thermochim. Acta* **2000**, *356*, 97-100.

(21) Freidina, E. B.; Fray, D. J.: Phase diagram of the system $CaCl_2$-$CaCO_3$. *Thermochim. Acta* **2000**, *351*, 107-108.

(22) Wenz, D. A.; Johnson, I.; Wolson, R. D.: $CaCl_2$-rich region of $CaCl_2$-CaF_2-CaO system. *J. Chem. Eng. Data* **1969**, *14*, 250-&.

(23) Chatterj.Ak; Zhmoidin, G. I.: Phase equilibrium diagram of system CaO-Al_2O_3-CaF_2. *Journal of Materials Science* **1972**, *7*, 93-&.

(24) Sano, N.; Tsukihashi, F.; Tagaya, A.: Thermodynamics of phosphorus in CaO-CaF_2-SiO_2 and CaO-CaF_2-$CaCl_2$ melts saturated with CaO. *Isij International* **1991**, *31*, 1345-1347.

(25) Tago, Y.; Endo, Y.; Morita, K.; Tsukihashi, F.; Sano, N.: The activity of CaO in the CaO-$CaCl_2$ and CaO-$CaCl_2$-CaF_2 systems. *Isij International* **1995**, *35*, 127-131.

(26) Tacker, R. C.; Stormer, J. C.: Thermodynamics of mixing of liquids in the system $Ca_3(PO_4)_2$-$CaCl_2$-CaF_2-$Ca(OH)_2$. *Geochimica Et Cosmochimica Acta* **1993**, *57*, 4663-4676.

(27) Poletaev, I. F.; Lyudomirskaya, A. P.; Ismailov, A. I.; Tsiklina, N. D.: $CaCl_2$-$CaCO_3$-CaO system. *Zhurnal Neorg. Khimii* **1976**, *21*, 2281-2284.

(28) Kondo, H.; Asaki, Z.; Kondo, Y.: Hydrolysis of fused calcium-chloride at high-temperature. *Metallurgical Transactions B-Process Metallurgy* **1978**, *9*, 477-483.

(29) Sudha, V.; Harinipriya, S.; Sangaranarayanan, M. V.: Dehydration energies of alkaline earth metal halides - a novel simulation methodology. *Chemical Physics* **2005**, *310*, 59-66.

(30) Partanen, J.; Backman, P.; Backman, R.; Hupa, M.: Absorption of HCl by limestone in hot flue gases. Part II: importance of calcium hydroxychloride. *Fuel* **2005**, *84*, 1674-1684.

(31) Molenda, M.; Stengler, J.; Linder, M.; Worner, A.: Reversible hydration behavior of $CaCl_2$ at high H_2O partial pressures for thermochemical energy storage. *Thermochim. Acta* **2013**, *560*, 76-81.

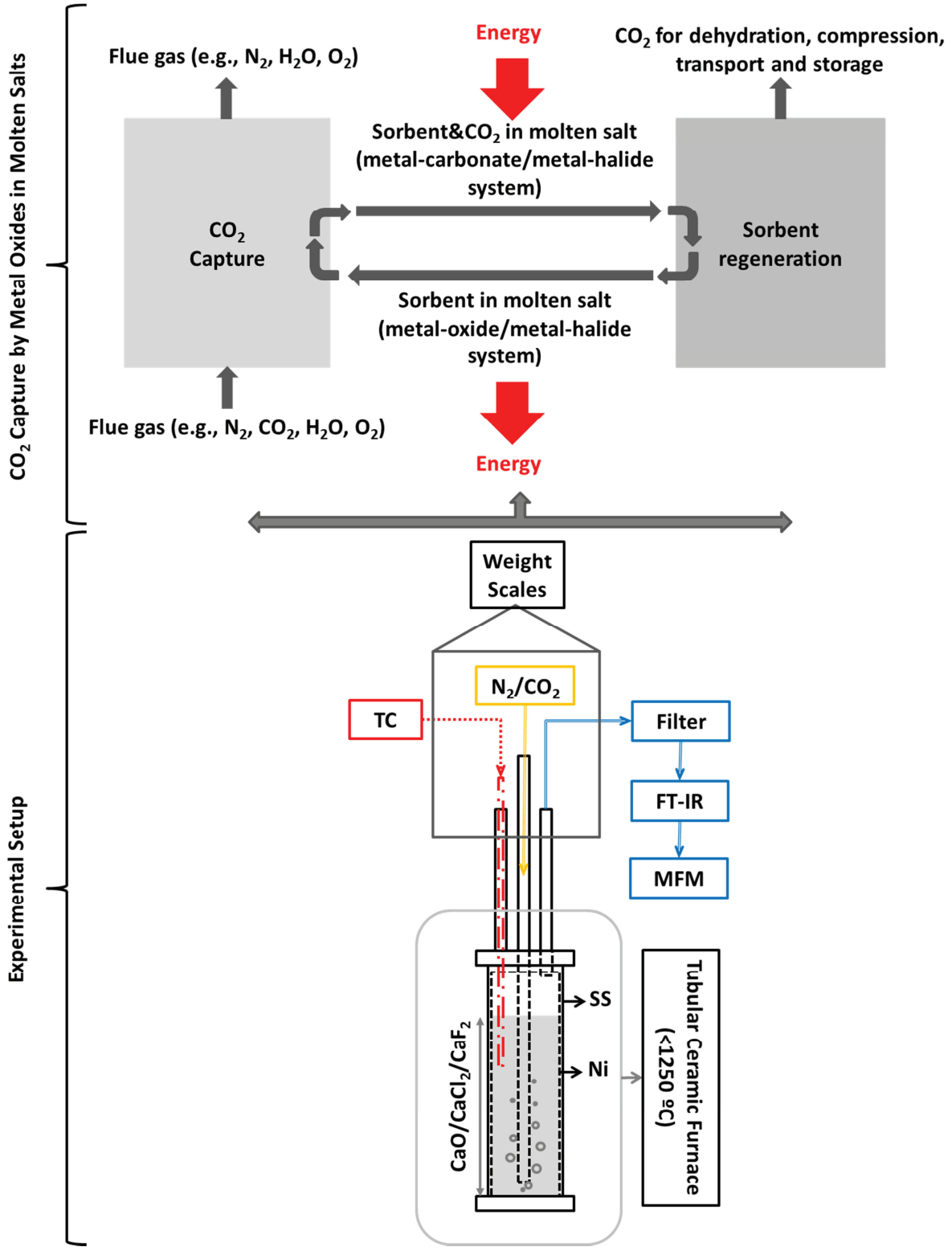

Figure 1. Block diagram of the continuously operating carbon dioxide capture by metal oxides dissolved or partly dissolved in molten salts. The experimental setup: FTIR gas cell apparatus, weight scales, electrostatic filter, mass flow meter (MFM), S-type thermocouple (TC), furnace and reactor (the outer compartment is made of stainless steel (SS), the inner crucible and the feed tube are made of nickel (Ni)).

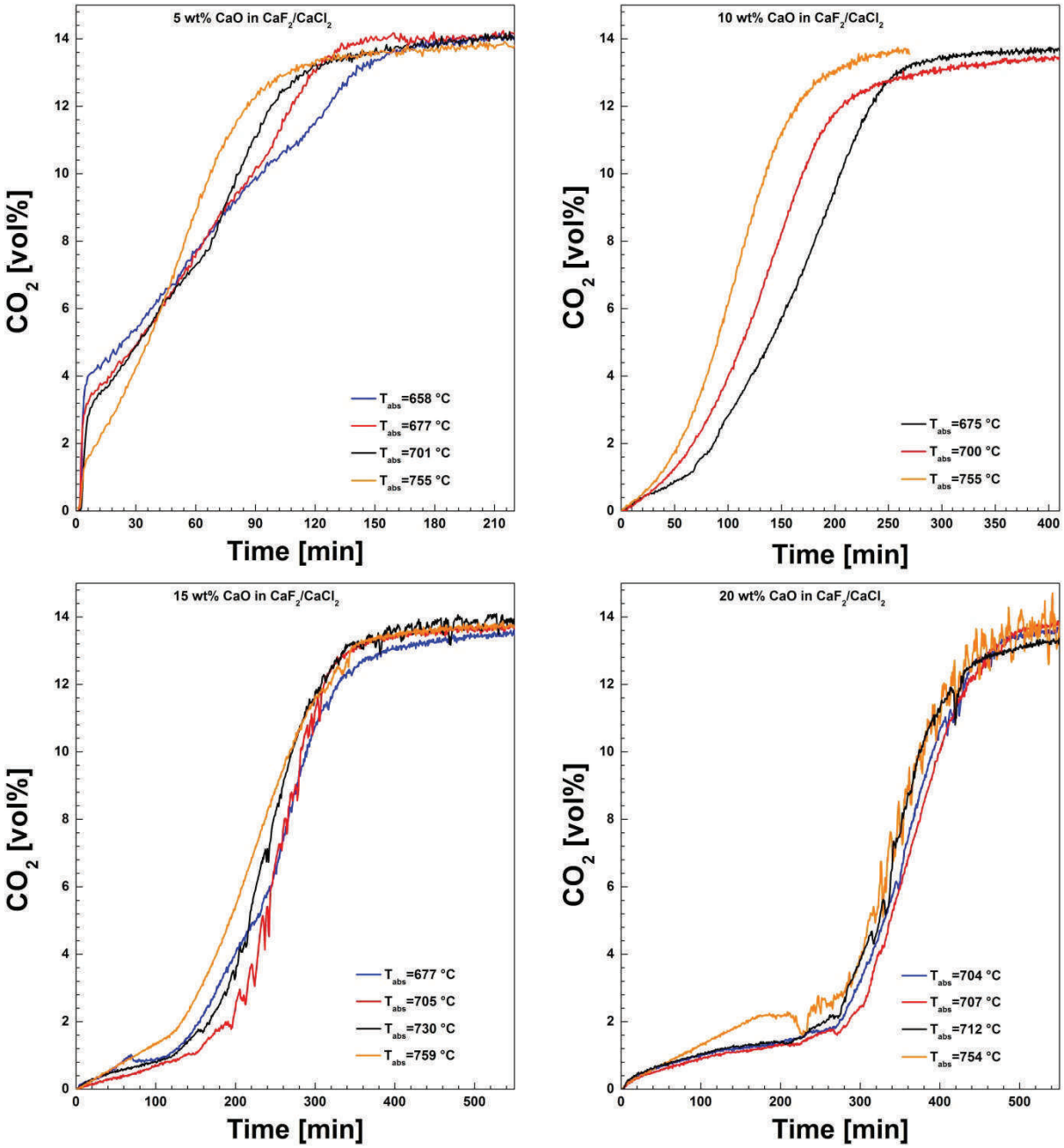

Figure 2. Influence of the temperature and CaO/metal halides (13.8 wt% CaF_2 in $CaCl_2$) mass ratio on CaO reactivity with CO_2. Carbonation of CaO dissolved or partly dissolved in the eutectic composition of $CaF_2/CaCl_2$ system was carried out under ~14 vol% of CO_2 in N_2.

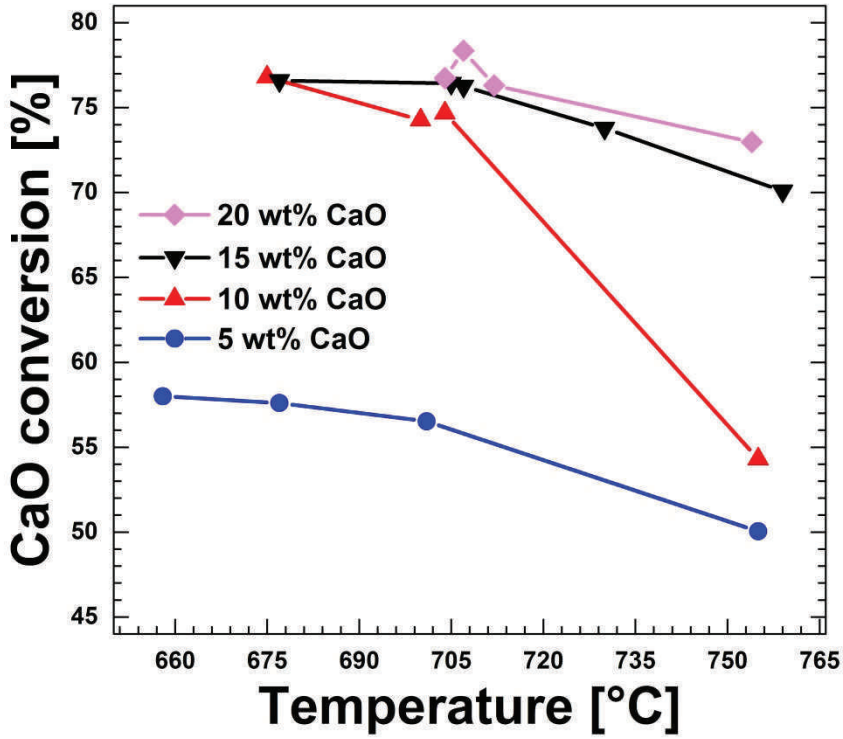

Figure 3. Carrying capacity dependence on the carbonation temperature and CaO concentration in the eutectic composition of $CaF_2/CaCl_2$ system.

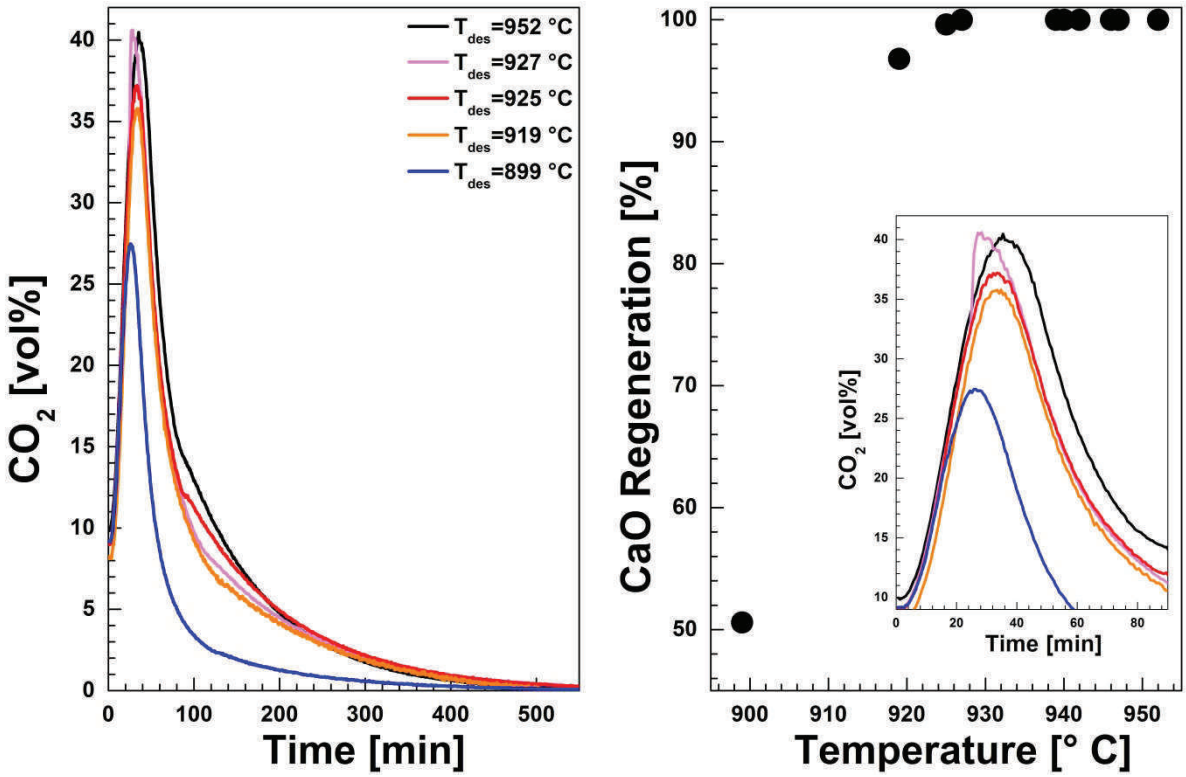

Figure 4. The impact of the system temperature on the formed carbonates decomposition in the eutectic mixture of $CaF_2/CaCl_2$ melt. The carbonation of the $CaO/CaF_2/CaCl_2$ (15/11.7/73.3 wt%) samples were performed at 695-705 ºC under 14vol% CO_2 in N_2. The decarbonation step was carried out at 899-946 ºC under pure N_2 for 550 min. The left graph show CaO regeneration efficiency dependence on decarbonation temperature. Inset: CO_2 concentration versus time (0-90 min).

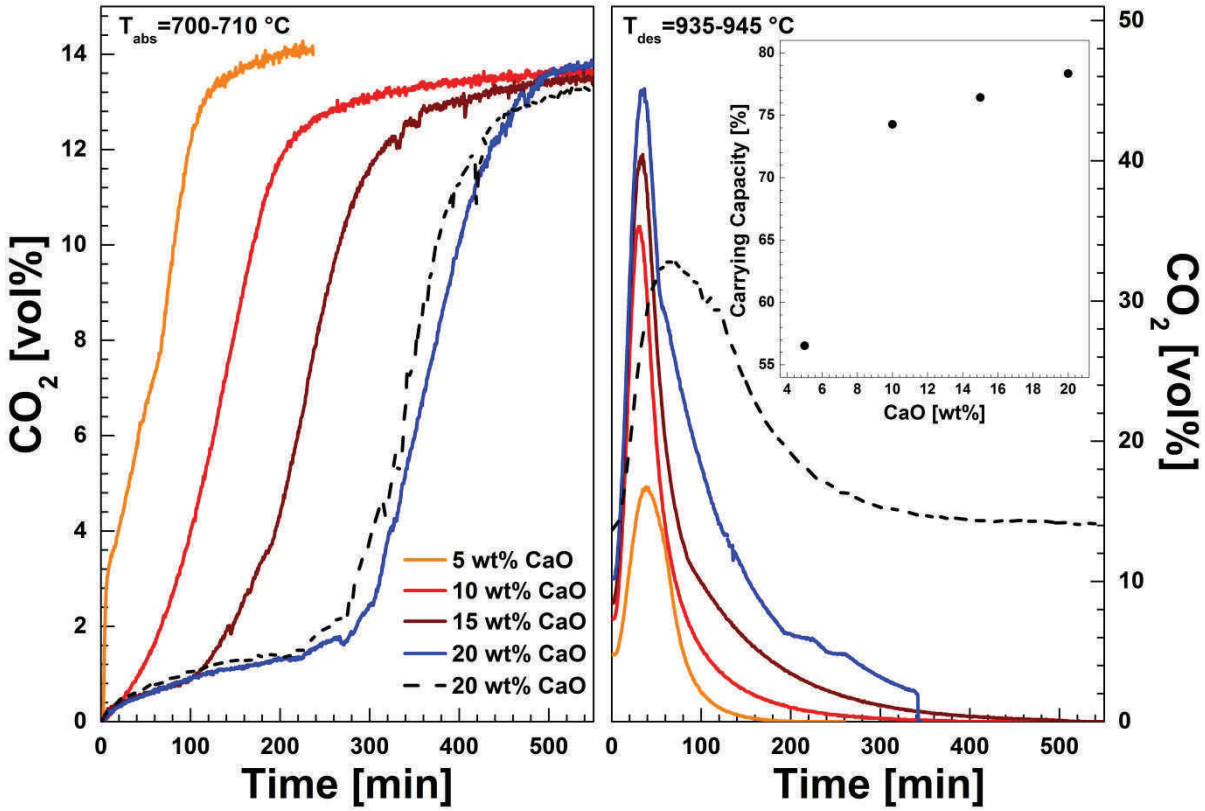

Figure 5. The impact of CaO variation in the $CaF_2/CaCl_2$ (13.8 wt% CaF_2 in $CaCl_2$) melts on the CO_2 capture process. CO_2 absorption was conducted by bubbling ~14 vol% of CO_2 in N_2 through the melt at 700-710 ºC. CO_2 regeneration was performed 935-945 ºC under pure N_2 and (--- black dash line) ~14 vol% of CO_2 in N_2 mixture for 550 min. Inset: Carrying capacity dependence on CaO concentration in the $CaF_2/CaCl_2$ melts fixed at eutectic composition.

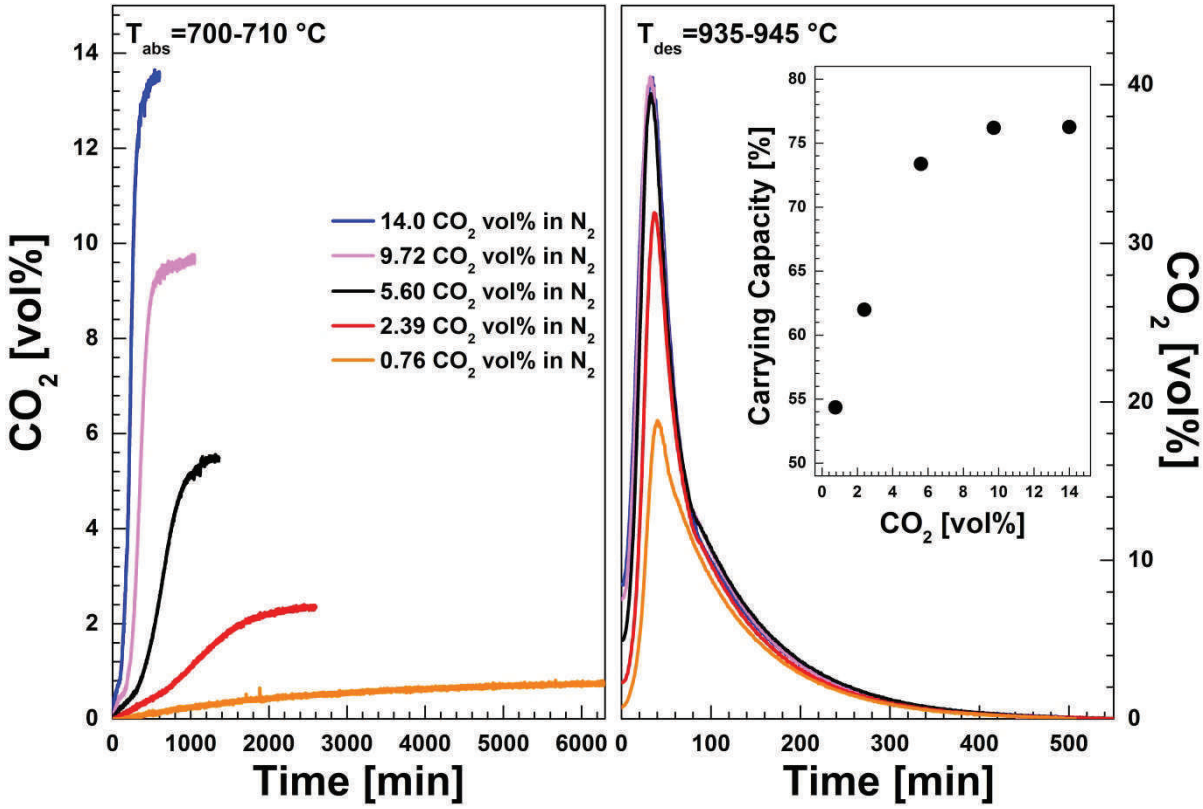

Figure 6. The impact of CO_2 concentration in N_2 on carbonation/decarbonation reactions. The sample of 15 wt% CaO, 11.7 wt% CaF_2 and 73.3 wt% $CaCl_2$ carbonation was conducted at 700-710 ºC under 14.0-0.8 vol% CO_2 in N_2. Decarbonation stage performed at 935-945 ºC under pure N_2. Inset: Carrying capacity dependence on CO_2 concentration in N_2.

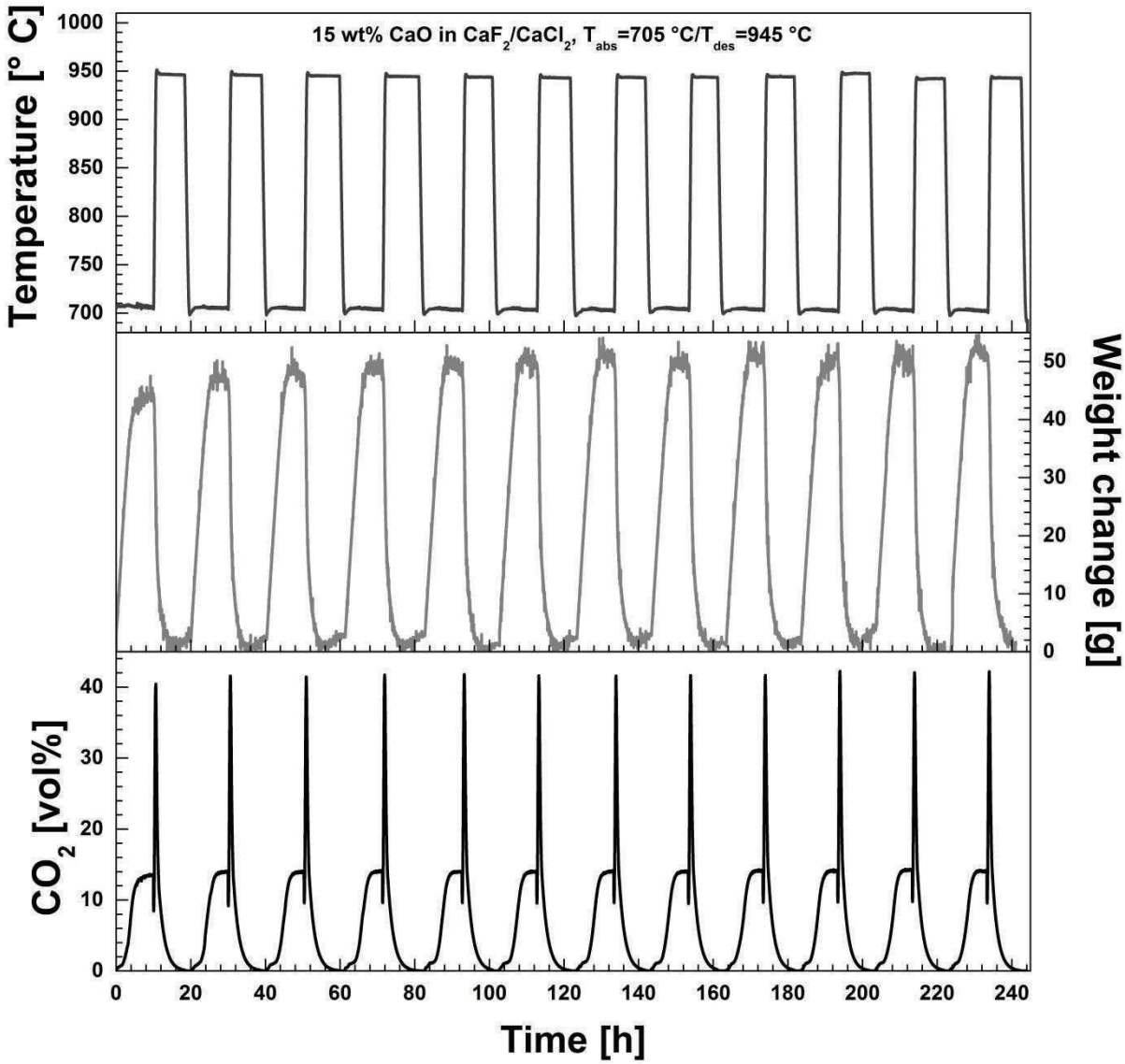

Figure 7. Cyclic CO_2 absorption/desorption by 15 wt% CaO in molten $CaF_2/CaCl_2$ (11.7/73.3 wt%). Carbonation of the sample was carried out at ~705 ºC by bubbling 14 vol% CO_2 in N_2 through the melt and decarbonation was performed at ~945 ºC under pure N_2.

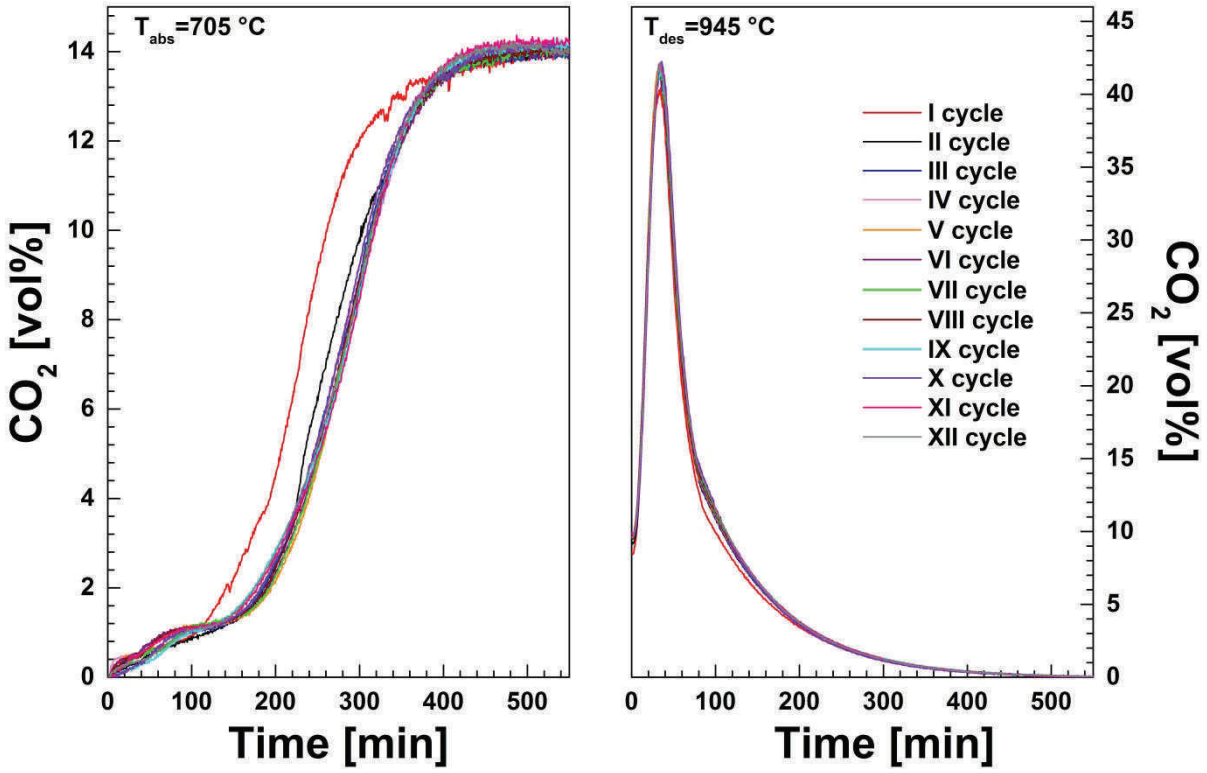

Figure 8. Comparison of 10 CO_2 capture cycles with carbonation temperature ~705 ºC of the 15 wt% CaO in molten $CaF_2/CaCl_2$ (11.7/73.3 wt%) sample under ~14 vol% CO_2 in N_2. Decarbonation was conducted at ~945 ºC under pure N_2.

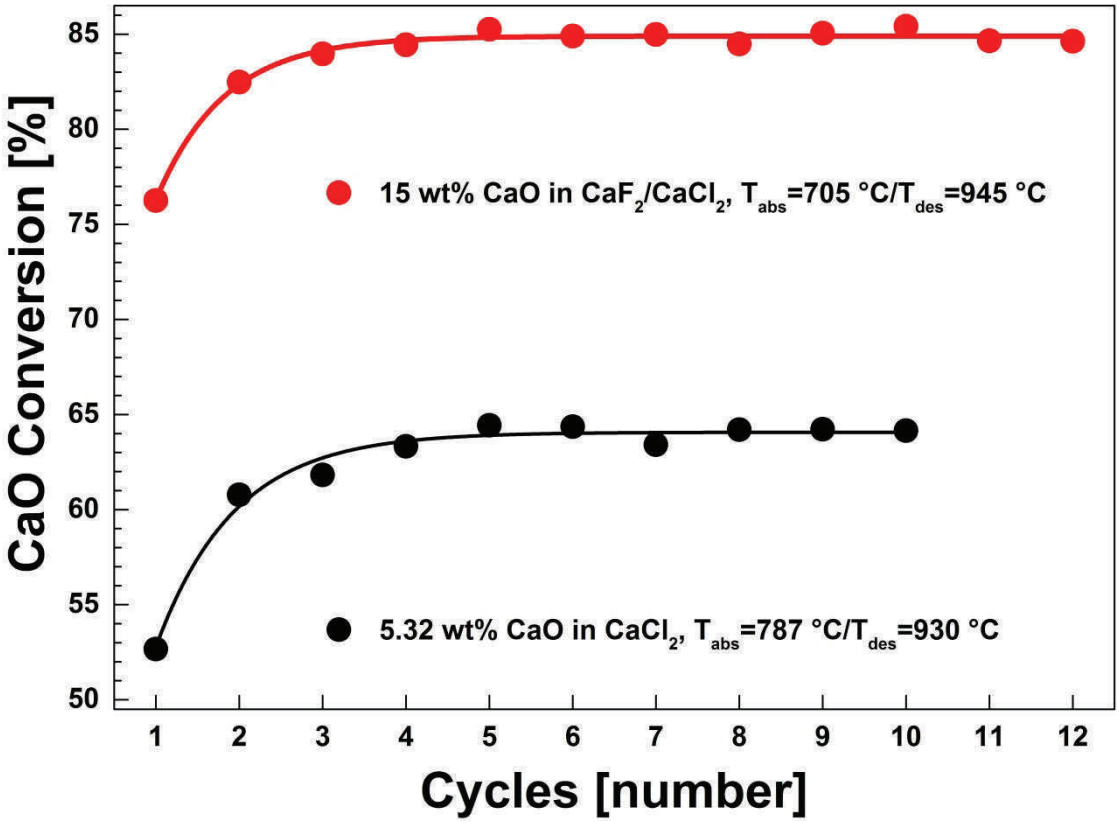

Figure 9. Carrying capacity investigation in cyclic carbonation/decarbonation of the $CaO/CaF_2/CaCl_2$ (15/11.7/73.3 wt%) sample. The results are compared to previously performed data on carbonation/decarbonation in the $CaO\text{-}CaCl_2$ system.[1]

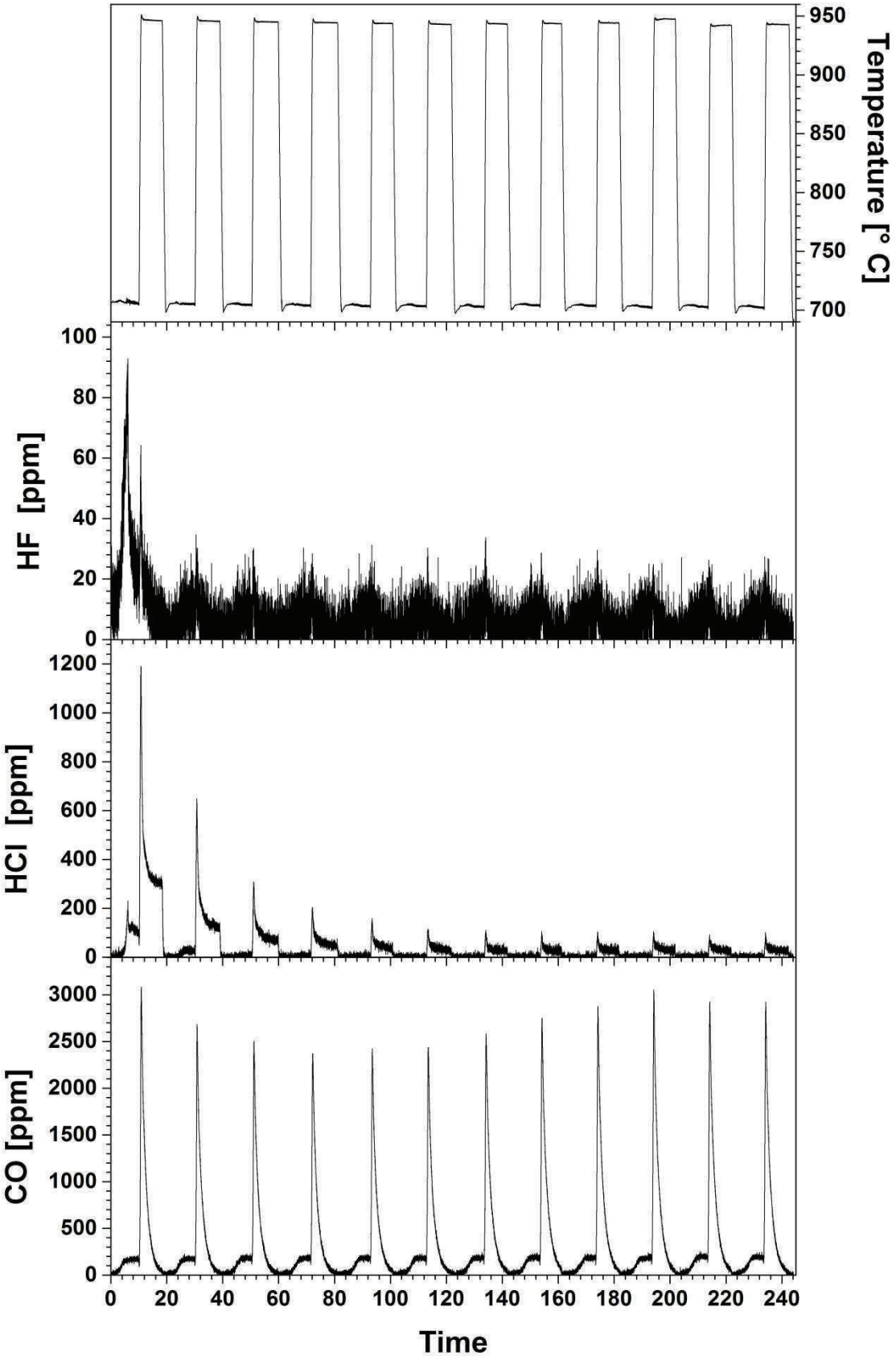

Figure 10. Hydrofluoric acid (HF), hydrochloric acid (HCl) and carbon monoxide (CO) formation in 12 CO_2 absorption/desorption cycles with 15 wt% CaO in molten $CaF_2/CaCl_2$ (11.7/73.3 wt%). The sample was carbonated at ~705 ºC in ~14 vol% CO_2 balanced by N_2 and decarbonated at ~945 ºC under pure N_2.

Paper V

Espen Olsen and **Viktorija Tomkute**. Carbon Capture in Molten Salts. *Energy Science & Engineering* 1 (2013) 144–150.

Energy Science & Engineering

Open Access

SHORT COMMUNICATION

Carbon capture in molten salts

Espen Olsen & Viktorija Tomkute

Department of Mathematical Sciences and Technology, Norwegian University of Life Sciences, Drøbakveien 31, N-1432 Ås, Norway

Keywords
$CaCl_2$, calcium looping, CaO, CO_2 capture, molten salt, NaF

Correspondence
Espen Olsen, Department of Mathematical Sciences and Technology, Norwegian University of Life Sciences, Drøbakveien 31, N-1432 Ås, Norway. Tel: +47 64965439; Fax: +47 64965401;
E-mail: espen.olsen@umb.no

Funding Information
We thank the Norwegian Research Council for financial support through the CLIMIT research program (199900/S60).

Received: 22 August 2013; Revised: 11 October 2013; Accepted: 22 October 2013

***Energy Science and Engineering* 2013; 1(3): 144–150**

doi: 10.1002/ese3.24

Abstract

Capture and storage of fossil carbon emitted to the atmosphere from anthropogenic sources has been identified as a key technology for keeping human-induced global warming below 2°C. Available technologies have not achieved widespread impact due to costs related to increased energy consumption and expensive, large process equipment. Here, we show how molten inorganic halide salt-based mixtures containing CaO may be utilized for selective capture and subsequent controlled release of carbon dioxide from diluted flue gases. Highly efficient absorption is demonstrated in a fluoride-based liquid, absorbing close to 100% of the CO_2 from a simulated flue gas with an absorbing column height of only 10 cm. Greater than 90% carbonation with >80% regeneration to CaO was recorded. Excellent cyclability has been achieved with a chloride-based liquid with 60% carbonation and 100% regeneration to CaO during four cycles. The high efficiencies may enable extraction of CO_2 from highly diluted gas mixtures.

Introduction

The capture and storage of CO_2 emitted from exploitation of fossil fuels has been identified as an issue, which should be aggressively pursued [1]. High-temperature post-combustion removal (HT-CCS) by carbonate looping has been identified by The European Technology Platform for Zero-Emission Power Generation (ZEP) as one of the most promising methods in the developing stage [2–15]. The concept relies on absorption of CO_2 by CaO with formation of $CaCO_3$ in the solid state. $CaCO_3$ is subsequently stripped for CO_2 and CaO is regenerated by raising the temperature [4–6]. CaO is frequently chosen as the active substance in the solid-state carbonate looping system, but other alkali-earth metal oxides may be used similarly. These oxides will exhibit thermal decomposition, each at their own, specified temperatures. The cycling may be described by the equilibrium in equation (1), here M denotes an alkali-earth metal element.

$$MO(s) + CO_2(g) \rightleftharpoons MCO_3(s) \quad \Delta G^{M=Ca}_{800^\circ C} = -12.4 kJ/mol \tag{1}$$

M: Mg, Ca, Sr, Ba

At lower temperatures, the equilibrium is shifted toward the right with the compounds on the left becoming increasingly stable at higher temperatures. This enables absorption and desorption of CO_2 to be performed, controlled by a simple thermal swing, either in a continuous flow reactor or a batch reactor. Thermodynamic modeling of the cycling has been performed and the Gibbs free energy for the equilibrium in equation (1) for the alkali-earth metals from Mg to Ba is plotted in Figure 1A.

Frequently, CaO is chosen as the active material due to its abundance and relevance with cement manufacture. CO_2 reacts with calcium oxide at a defined temperature to

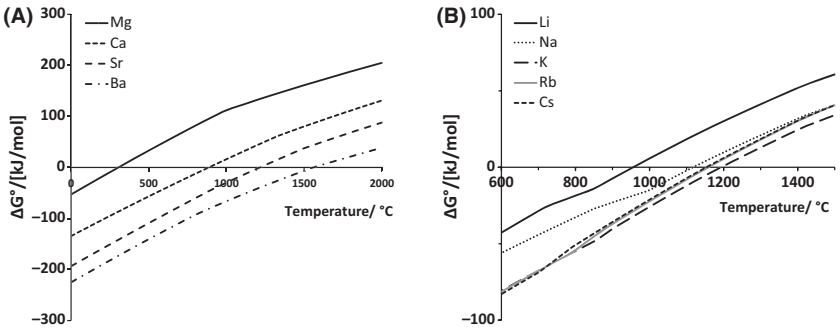

Figure 1. Thermodynamic modeling of the Gibbs free energy for the chemical reactions described by equation 1 (A) and equation 3 (B) [17].

form calcium carbonate in an absorption chamber (carbonation). The carbonate is then transferred to a second reactor chamber and decomposed to regenerate the oxide and pure CO_2 gas at a higher temperature (decarbonation). Transfer of the decarbonated solid (CaO) back to the absorption chamber completes the loop. Fluidized bed (FBR) reactors are normally used with these systems. Repeated absorption–desorption cycles introduce physical and structural stresses as well as sintering, leading to morphological changes in the particles [8,10,16]. For naturally occurring minerals, CaO-based sorbent reactivity is severely reduced after few (~3) cycles representing the main challenge identified with the technology [7–9].

We here report on a process based on the chemical principles involved in carbonate looping, but where the active substances are present as dissolved or partially dissolved in a liquid consisting of molten inorganic halide salts. By dissolving the active substances in a liquid, rapid gas–liquid reactions enable efficient absorption. A slurry state where the active substances are present in amounts exceeding their solubility limits has also been tested. As the active materials are present – at least partly, in dissolved states, they are constantly regenerated and the mechanisms leading to deactivation of solid sorbents will not be present.

Experimental Procedure

A sealed, one-chamber reactor was used for batch operation. The reactor chamber was made from stainless steel, with an inner crucible made of nickel (Ni) with inner diameter 5.0 cm containing 10 cm of liquid (400/500 g, NaF-CaF_2-CaO/$CaCl_2$-CaO). The experimental setup is schematically depicted in Figure 2. Reagent grade chemicals, all provided by Sigma–Aldrich (Steinheim, Germany) were used: CaO 96–100.5%, $CaCl_2$, anhydrous, ≥97.0, CaF_2

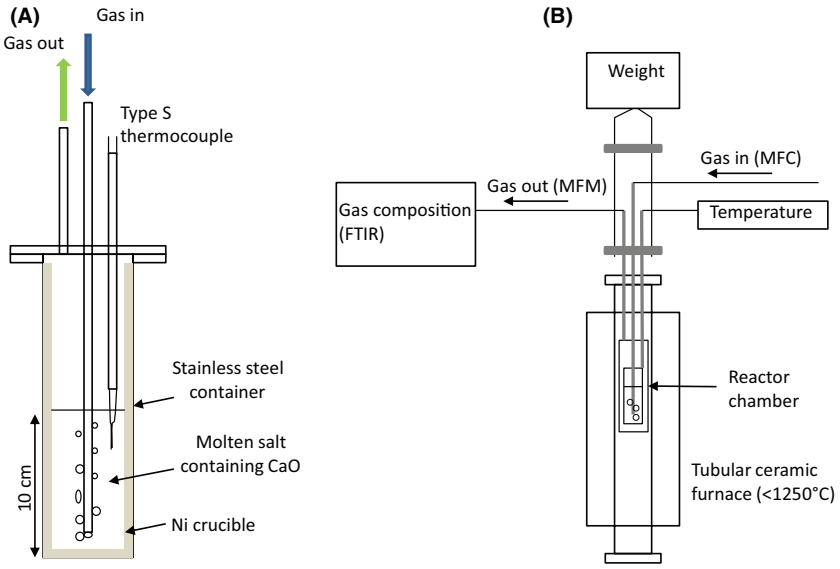

Figure 2. The experimental setup, schematically depicted. (A) The reaction chamber. (B) The full setup. The absorption–desorption processes are monitored by gravimetry and gas analysis (FTIR).

99.0–100.0%, NaF 98.5–100.0%, LiF 99%. To remove traces of water, the powders were dried in Ar at 200°C for 50 h, then slowly heated (200°C/h) to 850°C and kept for 10 h. The reactor chamber and gas lines were first purged by inert gas (N_2, 99.999%, AGA, Oslo, Norway) to remove air and to provide a stable environment while the salts and oxide originally added as powders were fused. Absorption was preceded by first bubbling nitrogen through the molten column for 1 h to remove traces of water. Gas analysis was performed continuously by an in-line Fourier transform infrared spectrometer (FTIR) (Thermo Nicolet 6700; Thermo-Fisher Scientific, Waltham, MA) equipped with a 2 m gas analysis cell. The weight of the assembly was monitored by an industrial balance (Mettler Toledo MS 8001S, Mettler-Toledo, Colombus, OH; 0.1 g). The experiments then commenced by submerging the Ni tube into the liquid while keeping the gas flowing. At this stage, CO_2 (AGA, instrument grade) was added to the gas flow. The content of CO_2 in the gas emitted from the reactor was monitored by FTIR while the weight change was recorded simultaneously. An electrostatic filter was employed in the gas line after the reaction chamber to protect the FTIR analyzer from potentially corrosive substances. Data were logged by using National Instruments Compact FieldPoint. Different molten salt systems were examined; compositions are given in weight% unless otherwise specified. A chloride-based system, which comprised of a 5.3% CaO/94.7% $CaCl_2$ mixture and two fluoride-based systems (48.2% NaF/41.8% CaF_2/10% CaO and 52% LiF/38% CaF_2/10% CaO) were used. Absorption was performed at 826°C (CaO/NaF/CaF_2), 800°C (CaO/$CaCl_2$), and 787°C (CaO/LiF/CaF_2). Carbonation was conducted by leading 0.6 Nl/min of a simulated flue gas (14 vol% of CO_2 in N_2) through the liquid column in the reactor chamber to the FTIR gas cell. The estimated residence time for the gas in the liquid was on the order of 1 sec. The height of the absorbing liquid column was 10 cm. Desorption was performed by stopping the flow of CO_2 and raising the thermal set point of the furnace to the temperature required for the CO_2 desorption process to commence, while monitoring both the gas composition flowing from the cell and the weight change. To demonstrate the possibility to desorb pure CO_2 at ambient atmospheric pressure (p_{CO_2} = 1 atm.), a molten salt containing 20% CaO in $CaCl_2$ was used. Here, the N_2 flow was stopped after carbonation had proceeded to its full extent. 100% CO_2 was kept flowing through the system while the temperature was raised stepwise to 1070°C. In this case, only the weight change was recorded. The sorption of CO_2 was calculated based on the gravimetric data and the efficiencies were estimated based on the measured weight gain/loss compared with the maximally achievable as 1 mol of CaO may absorb 1 mol of CO_2. X-ray diffraction (XRD) was performed by a Philips PW1730/10 diffractometer (Philips N.V., Eindhoven, Netherlands) using Cu-Kα (1.5418 Å) radiation and a Philips PW1711/10 proportional detector on melt samples rapidly quenched on an iron plate after removal from the experimental setup and remelting at 1200°C in the nickel inner crucible in a furnace open to the ambience.

Results and Discussion

Absorption with following desorption of CO_2 in the fluoride-based melts, as measured by gas analysis as function of time is depicted in Figure 3. Analysis of the gas composition after absorption reveals extremely efficient absorption of CO_2 initially. The total conversion rates from CaO into carbonate were in excess of 92% for both fluoride-based systems (CaO/LiF/CaF_2 and CaO/NaF/CaF_2). The decomposition of carbonate to oxide was recorded to be 47.5% for the NaF -containing, and 83.8% for the LiF-containing system. The content of CO_2 in the gas led through the reactor was registered to be below the detection limit of the analyzer (0 ppm recorded) for around 50 min in the initial carbonation stage. Following this, a slowly rising content of CO_2 in the emitted gas from the reactor was detected. The exothermic nature of the process was evidenced by a rise in temperature by 4–6°C from the set point when starting the carbonation reaction. The extremely efficient initial absorption was followed by a less efficient absorption stage initiated by an abrupt increase in the content of CO_2 being liberated from the reactor. This is seen in Figure 3 at around 200 min of elapsed time.

The high absorption efficiency in the fluoride-based melts is maintained by the simultaneously occurring exchange reaction described by equation (2).

$$CaCO_3(\text{diss}) + 2MF\ (l) \rightleftharpoons M_2CO_3(\text{diss}) + CaF_2(l) \quad (2)$$

M: Li or Na $\quad \Delta G_{800°C}{}^{M=Na} = -20.3$ kJ/mol

Equation (2) will be shifted toward the right for the NaF- or LiF-containing salt, keeping the activity of $CaCO_3$ in the system low. Unfortunately, no phase diagrams for the CaO-Li/NaF-CaF_2 system have been found in the literature, but the solubility of CaO in the Li/NaF-CaF_2 salts is most likely low at high NaF/LiF:CaF_2 molar ratios due to the Lewis basic character of both solute and solvent. Ten wt% CaO was added to this molten salt mixture, implying that this substance was present in quantities well above the solubility limit. This will fix the activity of CaO at unity early in the experiments and so lead to a low partial pressure of CO_2 to be established in the system. The combined, total reaction occurring with CaO and MF/CaF2 (M = Li or Na) as the active substances is described by equation (3). The Gibbs free energies for the combined reaction for the different alkali-earth metal elements are plotted in Figure 1B.

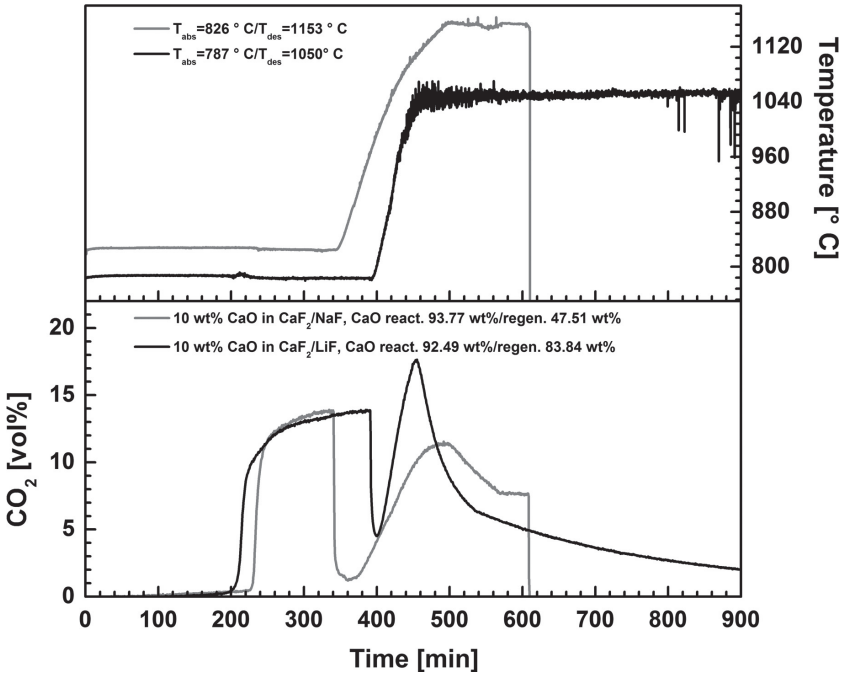

Figure 3. Absorption with subsequent desorption of CO_2 from a simulated flue gas (N_2 + 14 vol% CO_2) in fluoride-based liquids (grey line: 48.2% NaF/41.8% CaF_2/10% CaO, black line: 52% LiF/38% CaF_2/10% CaO). Desorption is performed by raising the temperature as indicated in the figure top panel. The figure shows the content of CO_2 in the gas emitted from the reactor (bottom panel) and the temperature (top panel) as functions of time.

$$\mathrm{CaO(diss,s) + CO_2(g) + 2MF\ (l) \rightleftharpoons M_2CO_3(diss) + CaF_2(l)} \quad (3)$$

M: Li or Na $\quad G^{M=Na}_{800°C} = -27.5$ kJ/mol

When the readily available (dissolved or dispersed) CaO was consumed, the partial pressure of CO_2 above the melt rapidly increased as the activity of CaO fell toward a low value and the carbonation commenced at a substantially lower rate. This is indicated by the rapid rise in CO_2 being liberated from the cell at around 200 min in Figure 3. Solid CaO (ρ = 3.3 g/cm^3) [17] is relatively heavy compared to the molten salt (ρ = 2.8 g/cm^3) [18] and may deposit toward the lower edges in the inner crucible during the initial melting of the powdery chemicals. Some of it may as such be less easily available for carbonation as it will need to dissolve in the rather basic melt in order to come into contact with the CO_2 being released in the center. This may explain the slower rate of the carbonation reaction from 200 to 400 min as recorded for the LiF-containing salt. The Gibbs free energy for the combined reaction (Eq. 3) with CaO and NaF as active substances becomes positive above 1120°C [17], shifting the equilibrium toward the left as the temperature increases. Thus, desorption of CO_2 in the $CaO/CaCO_3$/NaF/CaF_2 system was conducted by raising the furnace temperature to above this level (1150°C). Fast CO_2 desorption appeared as the temperature was raised (Fig. 3). Based on the FTIR gas analyses, 47.5% of the reacted CaO was regenerated in the NaF containing salt. XRD of samples, which remelted at 1200°C and then quenched, showed no signs of other phases than the initial (CaF_2, NaF, CaO), as evident in Figure 4, indicating that the decarbonation had proceeded fully at this temperature. Modeling showed that for a salt based on LiF, the liberation of absorbed CO_2 is supposed to commence at about 160°C lower in temperature as compared with the salt based on NaF [17]. As shown in Figure 3, this was also demonstrated experimentally, as rapid desorption was recorded from a melt containing $CaO/Li_2CO_3/LiF/CaF_2$ at 1050°C. The conversion rates from CaO into carbonate were in excess of 90% for both systems, while a higher decomposition rate of the formed carbonate back to CaO was observed in the melt containing LiF (83.8% of CO_2 desorbed) than in the NaF system (47.5% of CO_2 desorbed). Cycling was not performed for the fluoride-based melts as the higher desorption temperatures led to corrosion and deterioration of the outer stainless steel vessels by air.

Figure 5 shows absorption/desorption cycles in molten $CaCl_2$ with 5.3 wt% CaO added. The weight, temperature, and composition of the gas emitted from the reactor as

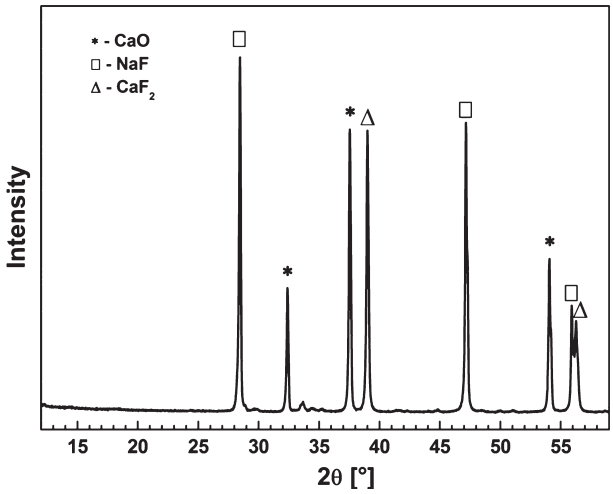

Figure 4. XRD pattern from a quenched fluoride-based molten salt after remelting in a crucible open to the ambient atmosphere. The desorption of CO_2 has proceeded to completion, as only CaF_2, NaF, and CaO is detected.

function of time is shown. In this system, there is no exchange reaction (Eq. 2), and the activity of $CaCO_3$ is not maintained at a low level. Furthermore, $CaCl_2$ exhibits a higher solubility of CaO than the fluoride-based melt (6% at 800°C) [19,20]. Absorption followed a predictable manner as the absorption efficiency started at a high level and then dropped, as reactive dissolved CaO in the liquid was consumed. This is evidenced by the recorded content of CO_2 in the gas emitted from the cell during each part of the cycle. During the initial carbonation, 46% CaO is converted into $CaCO_3$ in the first cycle during the first 70 min. This is followed by a slower reaction until carbonation stops after an additional 70 min. In the following cycles, increased CaO conversion is experienced. Figure 5 shows four completed cycles. The maximum value of CaO conversion into $CaCO_3$ in the $CaCl_2$ salt increased from 51.3% to 60.1% during the four performed cycles. When all available CaO had reacted and the gas escaping from the reactor resembled the composition being fed to the system, the feed of CO_2 was stopped and the temperature raised as described for the fluoride-based system. Rapid decomposition of $CaCO_3$ is evident from the sharp increase in the content of CO_2 in the liberated gas. The conversion efficiencies based on weight for CaO into $CaCO_3$ and for $CaCO_3$ back into CaO are plotted in Figure 6. The availability of CaO seemed to increase as higher values for conversion of CaO into $CaCO_3$ were observed with each cycle. 100% conversion into CaO was recorded in all cycles.

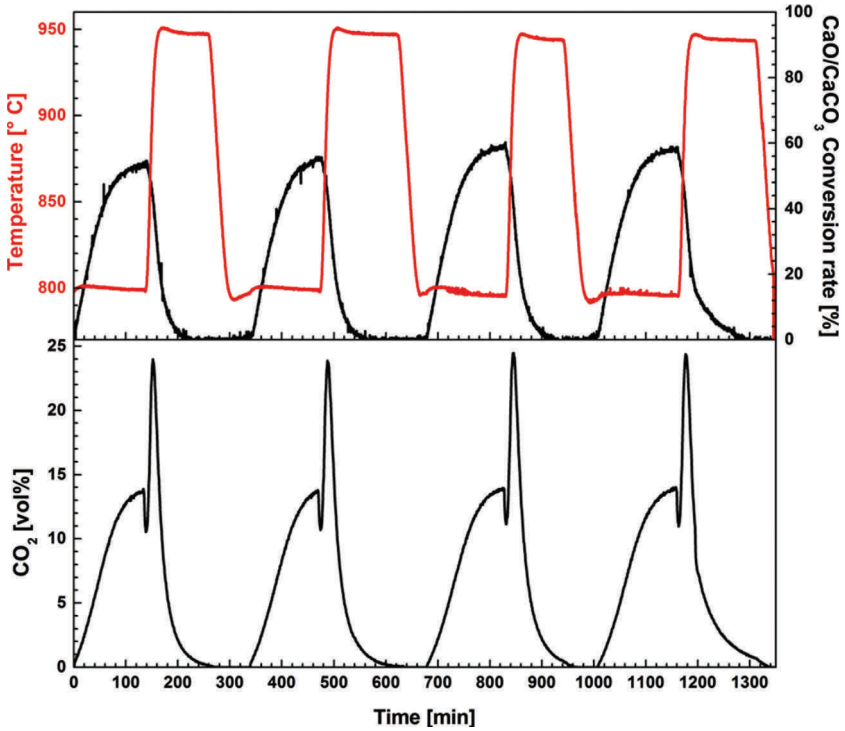

Figure 5. Repeated absorption–desorption cycling (4×, 800°C/950°C) from a simulated flue gas (N_2 + 14 vol% CO_2) with a chloride-based absorbing liquid ($CaCl_2$ + 5%CaO). The content of CO_2 in the gas emitted is shown in the bottom panel (black), while the mass of the reaction vessel (black) as well as temperature (red) is shown in the top panel.

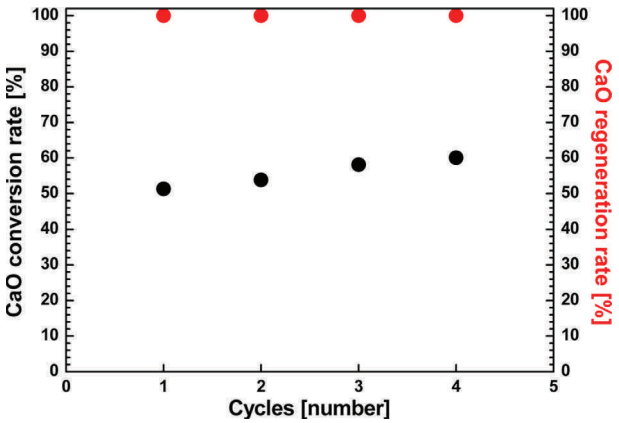

Figure 6. The conversion efficiency of the cycling between CaO and $CaCO_3$ during absorption (black) and desorption (red) in each of the cycles from Figure 3 based on weight measurements. The decarbonation of $CaCO_3$ by forming CaO and CO_2 is reaching 100% efficiency in all the cycles while the conversion of CaO into $CaCO_3$ during absorption shows a rising trend with each cycle.

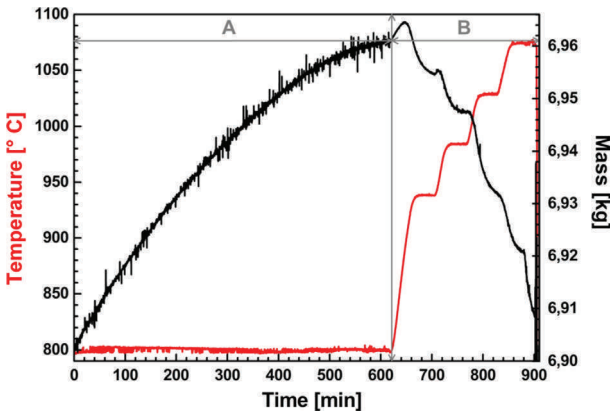

Figure 7. Absorption from a simulated flue gas with subsequent desorption in pure CO_2 atmosphere (pCO_2 = 1 atm.). Region A: Absorption. Region B: Desorption. Desorption was performed after absorption by stopping the flow of N_2 in the simulated gas while keeping the CO_2 flowing. The temperature was then raised in steps of 50°C until 90% of the CO_2 had desorbed according to weight measurements. The furnace was then shut down.

In processes for CCS based on thermal swing, CO_2 is often driven off by addition of superheated steam. Desorption of the pure CO_2 itself (i.e., a partial pressure of CO_2 of 1 atm.) is desirable as costs related to the condensation of water may be avoided. Decomposition at such conditions with a 20% CaO in $CaCl_2$-based molten salt was performed by stopping the flow of nitrogen while keeping the CO_2 flow. The temperature was then stepwise raised to 1070°C as described above. 74.2% of CaO had reacted with CO_2 when carbonation had proceeded to its full at 800°C. Additional carbonation (4.4% of CaO converted) was observed when the nitrogen was suspended in the gas flow and the temperature increased (Fig. 7). As the temperature increased beyond 900°C a loss of mass was recorded, indicating decarbonation and release of CO_2 from the liquid. A stepwise weight loss in accordance with the stepwise increase in temperature was recorded as depicted in Figure 7. A conversion rate of $CaCO_3$ into CaO on the order of 90% was found at 1070°C.

Concerns may be raised regarding the energy consumption for the thermal swing with a diluted liquid compared to a solid-based sorbent such as CaO (s). However, our experiments indicate that CaO can be present substantially above its solubility limit – most likely in the form of slurry. In this work, up to 20% CaO in $CaCl_2$ has been used while the solubility of CaO in $CaCl_2$ at 800°C is 6% [19]. At 74.2% carbonation, this is equivalent to an uptake capacity of CO_2 of 0.105 g/g liquid if 90% $CaCO_3$ to Ca conversion as recorded with this composition is assumed. This is similar to numbers recently reported for synthetic, stable sorbents in Ca-looping where CaO is present as nanostructures on a solid, inert carrier [21]. In practice, increasing viscosity will probably be the limiting effect as more CaO is added, however, this was not notable at a content of 20% CaO. Further work will concentrate on optimizing these conditions as they will be closely linked to the overall economics. Some molten salts may be subject to hydrolysis when exposed to water. Hydrolysis is, however, not thermodynamically favored for the salts used in this study [17]. A vapor pressure will be established over a free liquid surface. Potentially evaporated material will condense and deposit in cooler parts of the reactor or the gas line. Such condensate was, however, not found in any significant amounts, implying that the mass loss of due to evaporation was negligible.

To summarize, we have investigated a new method for selectively separating CO_2 from diluted gas mixtures exhibiting efficient gas–liquid reactions. An absorption column height of only 10 cm is shown sufficient to achieve high absorption efficiency. We propose that capture and release of CO_2 from very dilute gas mixtures may be possible with a fluoride-based melt containing NaF or LiF. Due to the robust inorganic chemicals, we propose that the method may be particularly suited for CCS on industrial emissions.

Acknowledgments

We thank the Norwegian Research Council for financial support through the CLIMIT research program (199900/S60), SINTEF Materials and Chemistry, Trondheim, Norway for experimental assistance and chief scientist Asbjørn Solheim for counsel.

Conflict of Interest

None declared.

References

1. Chu, S. 2009. Carbon capture and sequestration. Science 325:1599.
2. MacDowell, N., N. Florin, A. Buchard, J. Hallett, A. Galindo, G. Jackson, et al. 2010. An overview of CO_2 capture technologies. Energy Environ. Sci. 3:1645–1669.
3. Dean, C. C., J. Blamey, N. H. Florin, M. J. Al-Jeboori, and P. S. Fennell. 2011. The calcium looping cycle for CO_2 capture from power generation, cement manufacture and hydrogen production. Chem. Eng. Res. Des. 89:836–855.
4. Blamey, J., E. J. Anthony, J. Wang, and P. S. Fennell. 2010. The calcium looping cycle for large-scale CO_2 capture. Prog. Energy Combust. Sci. 36:260–279.
5. Abanades, J. C., E. J. Anthony, J. Wang, and J. E. Oakey. 2005. Fluidized bed combustion systems integrating CO_2 capture with CaO. Environ. Sci. Technol. 39:2861–2866.
6. Dobner, S., L. Sterns, R. A. Graff, and A. M. Squires. 1977. Cyclic calcination and recarbonation of calcined dolomite. Ind. Eng. Chem. Process Des. Dev. 16:480–486.
7. Li, Z., N. Cai, Y. Huang, and H. Han. 2005. Synthesis, experimental studies, and analysis of a new calcium-based carbon dioxide absorbent. Energy Fuels 19:1447–1452.
8. Chen, Z., J. R. Grace, and C. J. Lim. 2008. Limestone particle attrition and size distribution in a small circulating fluidized bed. Fuel 87:1360–1371.
9. Fennell, P. S., R. Pacciani, J. S. Dennis, J. F. Davidson, and A. N. Hayhurst. 2007. The effects of repeated cycles of calcination and carbonation on a variety of different limestones, as measured in a hot fluidized bed of sand. Energy Fuels 21:2072–2081.
10. Wu, Y., J. Blamey, E. J. Anthony, and P. S. Fennell. 2010. Morphological changes of limestone sorbent particles during carbonation/calcination looping cycles in a thermogravimetric analyzer (TGA) and reactivation with steam. Energy Fuels 24:2768–2776.
11. Abanades, J. C., G. Graca, M. Alonso, N. Rodriguez, E. J. Anthony, and L.-M. Romeo. 2007. Cost structure of a postcombustion CO_2 capture system using CaO. Environ. Sci. Technol. 41:5523–5527.
12. MacKenzie, A., D. L. Granatstein, E. J. Anthony, and J. C. Abanades. 2007. Economics of CO_2 capture using the calcium cycle with a pressurized fluidized bed combustor. Energy Fuels 21:920–926.
13. Dennis, J. S., and A. Pacciani. 2009. The rate and extent of uptake of CO_2 by a synthetic. CaO-containing sorbent. Chem. Eng. Sci. 64:2147–2157.
14. Working Group on Long-term R&D Plan for Capture Technology. 2010. Recommendations for research to support the deployment of CCS in Europe beyond 2020. European Technology Platform for Zero Emission Fossil Fuel Power Plants (ZEP), Brussels, Belgium.
15. Martínez, I., R. Murillo, G. Grasa, and J. C. Abanades. 2011. Integration of a Ca-looping system for CO_2 capture in an existing power plant. Energy Procedia 4:1699–1706.
16. Manovic, V., and E. J. Anthony. 2010. Sintering and formation of a nanoporous carbonate shell at the surface of CaO-based sorbent particles during CO_2-capture cycles. Energy Fuels 24:5790–5796.
17. Roine, A. 2008. Outokumpu HSC chemistry for windows 6.1. Outokumpu Research, Pori, Finland. ISBN-13: 978-952-9507-12-2.
18. Janz, G. J. 1967. Molten salt handbook. Academic Press, London, U.K.
19. The American Ceramic Society. 2010. ACerS-NIST Phase Equilibria Diagrams Database v. 3.1. The American Ceramic Society, Westerville, OH.
20. Wenz, D. A., I. Johnson, and R. D. Wolson. 1969. CaCl2-rich region of the $CaCl_2$-CaF_2-CaO system. J. Chem. Eng. Data 14:250–252.
21. Stendardo, S., L. K. Andersen, and C. Herce. 2013. Self-activation and effect of regeneration conditions in CO_2–carbonate looping with CaO–$Ca_{12}Al_{14}O_{33}$ sorbent. Chem. Eng. J. 220:383–394.